UNIVERSITA' DEGLI STUDI DI PARMA

Dottorato di ricerca in Scienze della Terra

Ciclo XXIII

Integrated Stratigraphy of the Upper Paleocene-Lower Eocene successions of the Tremp and Ager basins (south-central Pyrenees, Spain)

Coordinatore:
Chiar.mo Prof. Renzo Valloni

Tutor:
Chiar.mo Prof. Marco Roveri

Co-Tutor: Dott. Roberto Tinterri

Dottorando: Nicola Minelli

UNIVERSITA' DEGLI STUDI DI PARMA

Dottorato di ricerca in Scienze della Terra

Ciclo XXIII

INTEGRATED STRATIGRAPHY OF THE UPPER PALEOCENE-LOWER EOCENE SUCCESSIONS OF THE TREMP AND AGER BASINS (SOUTH-CENTRAL PYRENEES, SPAIN)

Coordinator:
Chiar.mo Prof. Renzo Valloni

Tutor:
Chiar.mo Prof. Marco Roveri

Co-Tutor: Dott. Roberto Tinterri

Ph.D. STUDENT: Nicola Minelli

alla mia famiglia

al mio amore

INDEX

-

1 - INTRODUCTION

The southern Pyrenees (or spanish Pre-Pyrenees) constitute a thrust-and-fold belt, formed through the southward propagation of thrust sheets in response to the continental collision between the Iberian and European plates, started in the late Cretaceous, that brought to the formation of the Pyrenean orogen.

Particular conditions, related to the areal extension of the décollement horizons, and with the combined effects of subsidence and eustatic variations, allowed the preservation of thick, relatively poorly-deformed successions of the southern pyrenean foreland (SPF). These successions are hosted in elongate basins, formed above the active thrust sheets and enclosed between roughly parallel thrust fronts, and display a syntectonic sedimentary record mainly expressed through the development of growth geometries and angular unconformities. The stratigraphic units enclosed between these unconformities are substantially tectonically-driven large-scale sequence-stratigraphic units ("allogroups", *sensu* Mutti et al., 1988), and the correlation of these units and their bounding unconformities throughout the SPF allowed former workers to establish a chronology of the tectonic deformation in this setting.

In the central portion of the SPF, the Tremp-Graus basin (hereafter "Tremp basin") hosts continental to shallow-marine deposits of early Paleogene age, that forms one of the most complete south-pyrenean stratigraphic successions in this period. Immediately south of the Tremp basin, the coeval Ager basin constitutes a narrower embayment, separated from the latter by the north-dipping Montsec thrust. In the Ager basin, the more constricted morpho-structural asset drove the formation of deposits, and related geometries of the sedimentary bodies, different from the ones observable in the Tremp basin (Mutti et al., 1988, 1994).

Uplift of the early Montsec thrust-related anticline caused the formation of basin-margin thinned successions on its flanks, and within these marginal successions unconformable stratigraphic relationships and growth geometries are in plain sight, or can be easily worked out through detailed section logging and local correlations.

Conversely, the axial successions of these basins are characterized by thick, aggrading successions, built up by the combined effects of subsidence, sealevel rise and abundant sediment availability. In these sections, the unconformable relationships recognized at the basin margins are often expressed by paraconformable contacts, where the presence of an allogroup or sequence boundary may only be expressed by sharp lithological changes, or changes in the faunal composition, suggestive of a significant drop in relative sealevel along a specific interface.

In the early Paleogene of the Ager basin, the northern marginal succession is represented by a limited exposure that allows the immediate recognition of two relevant unconformities, bounding a succession of early Ypresian age, whose correlations in the southern axial succession are only partially established, because of a poor coverage in chronostratigraphic data, and because of the structural setting of the basin, that prevents a direct physical correlation of stratigraphic units and surfaces.

In the Tremp basin, the stratigraphic relationships between the basin margin and the depocenter are well-established, primarily because of the continuity of the outcrops, and because of a greater amount of chronological informations provided by literature. However, in the marginal succession of the southern Tremp basin (i.e., the one bordering the Montsec structural high), angular unconformities are more subtle, and growth geometries are the most salient expression of the interaction of tectonics and sedimentation.

This work mainly deals with some problems in the definition of the allogroup boundaries and interposed units that formed in the upper Thanetian-early Ypresian of the Tremp and Ager basins; problems are mainly referred to the correlation, across the two basins, of major and minor sequence boundaries and interposed units, and also concern the significance of some of these boundaries as allogroup boundaries; as a direct implication of this, a dating of the main deformational stages occurring along the Montsec thrust front will be tentatively provided.

A further revision of the former stratigraphic investigations was conducted with the classic approach of field logging, facies analysis and sequence stratigraphic interpretation of the considered successions. This fieldwork took a period of approximately eight months, during which 23 sections were measured in detail, summing up to ~4000 m. No mapping was performed, because of the great detail already provided by aerial photograph mapping in some former investigations, that constituted the geological-cartographic basis for the present work (with particular reference to the Tremp basin's mapping provided by Waehry, 1999 and the Ager basin's mapping provided by Ghielmi, 1992 and Mutti et al., 1994).

The physical-stratigraphic approach was then integrated with a chemostratigraphic investigation in the field of the stable isotopes of carbon and oxygen.

The primary purpose of this approach was to overcome some limitations with the chronostratigraphic subdivision of the Ager basin, taking advantage of the global-scale correlation potential of an anomalous isotopic shift occurring at the Paleocene/Eocene boundary. This anomaly was formerly documented in the Tremp basin (Schmitz & Pujalte, 2003), and its relevance in the present work, apart from the obvious purposes of age determination, stands in its close stratigraphic relationship with a major sequence boundary or allogroup boundary. Functional to this specific objective, isotope analyses were applied in the whole Paleocene succession of the Ager basin (although it is in great part represented by the sole Thanetian), in order to obtain a first isotopic characterization of the main lithological and stratigraphic units, and to apply these results in a tentative correlation of the marginal and depocentral successions.

In the Tremp basin, the same geochemical analyses were conducted on shallow-marine carbonates of early Ypresian age, in order to evaluate the preservation of the isotopic signal in this setting, with the aim of integrating with chemostratigraphic informations the well-assessed physical stratigraphic subdivisions established in this basin by former workers; a secondary objective was the localization of another anomalous isotopic shift occurring in the early Ypresian, whose stratigraphic location was roughly constrained on the basis of other available chronostratigraphic data; however, this objective wasn't fulfilled, either because this specific horizon fell in a gap between the collected samples, or because it may coincide with a local stratigraphic gap related with a relatively pronounced sealevel fall.

An updated chronology for the studied successions was finally provided by the review of the published bio-, chemo- and magnetostratigraphic data in the light of recent early Paleogene age models, including a few new magnetostratigraphic data from the early Ypresian of the Ager basin.

In conclusion, the integration of these different stratigraphic approaches allows a better definition of the geological evolution of the Tremp and Ager basins in the early Paleogene; moreover, these successions, formed under the primary control of tectonics, are now framed in a global picture of long-term climate change, that allows a preliminary evaluation of the response of the local depositional systems to major climatic trends and events.

2 – GEOLOGICAL SETTING

This study was carried out in the central portion of the paleogenic foreland basin which developed along the southern border of the Pyrenean chain. The basin formed through the concomitant effects of active thrusting, longitudinal displacement of the thrust sheets and subsidence.

Deformation was diachronous across the whole foreland, both in longitudinal and transverse direction but, as a general rule, in the Pyrenean domain the compression started in the late Cretaceous and ended in the late Oligocene.

The Tremp and Ager basins developed upon a peculiar structural block ("Tremp Unit", auctt.), a condition that brought to a relative physiographic isolation from the eastern and western portions of the foreland; thrusting caused a compartmentalization of the basin in the longitudinal sense, causing the development of a number of parallel sub-basins. The E-W oriented Tremp and Ager basins, connected with a proto-Atlantic ocean to the west and extending from Lleida to the eastern Huesca provinces (Catalunya), are the better preserved of these sub-basins. Actually, the Tremp basin (sometimes referred to as the Tremp-Graus basin) hosts the most continuous sedimentary successions recording the whole history of the Pyrenean foreland.

2.1 – Strucural setting and geodynamic context

2.1.1 – The Pyrenees: surficial and deep structure.

The Pyrenees are a mountain range that separates the Iberian/African plates from the Eurasian plate, extending from the Cantabrian region to the NNW to the Mediterranean to the SSE (**figure 2.1**).

The extension of the chain was quantified in different ways; the whole complex reaches up to 1500 km in length from the Cantabric to Provence, but some authors only consider the 400 km ridge extending from the bay of Biscay to the Mediterranean (e.g., Sibuet et al, 2004); on a larger scale, moreover, the Pyrenees can be seen as the western end of the Alpine-Himalayan belt, because these mountain chains altogether formed in the common context of the Tethian convergence.

The orogen was classically subdivided into three, roughly parallel structural belts, that are the central Axial Zone and the northern and southern thrust-and-fold belts. At the outer margins of the thrust-and-fold belts lay the late foreland basins (Ebro and Aquitaine). The whole chain is doubleverging, and is characterized by a marked asymmetry, with the southerly-vergent structures (i.e., north-dipping) much more extended than the northern ones (Muñoz, 2002; **figure 2.2**).

STRUCTURAL MAP OF THE PYRENEES (redrawn from Muñoz, 2002)

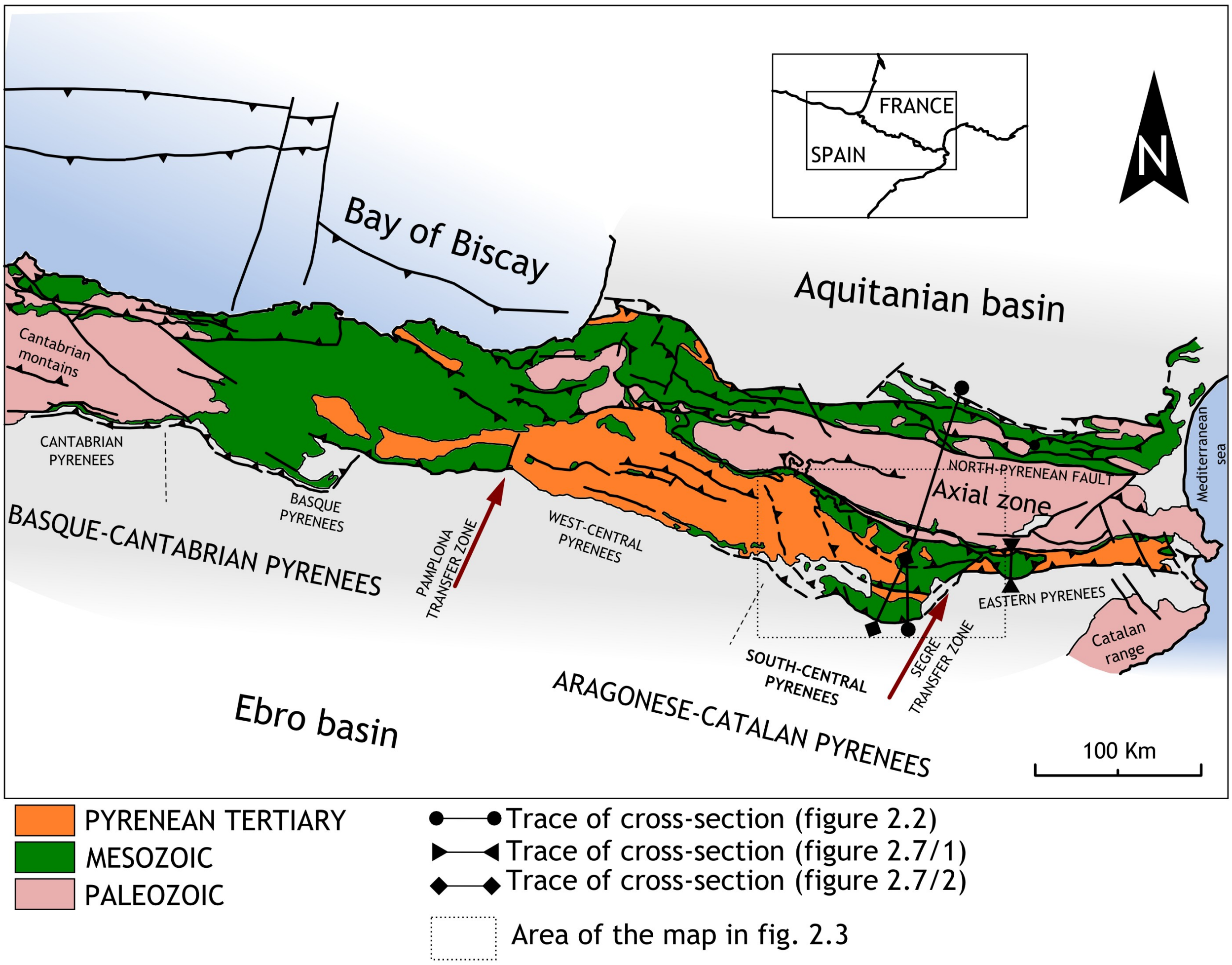

Figure 2.1

The North Pyrenean Fault (or fault zone), commonly considered as the boundary between the European and Iberian plates, separates the north- and south-vergent domains; it is made of vertically dipping transcurrent structures, bordering to the north the Axial Zone. In the central-eastern Pyrenees, the latter defines a sector dominated by duplex stacking and steeply dipping structures: this gives place to a bulging structure ("antiformal stack", auctt.), that is the highest across the pyrenean range. The duplexes involve Hercynian basement rocks, and overthrust the southern thrust-and-fold belts in the Eastern Pyrenees.

The southern thrust-and-fold belt (Southern Pyrenees) was developed through thrusting in the early southern foreland basin; structural lineaments were inherited from former extensional structures, through a process of fault inversion that, starting in the Santonian, is considered to have been the main driving factor of the Pyrenean orogeny (Muñoz et al, 1986).

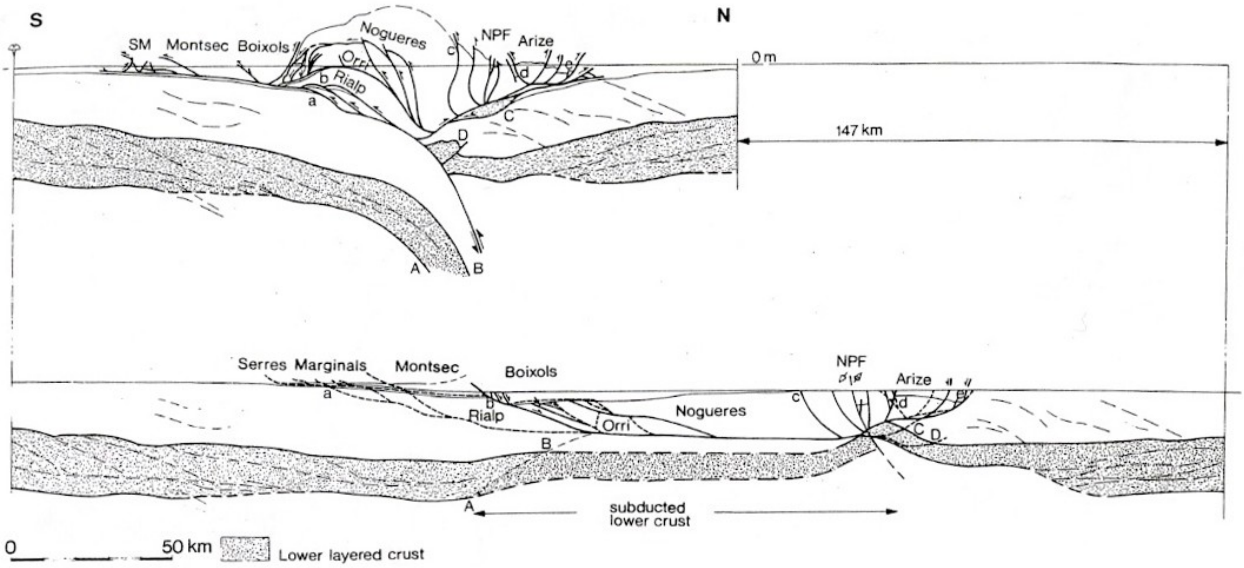

Figure 2.2 – Pyrenean crustal cross-section and restoration, based on the ECORS seismic profile, according to Muñoz, 1992.

2.1.2 – The Aragonese-Catalan Pyrenees

The south-eastern portion of the Pyrenean range (Aragonese-Catalan Pyrenees, in Muñoz, 2002) is longitudinally subdivided into three domains. These domains reflect a different structural style, mainly in response to the presence and areal extension of a basal evaporitic detachment layer, of late Triassic age, that allowed the dislocation of the thrust sheets in the southern foreland; where this soft layer was poorly developed, thrust sheets stopped advancing and began to pile up, as it is the case of the eastern domain; the central domain instead, is dominated by imbricate geometries of the thrust sheets, that eventually traveled further southwards because of a wider extension of the detachment layer. The boundary between the two domains is the Catalunya Fault (formerly Segre Fault), a large strike-slip structure with a NE-SW orientation.

The central domain, hosting the South-Central Pyrenean Foreland basin, will be treated in detail below; it is characterized by a discrete structural unit (named Tremp unit, or South Pyrenean Central unit) detached on a wide horizon of Triassic evaporites and delimited on its sides by lateral ramps, represented to the east by the Catalunya fault, and to the west by a complex, partly buried, fold and thrust system (Cotiella ramp; Morley, 1994, and references therein). Macroscopic features of the central domain are a sub-parallel orientation of the thrust fronts, and a minor amount of deformation if compared with the eastern ad western domains, that allowed a good preservation of the foreland basins that developed upon it.

The western domain is delimited to the east by the Cotiella ramp and to the west by a large transcurrent structure known as the Pamplona Fault, that divides the Aragonese-Catalan Pyrenees from the Basque-Cantabrian domain. Two main thrust and fold belts delimit to the north and to the south this region (Sierras interiores and Sierras exteriores), giving place to a large, relatively undeformed basin (Jaca or Hecho basin) in the middle.

2.1.3 – The South-Central Pyrenean Unit (Tremp Unit)

This unit, represented in the map and cross-section of **figures 2.3 and 2.4**, defines a region bordered to the north by the antiformal stack of the Axial Zone, and to the south by the frontal pyrenean thrust (Vallfogona thrust). Lateral ramps provided a relative isolation of the sedimentary basins since the Mesozoic, and the whole unit was slightly uplifted with respect to the eastern ad western regions. The main structural elements were inherited by Mesozoic pre-inversion structures, reactivated during the Santonian; the thrust sheets themselves mimic the geometry of portions of the Mesozoic extensional basins (Morley, 1994, and references therein).

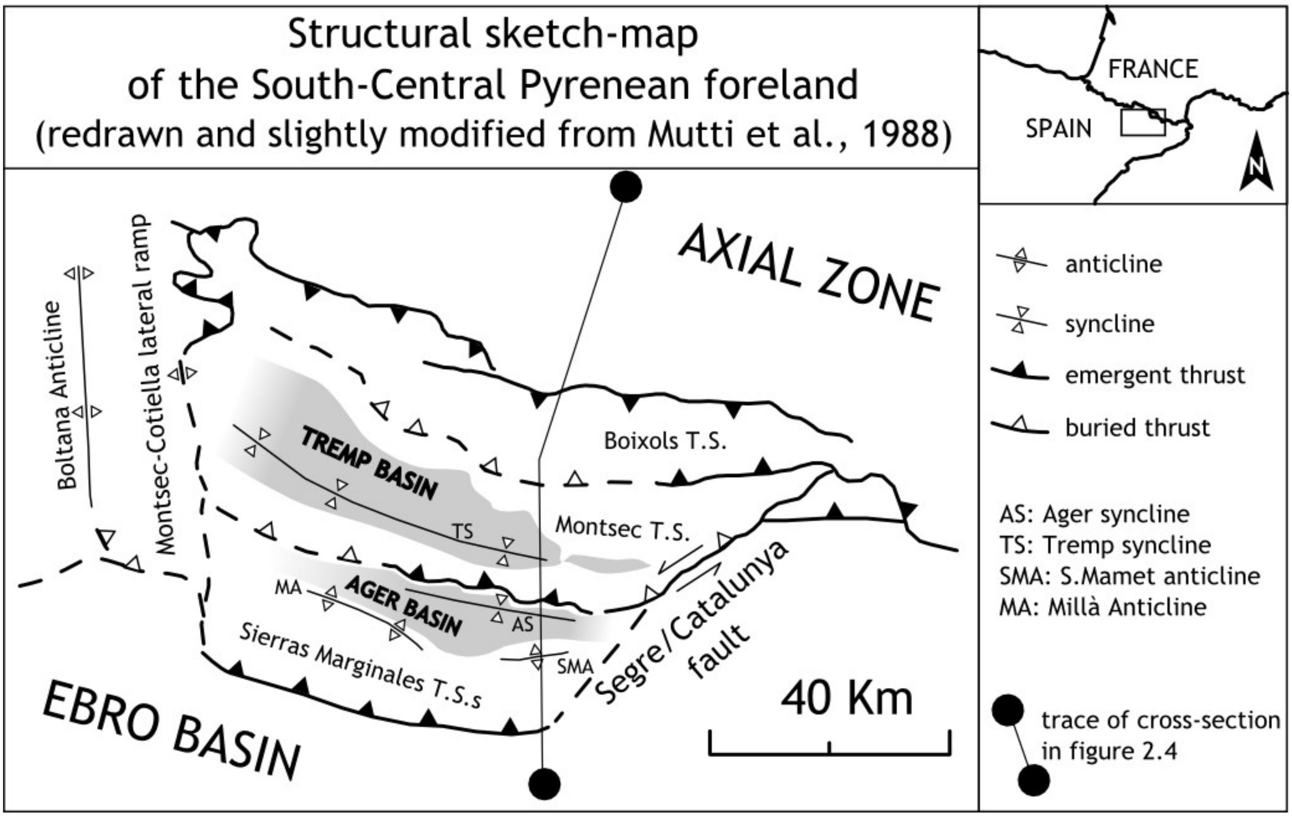

Figure 2.3

This region experienced thrusting since the late Cretaceous, and thrusts generated in a piggy-back sequence up to the middle Eocene; after that, further reactivations (that caused the most of the shortening, Muñoz, 1992; Fitzgerald et al., 1999) progressed in an out of sequence pattern until the late Oligocene. Three main thrust sheets can be clearly defined, both on surface and subsurface, that are, from north to south, the Boixols, Montsec and Sierras Marginales thrust sheets. The Boixols and Montsec thrust sheets show a relatively simple geometry and, especially the latter, poor structural disturbance.

The Boixols thrust sheets is delimited to the north by a backthrust (Morreres thrust) that acted passively with respect with the Axial Zone (Muñoz, 2002, and references therein); to the south, the frontal thrust crops out only in few locations, since it was buried during the late Cretaceous by syntectonic sediments. The thrust sheet is composed of a thick (~5000 m) succession of Cretaceous limestones, partly dismantled during the Tertiary.

The Montsec thrust sheet is the less deformed unit, developing as a wide flattened synform body. Structural complications are present on its eastern and western borders due to the interaction of the Montsec thrust with the lateral ramps; actually, the western ramp is an arcuate continuation of the thrust that was further folded as the Tremp Unit progressed in the foreland (Morley, 1994, and references therein). Similarly to the Boixols thrust sheet, the original Montsec thrust sheet was made of Mesozoic rocks, but since when it became a regional morphological feature, it hosted a piggy back basin of Paleocene to middle Eocene age (Tremp-Graus basin).

The Sierras Marginales thrust sheet is the most complex unit, being fragmented in many small imbricate units, with blind thrusts producing a surficial folded geometry. The mesozoic succession it hosts is thinner than that of the northern thrust sheets, as it is for the Paleocene and Lower Eocene successions (Meigs and Burbank, 1997). The inner (northern) anticlines of the Sierras Marginales, (Millà and St. Mamet anticlines) and the ancestral expression of the Montsec ("paleo-Montsec") delimited the Ager basin south of the Tremp basin.

2.2 – General stratigraphy and timing of tectonics in the South-Central Pyrenees

The history of the Pyrenean orogenesis has been fairly constrained both through stratigraphy and deep seismic studies. Moreover, the study of the magnetic anomalies in the bay of Biscay allowed various reconstructions of the relative movements of the iberian ad european plates.

Figure 2.4, redrawn from Muñoz (2002) resumes the main stages of movement of the thrust fronts in the south-central Pyrenees, much part of which were already identified in the 1970s and 1980s on the basis of the recognition of syntectonic deposits (Puigdefabregas, et al., 1986; Muñoz, 1992). **Figure 2.5**, from the same author, shows a reconstruction of the Pyrenean shortening during the main different evolutionary steps.

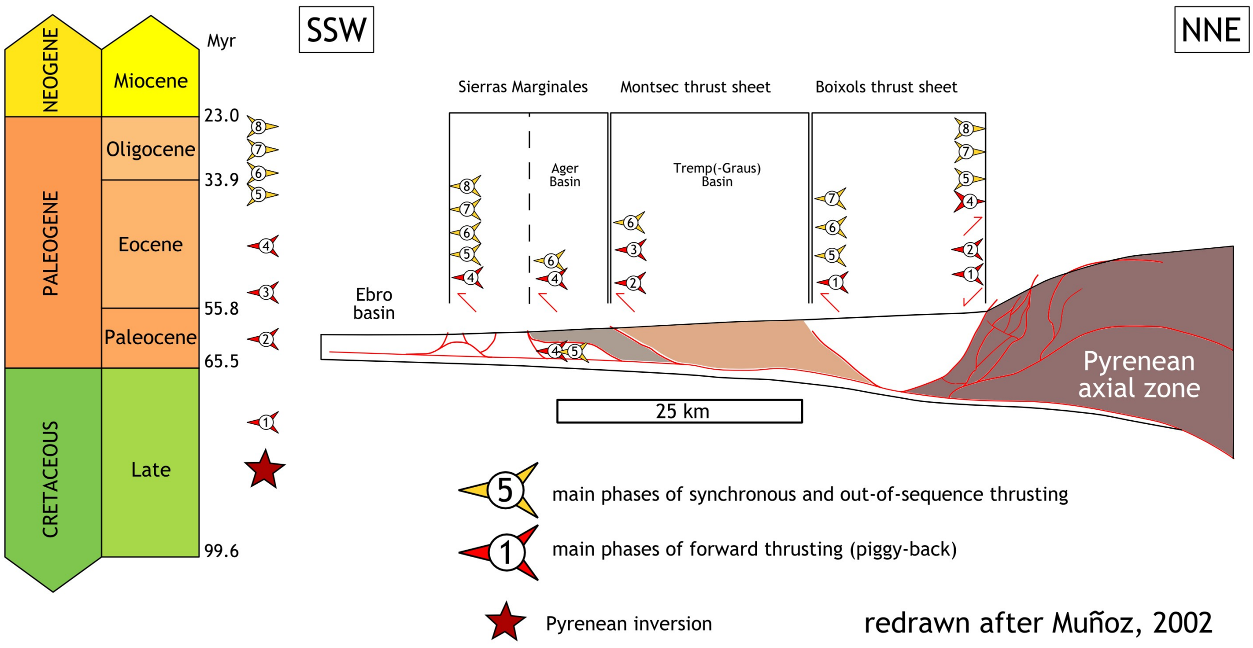

Figure 2.4 – Schematic cross-section (see figure 2.3 for section location) and synthesis of the main stages of thrust propagation in the South-Central Pyrenean foreland; slightly modified.

2.2.1 – Pre-orogenic stages

2.2.1.1 – *Rifting stage*

Permian and Triassic continental successions developed upon a Variscan basement and were subsequently fragmented at the start of the extensional stage related with the North Atlantic rifting. In the iberian peninsula and along the eastern and western plate boundaries, rifting began in the early Triassic, and in the Pyrenean region it brought to the formation of shallow basins bordered by continental areas. Two main stages of rifting, at the Jurassic/Cretaceous boundary and in the late lower Cretaceous, caused crustal thinning and the development of the main pyrenean extensional basins, together with the incipient opening of the Bay of Biscay (Vergés et al., 2002); by the late Albian (end of the extensional regime), a wide marine connection was realized between the tethyan and the atlantic domains. During this stage, carbonate deposition prevailed on both sides of the Pyrenean basin; in the deeper areas occurred the deposition of carbonate turbidites and anoxic sediments.

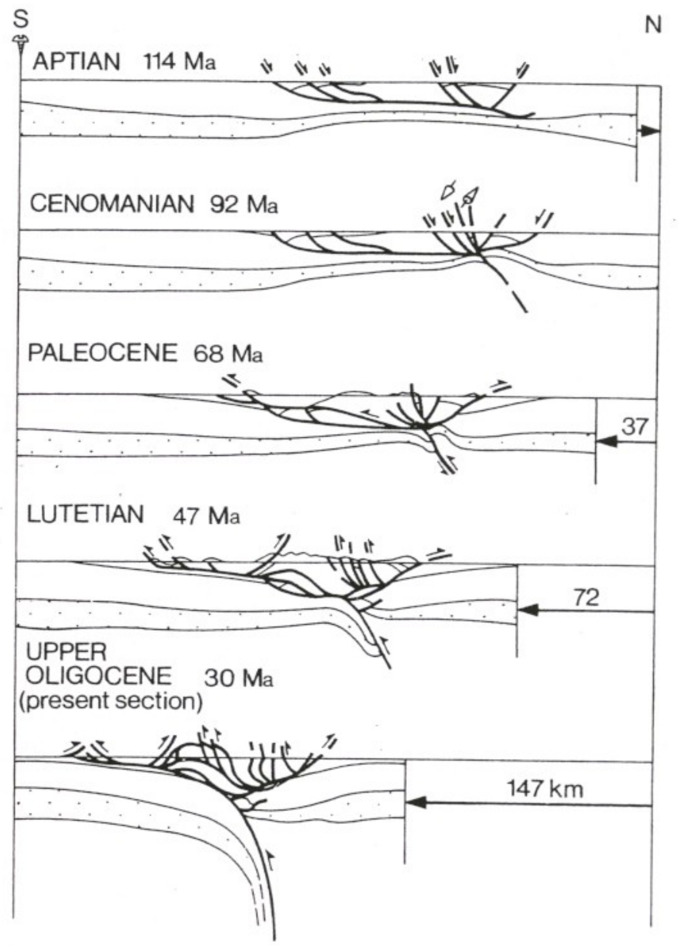

Figure 2.5 - Main stages of the pyrenean orogeny and assessment of the crustal shortening according to Muñoz, 1992

2.2.1.2 – *Intermediate stage*

Between the end of the rifting phase and the switching to a compressional regime, the Iberian plate underwent a ~35° anticlockwise rotation; the main stage of opening of the Bay of Biscay was related to this movement, and the same event drove the setting of transtensional conditions centered along the North Pyrenean Fault, with the associated formation of pull-apart basins, further crustal thinning and magmatism (summarized in Vergés et al., 2002; some authors – e.g. Choukroune et al., 1973, predate the rotation in the Barremian-Albian). A further geodynamic feature emerging from these conditions was a major spreading in the western areas, culminating in the production of oceanic crust, and a lesser evolution of the extensional systems to the east (summarized in Vergés et al., 2002).

2.2.1.3 – *Inversion stage*

The timing of the inversion was diachronous across the Pyrenean basin, and in some cases it anticipated the transtensional stage (Vergés et al., 2002). In the South-Central Pyrenees, starting from the Santonian, growth-faulting and fast sea level rise gave place to a cyclical drowning and backstepping of the carbonate shelves. This trend continued up to the late Santonian; between the late Santonian and the Maastrichtian the inversion had already occurred, as it is testified by deep shelf-margin erosion and chaotic and turbidite sedimentation (Campo Breccia; Puymanons Olistostrome; Vallcarga fm.). Basinal turbidites show a coarsening-upwards trend, and were interpreted by Simó (1986) as a signal of uplift in the source areas or, at least, a hint for increased tectonic activity.

2.2.2 – Syn-Orogenic stages

2.2.2.1 – *Upper Late Cretaceous*

In the Campanian-Maastrichtian interval, shallow water siliciclastics syntectonically buried an incipient Boixols thrust, as it is testified by clear unconformable relationships in the Arén Sandstone Group (Mutti et al., 1994). The Boixols thrust uplift (and the associated western Turbòn thrust) caused a major change in the paleocurrent distribution. Axial directions, that were more likely to occur in the axial portion of the Pyrenean basin, began to characterize this marginal region, and a general south-western direction of transport became at this point dominant. Moreover, the overall shallowing-upwards trend that characterizes the Arén Sandstone Group ultimately resulted in the deposition of a continental succession.

2.2.2.2 – *Early Paleogene*

During the Paleocene (but possibly already in the late Maastrichtian), tectonic stress shifted towards the foreland, and the Montsec thrust began to build up a relief. In this period, the Tremp and Ager basins began to delineate (Rosell et al., 2001); sedimentation was mainly continental in their inner sectors (“Garumnian” or Tremp fm., Mey, 1968), and it was occasionally interrupted by some minor marine ingressions proceeding from the west and causing the deposition of shallow-marine deposits.

A major marine ingression (“Ilerdian transgression”, auctt.) occurred in the earliest Ypresian, flooding both the Tremp and Ager basins, and causing the deposition of thick, shallow-marine successions up to the late Ypresian (Cadì fm./Alveolina Limestones, auctt., Baronia Sandstones fm. Mutti et al., 1972, 1985) , Tendruy fm. (Barberà et al., 1997). Activity of both the Boixols and Montsec thrust is recorded within these strata, and its most evident expression is the development of a strong differential subsidence between the basin margins and the depocentral areas (e.g., Fonnesu, 1984).

In the middle-upper Ypresian, tectonic uplift caused regression and renewal of clastic input (Mutti et al., 1988). As a consequence, the Tremp and Ager basins got overfilled, and continental conditions were met again between the upper Ypresian and early Lutetian (Mutti et al., 1988; Montanana Group, auctt.).

2.2.2.3 – *Late Paleogene*

While the early Paleogene was characterized by a forward-thrusting structural evolution, during the late Paleogene older structures underwent out-of-sequence reactivations. According to most reconstructions, the greatest part of the shortening in the south-Pyrenean foreland occurs during his period (extimates range between 50% and 80% of the shortening; e.g. Muñoz, 1992; Fitzgerald et al., 1999). The stratigraphic expression of this later deformational stage(s) is represented by a major unconformity between early Lutetian and Bartonian to Oligocene deposits (Escanilla and Collegats/Sìs/Pobla de Ségur fm., auctt.). Continental conditions were met in the upper Eocene throughout the whole southern Pyrenean region, including the lower Eocene foredeep sectors of the Ainsa and Jaca basins.

Late Paleogene reactivations also involved the Montsec thrust, and caused the overthrusting of most of the northern sector of the basin. Some problems in the early Paleogene Tremp-Ager correlation actually derive from this later structural developments.

2.3 – Early Paleogene South-Pyrenean allogroups

In the 60's and 70's two main approaches (structural and stratigraphic) were undertaken by researchers in order to unravel the geological history of ancient foreland basins. These two approaches eventually converged in the attempt to define the relationships between tectonics and sedimentation. Concerning the southern Pyrenees, the concepts of “tectono-stratigraphic units” and “allogroups” were applied by Puigdefabregas & Souquet(1986) and Mutti et al. (1988) respectively.

Both constitute regional-scale stratigraphic subdivisions, in part related with classic lithostratigraphic subdivisions and in part based on the presence and significance of major unconformities. Conceptually, allogroups as intended by Mutti et al. (1988) *are* tectono-stratigraphic units, since they are defined as sedimentary bodies enclosed between tectonically-driven unconformities; however, their definition follows more rigorous criteria, such as the possibility of correlating and mapping these units at the regional scale. Moreover, the allogroups of the upper Ypresian and Lutetian were correlated with the turbiditic deposits of the western foredeep located in the Ainsa-Jaca trough, stressing their relationship with cycles of uplift and erosion (Mutti, 1992; Mutti et al., 1988; 2003). In the present work, the nomenclature and subdivisions of the major stratigraphic units are mainly derived from the allogroup subdivisions proposed by Mutti et al. (1988) and further developed by Mutti et al. (1994) and Waehry (1999).

In the following sections, the main surfaces and stratigraphic units will be outlined; reference can be made to **figures 2.6 and 2.9** (although specifically referred to the study area) for comparisons between the discussed units.

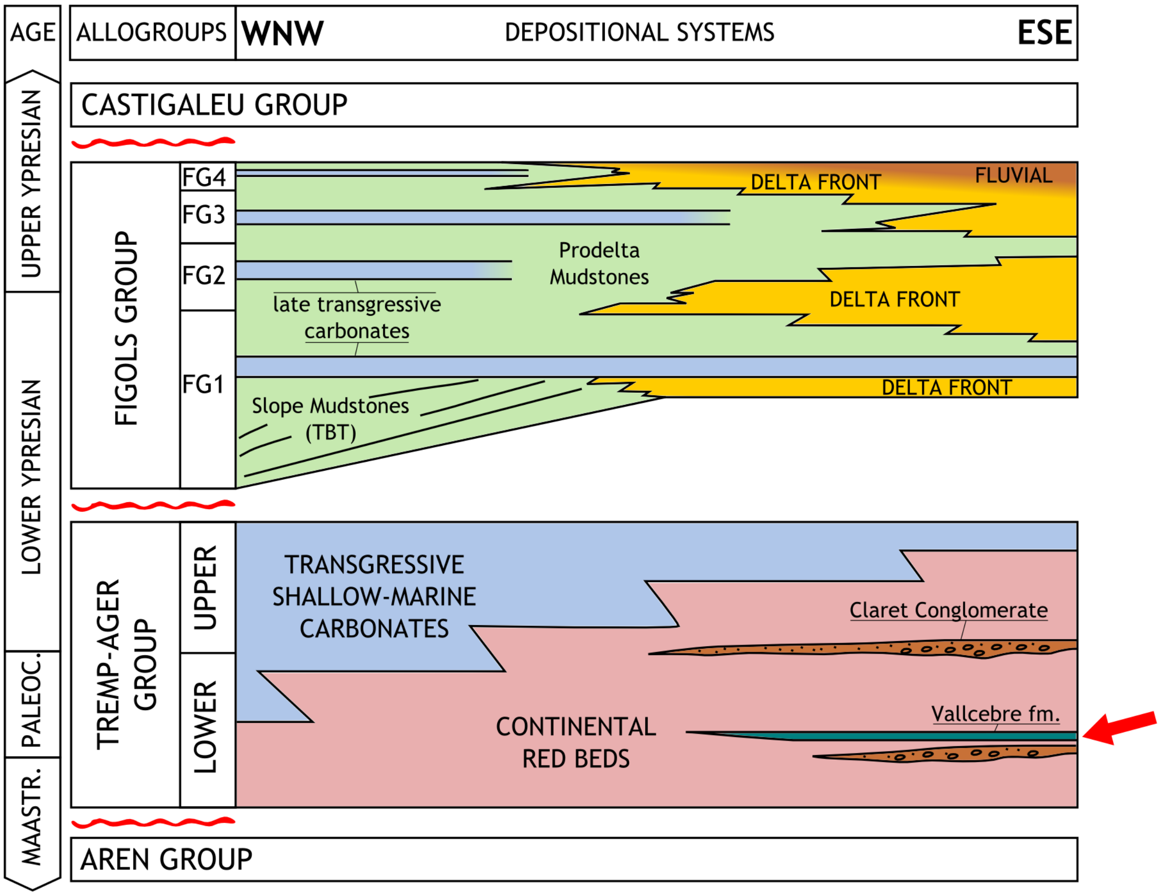

Figure 2.6 - Schematic reconstruction of the main tectono-stratigraphic units considered, in relation with the included depositional systems (redrawn and slightly modified from Mutti et al., 1994); the red arrow indicates the location of the "Middle Paleocene Unconformity" (see in the text below)

2.3.1 – Tremp-Ager Group

The Tremp-Ager Group (Mutti et al., 1988) is a rough definition for a large interval of upper Maastrichtian to lower Ypresian deposits. It is a very large scale unit, probably representing an higher-rank unit, if compared with the other allogroups defined in literature, and it wasn't studied in the same detail. It was divided in a lower, mainly continental unit (Lower Tremp-Ager Group in Waehry, 1999), and an upper, mainly marine unit (Alveolina Limestone Group in Mutti et al., 1988, or Upper Tremp-Ager Group in Waehry, 1999).

2.3.1.1 – *Lower Tremp-Ager group (LTAG)*

Apart from the different litho-stratigraphic subdivisions proposed for the stratigraphic interval represented by the Lower Tremp-Ager Group, (e.g., Liebau, 1973; Eichenseer & Kraus, 1985; Cuevas, 1992), it was studied mainly for chronostratigraphic and paleontological purposes; only a few works (e.g., Sole-Sugrañes 1970; Rossi, 1997; Rosell et al., 2001), deal with problems of physical stratigraphy.

The base of the LTAG is represented by a surface of subaerial exposure at the top of the Arèn Sandstones fm. (Mutti & Sgavetti, 1987; Mutti et al., 1994c), in the Tremp basin.

In the Tremp and Ager basins the LTAG is represented by an up to 1000m-thick succession of continental deposits (mainly paleosols and alluvial deposits, and subordinate continental carbonates), which pass to shallow-marine deposits to the west. Many small and large stratigraphic discontinuities are present within this succession, the most prominent of which develops in the middle Paleocene (Middle Paleocene Unconformity, MPU, after Baceta et al., 2001). In the study area, as well as in the south-eastern Pyrenees, it is recorded within the "Vallcebre fm."(Sole-Sugrañes, 1970; synonim: Millà fm., in Colombo & Cuevas, 1993), an horizon of lacustrine deposits widespread throughout the southern Pyrenean foreland during the Danian; the prolonged lowstand associated with this discontinuity occurred over an area wider than the sole Pyrenean domain (cf. Haq et al., 1988), and caused a hiatus in the study area that can be extimated between 2 and 3 My (Colombo & Cuevas, 1993; Baceta et al., 2001, 2007).

In the southern Ager basin, the MPU is recorded within the karstic horizons located in the upper portion of the Vallcebre fm.; in the Tremp basin, it was placed by Baceta et al. (2011) along an erosional surface slightly above the top of the supposed local equivalent of the Vallcebre fm.

Rosell et al. (2001), although considering the karstic surfaces in the Ager basin to be local features, depict a major unconformity at the K/T boundary, i.e., close to the base of the Vallcebre fm.; this unconformity follows a stage of basin narrowing and abundant fluvial sedimentation, and precedes (or is equivalent to) the onset of a paleo-Montsec high (**figure 2.7**).

Although the two versions disagree (it may even be possible that the MPU and Rosell et al.'s unconformities are actually two distinct events), the close vicinity of the MPU with signals of tectonic uplift may be supported by the E-W diachronicity of the deformation recorded within the Southern Pyrenees (F. Colombo, pers. comm.).

Above the MPU, in the Thanetian (cf. Colombo & Cuevas, 1993), sedimentation remained substantially similar to the Maastrichtian, dominated by paleosols and fluvial deposits; according to the subsidence patterns recognized in the stratigraphy of the southern Ager basin (Colombo & Cuevas, 1993, see **figure 2.10**; Rossi, 1997), during this period the inner anticlines of the Sierras Marginales already acted as structural highs.

A few marine ingressions reached the inner Tremp and Ager basins, the latter being flooded much farther (10s of kms) to the east than the former (e.g. Rossi, 1997), suggesting a structurally-lowered depositional profile in the Ager basin.

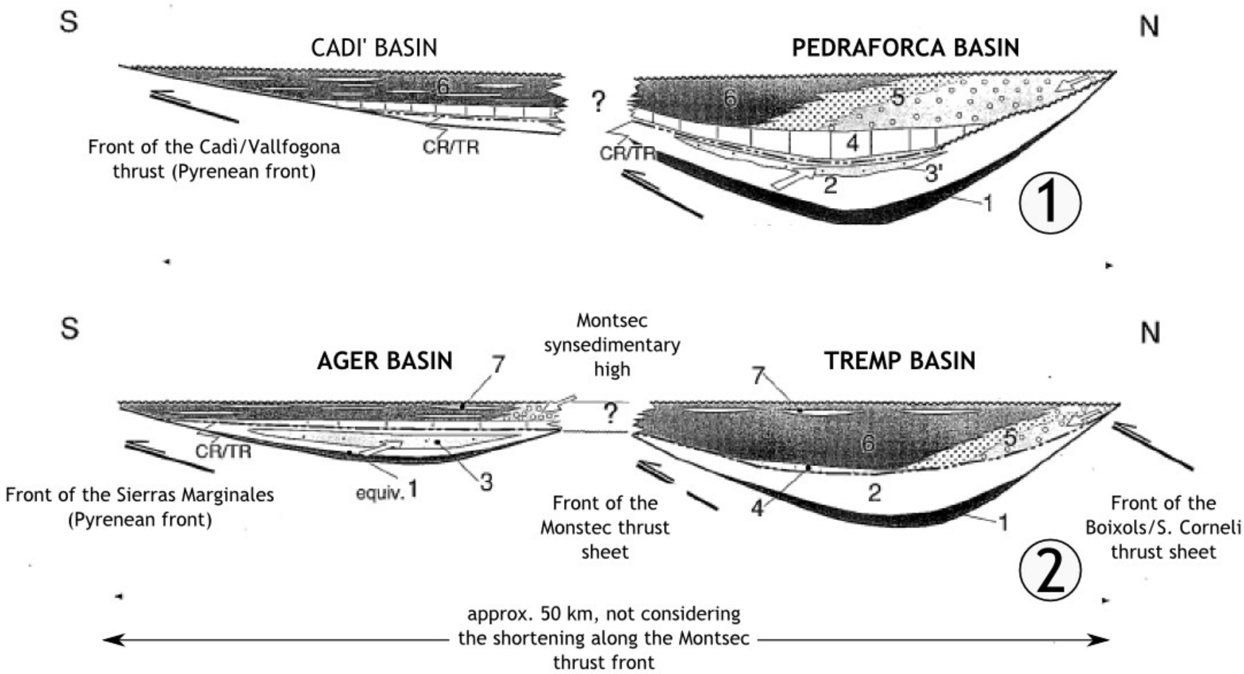

Figure 2.7 - Schematic cross-sections across the eastern (1) and south-central (2) Pyrenees during the deposition of the Lower Tremp-Ager Group, slightly modified from Rosell et al., 2001. See figure 2.1 for the location of the cross-sections; small numbers indicate the following units:

1. "Grey Garumnian" (lagoonal and palustrine deposits);

2., 3., 3'. "Lower Red Garumnian" (fluvial and alluvial deposits): 2. Red paleosols and subordinate fluvial deposits; 3, 3'. Braided stream fluvial deposits;

4. Vallcebre limestones and their lateral equivalents;

5., 6., 7. "Upper Red Garumnian": 5. Pebbly and sandy alluvial fans; 6. paleosols and lacustrine limestones; 7. Evaporites;

CR/TR: "Colmenar-Tremp horizon" (Eichenseer & Krauss, 1985), a regional keybed related with the Vallcebre fm. and the Middle Paleocene Unconformity (Baceta et al., 2011)

2.3.1.2 – *Upper Tremp-Ager group (UTAG)*

The boundary between the LTAG and the Upper Tremp-Ager group is marked by the widespread occurrence of a conglomerate unit ("Claret Conglomerate", auctt.) below the base of the shallow marine, mostly carbonatic deposits of the Ilerdian transgression. In some papers it is reported the existence of a relevant hiatus at its base (e.g., Serra-Kiel et al., 1994), and many agree on its interpretation as a lowstand deposit (eg., Eichenseer & Luterbacher, 1992; Mutti et al., 1988; Waehry, 1999).

Within the UTAG, a largely syntectonic succession developed in a shallow-marine environment. Growth strata and angular unconformities are reported within early Ypresian marine deposits in the whole south-Pyrenean domain (Fonnesu, 1984; Mutti et al., 1988; Meigs, 1997; Barberà et al., 1997). In the northern sector of the Tremp basin (Arèn-Iscles region) a major tectonic unconformity formed during the early phases of the Ilerdian transgression (Fonnesu, 1984).

The sedimentary succession included within the UTAG is characterized by an overall transgressive trend, as suggested by changes in faunal compositions (e.g., Eichenseer & Luterbacher, 1992). Within this general pattern, minor oscillations in the relative sea-level were recognized in high-resolution sequence-stratigraphic investigations in the Tremp basin (Fonnesu, 1984; Waehry, 1999; Angella, 1999).

With the exception of its basal interval, developed in a continental environment, UTAG sediments are mainly represented by carbonates of the Cadì/Alveolina Limestone fm.

In the Ager basin, as well as along the Tremp basin's margins, this unit is dominated by calcarenites, mainly composed of foraminifers and mollusks, (Mutti et al., 1972, 1973; Luterbacher, 1970), and subordinate coralline and foraminiferal boundstones (Plaziat & Perrin, 1992; Eichenseer & Luterbacher, 1992); in the Ager basin, tidal processes controlled sedimentation, while in the Tremp basin they were uncommon or less significant for carbonate buildup (Mutti et al., 1972, 1973).

In the axial sectors of the Tremp basin, the UTAG is instead dominated by a delta-front muddy succession (Tendrui fm. in Barberà et al., 1997), that is lateral and interbedded between the carbonate banks forming along the uplifted southern basin margin represented by the paleo-Montsec high (Guardia, Estorm and Alsina members of the Tendrui fm., Barberà et al., 1997, FIG). Coarse siliciclastics developed in the lower portion of the Tendrui fm. (base of Puigmaçana-Serrat de Cal Senàs depositional system in Fonnesu, 1984; estuarine channels in the Aransìs-Sant-Salvador de Toló sector, Eichenseer & Luterbacher, 1992). Siliciclastic (or mixed carbonate-siliciclastic) deposits are present also in the Ager UTAG, although they were observed in its upper part (Mutti et al., 1994, see “stop descriptions”). A relationship between these events in the two basins is anyway possible due to a major condensed succession or hiatus located in the upper part of the UTAG in the Ager basin, as it is suggested by biostratigraphic data (Ferrer et al., 1973; see **2.5.3**).

The top of the UTAG, as defined in Mutti et al. (1994) and Waehry (1999), corresponds with a regressive surface, associated with an angular unconformity in the Ager basin (Mutti et al., 1985, 1988) and in the southern Tremp basin (Barberà et al., 1997).

The UTAG in the Tremp basin was subdivided by Waehry (1999) in four “large scale sequences”, roughly equivalent to 4th order sequences (s*ensu* Vail et al., 1977), each composed by a variable number of medium to elementary depositional sequences (*sensu* Mutti, 1992, and Mutti et al., 1994); these were inferred to have formed under a cyclical, climate-forced control in the eccentricity (~100 ky) and precessional (~20 ky) ranges respectively.

2.3.2 – Figols Group

The Figols Group (*sensu* Mutti et al., 1994) records an interruption in the early Ypresian transgressive trend, and a shift in sedimentation to more terrigenous and/or coarser compositions. This change is a consequence of progressive basin narrowing, and uplift in the source areas (particularly in the Pyrenean Axial Zone). These factors contributed to a gradual infilling of the inner portion of the south-central pyrenean basins, that in the late Ypresian cause the permanent retreat of the sea (Castigaleu Group; Mutti et al., 1988).

The Figols Group was subdivided in four sequences by Mutti et al. (1994); Waehry (1999) chose to distinguish a Lower Figols Group, equivalent to the Figols 1 sequence, and an Upper Figols Group, equivalent to the Figols 2, 3 and 4 sequences, in order to stress the “transitional” character of the LFG, still affected by dominantly transgressive conditions, from the UFG where uplift prevailed over the sea level rise.

2.3.2.1 – *Lower Figols Group (LFG)*

Depending on the location within the Tremp and Ager basins, the UTAG/LFG boundary may display different features.

In the Tremp basin it is represented by a lithological change (sudden coarsening and thickening of sandstone beds; Serra-Puit depositional system in Fonnesu, 1984), associated with a transitional faunal change from a *Nummulites*-dominated to an *Alveolina*-dominated foraminiferal assemblage. Angular relationships associated with this boundary may be observed in a few locations along the southern margin of the basin (e.g., Barberà et al., 1997). In this sector, as well as in the south-western and northern sectors of the Ager basin, these angular relationships are expressed by the onlap of the Lower and Upper Figols beds on a tilted carbonate ramp belonging to the UTAG (Mutti et al., 1985).

The Lower Figols Group in the Ager basin is clearly represented by the succession of hybrid arenites (*sensu* Zuffa, 1980) and sandy mudstones of the Lower Baronia Sandstone (Mutti et al., 1985). Similarly to the UTAG deposits, these LFG deposits formed under the activity of strong tidal currents (Mutti et al., 1973, 1985); also in the Tremp basin, the LFG's lithologies and facies bear many similarities to the ones of the UTAG: they are represented by prevalently deltaic sandy and muddy deposits (Tendruy fm.) in the axial sector, and by shallow-water carbonate banks in the southern marginal sector ("Eroles" and S. Llucia mbs. – *sensu* Barberà et al., 1997).

The top of the Lower Figols Group can be easily recognized in the Ager basin, because it corresponds to the base of the Middle Baronia Sandstone (Mutti et al., 1985; Mutti et al., 1988), a thick and relatively coarse package of estuarine sandstones. The abrupt lithological change represented by this unit is also associated with channel erosion in the deposits of the Lower Baronia Sandstone in the south-western sector of the basin (Mutti et al, 1985). In the Tremp basin, because of problems of exposure, and lower chronostratigraphic resolution in the Upper Ypresian deposits, the recognition of a sharp boundary is more complicated. In the present work, the chosen boundary is slightly lower than the one chosen by Waehry (1999), being equivalent to the base of the "Alinya sequence" according to Eichenseer & Luterbacher (1992; cf. **Figure 2.9**).

According to this description, the LFG is composed of two "large scale sequences" (sensu Waehry, 1999; see **2.3.1.2**), each composed by five "medium scale sequences".

In the Ager basin, the LFG was subdivided in up to seven elementary depositional sequences (Ghielmi, 1991). This subdivision raises a problem in the relative significance of the EDS, as defined in the LFG of the Ager basin (see Mutti et al., 1994, 2000), with the "large" and medium scale sequences of the Tremp basin, and generally on the relative chronology of the two basins; high-resolution correlations, however, must be handled carefully between different basins, and may be critically hampered by the paucity of chronostratigraphic data in the Ager basin.

2.3.2.2 – *Upper Figols Group (UFG)*

The Upper Figols Group is composed of three main sequences ("very large scale sequences" in Waehry, 1999; FG2, 3 and 4 in Mutti et al., 1994), that represent the gradual fill of the basins operated by deltaic systems, culminating in the lower Cuisian (middle-upper Ypresian) with the compensation of the paleo-Montsec high and the intercommunication of the Tremp and Ager basins (FG4 sequence; Angella, 1999; Calabrese, 1999).

The basin overfill that occurred during the formation of the UFG was primarily driven by tectonics, as it is testified by the arkosic composition of its sandstones; this composition records the renewal of clastic input from the Pyrenean Axial Zone (Fonnesu, 1984).

2.4 – The Study Area and Interval: units, surfaces and problems

The Tremp and Ager basins were studied in the eastern sector of the South-Central Pyrenean Unit (**2.1.3**), i.e. in the sector included within the Rio Noguera Pallaresa and the Rio Noguera Ribagorçana. They are located in the Pallars Jussà and Noguera districts of the Llleida province (Catalunya, Spain). The classic outcrops of these basins are located in this area, that provides thick and laterally extensive exposures. The study area is represented in the map of **figure 2.8**.

The Tremp basin is structured as a gentle syncline, with its axis displaced to the south, where the hangingwall of the Montsec thrust rapidly ramps up due to a late Paleogene reactivation. Many gentle synclines and anticlines can be traced in a longitudinal and transversal direction (cf. Barberà et al., 1997). Some of these structures probably acted as synsedimentary features since the late Cretaceous through the late Paleogene (de Boer et al., 1991; Vincent, 2001; Fonnesu, 2011).

The Ager basin is structured as a strongly asymmetric syncline, with a northern thinned margin, only partially exposed, and a southern expansive sector (depocentral or peri-depocentral). This asymmetry is originally caused by northern uplift (initial activity of the Montsec thrust) and southern subsidence, and enhanced by the development of an onlapping Ypresian succession over a tilted early Ypresian carbonate ramp (Mutti et al., 1985). Late Paleogene reactivations of the Montsec thrust caused a further narrowing of the syncline; minor structures formed in the northern sector, hiding, disarticulating or removing a substantial portion of the Maastrichtian and Paleocene in this sector.

The studied stratigraphic interval is focused on the Lower Ypresian Upper Tremp-Ager and Lower Figols groups, but in the Ager basin it was extended in the Paleocene down to the Middle Paleocene Unconformity (**2.3.1.1**).

Figure 2.9 collects the stratigraphic subdivisions proposed in the former works discussed in this text; the adopted subdivision will be treated in chapter **6**. They encompass both lithostratigraphic and physical-stratigraphic units, that will be described in the next chapter, and their comparison is intended for reference purposes.

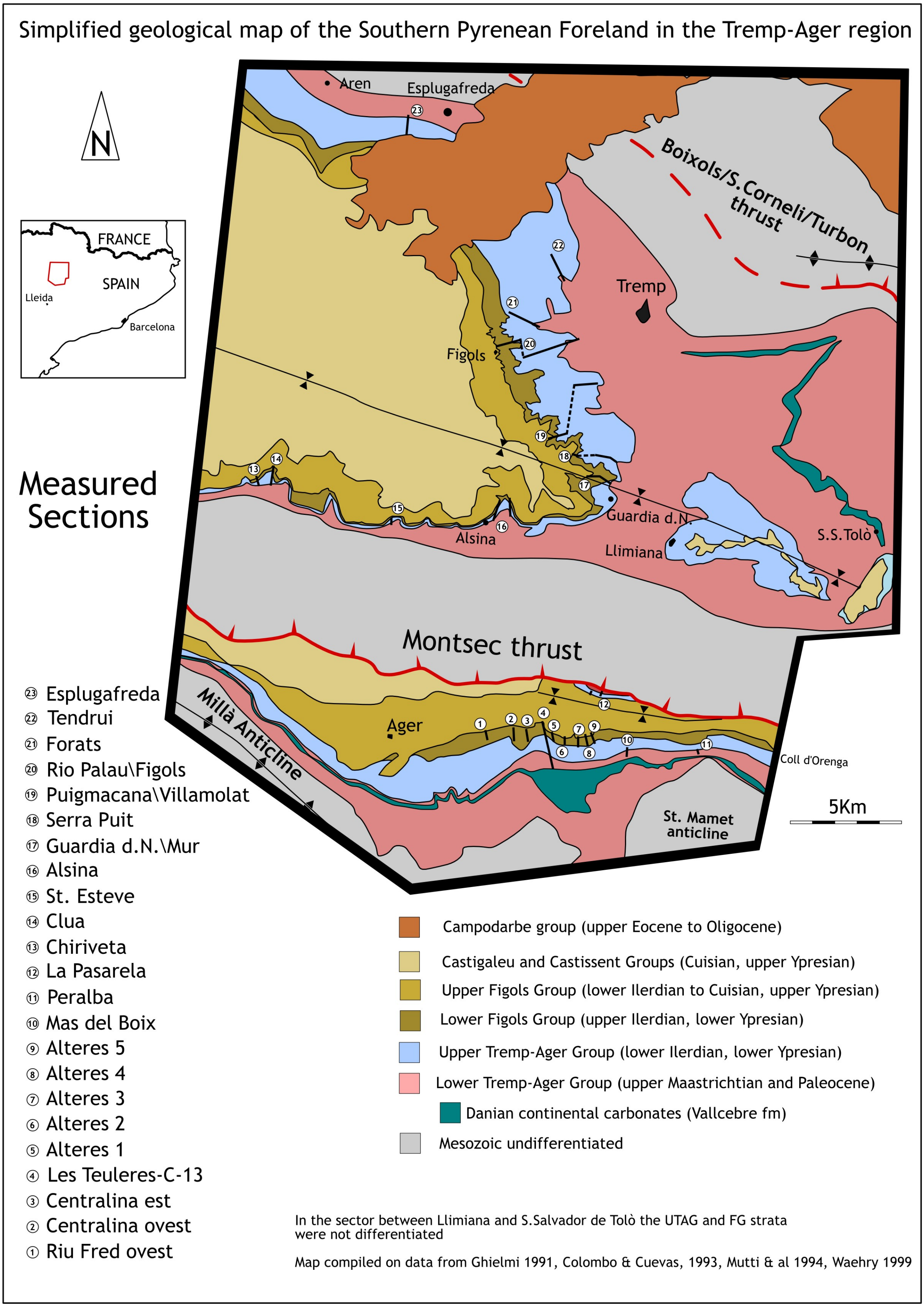
Simplified geological map of the Southern Pyrenean Foreland in the Tremp-Ager region
N
FRANCE
SPAIN
Lleida
Barcelona
Measured Sections
㉓ Esplugafreda
㉒ Tendrui
㉑ Forats
⑳ Rio Palau\Figols
⑲ Puigmacana\Villamolat
⑱ Serra Puit
⑰ Guardia d.N.\Mur
⑯ Alsina
⑮ St. Esteve
⑭ Clua
⑬ Chiriveta
⑫ La Pasarela
⑪ Peralba
⑩ Mas del Boix
⑨ Alteres 5
⑧ Alteres 4
⑦ Alteres 3
⑥ Alteres 2
⑤ Alteres 1
④ Les Teuleres-C-13
③ Centralina est
② Centralina ovest
① Riu Fred ovest
Aren
Esplugafreda
Boixols/S.Corneli/Turbon thrust
Tremp
Figols
Guardia d.N.
Alsina
Llimiana
S.S.Tolò
Montsec thrust
Millà Anticline
Ager
Coll d'Orenga
St. Mamet anticline
5Km
Campodarbe group (upper Eocene to Oligocene)
Castigaleu and Castissent Groups (Cuisian, upper Ypresian)
Upper Figols Group (lower Ilerdian to Cuisian, upper Ypresian)
Lower Figols Group (upper Ilerdian, lower Ypresian)
Upper Tremp-Ager Group (lower Ilerdian, lower Ypresian)
Lower Tremp-Ager Group (upper Maastrichtian and Paleocene)
Danian continental carbonates (Vallcebre fm)
Mesozoic undifferentiated
In the sector between Llimiana and S.Salvador de Tolò the UTAG and FG strata were not differentiated
Map compiled on data from Ghielmi 1991, Colombo & Cuevas, 1993, Mutti & al 1994, Waehry 1999

Figure 2.8

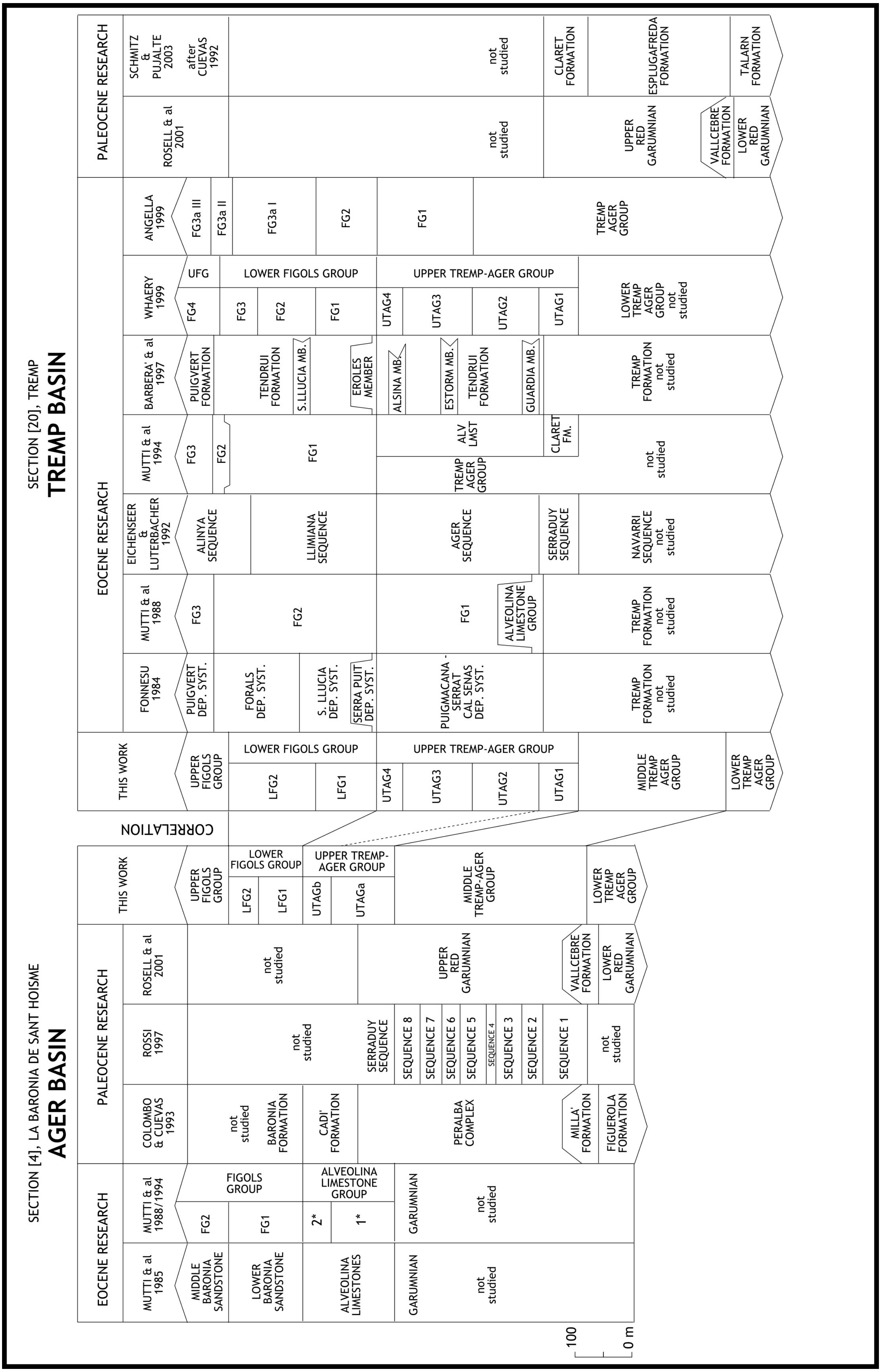

*Figure 2.9. The units and correlations applied in the present work are discussed in chapters **4, 5, 6***

2.4.1 Paleocene of the Ager basin

It was studied in the area east of the Rio Noguera Pallaresa, between the villages of La Baronia de San Hoisme and Peralba (sections [4] and [10]), and in the small roadcut exposure close to the Ager-Tremp-Balaguer crossroad (section [12]).

The maximum thickness (~400 m) reached in the Ager basin by Paleocene deposits is observed in the sector between the Millà and St. Mamet anticlines (cf. Colombo & Cuevas, 1993; **figure 2.10**). This trough, or more subsident sector, was considered by Rossi (1997) to be the ancestral expression of a tear fault between the two anticlines, and is a persistent morphological feature of the Ager basin throughout the whole Paleocene and lower Eocene.

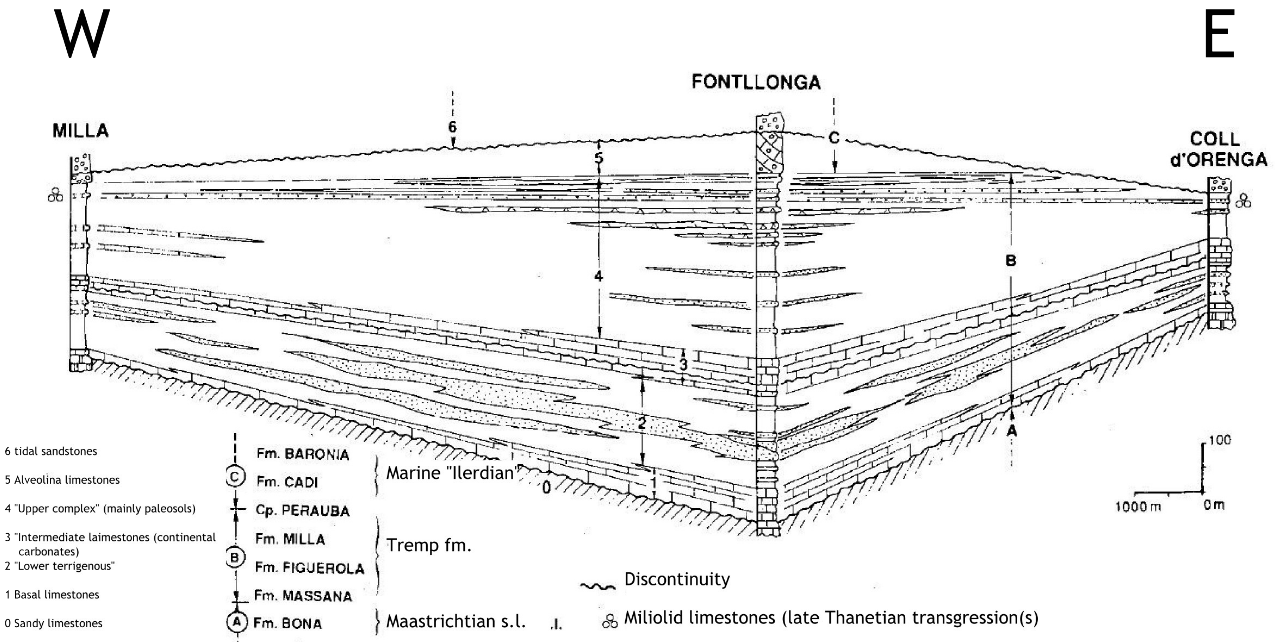

Figure 2.10 – Stratigraphy of the Tremp fm. in the southern flank of the Ager syncline (from Colombo & Cuevas, 1993, slightly modified). The base of the Paleogene is roughly located below the base of the "Millà fm." (= Vallcebre fm.).

During the Danian, this sector is one of the south-Pyrenean depocenters of the lacustrine Vallcebre fm. (Millà fm. in Colombo & Cuevas, 1993), here exceeding 50m in thickness. It is represented by a package of decimetric to metric layers of blue-grey to pink micrites, with abundant carophytes. Some layers of micritic breccia and at least one horizon of pedogenization (cf. FIG) – possibly representing the major discontinuity related with the MPU – are located within its upper part; silica nodules and Microcodium bioerosion are also common.

Rosell et al. (2001) suggest the presence of this unit in the northern Ager basin (cf. **figure 2.7**).

In facts, the base of the "Garumnian" continental succession in this sector is represented by a ~7m-thick white-pink micrite unit with micrite breccia horizons.

Above the Vallcebre fm., a succession of paleosols and fluvial deposits builds up for ~300 m in the southern sector (Peralba Complex in Colombo & Cuevas, 1993). In the upper portion of the Complex, fluvial deposits are unfrequent; lacustrine ("playa-lakes") to evaporitic and shallow-marine deposits are instead more common. In the late Thanetian, a few events transgressive events affect the western Ager basin, the latter of which actually floods the whole southern basin up to the Coll d'Orenga region (Colombo & Cuevas, 1993; Rossi, 1997). A further fall of the relative sea-level, and the development of continental deltaic sandstone bodies (equivalent to the "Claret Conglomerate; see **2.3.1.2** and **2.4.3.1**; Sole-Sugrañes, 1970; Rossi, 1997) indicates the passage to the UTAG.

In the northern Ager basin, this same boundary is marked by a sharp angular unconformity between continental deposits (of undetermined, but supposedly Paleocene age, following Rosell et al., 2001) and early Ypresian shallow-marine deposits (Ferrer et al., 1973).

2.4.2 – Paleocene of the Tremp basin

Despite the great number of exposures of this interval, only in a few places continuous sections can be studied; actually, most published researches describe this interval in very general terms. Amongst the most relevant papers on the Tremp fm. are the ones from Rosell (1965), Liebau (1973) and Eichenseer & Krauss (1985) and Cuevas (1992; **figure 2.11**).

The most continuous Paleocene exposure is represented by the Esplugafreda section (section [23], northern Tremp basin). It was recently reviewed by Pujalte & Schmitz (2005) and Baceta et al. (2011; **figure 2.12**), in their attempt to correlate the continental deposits of the inner Tremp basin with the marine Paleocene in the outer Tremp basin (Rio Esera sector), and with the coeval carbonate shelves in the Basque country.

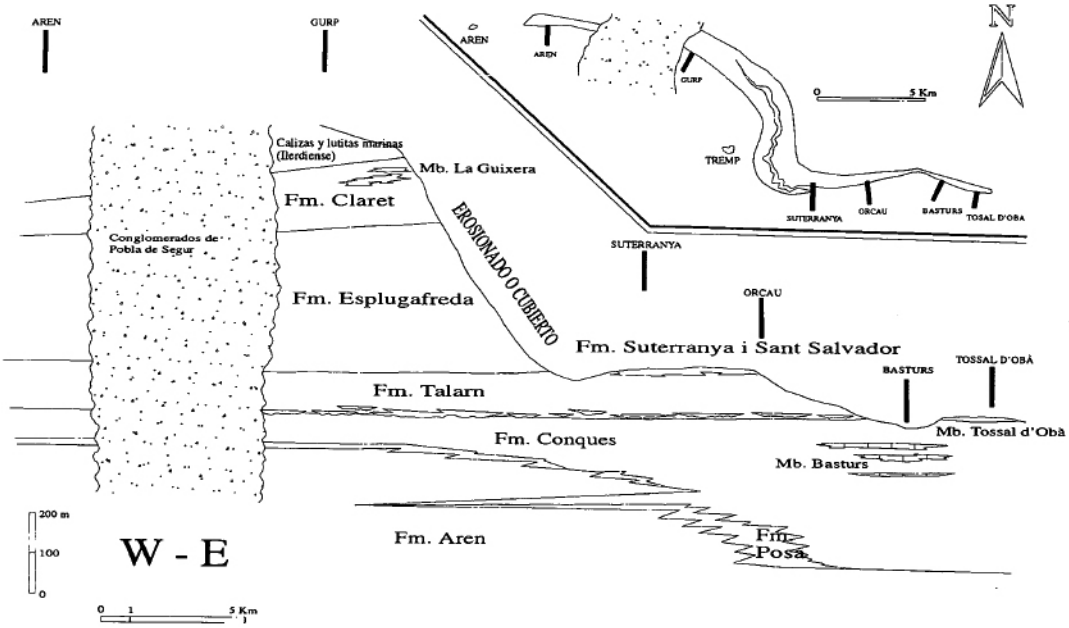

Figure 2.11 – Lithostratigraphic cross-section of the Tremp fm in the Tremp basin (according to Cuevas, 1992). The base of the Paleogene is located within the "Talarn fm."; the "Suterranya y Sant Salvador fm." is equivalent of the Vallcebre fm.

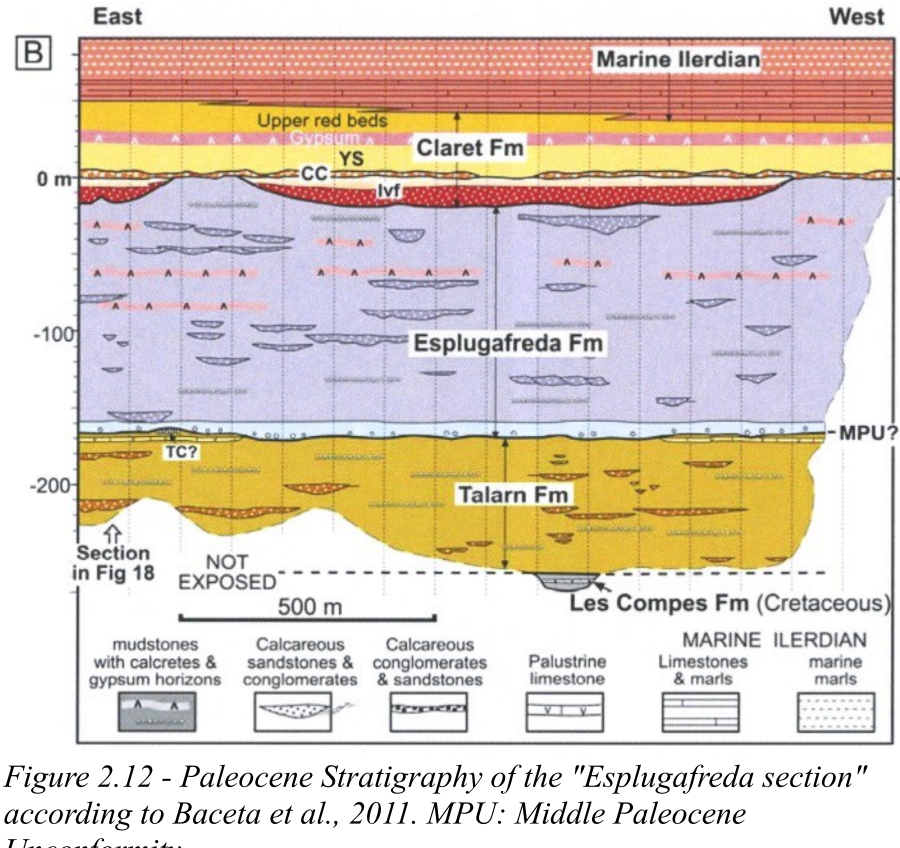

Figure 2.12 - Paleocene Stratigraphy of the "Esplugafreda section" according to Baceta et al., 2011. MPU: Middle Paleocene Unconformity

2.4.3 – The Claret Conglomerate and the Ilerdian transgression

Before introducing the early Ypresian successions of the Tremp and Ager basins, a few words must be spent for these two relevant horizons, because of their physical-stratigraphic and chronological significance.

2.4.3.1 – *The Claret Conglomerate and the Paleocene/Eocene boundary*

The Claret Conglomerate *s.s.* is a widespread composite sedimentary body composed of polymictic conglomerates and sandstones, developed at the southern border of the Boixols/Turbòn thrust front (**figure 2.13**). It reaches a maximum thickness of 6-7 m in the Claret (base of section [20] in the present work) and Esplugafreda exposures, and thins out to the south and west. It was either interpreted as a lowstand, flood-dominated fluviodeltaic deposit (Angella, 1999; Mutti et al., 2000), or as an highstand alluvial fan deposit (Pujalte & Schmitz, 2005); the latter authors, agree anyway on the fact that, at least locally, its base coincides with a major sequence boundary (i.e., the LTAG/UTAG boundary).

In the axial sector of the Tremp basin, this unit rapidly pinches out and disappears south of the Rio Palau. In the innermost sector of the basin (San Salvador de Toló/S. Martì de Barcedana) and along its southern margin, a relatively continuous sandstone body, exposed a few meters below the first marine Ypresian deposits, was picked for correlation by Eichenseer & Luterbacher (1992) and Waehry (1999), and it was considered an equivalent of the Claret Conglomerate.

In the southern Ager basin, Sole-Sugrañes (1970) established a correlation of the sequence boundary associated with the base of the Claret Conglomerate with a similar, "deltaic siliciclastic body" (in Rossi, 1997). This unit as well is the latest and more diffuse siliciclastic body formed before the Ilerdian transgression.

Aside from the physical-stratigraphic significance of the Claret Conglomerate, this has become a key-layer also for chronostratigraphic investigations. Schmitz & Pujalte (2003, 2007, and Pujalte et al., 2009b; **figure 2.14**) discovered evidence for the carbon isotopic excursion associated with the Paleocene-Eocene Thermal Maximum (see **5.2.1**) in the paleosols bounding the Claret Conglomerate. The onset of this extreme climatic anomaly, a possible driver – or enhancer – of the formation of the Claret Conglomerate, is the main criteria for the location of the P/E boundary. It is not clear whether this phenomenon started before or during the deposition of the conglomerate, but data from Domingo et al. (2009; **figure 2.14**) seem to support a consequential relation between the climatic event and the lithological change.

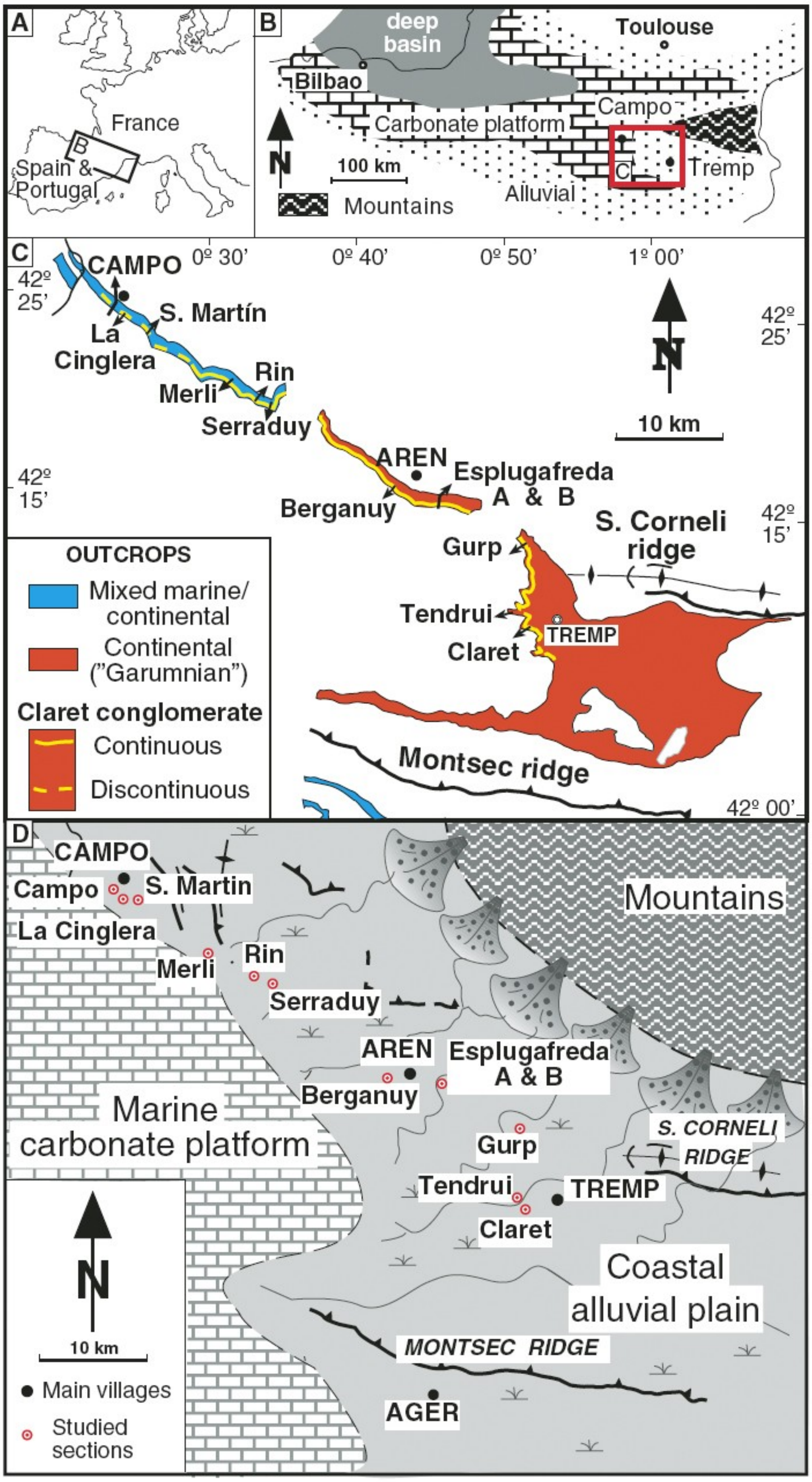

Figure 2.13 – Location of the Claret Conglomerate within the Tremp fm. in the Tremp basin, and paleogeographic reconstruction; from Schmitz & Pujalte, 2007

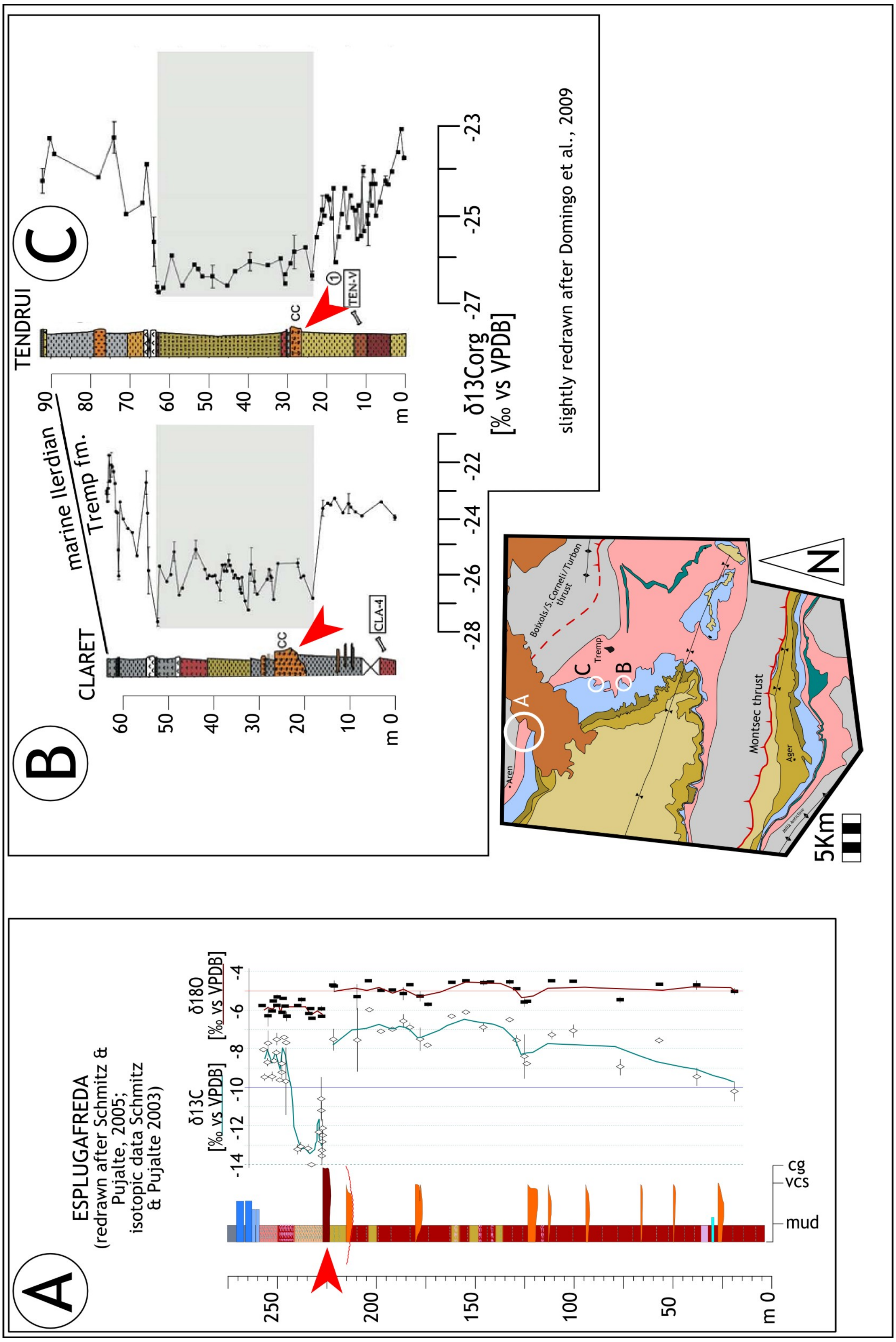

Figure 2.14 - Isotope stratigraphy of the Paleocene and basal Eocene in the Tremp basin; A: data from carbonate soil nodules; B, C: organic matter data. References included within the image.

A further problem, concerning the relationships between the Claret Conglomerate and the PETM, is the possible presence and magnitude of a hiatus, reported by Serra-Kiel et al. (1994) at the base of the Claret Conglomerate. Pujalte et al. (2003) found evidence for a minor amplitude of this hiatus in the western Tremp basin; the problem, anyway, would be overcome by an alternate positioning of the major sequence boundary in that range (i.e., the LTAG/UTAG boundary); this solution was proposed by Pujalte & Schmitz (2005). In the authors' interpretation, this boundary would be expressed by a lowstand incision ("incised valley") they recognize both in the Esplugafreda and Claret exposure; the Claret Conglomerate would be the terminal, highstand infill of this incision.

2.4.3.2 – *The Ilerdian transgression*

In the late PETM, evaporitic deposits formed in patches in the Tremp and Ager basin. A short time later, the Ilerdian transgression broke through the Tremp and Ager basins in the earliest Ypresian (cf. Hottinger, 1960; Eichenseer & Luterbacher, 1992; Pujalte et al., 2009b) and abruptly flooded the whole south-Pyrenean domain. This event is recorded throughout the whole peri-Tethyan domain.

The name "Ilerdian" refers to a local stage (although of Tethyan recurrence) that has both biological and lithological significance (see 2.5.2.1). The "Tremp section" (section [20] in the present work) represents its stratotype (cf. Eichenseer & Luterbacher, 1992, and references therein).

The Ilerdian transgression proceeds from west to east; in the Ager basin, it is heralded by the development of a relatively thick lacustrine succession, suggesting an initial rise of the base level. Something similar occurs in the Tremp basin, with a vertical transition from calcimorph paleosols above the Claret Conglomerate to "gley" paleosols and palustrine mudstones (Eichenseer & Luterbacher, 1992).

In the study area, the marine ingression is testified by the diffusion of lagoonal carbonate and subordinate muddy deposits, characterized by miliolids- and alveolinae-dominated faunal compositions.

2.4.4 – Lower Ypresian of the Ager basin

Lower Ypresian deposits, encompassing the UTAG and LFG allogroups, are exposed in the southern limb of the Ager syncline (sections [1] to [11]) between Millà and Villanova de Meià, and in a small sector along the northern limb (roughly centered at the Ager-Tremp-Balaguer crossroad)

In the most subsiding sector of the Ager basin (section [4]), above the initial Ilerdian transgression, a ~50m-thick succession of tide-influenced shallow-water calcarenites (Alveolina Limestones or Cadì fm, auctt.) builds up in an overall deepening-upwards trend (Ferrer et al., 1973; Mutti et al., 1973, 1985, 1988, 1994; Colombo & Cuevas, 1993). This succession was never studied in great detail, because most of it is exposed along steep cliffs; some unpublished or partially published works (e.g., Ghielmi, 1992; Rubino et al., 1985) marginally deal with its uppermost interval. In facts, that is a problematic issue of the Ager basin's succession, as suggested by Mutti et al. (1994, "stop descriptions"). As anticipated (**2.3.1.2**), within the upper ~20m of the calcarenitic succession, evidence for general transgressive to highstand conditions (Mutti et al., op.cit.) is accompanied by the input in the basin of east-sourced terrigenous materials (Rubino et al., 1985, and E. Mutti, pers. comm.), possibly associated with a sequence boundary (Mutti et al., 1988; cf. **figures 2.17** and **2.19**; lower boundary of "UTAG b" unit), and substantially heralding the passage to the Figols Group. The interpretation of this interval is further complicated by the apparent presence of a condensed interval, or a large hiatus within it (see **2.5.3**).

The northern succession (section [12]) of the Alveolina Limestones is similar in thickness and composition to the southern one, although some problems in their correlation are still unsettled.

First, it is included within two angular unconformities (Mutti et al., 1985, 1988), both of which are likely to be associated with a major hiatus in that location; secondly, chronostratigraphic control is almost missing (with the exception of its lowermost interval, at least partly coeval with the early stage of the Ilerdian transgression – Ferrer et al., 1973); and finally, the exposure is so limited that depositional geometries can be barely appreciated.

A significant observation, reported by Mutti et al. (1985, 1988; **figure 2.18**), concerns the presence of pebbly horizons (in some cases true conglomeratic layers) interbedded within the lower limestone bodies, and interpreted as Montsec-sourced alluvial fan deposits fringing in the shallow waters of the early Ypresian shelf.

The top of the Alveolina limestones, througout the whole Ager basin, is unconformably overlain by onlapping Figols deposits (**2.3.2.1** and **figures 2.15**, **2.16**, **2.18**, **2.19**). These are represented by the tide-dominated deltaic succession of the Baronia sandstones (**figure 2.17**) and their carbonate equivalents in the south-western sector of the basin (Mutti et al., 1985, Rubino et al., 1985; Ghielmi, 1991; Mutti et al., 1994; Angella, 1999; Calabrese, 1999).

According to the original paper from Mutti et al., the Baronia sandstones accumulated for almost 500m after a deformational stage that critically transformed the basin, and formed (or enhanced) a relief in the northern and southern sectors. This caused the Figols strata to accumulate unconformably on a tilted carbonate shelf (onlap).

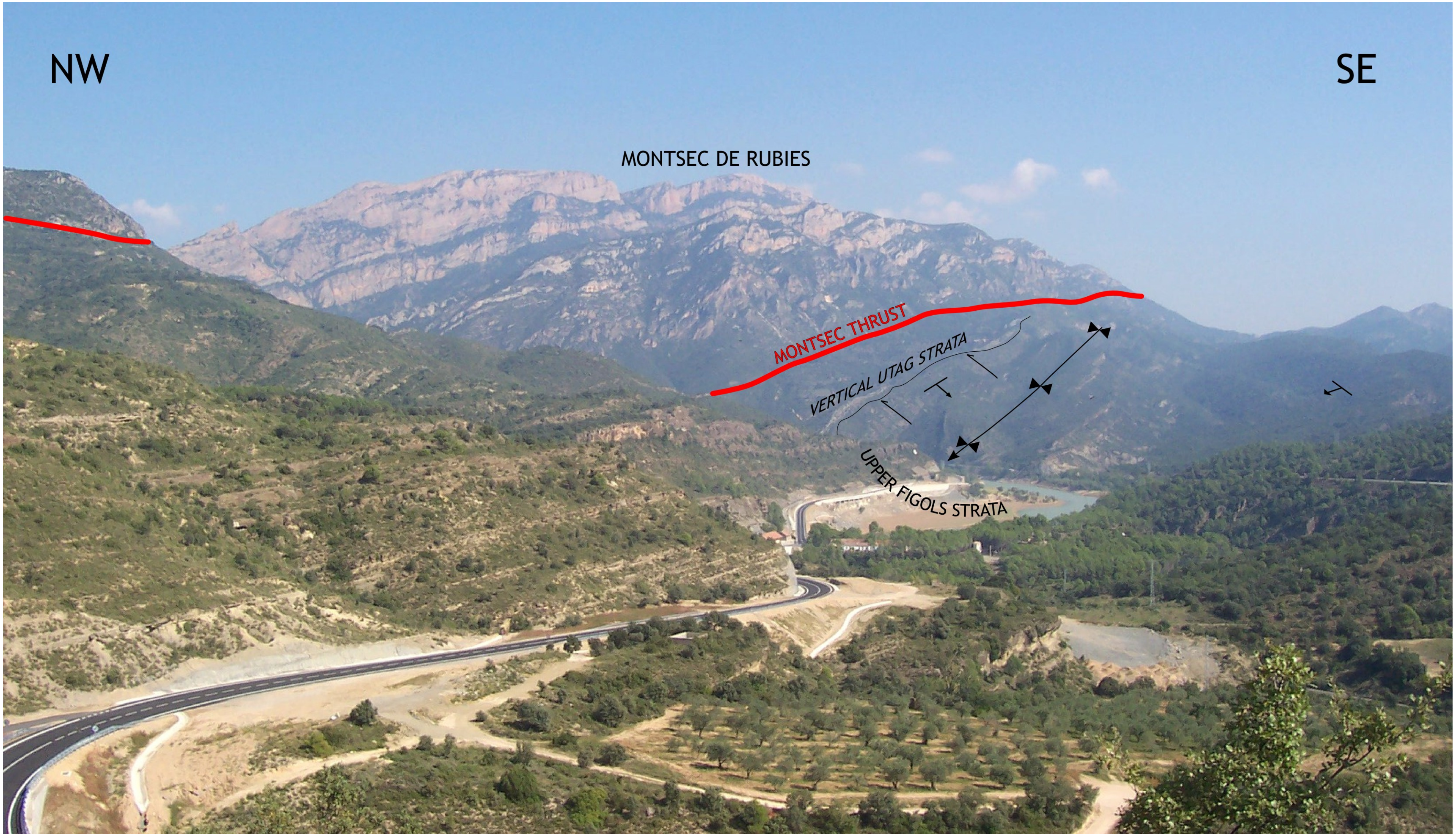
NW
SE
MONTSEC DE RUBIES
MONTSEC THRUST
VERTICAL UTAG STRATA
UPPER FIGOLS STRATA

Figure 2.15 (former page) – Panoramic view of the Ager syncline; compare with figures 2.16 and 2.17

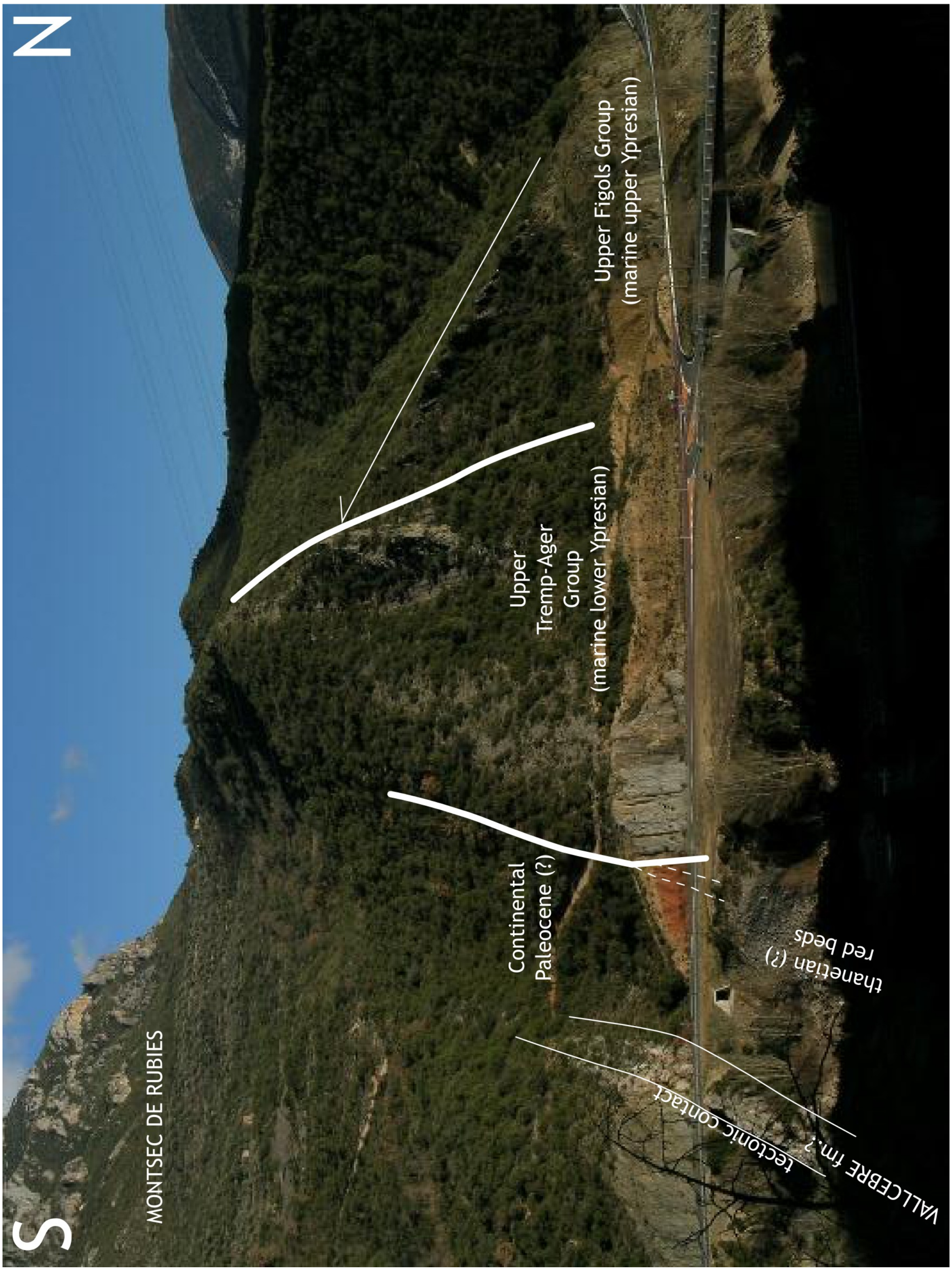

Figure 2.16 – Panoramic view of the "Pasarela" exposure (Tremp/Ager/Balaguer crossroad), displaying the main unconformities that bound the UTAG in this sector. Inspired by Mutti, 1985, 1994; compare with figure 2.17

Figure 2.17 – Panoramic view of the Baronia Sandstones at La Baronia de Sant Hoisme; the minor subdivisions within the LFG and UTAG will be discussed in chapter 4.

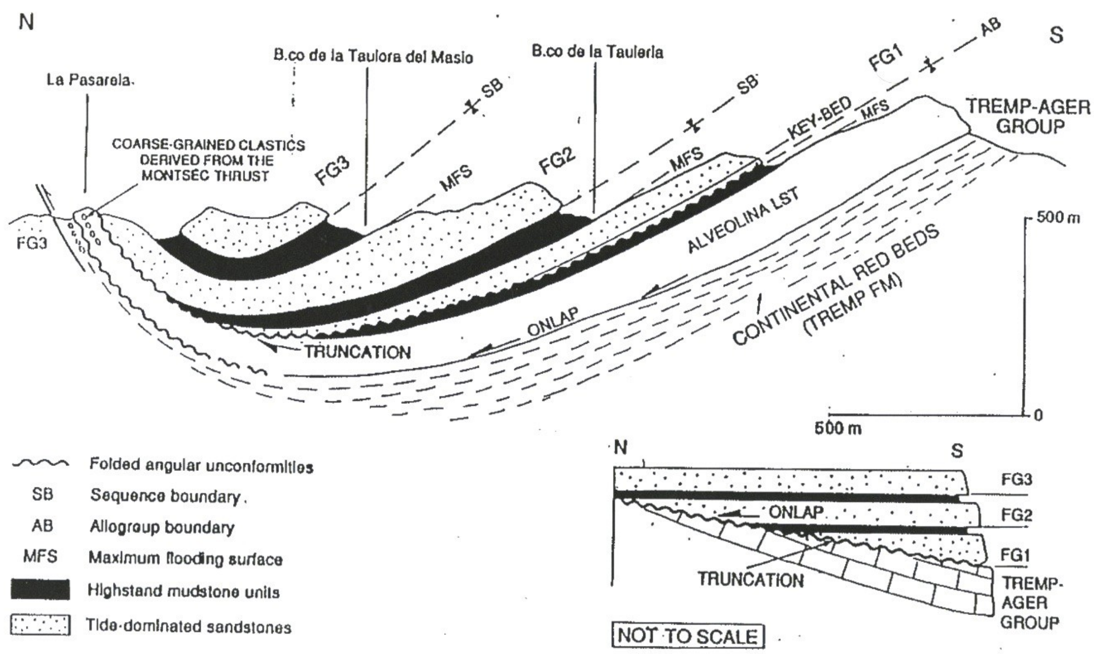

Figure 2.18 – Transversal (N-S) cross-section of the Ager syncline. FG: Figols Group; AB: allogroup boundary; SB: sequence boundary; MFS: maximum flooding surface. From Mutti et al. (1994)

Both the Alveolina Limestones (UTAG) and the Lower Baronia Sandstones (LFG; up to ~100m-thick) reflect a stage of intense tidal action in the Ager basin, directly related with its shape, that caused conditions of tidal resonance during periods of low sea-level (Mutti et al., 1985). This energetic environment caused grain size to keep relatively coarse; wedges of highstand mudstones and sandy mudstones separate the main sandy or carbonatic bodies, that are composed by metric, almost tabular packages of tidal bars (*sensu* Mutti et al., 1985; **figures 2.17**, **2.18** and **2.19**).

In the Cuisian (upper Ypresian), these conditions would have changed – either because of a change in the basin structural setting, general sea-level rise or enhancement of deltaic input. This brought the “purely” tidal deposits to be substituted by estuarine to fluviodeltaic deposits of the Middle and Upper Baronia Sandstones, and “Amettla Delta”.

This setting in the Eocene is consistent with the description of the Ager basin as a gulf, interested, during different stages of its history, by south and east-sourced deltaic inputs.

Figure 2.19 (next page) – Longitudinal (W-E) cross-section of the southern limb of the Ager basin. AL: Alveolina limestones; FG: Figols Group; MFS: maximum flooding surface. Notice the sequence boundary within the Alveolina limestones and the onlap of the FG1 and FG2 sequences on the tilted carbonate ramp (from Mutti et al., 1988)

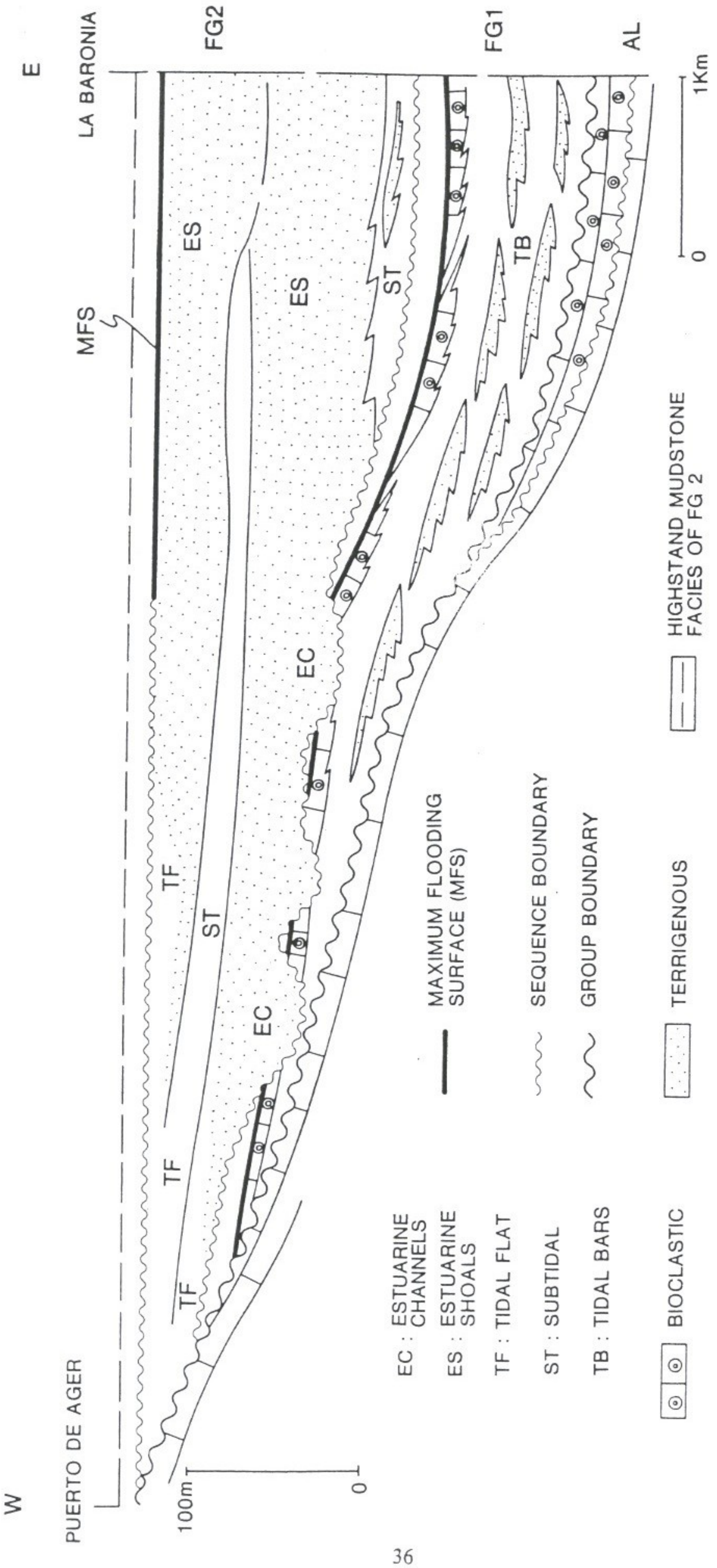
W
PUERTO DE AGER
E
LA BARONIA
FG2
FG1
AL
MFS
ES
ST
TB
EC
TF
100m
0
1Km
EC : ESTUARINE CHANNELS
ES : ESTUARINE SHOALS
TF : TIDAL FLAT
ST : SUBTIDAL
TB : TIDAL BARS
MAXIMUM FLOODING SURFACE (MFS)
SEQUENCE BOUNDARY
GROUP BOUNDARY
BIOCLASTIC
TERRIGENOUS
HIGHSTAND MUDSTONE FACIES OF FG 2

2.4.5 – Lower Ypresian of the Tremp basin

Lower Ypresian deposits are exposed in a continuous outcrop belt bordering the southern Tremp basin from the Congost de Mont Rebei (Rio Noguera Ribagorçana valley) to San Miguel de la Vall (east of the Rio Noguera Pallaresa), and in a transversal cut, west of the Rio Noguera Pallaresa from Guardia de Noguera to Gurp. Most of the northern margin of the basin isn't preserved, mainly due to erosion and later sedimentary cover.

The Lower Ypresian succession extends from the Claret Conglomerate to the lower UFG. The main features of this succession were anticipated in chapter **2.3**: it is a shallow-marine succession with a distinctly subsiding axial sector and marginal sectors affected by tectonic uplift; sedimentation is mud-dominated in the axial sector and of deltaic origin (Fonnesu, 1984; Mutti et al., 1994; 1996, 2000), while the thinned basin margins host a mainly carbonatic succession.

Correlations between these two domains were proposed in a great number of papers, the most influential of which are the works of Fonnesu (1984), Eichenseer & Luterbacher (1992), Serra-Kiel et al. (1994). High-resolution correlations were performed by Waehry (1999) and Angella (1999), and their results are partly published in Mutti et al. (1994, 2000).

Sediments belonging to the UTAG and LFG are more monotonous than in the Ager basin; the main widespread lithological changes are related with a few stages of exceptional progradation of the southern carbonate shelf in the axial region or, conversely, major stages of forestepping of the deltaic systems (Fonnesu, 1984; Barberà et al., 1997; Waehry, 1999).

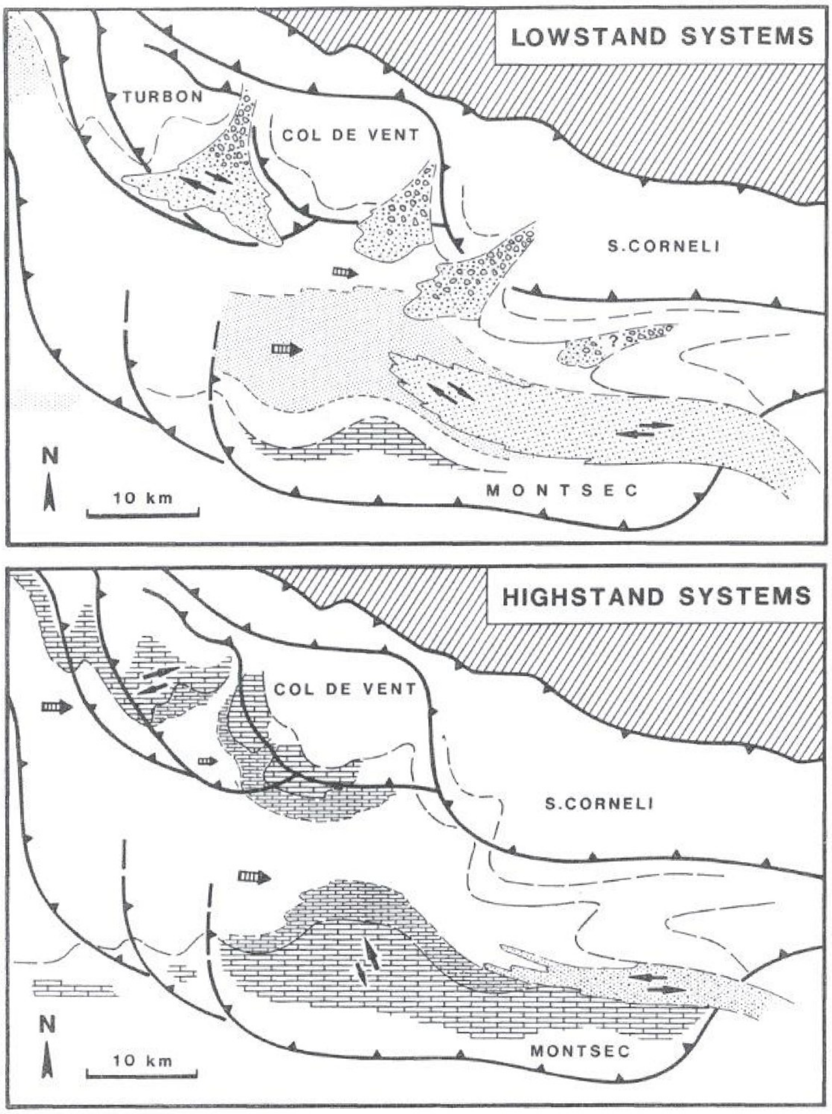

Figure 2.20 – Paleogeographic reconstructions of the Tremp basin during the Lower Ypresian. Notice the different distribution of carbonate and siliciclastic systems in relation to structural highs and lows, and the expansion of these systems with changes of the relative sea-level. From Eichenseer & Luterbacher (1992).

2.4.5.1 – *The southern carbonate ramp*

The marginal deposits of the Tremp basin are mainly composed of calcarenites, organized in a few main banks interbedded by marly/muddy deposits. Stratigraphic studies and environmental interpretations were provided by Luterbacher (1970), Fonnesu (1984), Eichenseer & Luterbacher (1992), Barberà et al. (1997) and finally Waehry (1999). A review of these deposits at the western end of the study area (sections [13, 14]) was recently proposed by Baceta et al. (2011). Barberà et al. (1997) provided a lithostratigraphic subdivision of these bodies as members of the muddy

Tendrui fm., and described their general growth geometries (**figure 2.21**). These are the Guardia, Estorm, Alsina, Eroles and S.ta Llucia members (a further unit, the Mur mb., is located in the UFG and wasn't considered in the present work).

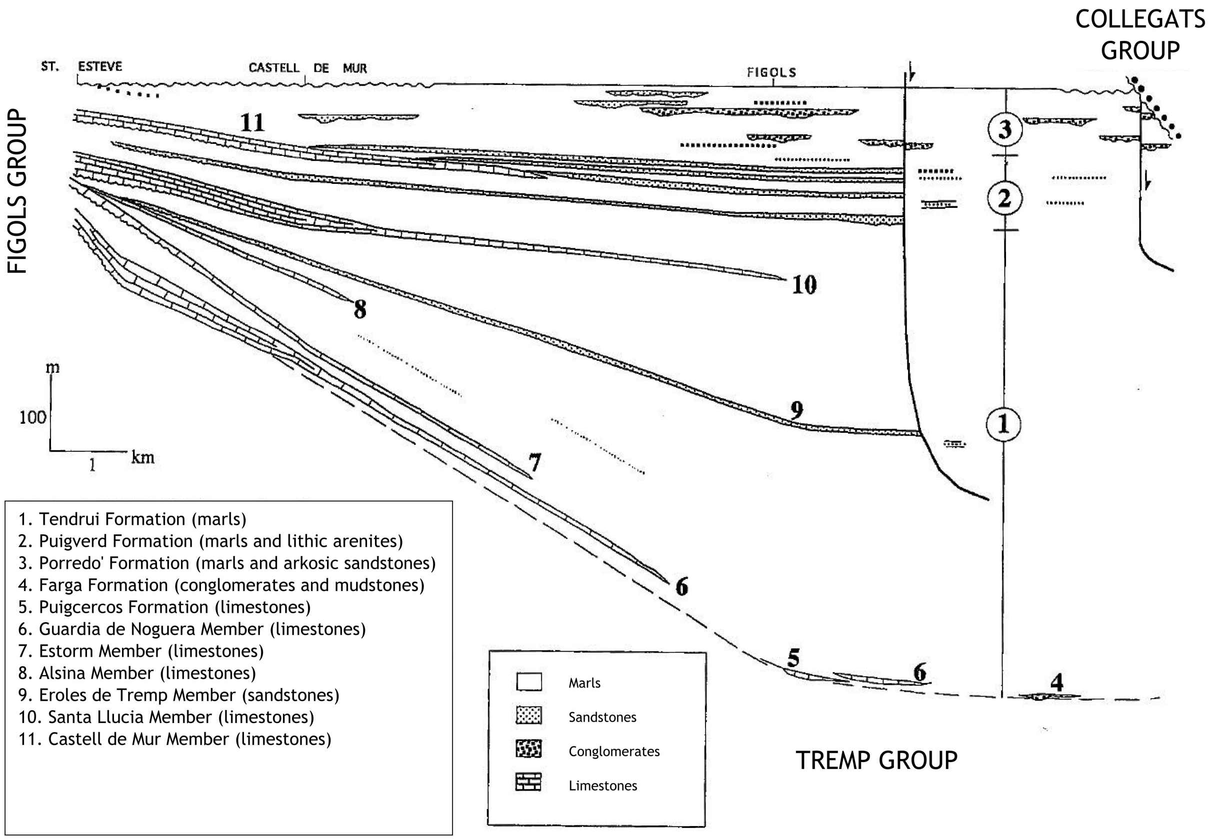

Figure 2.21 – Lithostratigraphic subdivision of the Tremp basin during the Ypresian according to Barberà et al. (1997, slightly modified); notice that the Figols Group as intended by the authors correspondss with the UTAG and FG altogether. The Lower/Upper Ypresian boundary falls within the "Puigvert Formation", roughly equivalent to the lower portion of the UFG (cf. figure 2.9).

The Guardia mb. is a 30-40 m thick package of packstones and wackestones hosting fossil assemblages typical of lagoonal to inner shelf settings, i.e., dominated by porcellanaceous foraminifera (Alveolina and miliolids; Luterbacher, 1970). It represents the stage of maximum diffusion of the carbonate environments in the Tremp basin during the initial Ilerdian transgression; minor sedimentological changes occur to the north, where the Guardia mb. is interfingered with muddy lagoonal deposits. In this direction, calcarenites display a growing nodular facies, indicating an increase in their mud content (Fonnesu, 1984).

The Estorm mb. is a smaller unit, never exceeding 20m in thickness, substantially similar to the Guardia mb. in terms of facies, with the exception of its upper portion, characterized by a muddier lithology (wackestones) and a deeper faunal composition (nummulitids and dyscocyclinids; Waehry, 1999). It has a limited areal extent, and transitionally passes to muddy deposits in the Guardia de

Noguera sector. However, Angella (1999) observed that a single bed, of mixed siliciclastic/biocalstic composition, correlates with the base of the Estorm member throughout the whole inner Tremp basin.

The Alsina mb. is in turn smaller than the Estorm mb. (less than 10m at its thickest), and it is represented by lenticular, cross-bedded bodies composed of nummulitic packstones/wackestones. According to Barberà et al. (1997), it rests unconformably on the Estorm mb.

The “Eroles mb” mainly refers to a sandy unit, equivalent to the Serra-Puit depositional system of Fonnesu (1984; see **2.4.5.2**): it would be more appropriate to name the carbonate equivalent of this unit in the southern basin in a different way; in the present work it will be named “Alsina-2” unit (see chapter **4**). This unit, resting unconformably on the Alsina mb. (Barberà et al., 1997; cf. Waehry, 1999), is shallower and more discontinuous than the former, and it is constituted by grainstones and packstones recording an initial shallowing followed by a fast transgression (faunal compositions shifting from alveolina/miliolid-dominated to nummulite-dominated; Waehry, 1999). The base of the Alsina-2 unit corresponds with the base of the Figols Group (Waehry, 1999).

The “S.ta Llucia mb.” records a major stage of progradation of the carbonate environments throughout the Tremp basin. It reaches a maximum thickness of ~30m north of Guardia de Tremp; in this location it abruptly terminates or transitionally pass to muddy deposits. In the axial sector, a few layers of nodular outer shelf limestones might constitute a lateral equivalent on this unit, although not all of the proposed correlations agree on this point (cf. Fonnesu, 1984; Waehry, 1999; Angella, 1999).

2.4.5.2 – *The axial deposits*

The axial deposits in the Tremp basin are fundamentally represented by fluviodeltaic sediments (Mutti et al., 1994; 1996; 2000; Waehry, 1999; Angella, 1999). These are represented by a full range of facies from fluvial mouth bars to distal lobes. Large part of the mudstones – that constitute the dominant lithofacies of the succession – were interpreted as prodelta deposits.

Carbonate facies are rare; they are limited to the base of the marine succession (a small tidal channel and residual beach deposits coeval with the Guardia mb.; Fonnesu, 1984; Eichenseer & Luterbacher, 1992), and to the supposed axial equivalent of the S. Llucia mb. (see **2.4.5.1**).

“Mixed” carbonate/siliciclastic beds are more frequent (Waehry, 1999); actually, very few sandstone layers display a purely terrigenous composition, and are mainly located in the lower part of the marine succession (“Farga mb.” in Barberà et al., 1997) and within the Figols Group.

Similarly to the southern ramp and the Ager basin's successions, the axial succession deepens upwards. In the early stage of the Ilerdian transgression, and later, in the middle/upper Ilerdian, abrupt relative sea-level falls interrupt this transgressive trend, and are recorded by a fast forestepping of deltaic deposits, and by faunal changes (Eichenseer & Luterbacher, 1992; Waehry, 1999). The first event is clearly recognizable in the northern sector of the basin (Tendrui and Esplugafreda sector, sections [22, 23]; basal unit of the Puigmaçana/Serrat de Cal Senàs depositional system in Fonnesu, 1984; "Farga mb." in Barberà et al., 1997); the second one is represented by an up to 10m-thick package of medium-coarse sandstones (and subordinate mudstones and shallow-water calcarenites), interpreted as proximal deltaic lobes, that can be followed in most of the basin (Serra-Puit depositional system of Fonnesu, 1984; Eroles mb. in Barberà et al., 1997); in the hill named "Serra-Puit", north of Guardia de Noguera, pebbly, cross-bedded mouth-bars deposits can be observed.

The base of the Serra-Puit beds correlates with the unconformity between the Alsina and Alsina-2 mbs. (**2.4.5.1**), and constitutes the base of the Figols group (Mutti et al, 1994; Waehry, 1999).The definition of this surface has changed through time, and Angella (1999), chose a lower location, equivalent to the one originally proposed by Mutti et al. (1988), and coincident with the keybed at the base of the Estorm mb. (**2.4.5.1**). The problem of the base of the Figols group is related to the fact that in the inner Tremp basin no major unconformities can be recognized, with the exception of the ones observed along the marginal sectors; in the Ager basin instead, the TAG/FG boundary is clearly expressed by an angular unconformity (**2.4.4**) and an associated sharp lithological change (base of the Baronia sandstones). The different implications related with the base of the Figols Group will be discussed in **6.1** and **6.3**.

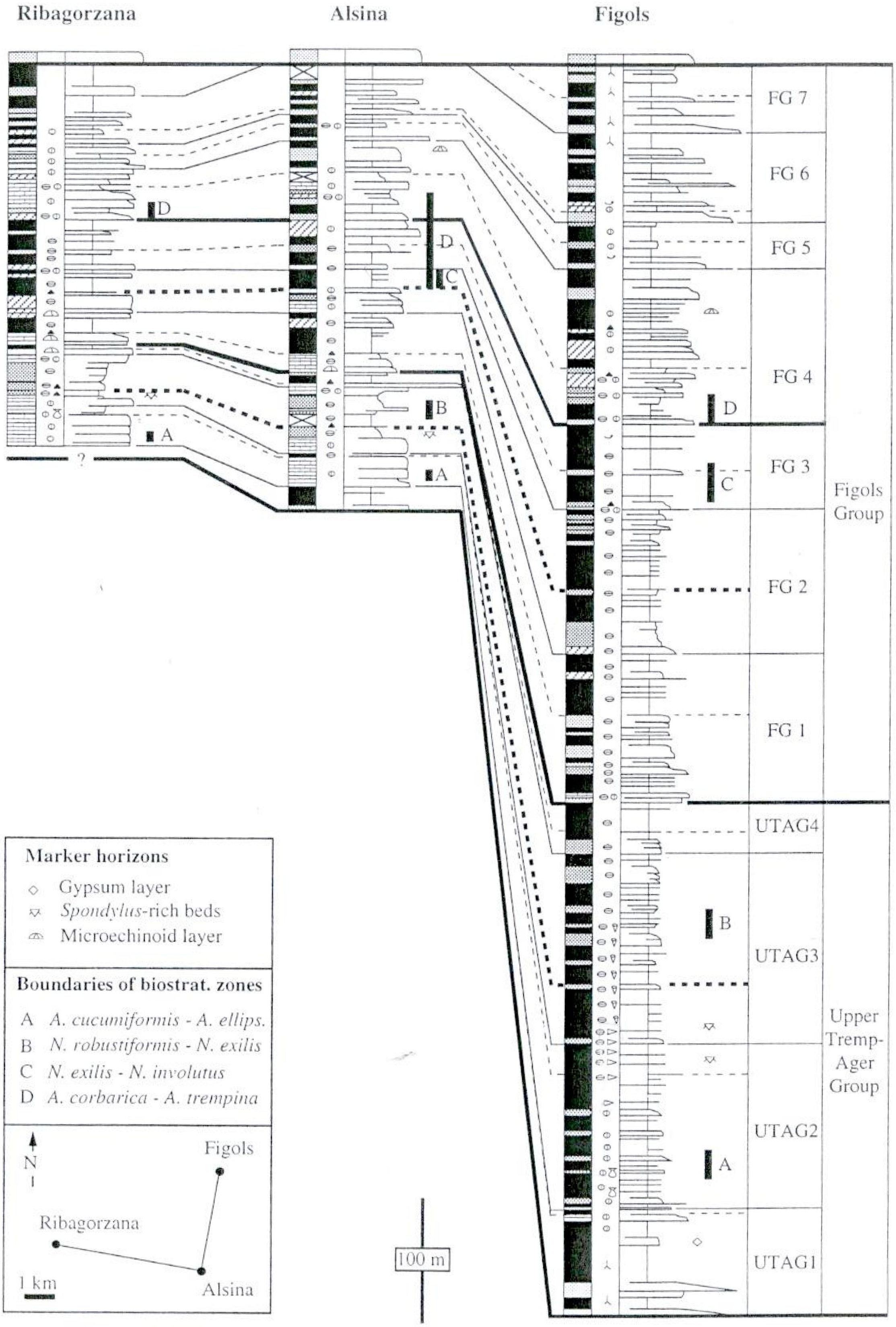

Figure 2.22 – High-resolution stratigraphic cross-section of the inner Tremp basin according to Waehry (1999); Ribagorzana, Alsina and Figols sections are equivalents respectively of sections [13, 14], [16] and [20] in the present work.

2.5 – Integrated stratigraphy of the studied successions

The history of the south-central Pyrenean foreland basin (SCPFB) as a distinct structural and physiographic element mostly spans through the early and middle Paleogene. The stratigraphic interval studied in both the Ager and Tremp basins is represented by the lower and middle portions of a regional stage historically known as “Ilerdian” (Hottinger & Schaub, 1960), substantially equivalent to the lower Ypresian (Early Eocene).

This chapter is dedicated to the chronostratigraphic features of the studied successions, based on published data reviewed in the light of modern early Paleogene age models.

2.5.1 – Early Paleogene integrated stratigraphy

The Early Paleogene (EPG) is probably the oldest period where advanced and fully-integrated techniques of chronostratigraphic research are applied (examples relevant for this work can be found in Cramer, 2003; Lourens et al., 2005; Hilgen et al., 2010; Westerhold et al., 2007, 2008, 2009, 2011). The greatest improvements were performed in the last ten years, thanks to the collection of continuous logs – apparently hosting complete time-series – from deep-sea drilling programs, that were studied with growing sampling resolution.. The greatest outcome of these studies is an high-resolution relative age model for the Early Paleogene, commonly considering the Paleocene/Eocene boundary as the datum layer. Uncertainties are still related to the error range of the few reference layers where an absolute dating was investigated with the study of radioisotopes (Westerhold et al., 2007; 2009).

Although in this work a specific option for absolute dating was chosen (see below), it should be clear that absolute dating is irrelevant for this work's purposes; more critical is the choice of the relative age model, that is, the chronology of global events and geological cyclicity occurring in a given stratigraphic interval. The most refined relative age model is represented by the “Westerhold options”, based on the comparison of data from early Paleogene logs collected both in the subsurface and in exposed sections (Westerhold et al., 2009). Through this approach, the problems in the chronological reconstructions due to local hiatuses and condensed successions were minimized.

These age models were built exploiting reference layers of global chronostratigraphic significance such as EPG hyperthermals and magnetic reversals. Across the considered intervals, cyclostratigraphic investigation was applied on different data sets built upon geochemical and geophysical properties of these rock records, such as magnetic susceptibility, luminous reflectance and stable isotopes (primarily carbon isotopes). The common procedure for cyclostratigraphic analyses requires the data sets to be statistically tested in order to verify the non-stochastic distribution of data; finally, data are processed with spectral analysis to recognize characteristic bandwidths in their distribution.

The independent data sets (e.g., susceptibility and luminescence data) from individual sections, collected with cm-scale resolution, coherently showed that the studied successions developed with a cyclical stacking over a limited number of bandwidths, that clearly reflected astronomical cyclicities in the classic "Milankovian" range (Milankovitch, 1941), that are substantially precessional and short-,mid- and long-term eccentricity ciclicities (periods of respectively ~21, ~95, ~405 and ~2250 ky duration are commonly considered). These periodicities constitute the framework for a relative timescale that allows an error range in the scale of its minimum constituent, that is the precessional scale – i.e., ±21ky.

The hingepoint commonly considered for the relative dating is the onset of the Paleocene-Eocene Thermal Maximum (oPETM, see chapter **5.2.1**), primarily because of its ease of recognition, and its official designation as a GSSP for the Paleocene/Eocene boundary (Aubry et al., 2007). With a "zero" age established in the middle of the cyclostratigraphic data set, cycles are counted and relative ages are established. Discrete horizons are dated, and intervals are quantified.

2.5.1.1 – *Orbital solutions*

A further advancement in cyclostratigraphic chronology aims to its use as an absolute dating tool.

Aware of the well-assessed control that Earth's orbital parameters operate in the high-frequency variability of global climate, some groups of researchers began in the late 1980s to model the variability of these orbital parameters in time. This approach invested in computational modeling for considering a growing number of parameters, that would influence Earth's movements with respect to the sun, and finally obtain the variable pattern of Earth surface insolation in time.

These models are named "orbital solutions". The most recent models of this kind are named La2004 and La2010 and were published by Laskar et al. (2004, 2011); the latter reached such a level of complexity to consider, altogether with the orbits of the sun, the moon and the planets of the solar system, the orbits of five major asteroids.

"La" orbital solutions project the variability of Earth's individual orbital parameters in the past and future 250 million years (this implies that potentialities of this instruments go far beyond than the scopes of geochronology). Quaternary and Neogene research have successfully applied orbital solutions and verified their reliability in concert with other investigation techniques; correlation of cyclostratigraphic data with the orbital solutions can be successfully brought down to the full Oligocene (Pälike et al., 2006).

A problem in the application of every orbital solution developed up to now, hampers their application in older stratigraphic successions. Apart from the individual precessional and obliquity movements, whose rhythms are apparently coherent in deep-time (Laskar et al., 2004), the rhythms of eccentricity cannot be reliably tracked over ages older than ~50 My (and successively to the next 50 My; the ±50 My threshold was reached in the latest La2010 solution). This problem is related with a chaotic behavior in the solar system, due to phenomena of resonance between some specific parameters (Laskar, 1989).

The critical effect for geoscience applications is that, in the different tests performed to assess the reliability of the model, amplitude and phase of the short- ad long-term eccentricity cycles begin to shift unpredictably before this age: this means that, although components such as the precessional movements can be individually applied, the unpredictability of the eccentricity component produces unpredictable insolation patterns.

2.5.1.2 – *EPG research and orbital solutions*

Since the 50 My boundary falls in the Ypresian, EPG research has only tentatively applied orbital solutions to obtain an orbital tuning; in other words, while the presence of cycles of different order, reliably attributable to specific orbital parameters, can be extrapolated from the geological record, they cannot be correlated with cycles with a precise age according to a given orbital solution.

Moreover, because of the ultimately discontinuous nature of the geological record, cross-correlation of cycles cannot start from the computationally more predictable high-frequency cycles: in deep-time, where longer-term trends are commonly more easily read than the shorter ones, the eccentricity parameter becomes more relevant for geological interpretations.

This problem, in conjunction with some uncertainties in radiometric absolute dating (Westerhold et al., 2007, 2009; Machlus et al., 2004) brought researchers to propose different tuning options over “floating” timescales.

2.5.1.3 – *Westerhold & Rohl (2009): comparison with former EPG age models*

The Berggren '95 chronology, adopted in the last papers concerning the stratigraphic succession examined in this work, was substantially modified for the early Ypresian in the official 2004 GPTS (Gradstein et al., 2004). Apart from absolute age considerations (that have been positioning the whole succession to older ages), the relative duration of some intervals have sensibly changed. These changes are summarized in Westerhold & Rohl (2009), together with their age models and alternative recent age models (Smith et al., 2008; Machlus et al., 2004). If we consider the interval containing the horizons listed above, the most relevant changes were brought by the 2004 GPTS, with a ~200 ky longer interval between the oPETM and the base of chron C24n. Westerhold & Rohl (2009) early Eocene chronology doesn't apply changes in this interval, but the full length of Chron C24 was further expanded by ~170 ky, with a longer portion of C24r expanding below the oPETM; the duration of the short C24n.2n was expanded as well.

For the sake of completeness, "Westerhold options" for absolute dating are here reported for the oPETM reference layer (according to Westerhold et al., 2008), from younger to older:

Wo1: 55,53 My
Wo2: 55,93 My
Wo3: 56,33 My

Notice that these options are offset by exactly a ~405 ky eccentricity cycle; error was extimated by the authors in the range of ±10 ky. In this work, Wo2 was chosen just for its proximity with the dating proposed in the official GPTS 2004 (Gradstein et al., 2004).

2.5.2 – EPG stratigraphy and the South-Central Pyrenean basins

The relative age-model from Westerhold et al. (2007, 2009) was chosen as a chronostratigraphic reference for the Ypresian interval studied in the present work. Major uncertainties still affect the Paleocene cyclostratigraphy (cf. Westerhold & al., 2007, and Hilgen 2010), so the official Gradstein et al. (2004) chronology will be applied for this interval.

By assessing the wealth of bio-, magneto- and cyclostratigraphic data collected by modern EPG research, the ages relative to the chronohorizons formerly recognized in the SCPFB were adopted. These horizons are, from the younger to the older:

a. The upper and lower boundaries of magnetochron C24n.3n (formerly referred-to as n.2n before the discovery of a very short normal interval in the middle of C24n; dating from Westerhold and Rohl, 2009);

b. The upper and lower boundaries of the distribution of the calcareous nannofossil *Tribrachiatus contortus* (NP10d/CP9a biozones; Martini, 1971, modified by Aubry, 1996; Okada & Bukry, 1980; dating by Agnini et al., 2007);

c. The upper and lower boundaries of the PETM carbon isotopic excursion (Westerhold et al., 2009).

These boundaries are relative to the P/E boundary and the early Ypresian. Below are the bibliographic references for the original collection of each data in the study area:

a. collected by Pascual et al., 1992; Waehry, 1999;
b. originally reported by Kapellos and Schaub, 1973;
c. documented by Schmitz &Pujalte, 2003; this work for the PETM location in Ager basin and southern Tremp basin.

Planktonic foraminifera data are scarce because of the shallow setting of the marine deposits in the study area. Planktic stratigraphy mostly relies on the correlation with the Campo section (Molina et al., 2003), and from the few data from Tremp section deepest interval (Luterbacher, 1970; von Hillebrandt, 1965, 1975; Serra-Kiel et al., 1994).

Below are summarized the most relevant informations on biostratigraphically-significant planktic foraminifera taxa collected in the study area by former workers, and some problems in their age attribution.

Waehry (1999) reports a *Morozovella velascoensis*/*M. edgari* boundary at ~2/3 of the reverse polarity interval between the base of Tremp section (section [20] in the present work; ~equivalent to the oPETM) and the C24r/C24n reversal; in a slightly higher position, Serra-Kiel et al. (1994) report a *M. aequa*/*Pseudohastigerina wilcoxensis* boundary, that they approximated to the P6a/P6b boundary (sensu Berggren & Miller, 1988). Both of these boundaries occur inside *T. contortus*' stratigraphic range, apparently in contrast to older zonations, which located the *M. velascoensis*/*M. edgari* boundary in NP9 (see biostratigraphic framework in Eichenseer & Luterbacher, 1992). Actually, *M. edgari* has lost its biozonal significance. Therefore, the only datum that will be considered for chronostratigraphic purposes will be *M. velascoensis* HO, former P5/P6 boundary, that in Wade et al. (2011) is dated at 54,5 My before present, and that constitutes their boundary between Planktonic Foraminifera zones E2/E3 (following Berggren & Pearson, 2005); it is still a problematic issue the relationship between *M. velascoensis* HO and the LO of *T. contortus*: Agnini et al. (2007) give an average age of ~ 54,3 My for *T. contortus*' LO, based on Wo1 absolute dating for the oPETM (see previous chapter); since this oPETM dating is similar to the one applied by Wade et al. (2011), it turns out that *M. velascoensis*' HO is older, accordingly to former biozonations, and that the co-occurrence of these taxa as reported by Waehry (1999) might be caused by reworked tests of the foraminifer.

2.5.2.1 – *Stratigraphy of the Ilerdian stage and the Shallow Benthic Zones*

The Ilerdian stage was actually defined in the Tremp region (the name Ilerdian refers to the latin name of Lleida, the provincial capital), and Tremp section (section [20] in the present work) was designated as the stratotype of the Ilerdian stage; a parastratotype was designated as well in the SCPFB, that is the Campo section, some 50 km west of Tremp, in order to overcome problems concerning the discontinuity of Tremp section and, most of all, its poor content in planktonic foraminifera.

Together with the Cuisian stage (upper Ypresian), these two regional stages are very effective for describing specific portions of the exposed successions; nevertheless, the stratigraphic investigations performed by Orue-Etxebarria (2001) and Schmitz and Pujalte (2003, 2007), brought the authors in recent years to propose an equivalence between the base of the Ilerdian and the P/E boundary (Pujalte et al, 2009b).

The Ilerdian and Cuisian stages have not only a characteristic geological expression in the inner SCPFB – that could be roughly synthesized in a carbonate/mixed Ilerdian vs. a terrigenous Cuisian – but they are directly related with the evolution of the large benthic foraminifera. More specifically, the Ilerdian stage was defined by Hottinger & Schaub (1960) to account for major evolutionary changes in the *Alveolina* and *Nummulites* macroforaminifera in the tethyan realm.

Actually, the base of the Ilerdian corresponds to the first common occurrence of “true” alveolinids, and to a major radiative event for nummulites. This faunal change, addressed in later literature as the “Large benthic foraminifera turnover” (LBFT, or LBT), is a critical biotic event that had been related to the PETM climatic crisis (Baceta, 1996; Pujalte et al., 2009a). Since this turnover, alveolinids and nummulitids become a prominent constituent of tethyan shelfal sediments, and they are subject to a fast evolution, so that a biostratigraphic subdivision based on large benthic foraminifera was established in the 1960s (Hottinger, 1960; Hottinger & Schaub, 1960), and its correlation with planktic foraminifera (Luterbaher, 1970; von Hillebrandt, 1965, 1975) and nannofossil biozones (Kapellos & Schaub, 1973) were, at least partially, settled.

Since the beginning, workers were aware of the limits of the use of benthic foraminifera for a biozonation, because of their great environmental sensitivity – in fact, they make excellent paleoenvironmental indicators. This problem was partly overcome by the early observation that both shallow and deeper-living genera (commonly alveolinae and nummulites) shared common evolutionary steps. Luterbacher (1998) pointed out that, at least for the Tremp basin, these steps are frequently associated with sequence boundaries or condensed successions, so that their effective sinchronicity couldn't be assessed.

The latest effort to consolidate EPG larger benthic foraminifera stratigraphy was made by Serra-Kiel et al. (1998) with the definition of an updated biozonation based on alveolinids, nummulitids and orthophragminids from tethyan successions. These biozones were named “Shallow Benthic Zones” (SBZ), and were considered by the authors to have a solid chronostratigraphic significance in their correlation with P and NP zones.

Since the 1998 SB zones were dated on the basis of the Berggren et al. (1995) timescale, a tentative adaption to more recent age models was performed.

The zonation proposed by Pujalte & al (2009) considers new integrated datas from bio-, magneto-, and chemostratigraphy at che Campo section in the SCPFB (Pujalte et al, 2003); the informations they provide unquestionably narrow the potential location of the SBZ4/SBZ5 boundary to a ~10 m continental horizon containing the Paleocene/Eocene boundary as established by chemostratigraphy. Their zonation (Pujalte et al 2009b) must anyway be corrected because it doesn't account for the long (~900 ky) interval between the top of chron C25n and the PETM CIE, as estabilished by Ogg & Smith's (2004) magnetostratigraphy - used for the 2004 GPTS (Gradstein & al, 2004) - and furtherly constrained in successive papers (Cramer et al., 2003, Lourens et al., 2005, Westerhold et al., 2007).

In the present work, the problem at stake is not the correlation of global and local stages (Yresian vs Ilerdian), but the zonal relationships along a few, well-constrained timelines, that are the onset of hyperthermals, such as the PETM and ETM2 (see chapter **5**), and the magnetochron boundaries. The fundamental controversy that stems out from the published material is that the redefined relationships in Pujalte et al. (2009b) imply a P5 (sensu Berggren & al 1995) attribution of great part of SBZ4, that have been seemingly excluded by Serra-Kiel et al. (1998) Shallow Benthic Zonation. This causes a longer duration of SBZ4, formerly limited to the C25n interval: in facts, it should overlap a ~1My interval in the lower C24r magnetozone.

Working out this controversy is clearly beyond the scope of this work; it is here chosen to follow Pujalte et al. (2009a) solution for the PETM-LFT correlation on the basis of the relevant data they brought to constrain the Larger Foraminifera Turnover location with the PETM CIE.

The immediate problem to be faced at this point is the actual temporal extension of the SBZs between the oPETM and the C24r/C24n reversal.

The boundary between SBZ5 and SBZ6 should run on the nannofossil CP8a/b boundary (sensu Okada & Bukry, 1980, according to Serra-Kiel et al., 1998); but on the basis of Gradstein et al. (2004) chronology, this nannofossil boundary is located in the Paleocene, so there are no major constraints on the location of SBZ5/SBZ6 boundary.

SBZ6/SBZ7 boundary falls close to the top of both P5 and NP9.

SBZ7/SBZ8 boundary must be included within planktonic foraminifera zone P6a (E3 in Wade et al, 2011), invariably before the NP10/NP11 boundary (sensu Martini, 1970); in Tremp section, SBZ7/SBZ8 boundary follows the LO of *T. contortus*, that is, the CP8b/CP9a (sensu Okada & Bukry, 1980) boundary (data form Serra-Kiel & al, 1998; Waehry, 1999) or the NP10c/NP10d boundary according to Aubry (1996).

Finally, the SBZ8/SBZ9 boundary is closely related with the top of C24n.3n, and the top of SBZ9 – defining the top of the Ilerdian stage – falls in the very short reverse interval of C24n.1r.

Figure 2.23 depicts the results of this rationalization, with the tentatively-corrected locations of the shallow benthic zonal boundaries. The implemented age model is the one from Westerhold & Rohl (2009), using their “option 2” for absolute dating.

2.5.2.2 – *Paleocene of the Ager basin*

Paleocene chronostratigraphy was not studied in a comparable detail, mostly because the studied paleogene succession lacks detailed chronostratigraphic studies; this because of inherent problems in the absence of good biostratigraphic markers (the succession develops in continental deposits for most of its extension).

According to Feist & Colombo (1983) and Galbrun et al. (1993), the basal unit of the studied succession (Vallcebre fm., see **2.3.1.1**; **2.4.1.1**) is of Danian age, including part of the Selandian, because it apparently spans through chrons C27r to part of C26r (Galbrun et al., 1993). This same unit, however, hosts the Middle Paleocene Unconformity (see **2.3.1.1**), that extends up to the Thanetian (upper Thanetian in the old subdivision adopted by Feist & Colombo, 1983).

The presence of wide covered intervals, both below and above the Danian limestones, substantially hampers a better chronostratigraphic investigation for this interval.

Slightly better chronological constraints are available for the upper portion of Ager basin's Paleocene, where the location of SBZ4 and the top of SBZ3 (formerly *Glomalveolina levis* and

Glomalveolina primaeva biozone) were defined by Rossi (1997). The location of the Paleocene/Eocene boundary is inferred from geochemical data collected for the present work (see chapter **5**. **Figure 2.24** provides a synthesis of these chronostratigraphic data, dated on the basis on the 2004 GPTS (Gradstein et al., 2004).

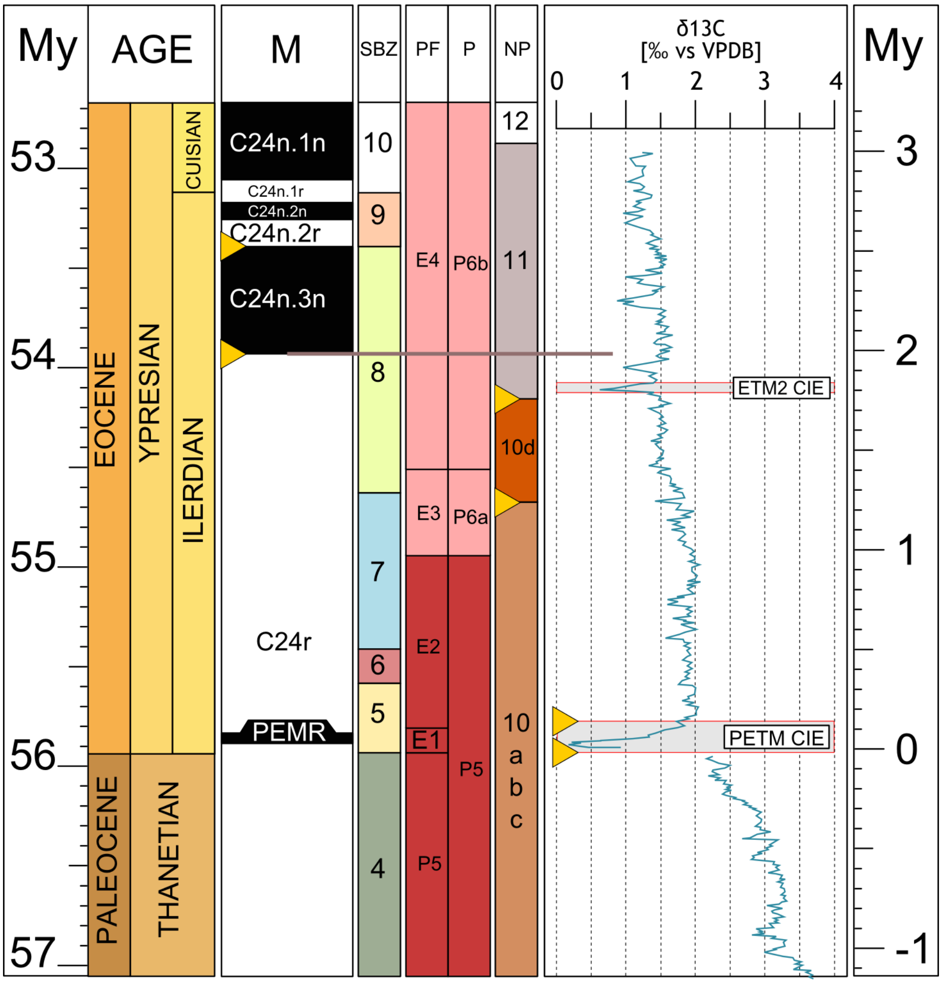

Figure 2.23 - Chronostratigraphy in the range of the Ilerdian regional stage; upper and lower limits are the boundaries of chron C24; on the left, absolute ages according to Wo2 age model; on the right, relative ages from the onset of the PETM (according to Westerhold & Rohl, 2009); carbon isotope stratigraphy from Zachos et al. (2010), redrawn; PF and P zones according to Wade et al., 2011; NP zones according to Aubry, 1996; the applied NP zonation is dated by Agnini et al. (2007) on the basis of Westerhold et al. (2007) relative age model. Notice that the applied NP zonal boundaries are the ones consistent with published nannofossil distribution data from the Tremp section (see text for references); Shallow benthic zones adapted from Serra-Kiel et al. (1998) and Pujalte et al. (2009b) – see text for details. Yellow markers indicate the most reliable chronohorizons documented in literature in Tremp section (section [20] in this work; see text). The "PEMR" normal microchron occurring during the PETM (Lee & Kodama, 2009) has been depicted for completeness, but no evidence for this event has yet been found in the studied successions.

2.5.3 – Age model of the Tremp and Ager basins

Figure 2.24 displays the correlation of the successions of the Tremp and Ager basins with the chronostratigraphy of the early Paleogene. Numbered horizons and intervals are discussed below.

1. **Base of the Vallcebre formation**. This unit, well expressed in Ager basin, is only locally recorded in Tremp basin. According to Pujalte & Shmitz (2005), it is represented by a thin horizon of palustrine limestones supposedly associated with a paleosol horizon of regional extent (Tremp-Colmenar horizon of Eichenseer, 1988).
2. **Middle Paleocene hiatus; base of the Middle Tremp-Ager Group**. This hiatus, associated with the MPU (**2.3.1.1**) is clearly documented in Ager basin, and on the basis of published data its base – and consequently, the base of the here-defined Middle Tremp-Ager Group (see chapter **6**), should be located in the Selandian (chron C26r Galbrun et al., 1993; according both to the 1995 and 2004 GPTSs the Selandian begins before the end of C27n); the red paleosols above it were reported to be of Thanetian age (Feist and Colombo, 1983). Concerning Tremp basin, a revised stratigraphy of the Paleocene of Tremp basin proposed by Pujalte & Schmitz (2005) and Baceta et al. (2011) hypothesize the location this hiatus in correspondence to an erosive surface, that cuts through the Tremp-Colmenar horizon and the Vallcebre formation. The duration of this hiatus in Tremp basin, as proposed by Baceta et al. (2004, 2011), is about 2My, although chronostratigraphic control in this setting is poorly reliable, and the authors' extimate is based on the extension of this hiatus in the correlative Paleocene carbonate shelf in the Basque country.
3. **SBZ3/SBZ4 boundary**. This boundary, reported by Rossi (1997), in Ager basin reference section (section [4]) falls in a continental interval, and its location is inferred on the basis of the correlation proposed in the cited paper with Thanetian marine deposits located to the west.
4. **Base of the Upper Tremp-Ager group; onset of the PETM**. This boundary, equivalent to the base of the Serraduy sequence in Eichenseer & Luterbacher (1992), is closely associated with the onset of the PETM, as documented by Schmitz ad Pujalte (2003) for northern Ager basin. The proposed location of the associated carbon isotopic shift in Ager basin is documented in chapter **5**).
5. **Ilerdian transgression**. This major transgressive event have been documented in many papers, since it is a salient feature of the SCPFB. Schmitz and Pujalte (2003) isotopic data document the total remission of the PETM isotopic excursion in a position very close to the level of the marine ingression in the inner Tremp basin. In the present work (see chapter **5**), it wasn't possible to locate the end of this excursion in Ager basin, because of complications related with changing lithologies, so a precise dating of the marine ingression cannot be established.

6. **Top of SBZ5**. Shallow benthic data in the studied successions are problematic under many aspects, primarily because of the close relationship of zonal boundaries with sequence boundaries and condensed successions (Luterbacher, 1998). In the specific case of SBZ5, the top of this biozone in Ager basin (Ferrer et al., 1973) might be postdated because of tidal activity. A further problem arises because of the relation of this horizon with a major condensed succession.

7. **Lower Ypresian condensed succession in Ager basin, and its temporal equivalent in Tremp basin** . In Tremp basin, a condensed succession was documented by Eichenseer & Luterbacher (1992) a few meters above the top of SBZ5; in Ager basin, benthic foraminifera biostratigraphy from Ferrer et al. (1973) suggest a lower rate of sedimentation in this interval, but the presence of a major condensed succession is further constrained by the presence of glauconite (Mutti et al., 1994, stop descriptions) and from magnetostratigraphic data presented in this work (see Appendix 1). The stratigraphic expression of the Tremp basin's condensed succession is much less significant, and clearly covers a shorter time interval.

8. **Base of chron C24n**. This horizon was very well documented in Pascual et al. (1992) for Tremp section. In the present work, a targeted magnetostratigraphic sampling was performed in the range of the “lower Baronia sandstones” (Mutti et al., 1985), showing that the base of this unit falls already in a normal interval (see [CHAP-appendice]). These data diminish the stratigraphic expression of the lower Ypresian condensed succession of the Ager basin, spanning for a greater time interval if compared with its equivalent within the Tremp basin.

9. **Base of the lower Figols Group**. This boundary, equivalent to the lower sequence boundary of the Llimiana sequence in Eichenseer & Luterbacher (1992), was proposed in Mutti et al. (1994) and Waehry (1999). It is slightly younger than the base of C24n, although a possible hiatus due to erosion might be present, as it is apparent from the vertical distribution of *T. contortus* (NP10d, Aubry, 1996 after Martini, 1972) in Tremp section, by comparison with the chronostratigraphic table. Following recent EPG research papers (Agnini et al., 2007), these two boundaries constrain the location of the ETM2 hyperthermal in the SCPFB succession.

10. **Base of the upper Figols Group**. This boundary, equivalent to the FG2 lower sequence boundary in Mutti et al. (1994), and located in a slightly lower position if compared with Waehry (1999), falls in the narrow reverse subchron C24n.2r. Published chronostratigraphic data in this interval are very doubtful, and only Waehry (1999) reports unpublished data from J. Channell indicating the presence of a small normal interval a few ten meters above it, possibly the short C24n.2n (at that time unknown). Notwithstanding this consideration, it is evident that the deposition of the lower Figols Group occurs in a relatively short time interval, that can be assessed between 400 and 500 ky. A further hypothesis, that would identify the normal chron reported in Tremp

section by Pascual et al. (1992) as the whole C24n is considered unlikely on the basis of biostratigraphic data.

Figure 2.24 (next page) - Chronostratigraphic diagram sinthesizing the available chronological data for the reference sections of the Ager and Tremp basins. See the text for comments.

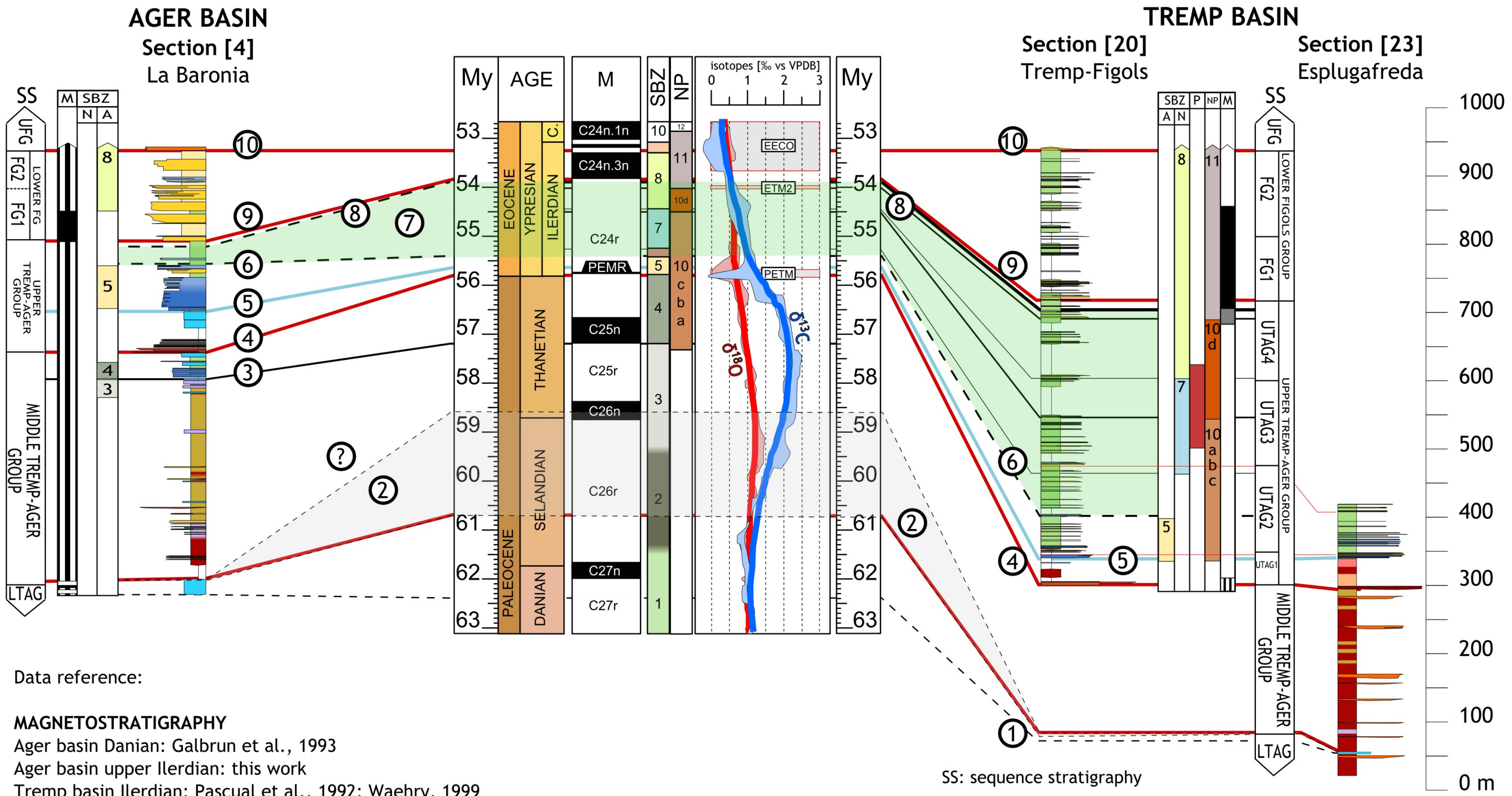

Data reference:

MAGNETOSTRATIGRAPHY
Ager basin Danian: Galbrun et al., 1993
Ager basin upper Ilerdian: this work
Tremp basin Ilerdian: Pascual et al., 1992; Waehry, 1999

BIOSTRATIGRAPHY
Ager basin upper Thanetian: Rossi, 1997
Ager basin Ilerdian: Ferrer et al., 1973
Tremp basin Ilerdian: Serra-Kiel et al., 1994

Esplugafreda section according to Pujalte & Schmitz, 2005 (marine segment: this work)

CHEMOSTRATIGRAPHY
Stable isotopes curves redrawn and adapted from Zachos et al., 2001, on 2004 GPTS (Gradstein et al., 2004)
P\E boundary: Tremp/Esplugafreda: Schmitz & Pujalte, 2003; Ager: this work

SS: sequence stratigraphy
SBZ Shallow Benthic Zones (Serra-Kiel & al 1998, modified)
A, N: Alveolina vs Nummulites data
P Planktic Foraminifera Zones (Berggren & al 1995)
NP Calcareous Nannoplankton Zones (Martini 1971; cf Agnini, 2007)
M Polarity: normal; reverse; uncertain; no data

Sequence stratigraphy for Ager basin Ypresian according to Mutti et al. (1994); Tremp basin: Waehry (1999), both with some modifications

3 – OBJECTIVES AND METHODS

The main objective of the present work is to establish a correlation between the Tremp and Ager basins in the early Ypresian. The focal element of this correlation is the paleo-Montsec high, whose synsedimentary uplift controlled the local development of angular unconformities in the southern and northern marginal areas of the Tremp and Ager basins respectively.

The main problem in this investigation resides in the N-S (“margin to depocenter”) correlation of the Ager basin's major unconformities, that is presently hampered by the strong deformation that occurred in the footwall of the Montsec Thrust during late Paleogene reactivations. Extrabasinal correlations require then to recognize surfaces (or intervals) equivalent to these unconformities in the Tremp basin (**2.3**, **2.4**).

In order to fulfill this objective, the Lower Ypresian deposits of the inner Tremp and Ager basins (also including the Paleocene of the Ager basin) have been studied with a classic fieldwork approach integrated with geochemical investigations.

3.1 – Fieldwork

The fieldwork lasted approximately 8 months and involved the study and logging of ~4000m of sedimentary successions.

These successions were studied through facies analysis, vertical logging and, where possible, direct correlation. Most of this study was substantially a review of former high-detail studies (**2.4**); the successions were subdivided in informal, descriptive lithostratigraphic units, and then interpreted in terms of physical stratigraphy (see **3.2**). Intra-basinal correlations were mainly founded on the recognition of sequence boundaries and transgressive surfaces, following the guidelines for high-resolution sequence stratigraphy proposed by Mutti et al. (1994). Extra-basinal correlations were mainly based on a chronostratigraphic approach, by using updated published informations (see **2.5.3**) and by integrating them with original isotope-stratigraphic data or magnetostratigraphic data.

The high-resolution photogeological maps drawn by Ghielmi (1992) and Waehry (1999) provided an excellent field guide for the Lower Ypresian interval, so no further mapping was performed (with the exception of a small area of the southern Tremp basin, where mapping on ortophotomaps and high-detail logging was needed to investigate in detail the geometries of the southern carbonate ramp; chapter **4.4.1**).

3.2 – Physical-stratigraphic interpretation

The physical stratigraphy approach to the study of stratigraphic successions and basin analysis is based on the definition of units, coeval within their bounding surfaces, whose development is driven by well-assessed external phenomena, such as eustatism and tectonics. Physical stratigraphy is based on the sequence-stratigraphic concepts developed by Vail et al. (1977) and Wilgus et al. (1988); the main implication of this, is the fact that the development of sedimentary successions is ultimately controlled by relative variations in the sea-level, that cause changes in the geometry and facies distributions of the depositional systems that develop, within a certain time-interval, throughout a basin.

3.2.1 – Main sequence-stratigraphic concepts

Sequence stratigraphy (formerly "seismic stratigraphy", Vail et al., 1977; Wilgus et al., 1988) represents the main theoretical advancement of the 20th century in the study and interpretation of sedimentary successions, with practical consequences that were critical both for academic research and industrial applications.

Its main principle is that the primary control in the stacking pattern of a sedimentary succession (including the geometries and latero-vertical distributions of depositional systems) are primarily controlled by relative variations of the sealevel (rsl). These variations occur as a combination of eustasy and subsidence, causing changes in the space available for sedimentation ("accommodation") in time and along the depositional profile.

The fundamental unit for sequence stratigraphy is the depositional sequence, i.e., a stratigraphic unit bounded by unconformities (and their correlative conformities) formed during two successive relative sealevel falls (Van Wagoner et al., 1988).

Sequences are subdivided in systems tracts, i.e., packages of consanguineous depositional systems formed during a specific stage of the sealevel variation, and located in a specific position within the sequence; these are termed "lowstand" (LST), "transgressive" (TST) and "highstand" (HST) systems tracts; a further category of systems tract was introduced by Nummedal (2001), that is the "falling stage" systems tract (FSST), encompassing, when present, the upper part of the HST.

The composing elements of a sequence are depicted in **figure 3.1**, and are described below.

According to the classical model, developed on passive-margins successions and at the seismic scale (Vail et al., 1977), LSTs develop in the time interval during which the sealevel is at its minimum, when part, or all of the continental shelf is exposed, thus causing the formation of an erosional unconformity, a more or less abrupt forestepping of shallow-water depositional systems ("Prograding Lowstand Wedge"), and the accumulation of turbidites at the basin floor ("Basin Floor Fan").

TST form when rsl starts to rise with a significant rate. This rise causes depositional geometries to switch from a progradational to aggradational pattern (increased accomodation). At the same time, a greater area is made available for sedimentation on the continental shelf, due to the progressive encroachment of the shoreline on formerly-exposed sectors. Aggradational patterns are then associated with a progressive backstepping of depositional systems, and the development of condensed successions in the basinal areas.

The rate of rsl rise may then reach a critical threshold, past which sedimentation does not succeed in filling all of the accomodation space. This may occur in siliciclastic settings, with the drowning of deltaic systems and the sequestration of fluvial sediments in the alluvial plain; in carbonate settings, aggradation of the shelf may terminate when depth exceeds the limit below which carbonate communities flourish, typically related with light intensity on the seafloor (shelf drowning *sensu* Schlager, 2005, and references therein). This critical boundary is termed "Maximum Flooding Surface", and may be associated in marine settings with a basin-wide condensed succession, typically characterized by the formation of authigenic minerals, such as glauconite, or hard-ground surfaces.

HSSTs begin to develop when the rate of rsl rise gradually drops, and sedimentation may start over by filling of the accomodation space. Sediments once limited to the alluvial plain are free, or forced, to start over with prograding on the continental shelf. HSSTs typically display aggradational patterns, that may turn to progradational in the early stages of sea-level fall (orange boundary in **figure 3.1**). Due to the gradual reduction of accommodation space, progradational geometries might become dominant. This causes the formation of a "Falling Stage Systems Tract" (*sensu* Nummedal, 2001).

As soon as the rate of sea-level fall greatly exceeds subsidence rates, shelfal deposits are exposed and eroded, causing the development of an unconformity, and the development of a new sequence. As a consequence of erosion, the FSST may not be preserved.

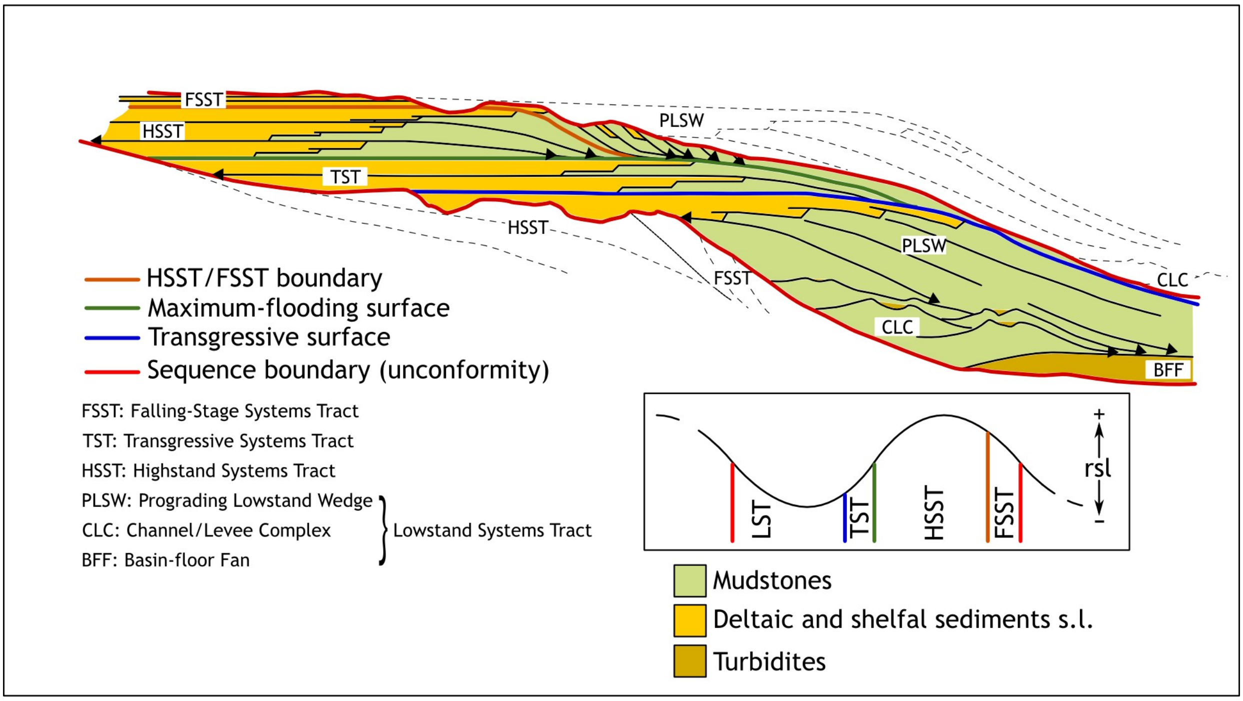

Figure 3.1 – Conceptual model of a 3rd order sequence (typically developed on vertical scales of hundreds of meters), based on seismic stratigraphy of passive margins; slightly modified from Mutti (1992) in order to include the FSST.

3.2.2 – Sequence-stratigraphic hierarchical subdivisions.

The concept of depositional sequence is scale-independent. Different "orders" were established on the basis of the physical and temporal scale during which sequences develop (Vail et al., 1977), that correspond to the different orders of rsl variations with time.

Up to six orders were established, depending on different controlling factors. Physical and temporal scales associated with the sequences decrease from the fist to the sixth order.

Higher order sequences (4th to 6th order) form under the control of eustatic variations, ultimately driven by high-frequency climate changes controlled by astronomical parameters (typically precession and eccentricity). Lower-order sequences are instead controlled by geodynamic parameters, such as continent formation and breakup, thermal subsidence in passive margins, and tectonic uplift in foreland basins (Vail et al., 1991; Mutti et al., 2009, their figure 26).

3.2.3 – High-resolution sequence stratigraphy

With the increase of resolution of seismic prospections, and the application of the sequence-stratigraphic concepts on exposed successions, more insight was provided in the stacking pattterns and significance of higher-order sequence-stratigraphic units.

Initially (Wilgus et al., 1988; Van Wagoner et al., 1990), the elementary sequence-stratigraphic units were envisaged in the "parasequences", i.e., small-scale (metric to decametric) stratigraphic units bounded by flooding surfaces.

Mutti et al. (1992, 1994) first observed that the elementary building blocks of sequence stratigraphy should be instead represented by elementary sequences, implying the need and possibility of defining sequence boundaries also in the higher-order sequence stratigraphic subdivisions.

The concept of "elementary depositional sequences" (EDS, op. Cit.; **figure 3.2**) was proposed, defined as the elementary mappable stratigraphic units expressing a regressive/transgressive cycle.

This concept was developed primarily from field research, founded on facies analysis and detailed mapping, in the exposed shallow-water successions of foreland basins. Facies analysis was considered as the primary tool to define, at the outcrop scale, the lateral shifting of the depositional systems in relation with the depositional profile, allowing the definition of sequence boundaries, flooding surfaces and systems tracts within elementary sequence boundaries. Detailed mapping, performed with the use of aerial photographs and field survey, substantiated the lateral continuity of the EDS in shelfal deposits.

3.2.4 – Foreland basin tectonics and sequence-stratigraphy

In foreland basin successions, sedimentation directly interacts with tectonics.

The activation and evolution of thrust fronts is primarily reflected in the development of basin-wide unconformities, and differential subsidence causes the formation of growth strata at the basin margins; at the same time, depocenters gradually subside, due to the combined effect of thrust and sediment load, and eventually shift with the advancement of thrust sheets.

In the SCPFB, the first description of these dynamics was provided by the concept of "progressive unconformity" (Riba, 1976), exemplified by a succession of stratigraphic units displaying an increase in dip from the younger to the older units; each unit was then separated from the other by an angular unconformity; Mutti et al. (1988), applied the concept of allogroups, or UBSU (unconformity-bounded stratigraphic units) to define the main tectono-stratigraphic units in a sequence-stratigraphic framework

In terms of scale, allogroups may represent 2nd and 3rd order sequences.

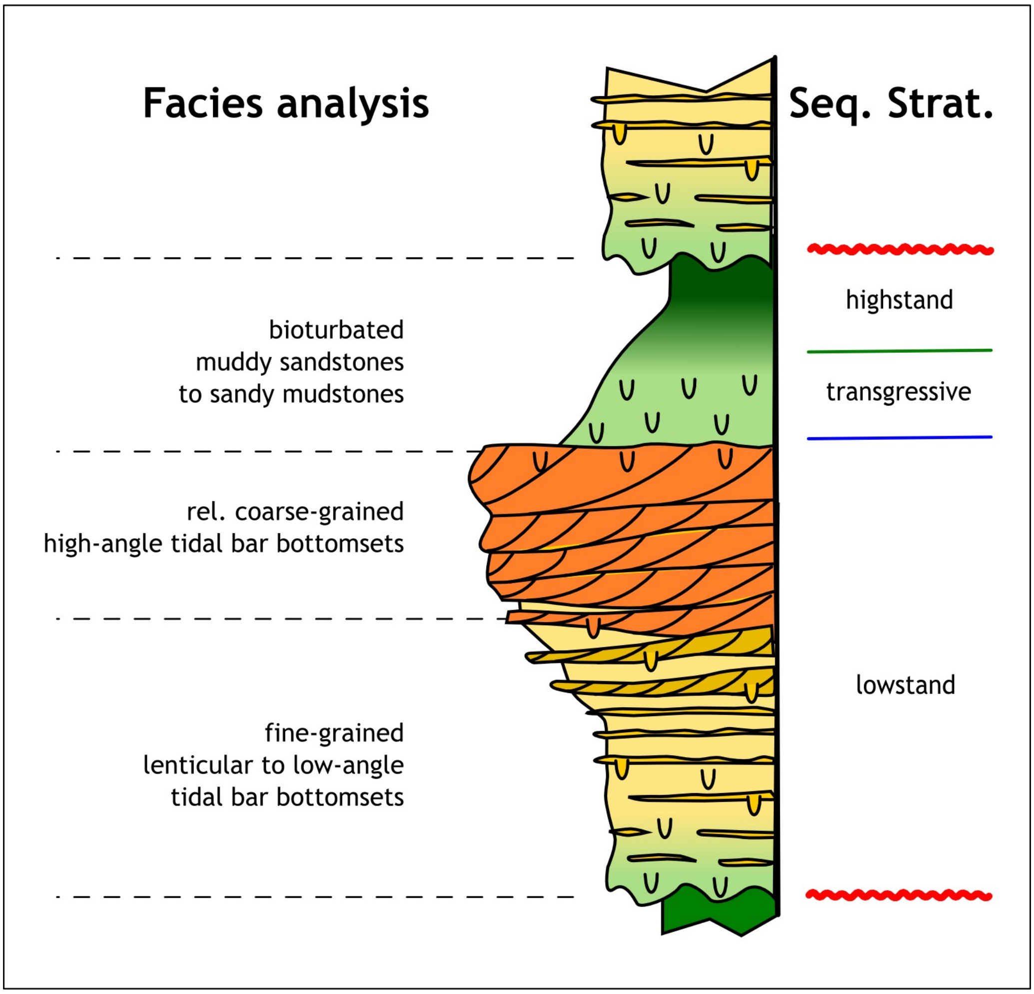

Figure 3.2 – Conceptual model of an EDS based on the tide-dominated deposits of the Lower Baronia Sandstones (Ager basin). These units typically develop over metric to decametric scale. Based on Mutti et al., 1985, 1994, 1996; see 4.2.1.5 for details concerning facies and facies associations.

3.2.5 – Sequence-stratigraphic interpretation of the marine foreland successions of the Tremp and Ager basins

The problems in the application of sequence-stratigraphic concepts in the study area are related with the co-occurence of eustatic cycles and subsidence variations (both positive and negative) driven by tectonics (e.g., Mutti & Sgavetti, 1987).

The problem is further complicated in the marine Ypresian of the Tremp basin, because of the co-occurrence of siliciclastic and carbonate deposits whose mutual relations are relatively complicated. The main problems concern difficulties in establishing the relative depth of the marginal and depocentral areas, the possible presence and significance of longitudinal morphological thresholds (e.g., a shelf margin in the southern ramp), the basically unknown sedimentation rates of both the deltaic and carbonate depositional systems that characterized this basin. The latter problem is mainly related with the applicability of modern analogues to depositional systems that are, both in the siliciclastic and carbonate realm, specific to a very peculiar geodynamic and climatic setting (foreland basin sedimentology during the greenhouse world of the Early Eocene).

Angella (1999) proposed a sequence-stratigraphic model mainly founded on a tectonic interpretation of the succession.

The author interpreted the main the carbonate banks of the southern ramp (see **2.4.5.1**; **4.3.1.6**; **4.4.1**) as progradational units formed in response to stages of uplift of the Montsec thrust. Basin-wide sea-level fall occurred concomitantly with the uplift.

The axial deltaic deposits similarly responded to uplift events, possibly in relation with tectonically-increased gradient of the fluvial systems, fed by northern and eastern sources.

This caused the deposition of widespread sandy deposits, deposited by bottom water hyperpicnal flows developed at the fluvial entry points (turbidite-like shelfal sandstone lobes, *sensu* Mutti et al., 1996, 2000, 2003; see also Mulder & Syvitski, 1995).

Given certain conditions (e.g., major floods, or entry points located closer to the carbonate ramp) these currents could have reached the lateral ramp, collecting and reworking bioclastic material.

During relative sea-level rise, deltaic systems gradually backstepped, as suggested by thinning- and fining-upwards packages of sandstone/mudstone beds.

With increased axial subsidence and/or sea-level rise, also the carbonate ramp could have backstepped.

Both siliciclastic and carbonate depositional systems were finally drowned by outer shelf mudstones during highstands. These probably were accumulated by background fluvial activity (hypopicnal plumes developed during periods of diminished fluvial activity, or distal equivalents of the sandstone lobes).

A similar approach in the interpretation of the margin-depocenter relations was followed by Waehry (1999).

This model, synthesized in **figure 3.3**, was followed for the sequence-stratigraphic subdivisions operated in the present work, although some horizons were correlated in a slightly different manner.

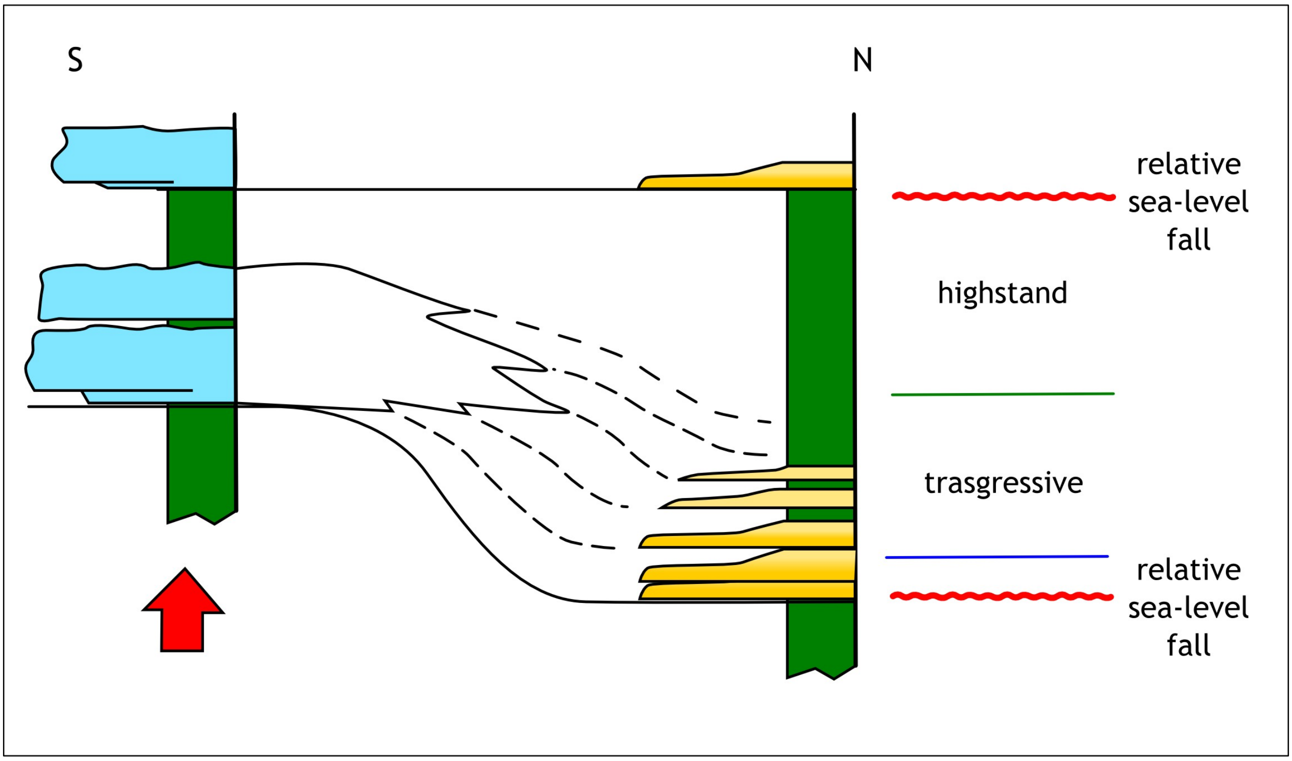

Figure 3.3 – Conceptual model of the sequence-stratigraphic implications of the margin/depocenter correlation in the Tremp basin based on Angella (1999).

3.3 – Isotope Stratigraphy

The geochemical investigation (chapter **5**) was performed in the field of stable isotopes of carbon and oxygen. Following the papers of Schmitz & Pujalte (2003, 2007), the location of the PETM in the Ager basin and in the southern Tremp basin was investigated; this because of the close stratigraphic position between the PETM isotopic anomaly and the base of the UTAG (**2.4.3**).

This part of the work required to extend the studied interval in the Paleocene of the Ager basin, and a basic isotopic characterization of this interval (**5.4**), in order to document the possible preservation of the isotopic signal. As a secondary outcome of this characterization, the isotopic signatures of some Paleocene units were used as a correlation tool to test some hypotheses in the N-S correlation within the Paleocene of the Ager basin (**2.3**; **5.5**).

Finally, the close stratigraphic position of some allogroup boundaries (lower and upper boundaries of the UTAG) with the PETM and ETM2 isotopic anomalies, and the development of long-term global climate changes during the formation of the studied successions were considered, in order to evaluate the potential role of climate trends and anomalies on the stratigraphy of the South-central Pyrenees. This side of the problem was mainly based on chronostratigraphic features, and a tentative isotope investigation of the southern carbonate ramp of the Temp basin was performed in order to verify the main chronological assumptions (chapter **5.6.2**).

The materials and methods of the geochemical analyses are treated in detail in **5.3**.

4 – FIELD DATA, FACIES ANALYSIS AND PHYSICAL STRATIGRAPHY

4.1 Measured sections

An overview of the measured sections, including some general stratigraphic remarks, is here provided. The same or equivalent logs, measured by former workers, are reported as well.

SECTION [4]

This section was measured along and in proximity ("Les Teuleres" outcrop) of the C-13 roadcut close to the village of La Baronia de Sant Hoisme.

It represents a time interval extending from the lower Danian to the lower Ypresian, and hosts a major hiatus close to its base (Middle Paleocene Unconformity, CHAP).

The section includes continental (and subordinate marine) deposits of Paleocene and Lower Ypresian age, and a marine succession of lower Ypresian age mainly represented by carbonate deposits of the Cadì fm. and hybrid arenites of the Lower Baronia fm.

The succession hosts three main sequences or allogroups that belong to the Lower Tremp-Ager Group (LTAG), the Upper Tremp-Ager Group (UTAG) and the Lower Figols Group (LFG).

Compare the lower part of this section (Paleocene) with Fontllonga section in Colombo & Cuevas, 1993 (including the lower Ypresian Cadì fm.) and the Lower Ypresian interval with the Ager section in Ferrer et al., 1973; Ager section in Mutti et al. (1994, plate II; section 5 in plate III); reference section in Ghielmi (1991); Ager section in Angella (1999).

SECTION [10]

This section was measured in proximity of a local relief named "Mas del Boix", about 2,5 Km east of section [4].

It represents a time interval included between the latest Thanetian and the earliest Ypresian and it hosts the LTAG\UTAG allogroup boundary.

SECTIONS [1, 2, 3, 5, 6, 7, 8, 9]

These sections only encompass the LFG sequence, and were measured in a relatively continuous outcrop belt from the "Barranco de Marcò" to the west and the eastern end of the cliff named "Les

Alteres".

Compare with the logs from the FG 1 stratigraphic cross-section in Ghielmi (1991), Mutti et al. (1994, plate III).

SECTION [11]

This is a very short log, measured only to verify the lateral continuity of the units exposed in section [10] in the most thinned sector of the Paleocene of the Ager basin, in proximity with the local culmination of the St. Mamet anticline, on a local relief named "Rocaspana", near the village of Peralba.

SECTION [12]

This is a composite section measured on both sides of the Rio Noguera Pallaresa in the northernmost reaches of the Ager syncline (close to the Ager/Temp/Balaguer crossroad). It hosts a thin continental succession, correlated in this work with the lower portion of section [4], that comprises the Middle Paleocene Unconformity (see chapters **5.x** and **6.x** CHAP), and a marine succession of Lower Ypresian age; this is in turn unconformably overlain by middle/upper Ypresian deposits of the Upper Figols Group (UFG).

The sequence stratigraphic subdivision of this interval is discussed in chapter **6.x CHAP**, but it clearly encompass part of the LTAG, and part of the UTAG.

The only formerly published versions of this section are apparently the ones from Ferrer et al. (1973) and Mutti et al. (1985); both papers refer to it as the "Pasarela Section", and only document its lower portion.

SECTION [13, 14]

This is a composite section measured on both sides of the Rio Noguera Ribagorçana, in the locality named "Congost de Mont Rebei". It hosts a thin continental succession, including the top of the LTAG, and the whole UTAG and LFG, expressed by prevalently marine carbonatic and muddy deposits.

Compare with the Ribagorçana section in Waehry (1999) and Mont Rebei section in Baceta et al. (2011).

SECTION [15]

It is exposed along the roadcut between between the villages of St. Esteve de la Sarga and Castellnou del Montsec, and was measured only to check on thicknesses in the lower interval of the

UTAG as observed in section [13, 14].

SECTION [16]

This is a composite section measured between the villages of Alsina and Moror. It encompasses a marine, mainly carbonatic succession, including the whole UTAG and LFG, and is treated in detail in CHAP of this chapter.

Compare with Alsina section in Waehry (1999).

SECTION [17]

This is a composite section measured along the relief comprised between the villages of Guardia de Noguera and Mur, an it hosts a marine carbonate/muddy succession, comprising most of the UTAG and the whole LFG.

Compare with section 6 in Fonnesu (1984) and Guardia de Noguera section in Angella (1999).

SECTION [18]

This section was measured along the hill named “Serra Puit”, and is mainly represented by marine deposits (mudstones and subordinate carbonate and mixed carbonate-siliciclastic beds). It includes part of the UTAG and LFG.

Compare with section 7 in Fonnesu (1984) and Serra Puit section in Angella (1999).

SECTION [19]

This is a composite section measured between the villages of Puigmaçana and Villamolat.

The upper portion of the succession, above the UTAG\LFG boundary, is poorly exposed, so correlations in this interval are not reliable; nevertheless, the overall thickness of the LFG was reliably measured. Section [19] hosts a muddy succession with subordinate sandstones and sandy limestones, comprising most of the UTAG (the location of UTAG base is uncertain) and the LFG.

Compare with Puigmaçana section in Angella (1999).

SECTION [20]

This is a composite section equivalent to the classic “Tremp section”.

The lower portion was measured in the Rio Palau incision, west of Palau de Noguera, along the “Tossal” hill and the C-1311 roadcut (between Tremp and the Montllobat pass) in its upper part.

It hosts a marine muddy succession, with the exception of its lowermost interval represented by continental deposits. The muddy succession is punctuated by sandstone and mixed carbonate-siliciclastic beds, and subordinate limestones and sandy limestones.

This section encompasses the full UTAG and LFG, but wide intervals are incomplete in the upper portion of UTAG because of plant cover.

Compare with sections 15 and 17 in Fonnesu (1984), Tremp section in Mutti et al. (1988), Eichenseer & Luterbacher (1992) and Angella (1999).

SECTION [21]

This section was measured in the “Barranc de Forats” incision, north of the C-1311 road.

It only encompasses the lower UTAG sequences, and it hosts a muddy succession similar to the one of section [20], including the basal continental deposits.

Compare with Eroles section in Angella (1999).

SECTION [22]

This section was measured in the “Barranc de Tendrui” incision, north of the village of Tendrui.

It encompasses the same stratigraphic interval of section [21].

Compare with section 23 in Fonnesu (1984) and S. Adrià section in Angella (1999).

SECTION [23]

This section was measured along a cliff exposure between the villages of Arèn and Esplugafreda.

The lower, continental interval of the succession, including the upper part of the LTAG, is taken from Schmitz & Pujalte (2005) and Baceta et al. (2011). The upper, marine interval, mainly represented by limestone bodies and mudstones, with subordinate sandy deposits, is unconformably overlain by upper Eocene continental deposits, and it only encompasses the UTAG1 and2 sequences.

4.2 – <u>Lithostratigraphy and Facies</u>

The main lithostratigraphic subdivisions, both formal and informal, were anticipated in chapters **2.3** and **2.4**. An informal lithostratigraphic subdivision will be proposed here in order to describe some intervals (e.g., the Paleocene of the Ager basin).

4.2.1 – Ager basin

The main lithostratigraphic subdivisions for Ager basin are adapted from different former papers (Mutti et al., 1973; 1985; Colombo & Cuevas, 1993, and references therein; Rossi, 1997, and references therein; Rosell, 2001, and references therein).

Although the following units were not ordered by a uniform, formal criterion, they provide a good reference for describing the great lithological variety encountered in the studied successions.

These units are, from the base to the top, the Vallcebre Formation, the Upper Red Garumnian, the Cadì Formation and the Lower Baronia Sandstones.

4.2.1.1 – *Vallcebre Formation*

The base of the studied interval (section [4]) is equivalent to the base of the Vallcebre fm. Detailed descriptions of this unit in the Ager basin are provided by Colombo & Cuevas (1993, “Millà fm.”).

It is represented by a package of white, grey and pink micrites, organized in decimetric and centimetric beds (**figure 4.1**). The typical weathering color is dark blue. These beds are in some cases finely-laminated, but more commonly massive and bioturbated. Carophyte fossils are relatively common, indicating that this unit formed in a lacustrine setting (Colombo & Cuevas, 1993). In the middle-upper portion of the Vallcebre Formation, micritic breccia layers are very common, in some cases associated with incipient pedogenic features (e.g. red clay horizons); these features were interpreted as the product of karst/pedogenic processes (op. cit.).

The Vallcebre fm. reaches its maximum thickness in the southern Ager basin in proximity of the Rio Noguera Pallaresa (~70m), and thins out to the west.

A possible equivalent of the Vallcebre fm. (cf. Rosell et al., 2001; **figure 2.7/2** and **4.3**) is exposed in the northern succession. It displays many similar lithological features (although the presence of carophytes wasn't ascertained), including the micritic breccia layers; bedding is less defined, and calcite-filled fractures are commonly found. This unit is delimited at its base by a tectonic contact, and it is ~7m-thick.

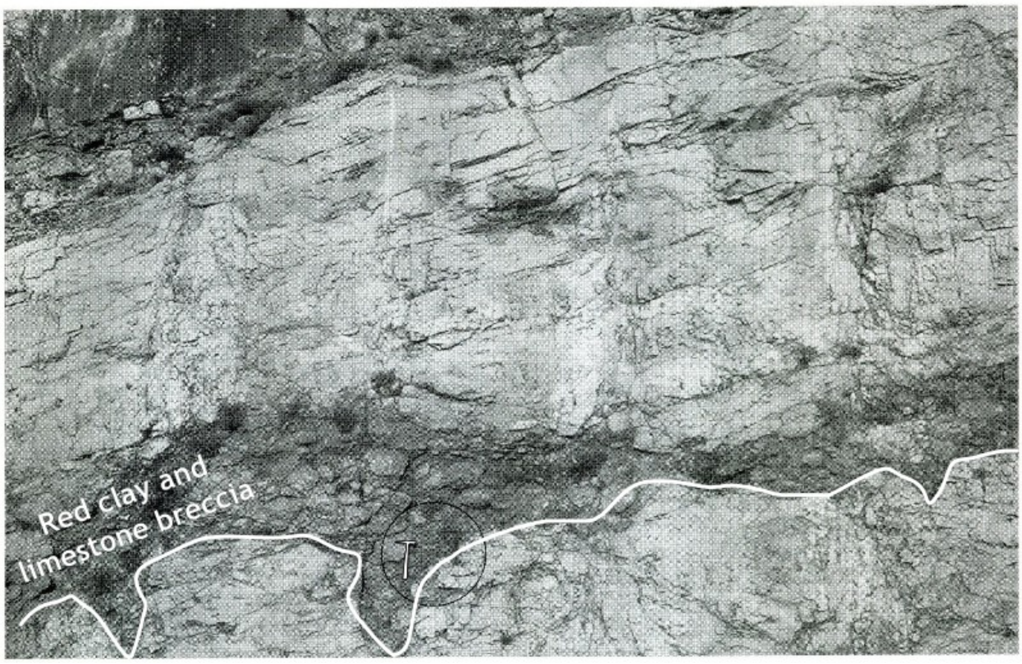

Figure 4.1 - Close-up view of the main karst surface within the Vallcebre fm. (picture from Colobo & Cuevas)

4.2.1.2 – *Upper Red Garumnian*

This unit (Rosell, 1965) extends between the top of the Vallcebre fm. and the base of the lower Ypresian marine deposits **(figure 4.2).** It can be subdivided in 6 informal units.

UNIT URG 1 – Red beds

In the southern Ager basin, it is represented by a succession of dark red mudstones, with subordinate sandstone beds and rare grey or yellow mudstone layers. This interval is roughly equivalent to Sequences 1 of Rossi (1997). In the northern Ager basin, a similar unit is recognized between the top of the (presumed) Vallcebre fm. and the unconformable contact with the lower Ypresian deposits; its equivalence with Unit URG1 is therefore inferred (cf. Rosell et al., 2001). In the two different locations, however, some substantial differences were observed.

Dark red mudstones of the southern Ager basin are mainly composed of clay, with a variable content of silt and sand. They show a distinctive blue-grey mottling and are locally rich in gypsum nodules or veins. Bedding surfaces can be recognized only where a lithological contrast is present (e.g. with sandstone or differently colored mudstones).

Sandstones are fine-grained (fine sandstones and subordinate very-fine sandstones), thin-bedded (individual beds never exceed 50-60 cm; most beds are less than 20dm-thick) and lenticular, with the exception of a very continuous (up to the Coll d'Orenga sector, to the east), sheet-like package of 5-6 sandstone beds in the middle portion of Unit URG 1.

Sandstone beds display yellow and red color, in some cases with blue and yellow mottling, and are frequently bioturbated (in-situ *Microcodium*; Rossi, 1997); horizontal laminations are rarely observed.

A couple of yellow mudstone layers were observed in the middle and upper portion of this unit. The lower one is located in the middle portion of Unit URG 1, and hosts a very thin grey/green mudstone horizon; the upper one is located in the upper portion of Unit URG 1 and it includes a sandy siltstone; this horizon as well is of continuous for some kilometers. Yellow mudstones are commonly characterized by a grey mottling.

In the northern succession (section [12]; **figure 4.3**), dark-red mudstones are locally rich in yellow and white micrite nodules; in the upper portion of Unit URG1, they are also sand-rich and pebbly.

Still close to the top of this unit, up to four conglomerate layers are present (Rosell et al., 2001, references therein). These conglomerates display a lenticular geometry, with the thickness of individual beds never exceeding 30 cm; they are almost entirely composed of subangular limestone clasts. Above and below these beds, two very thin, hardened, yellow mudstone horizons are present.

Unit URG 1 is approximately 50m-thick in both exposures (sections [4] and [12]). In the southern Ager basin, however, it pinches out to the east and west (Rossi, 1997).

Facies interpretation

The succession represented Unit URG 1 in the southern Ager basin clearly represents an alluvial plain facies association (Rossi, 1997). Red mudstones represent paleosols (with or without carbonate soil nodules) formed in a relatively arid climate (cf. Kraus & Riggins, 2007; Schmitz & Pujalte, 2003), with poorly-developed fluvial systems (lenticular thin-bedded sandstones). The more continuous, sheet-like package of sandstones might indicate a period of increased fluvial activity. Rossi (1997) interpreted these deposits as crevasse-splays; alternatively, this body could be related with the conglomerates exposed in the northern succession. These were interpreted as Montsec-sourced proximal fan deposits (Rosell et al., 2001, and references therein); the sheet sandstones in the southern succession could actually represent a distal fringe of this south-vergent discharge system.

Figure 4.2 - panoramic view of the Thanetian deposits along the southern limb of the Ager Syncline, "Les Teuleres" outcrop

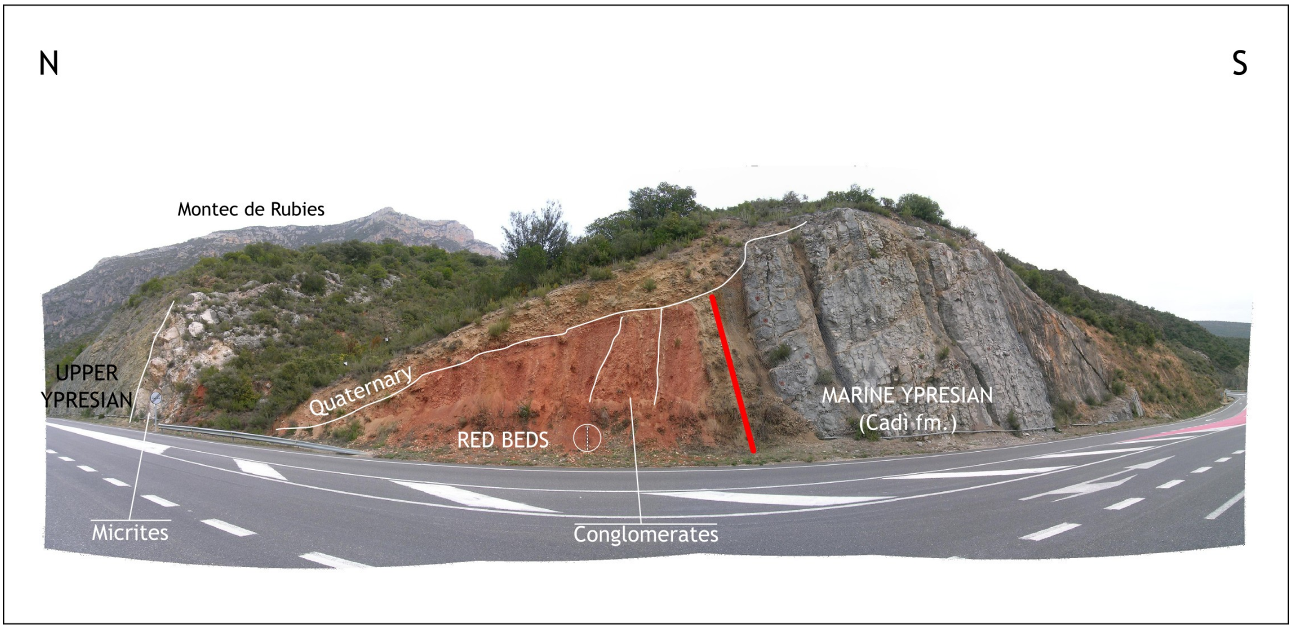

Figure 4.3 - Red beds exposed along the northern limb of the Ager syncline; notice that the micrites to the left are in tectonic contact with upper Ypresian deposits; the thick red line indicates the angular unconformity between "Garumnian" and "Ilerdian" deposits

UNIT URG 2 – Sandstones and varicolored mudstones

This unit is well exposed from section [4], where it is ~50m-thick, up to the Coll d'Orenga sector to the east, and it is roughly equivalent to Sequence 2 from Rossi (1997).

It is represented by an interval of lenticular sandstones, locally very coarse, associated with yellow, grey, brown, red, pink and purple mudstones, and subordinate micritic layers (**figure 4.4**).

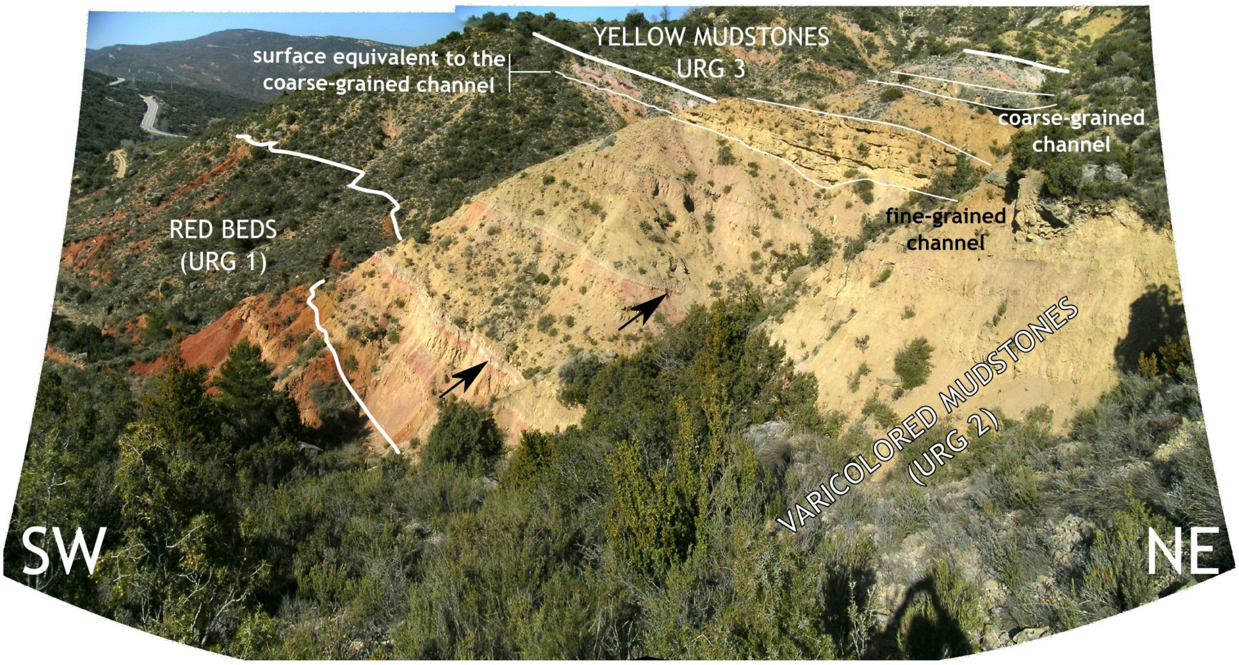

Figure 4.4 - View of Unit URG 2, "Les Teuleres" outcrop. Notice the cyclical organization of the varicolored mudstones; black arrows indicate the "pseudogonglomeratic" micritic layers.

Mudstones

Yellow mudstones are the main constituent of this interval. They are characterized by an intense grey and purple mottling and display a siltier composition if compared with the underlying red beds.

Grey mudstones are represented by a relatively thick horizon (~7 m) in the lower-middle portion of Unit URG 2, and by a number of thin layers (commonly a few cm-thick) interbedded within the upper portion of the unit, apparently related with pink mudstones and micritic layers. They are either non-mottled or yellow-mottled.

Brown (or yellow-brown) mudstones are located at the base of Unit URG2, where they contain abundant gypsum veins and display a variegated mottling, and in the middle of the Unit, where they are characterized by grey mottling.

Red mudstones occur as a thin (a few dm-thick) layer close to the top of the Unit, and do not display significant features.

Pink mudstones, although poorly significant in thickness, are highlighted within the succession because of their association with micritic/carbonatic *s.l.* layers. They occur either below the “pseudoconglomeratic” micritic layers (see below), or at the top of Unit URG 2, where they are represented by a few m-thick horizon at the top of the coarsest sandstone bed in this unit; this horizon is characterized by an hardened erosional profile, a sharp top, and an abundant content of $CaCO_3$.

Purple mudstones are rarely encountered, in the lower and intermediate portion of Unit URG 2. They display grey/blue or yellow mottling, in some cases very intense, and may be a carbonate-poor equivalent of the pink mudstones.

Sandstones

URG 2 is the most sandstone-rich unit within the Upper Red Garumnian, .

Most of these sandstones are characterized by yellow color, fine grain-size and a very limited areal extent. In the lower half of this unit they occur as individual lenticular beds, continuous over a few tens of meters, with maximum thicknesses not exceeding 40-50 cm, and average thickness ranging between 10 and 20 cm; normal grading was observed in some of these beds; a pink-purple mottling is in some cases present.

In the upper half of Unit URG 2, sandstones are organized in larger lenticular bodies, with concave base and flat top, composed of amalgamated, fine to very fine sand beds, locally including silty and/or muddy intercalations (commonly yellow or grey). Where amalgamation is less developed, individual sandstone beds display a maximum thickness of 20-30 cm. Current laminations (megaripples) are sometimes found within these beds, and display roughly east- and west-directed paleocurrents.

In the uppermost portion of Unit URG 2, a coarser unit is found. It is a few m-thick, medium to very-coarse pebbly sandstone (coarser at the top), resulting from the lateral amalgamation of lenticular bodies and continuous throughout the south-eastern sector of the basin; the individual bodies that compose this unit display a lateral extension in the order of some tens of meters. Similarly to the yellow sandstones described above, they are in turn composed of many amalgamated decimetric beds; mudstone intercalations (commonly grey) can be locally observed, typically away from the thinned borders of the lenticular bodies, where internal stratifications may hardly be recognized.

This body displays a sharp lithological contrast, since it is characterized by a blue weathered color, and it is topped by a hardened horizon of pink mudstones (se above).

Micrites

Micrite beds are relatively abundant within Unit URG 2. They commonly occur in lenticular beds, not thicker than ~10 cm. They are yellowish or white beds, displaying sharp base and top, devoid of macroscopic structures; frequently, they are characterized by a characteristic diagenetic nodular/botryoidal texture that affects the upper portion of originally massive micrites; in some cases, the whole bed is nodularized. These beds were in fact named “pseudoconglomeratic limestones” (*sensu* Freytet & Plaziat, 1982; in Rossi, 1997), and were interpreted as palustrine carbonates which underwent pedogenic processes.

The pseudoconglomeratic micrites have been observed to commonly occur within a lower, pink mudstone and an upper, grey horizon; unaltered micrites are more commonly found within grey horizons. This kind of succession is repeated cyclically within the yellow mudstones of Unit 2 (see **figure 4.4**). With minor changes (the micritic layer may be missing), these cycles are laterally continuous to the east; to the west, they correlate with lacustrine deposits (Rossi, 1997).

Facies interpretations

This succession of varicolored mudstones (paleosols) clearly indicates a significant change from the lower, monotonous succession of red paleosols. Following the guidelines proposed by Kraus & Riggins (2007) for paleosol interpretation, yellow, pink-purple and grey paleosols can be associated with increasing moisture conditions (or less efficient drainage). The development of palustrine to lacustrine deposits throughout the basin within this interval (Rossi, 1997) supports this interpretation. The apparent cyclical stacking of pink paleosols, palustrine micrites and grey paleosols might be related with cycles of flooding and abandonment; the yellow paloesols might instead indicate the re-establishment of relatively dry or sub-humid conditions.

The sandstones represent channelized fluvial deposits (Rossi, 1997). Most of these bodies develop concomitantly with color shifts in the paleosol succession, from yellow to purple or grey. This suggests that fluvial activity could have been enhanced in this interval under a climatic forcing (i.e., increased precipitations) better than in response to a relative sea-level variation (e.g. lowstand).

UNIT URG 3 – yellow mudstones and evaporites

This is a ~200m-thick unit, which includes a poorly-exposed interval, characterized by a dominant yellow color of the mudstones, scarcity of sandstone beds, and by the presence of evaporitic and subordinate micritic and dolomitic layers in its upper portion. It roughly corresponds with Sequences 3 to 7 of Rossi (1997).

Mudstones

Yellow mudstones are substantially similar to the ones in Unit URG2, and they are apparently the main constituent of this succession; however, in the lower and upper portion of the exposure, where plant cover is less pronounced, a varicolored succession was observed; the cyclical stacking of the color bands, and their lateral continuity, suggests that this organization may persist at least in part of the poorly-exposed intervals.

Similarly to Unit URG2, these cycles display a lower, red or light red interval, and an upper grey interval; however, limestone intercalations are rare; the "pseudoconglomeratic" fabric is here absent. A brown interval may be present below the red one.

In the middle Unit URG3, some horizons of grey mudstones occur in relation with evaporitic deposits, and they are rich in nodules and gypsum veins.

Finally, thin intercalations of dark mudstones rich in organic matter are present within the evaporitic beds at the top of Unit URG3.

Micrites

In the upper Unit URG 3, a few-m-thick, lenticular package of micrites (**figure 4.5**) is exposed below the uppermost evaporitic interval. It is constituted of grey-blue (lower) to dark yellow (upper) micrites, organized in centimetric and decimetric beds. It formed above an horizon of red mudstones of great lateral continuity; the micrites are instead limited to the central and western sector, where they pass to coastal deposits (Rossi, 1997).

Evaporites

According to former workers (Colombo & Cuevas, 1993; Rossi, 1997), evaporites in the Paleocene of the Ager basin are limited to the subsiding sector between the Millà and St. Mamet anticlines (section [4]); to the west, they are substituted by peritidal carbonates and sabkha dolomites (Rossi, 1993).

The evaporites encountered in section [4], in the intermediate and upper portion of Unit 3, are the same described by Colombo & Cuevas (1993), and display massive to laminar and nodular textures (**figure 4.6**); in the eastern portion of the "Les Teuleres" exposure, they pass to a muddy facies with abundant scattered gypsum crystals and gypsum veins.

Gypsum beds are organized in packages composed of decimetric to metric beds, seldom interbedded with grey or dark mudstones.

The upper evaporitic interval includes at its base and top some thin (commonly decimetric) white-yellow carbonate beds. These beds, displaying a significant dolomite content, probably correspond with the "peritidal" sabkha deposits reported by Rossi (1997), that constitute the western equivalents of the gypsum beds.

Figure 4.5 - Micritic horizon close to the top of Unit URG 3 (roughly 3 m thick);

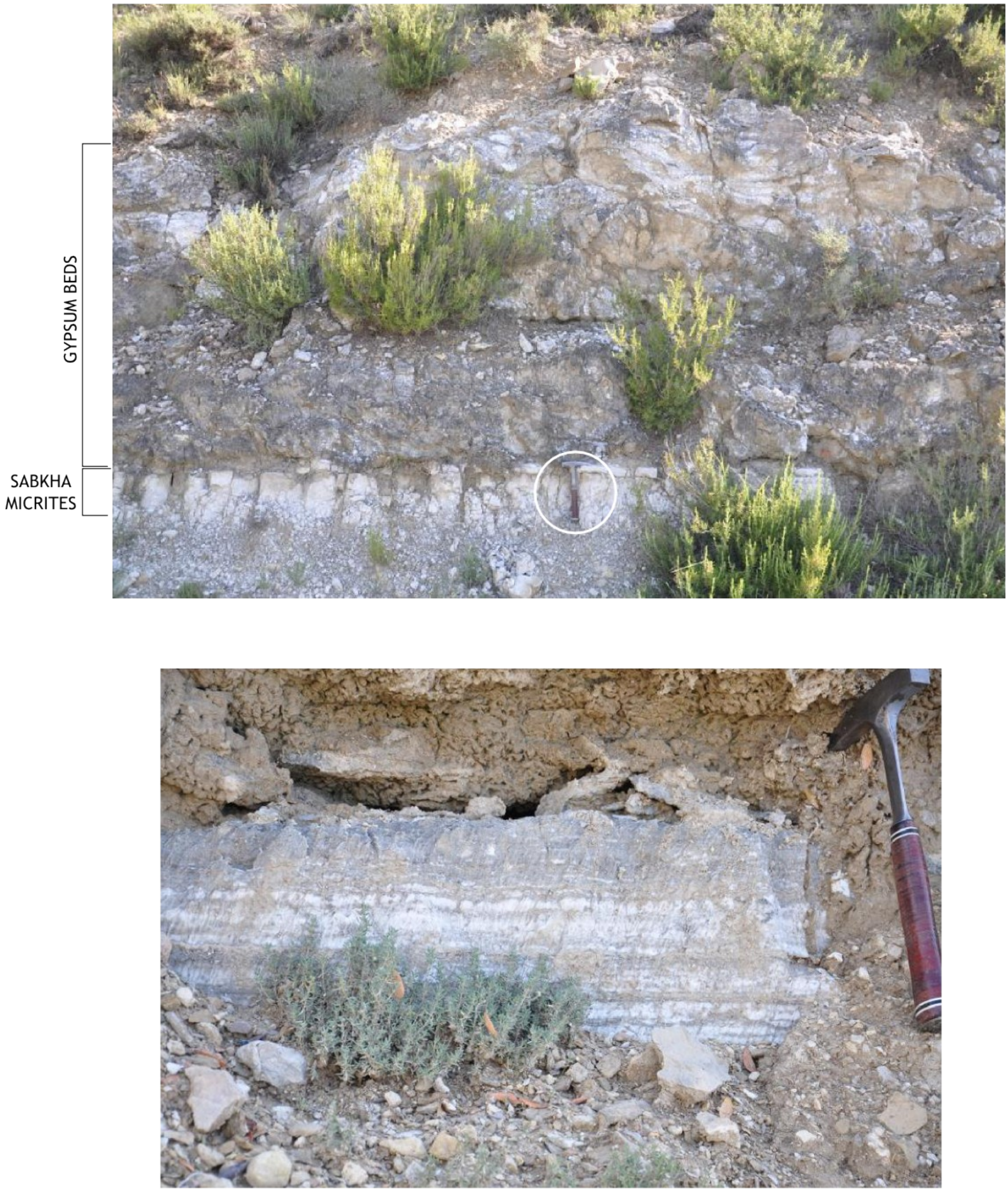

Figure 4.6 - Evaporite horizons in the upper portion of Unit URG 3

Sandstones

Sandstones only occur in the lower interval of Unit URG 3 (although more sandstone beds could be present in the poorly-exposed interval; however, the presence of stratigraphically-significant sandstone bodies in this unit can be excluded). They are substantially similar to the individual, fine-grained lenticular sandstone beds in the lower portion of Unit URG 2 (see above), with maximum thickness ranging between a few cm to 20-30 cm.

Facies interpretations

Starting from the "humid interval" represented by Unit URG 2, Unit URG 3 indicates a transition to a relatively more arid climate. This is testified by the abundance of yellow paleosols, and the occurrence, on top of the unit, of evaporitic layers, interpreted as a sabkha succession by Rossi (1997). The apparent cyclical stacking of brown, red and yellow paleosols recalls the Thanetian deposits described in the Esplugafreda section (section [23]; see **4.3.1.2**) by Schmitz & Pujalte (2003), Pujalte & Schmitz (2005) and Baceta et al. (2011), where an alternation of nodular and non-nodular red paleosols was interpreted as an effect of cyclical variations in soil moisture.

UNIT URG 4 – marine carbonates

This unit is equivalent to Sequence 8 of Rossi (1997), and is included in sections [4], [10] and [11] (only partially exposed). It is mainly composed of shallow-marine calcarenitic, muddy and micritic deposits, and its top is delimited by a surface of subaerial exposure (Rossi, 1997). A sandy, cross-bedded unit is locally included within the calcarenitic succession.

Mudstones

Mudstones of Unit URG4 are characterized by a grey color and abundant macrofossil content, mainly represented by oyster shells, both scattered and grouped in patches; plant remains are commonly found.

Calcarenites

These are mainly represented by three main wackestone/packstone bodies, characterized by an abundant content in miliolids, gastropods and lamellibranchs (almost exclusively oysters, concentrated in distinct layers). The thickness of these bodies ranges from ~4,5m to ~1,5m, and they are disposed in a thinning-upwards order; they also thin out to the east; anyway, they can be followed throughout the whole southern Ager basin (Colombo & Cuevas, 1993; Rossi, 1997; **figures 4.7**, **4.8** and **4.40**); to the west, they correlate with grainstone/packstone beds rich in glomalveolinids (Rossi, 1997).

Each of these main bodies is horizontally stratified; bedding is evidenced by alternations of more or less muddy intervals.

Most of these beds are intensely bioturbated, but they locally preserve some depositional structures, such as thin wavy to oblique laminations.

A couple of decimetric grainstone/packstone layers with locally abundant glomalveolinids were observed in the upper portion of Unit URG 4. These beds range from 30 to 50 cm in thickness, and display sharp base and top and an overall tabular geometry at least between section [4] and [10].

Figure 4.7 - Upper Thanetian fine-grained calcarenitic deposits and mudstones; Unit URG 4; C-13 roadcut near La Baronia de Sant Hoisme

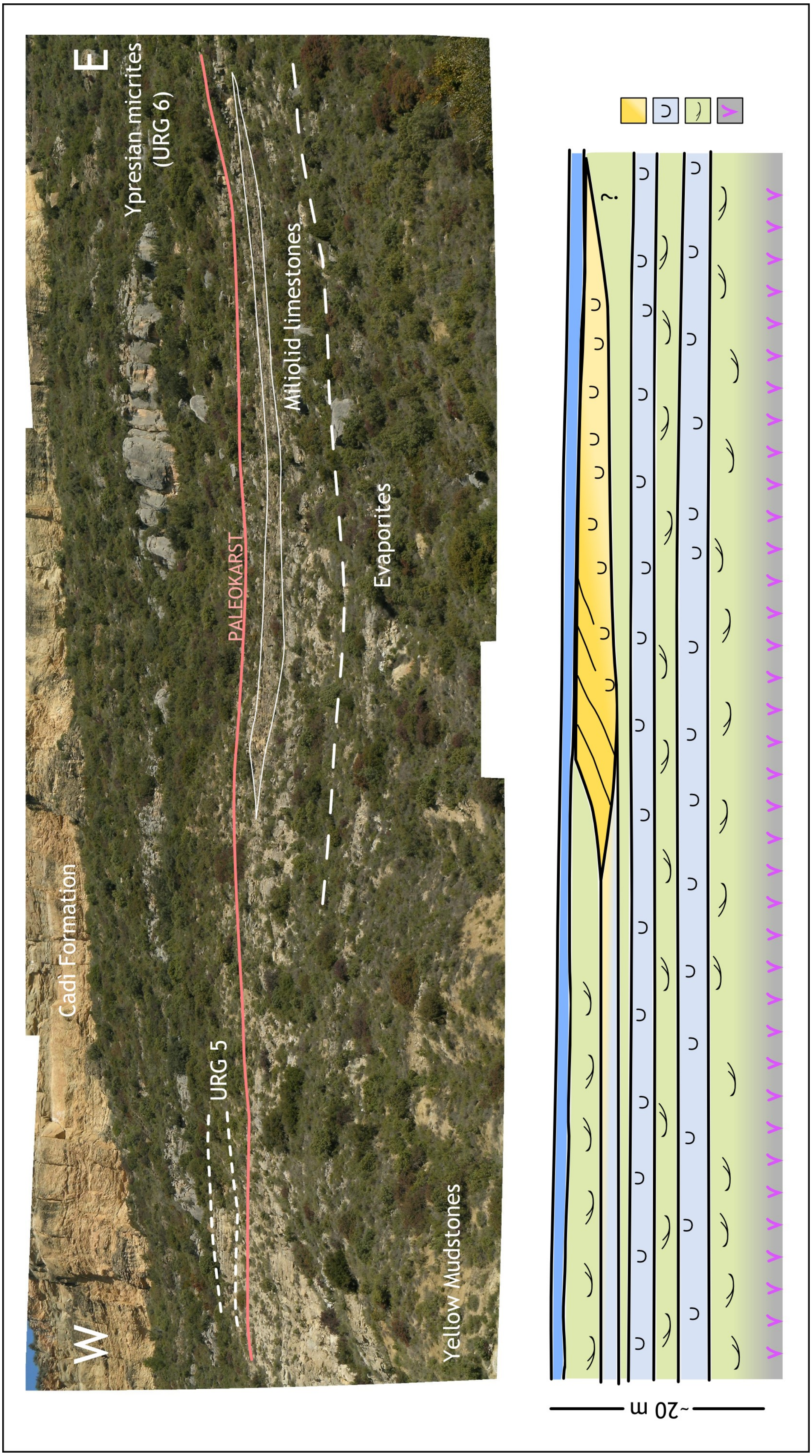
W
E
Ypresian micrites
(URG 6)
Miliolid limestones
Evaporites
PALEOKARST
Cadí Formation
URG 5
Yellow Mudstones
?
~20 m

Figure 4.8 (former page) – Tentative reconstruction of the stratigraphic relationships intercurring between the calcarenites and sandstones in Unit URG4

Sandstones

In the “Les Teuleres” outcrop (section [4]), the upper portion of the calcarenitic succession hosts a lenticular sandstone body characterized by W-dipping large-scale oblique to tangential stratifications (**figure 4.8**). Above the C-13 road cut, i.e., a few hundred meters to the west, this body is missing, but the upper calcarenitic layers locally display an abundant sand content; moreover, this body is delimited to the top of by the lower grainstone layer, apparently missing on the road-cut exposure.

This unit was only partially studied; it is a few m-thick bar mainly composed by fine sand and fine skeletal debris; bioturbation is abundant throughout the whole body.

It shows an overall bar geometry, with a lateral extension in the E-W direction of some tens of meters.

Micrites

Micrites are organized in beds of decimetric thickness, and occupy the upper portion of Unit URG 4. They display a white-grey color that turns to yellow-brown at the top of the unit. Marine fossils, mainly miliolids and a few gastropods have been observed within most of these beds in section [4], but in section [10] the uppermost micritic beds are apparently devoid of fossils. They are also characterized by micritic breccia horizons and abundant bioerosional structures (cf. *Microcodium*); these features were formerly interpreted as the product of karstification of a coastal carbonate succession (Rossi, 1997; **figure 4.9**).

Facies interpretations

The “miliolid limestones” record a transgressive event affecting the entire Ager basin. They were interpreted by Rossi (1997) as intertidal deposits; the common occurrence of miliolids and oyster shells suggest a lagoonal setting for the deposition of these beds. The occurrence of sandstones in the upper portion of this unit might be related with the conclusion of the transgression and the beginning of a regressive trend, that ultimately brought to the subaerial exposure of this shallow-marine succession (karst surface of Rossi, 1997).

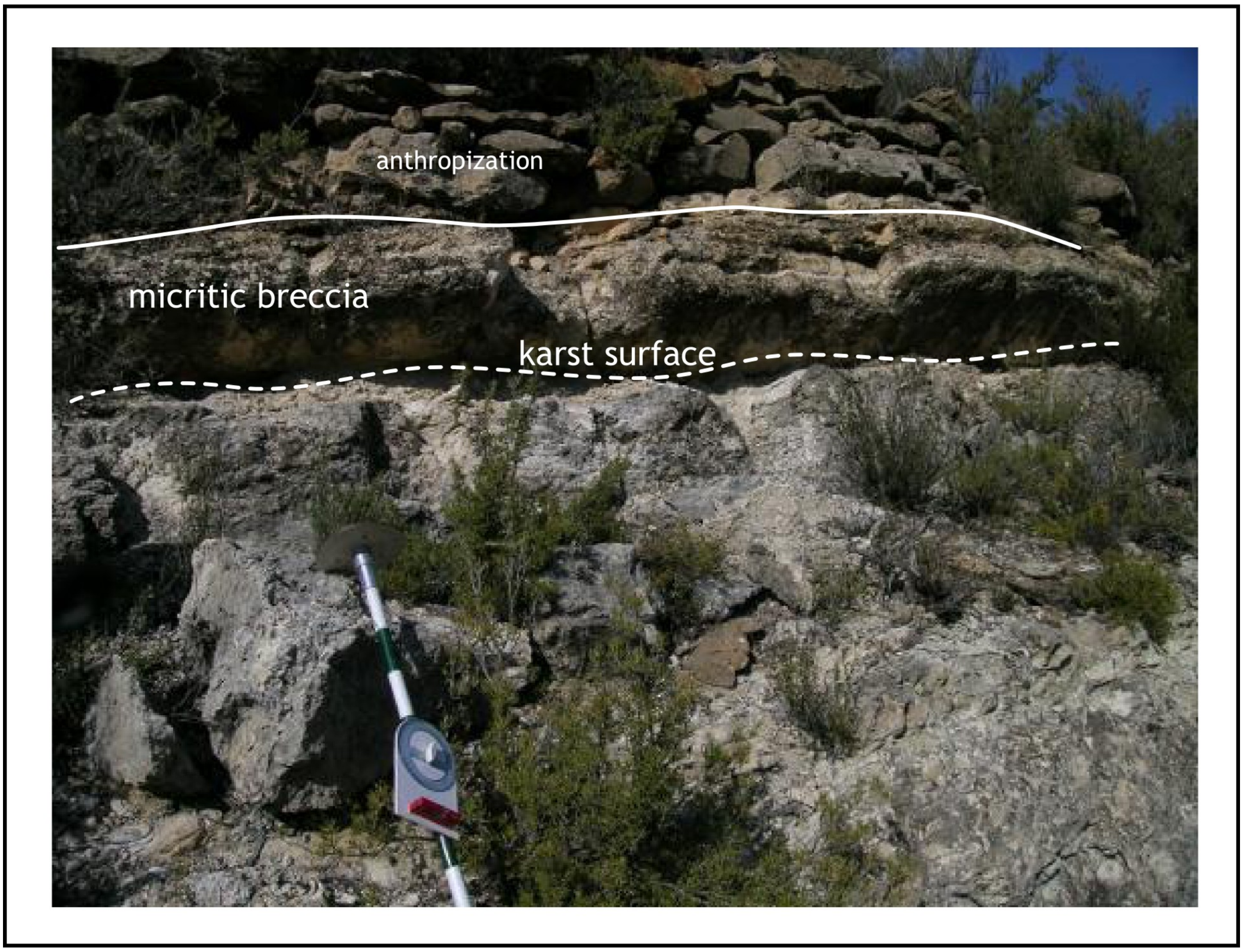

Figure 4.9 - Surface of subaerial exposure on top of Unit URG 4; section [10]

UNIT URG 5 – deltaic sandstones

This unit is exposed within two covered intervals that separate it from units 4 and 6, and it is mainly composed of sandstones. According to the 1:25000 geological map of the Institut Cartogràfic de Catalunya, the covered intervals should be represented by red mudstones; the lower one, whose upper portion was encountered in section [10], is represented by grey-yellow mudstones just below the contact with the sandstone beds.

This unit was studied in detail in sections [4] and [10] (**figure 4.10**). In section [11] it is not exposed, but sandstone blocks were found within the plant cover, thus testifying its presence also in the innermost and narrower sectors of the basin (**figure 4.40).** It is composed by a lower, relatively coarser package of amalgamated lenticular bodies, and an upper, finer-grained and thinner-bedded interval only exposed in section [4]; here, the whole succession is about 25m-thick.

The whole succession contains locally abundant plant fragments; no fossils were encountered.

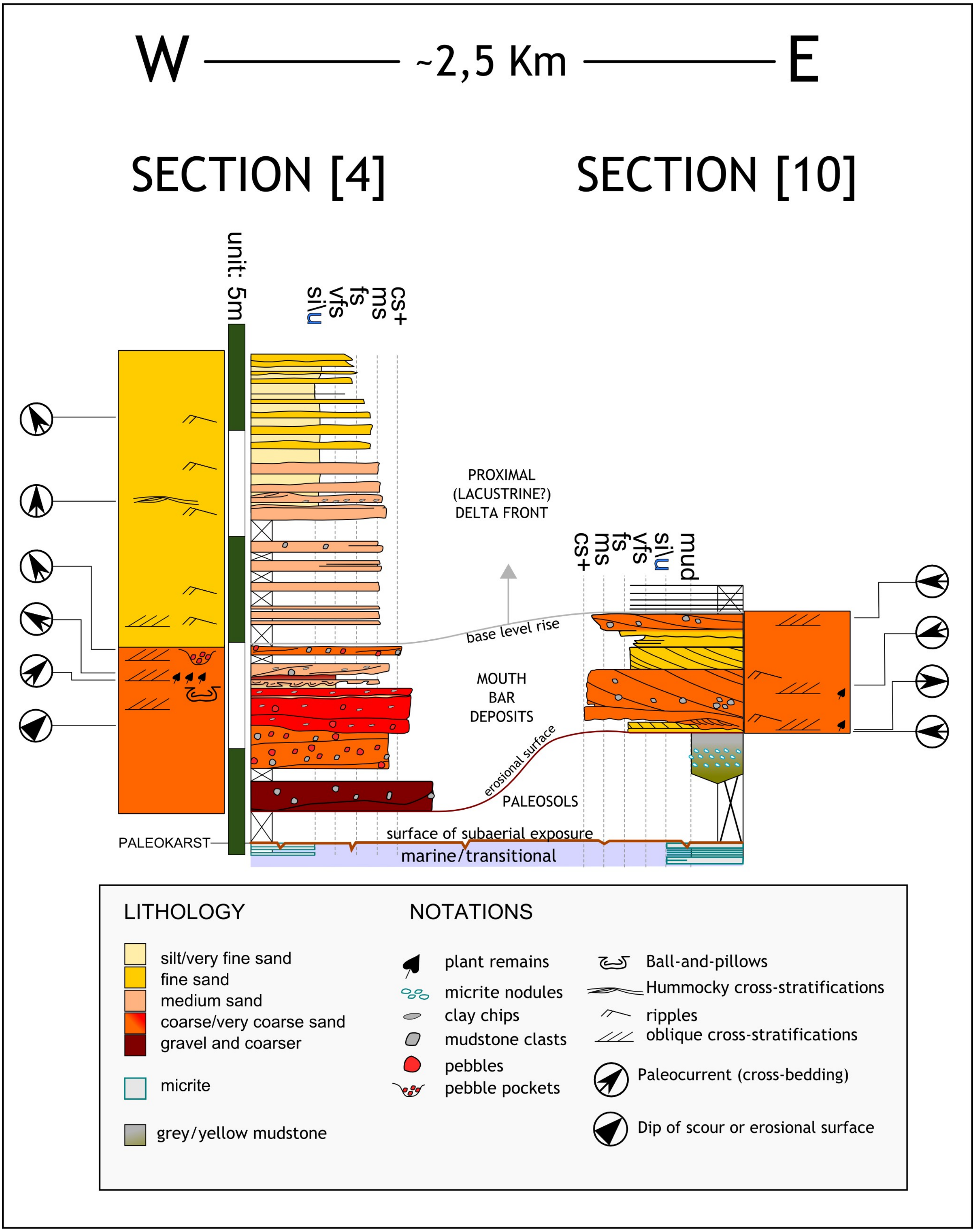

Figure 4.10 - Detailed logs of Unit URG 5 (see text in the next pages)

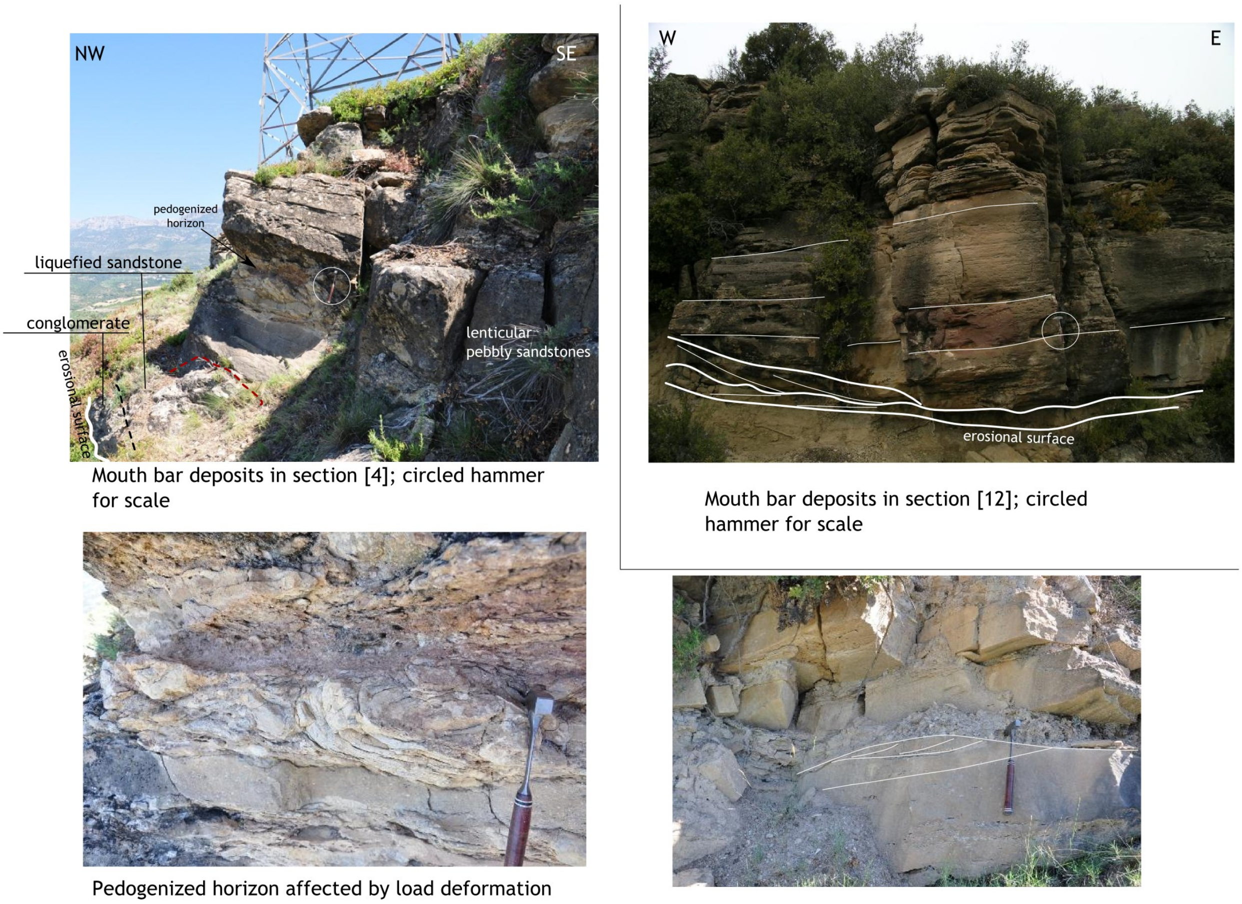

Mouth bar deposits in section [4]; circled hammer for scale

Mouth bar deposits in section [12]; circled hammer for scale

Pedogenized horizon affected by load deformation following a local mouth bar reactivation; section [4]

Proximal lobe, with asymmetrical HCS structure and clay chips in its lower interval; section [4]

Figure 4.11 - Close-up views of the characteristic facies that compose Unit URG 5

Grey-yellow mudstones

They are characterized by yellow mottling and by the presence of very thin (< 1 cm) micritic layers and isolated micrite nodules of similar size.

Lower lenticular sandstones

The lowermost unit that compose Unit URG 5 is a ~1m-thick, poorly-sorted orthoconglomerate, characterized by a very heterogeneous composition, primarily represented by clasts (small pebbles, never exceeding 1,5 cm in diameter) of sedimentary rocks, including sandstones and limestones; the matrix is mainly composed by sand; small mudstone clasts are also present. Some small (sub-cm), spherical, white and yellow micrite clasts were encountered (FIG-5.x-isotopi). The geometry of this conglomerate bed is probably lenticular, because it was recognized only in one outcrop.

Above the conglomerate unit, a small interval of cover hampers a clear understanding of its relationships with the overlying deposits.

The first unit above the conglomerate is represented by a ~2m-thick, intensely weathered, poorly sorted, pebbly-sandstone rich in mudstone clasts.

This interval is truncated by a lenticular, cross-bedded, pebbly sandstone with abundant “clay chips” (i.e., thin tabular mudstone clasts), and a wavy laminaset at its top. The basal erosional surface of this unit dips in an approximate NE direction. The top of this unit presents some small-scale oblique laminations dipping to the NE, and is characterized by slightly finer grain-size, although small pebbles are still present. The whole lenticular body ranges in thickness from ~50 to ~150 cm.

Above this unit, a finer-grained interval was observed. It is composed of a lower, ~20 cm-thick fine-sand/silty unit and an upper, reddish, sandy/muddy unit of similar thickness. The lower part is characterized by a convolute, partially liquefied laminaset, locally displaying small ball-&-pillows structures. The upper muddy horizon displays a scaly fabric, and its sediments are partially collapsed within the lower liquefied interval. It is also characterized by abundant plant remains.

Above this fine-grained horizon, a further lenticular coarse-grained body is present. It is composed by medium to coarse sand, with pebbles, mud clasts and clay chips; it is internally subdivided in 5-6 units expressed by a rhythmic alternation of couplets of decimetric and centimetric laminasets. The internal stratification of this body apparently dips to the NW. Its base is erosional; its thickness varies from ~60cm to at least 1m.

An upper lenticular body, slightly coarser than the former, concludes the lower portion of Unit URG5. Similarly to the former ones, it is characterized by an erosional base and internal oblique stratification, apparently dipping to the N or NW. A peculiar feature of this body is the fact that pebbles appear locally concentrated in small internal scours; mudstone clasts are present; it does not exceed 60 cm in thickness.

In section [10], this interval displays some lithological changes; common elements are the average coarse grain-size, the lenticular geometry of the sandstone units that compose it, their internal cross-bedding and the abundant presence of mudstone clasts.

The basal conglomerate is absent, and the base of the unit directly rests on grey-yellow mudstones. This contact is sharp with a relatively flat geometry.

On this basal contact lies a relatively fine-grained unit, approximately 40 cm-thick, mainly composed of fine and medium-grained sandstone. It is characterized by oblique stratification, dipping to the west, and cm-size mudstone clasts. It is overlain by a thin, poorly exposed finer-grained layer. These two units altogether are erosionally truncated by the upper units.

The first of them is a pebbly, coarse to very coarse sandstone unit, rich in mudstone clasts, with a crude, low-angle oblique stratification, approximately dipping to the east. The top of this unit gently downlaps coherently with its internal stratification, and it is sharply overlain with an oblique contact by the successive unit.

The latter displays a similar grain-size and texture, including big, sometimes elongated mudstone clasts (max. diameter ~15 cm). It is characterized by WSW-dipping oblique laminations, locally highlighted by thin mudstone partings. Grain size is coarser at the base, and finer at the top (medium to coarse sand); the finer interval is also characterized by thicker mudstone partings. This unit and the former sum up for a total thickness of about 4m.

Their top is slightly truncated by a ~2m-thick coarse sandstone unit, with horizontal to gently oblique, W-dipping bedding.

Upper "tabular" sandstones

These beds are exposed in section [4]. They form a ~15m-thick, fining- and thinning-upward succession..

A rough subdivision can be made between a lower and an upper unit.

The lower unit is composed of medium grained sandstone beds, ranging in thickness between 60 and 30 cm, with sharp base and undulate top; mudstone clasts and clay chips are sometimes present the latter more concentrated at the base of the beds. Low-angle oblique laminations and hummocky cross-stratifications (HCS) were observed in some beds. Grey mudstones/siltstones are interposed between individual beds.

The upper unit is characterized by thinner and finer-grained beds (medium to fine sandstones). Horizontal and wavy laminations are more common than oblique laminations (with the exception of rare ripples indicating roughly N-directed paleocurrents); mud clasts are absent. Bed thickness ranges between 15 and 40 cm; silty mudstones are interposed between each bed, but a few sandstone layers are locally amalgamated.

These upper beds display a tabular geometry, with relatively flat base and top; nevertheless, their effective lateral continuity cannot be ascertained.

In section [10] a possible equivalent of the upper sandstones of Unit URG5 is represented by thin-bedded (< 10 cm) and very-fine grained beds, only patchily exposed.

Facies interpretations

In Rossi (1997), the deposits of Unit URG5 are only marginally reported as "deltaic siliciclastics".

These deposits rest on a poorly-developed gley-like paleosol ("grey-yellow mudstones"). The correlation panel of **figure 4.10** clearly shows that the base of the lower lenticular sandstones deeply erodes through the underlying mudstones in section [4]; the abundance and size of mudstone clasts within the sandstones in section [10] suggests that significant erosion occurred also in this location. The micritic clasts hosted within the basal conglomerate of section [4] might either imply erosion of a pedogenic nodular horizon, or upstream erosion of the lower shallow-marine micrites (see also **5.4.1.1**).

The lenticular sandstones (and subordinate conglomerates; **figure 4.11**, above) are characterized by a great variability in the directions of accretion (dip of foresets); however, most of these directions are apparent due to the orientation of the exposures; where dihedral cuts are available, a recurrent northern component in foreset accretion can be recognized.

An interesting feature is represented by the presence of a red horizon, within these lenticular bodies, affected by load deformation (**figure 4.11**, lower left). This indicates at least one interval of prolonged deactivation of the system, followed by a relatively fast deposition of the successive coarse-grained sandstone unit, that ultimately caused the partial liquefaction of the underlying sediments; a similar phenomenon might have interested the lower part of the succession, although its bad exposure does not allow detailed observations on the field.

The coarse grain-size, overall bad sorting and the development of load structures suggest conditions of en-masse deposition and minimal development of traction structures, typical of catastrophic flows entering a water body (deltaic mouth bar *sensu* Mutti et al., 1996).

All of these features considered, the facies of the lower lenticular interval can be attributed to a deltaic mouth-bar complex roughly developed in an E-W direction, discharging sediment-laden stream flows in a northern trough.

The facies of the upper "tabular" sandstones (**figure 4.11**, lower right) can only be studied in a limited exposure; however, the absence of pedogenic deposits within these beds likely indicates a backstepping of the system (shifting from mouth bars to shallow-water deposits) rather than an forestepping (i.e., a shift from mouth bars to alluvial plain deposits).

Moreover, these beds bear many similarities with the flood-generated, deltaic sandstone lobes described by Mutti et al. (1994, 1996, 2000) in marine and continental deposits of the south-central Pyrenees and other foreland basins. Diagnostic features recognized in this succession are the relatively good sorting, the presence of mudstone clasts and HCS. According to the authors, the latter structure indicates catastrophic floods entering water, causing the development of on oscillatory component that, combined with the unidirectional input of a fluvial flood, would ultimately cause the development of combined-flows structures. More specifically, the HCS recognized within this succession are anisotropic HCS (*sensu* Mutti et al., 1994; Tinterri, 2011).

The lobes are organized in a fining- and thinning- upwards trend, suggesting a progressive deepening of the depositional profile. The absence of marine fossils suggest that these flows were discharged within a lacustrine basin.

UNIT URG 6 – continental carbonates

This is the highest unit of the "Upper Red Garumnian"; in section [4], it is expressed by a ~25m-thick succession of micritic and dolomitic carbonates; its thickness is highly variable in the southern Ager basin (**figures 4.2**, **4.8**, **4.40**). Despite that, this unit can be almost continuously followed in the southern Ager basin and in maps up to section [11]; between sections [10] and [11] it locally forms a distinctive dip-slope.

It is composed by a lower, mainly micritic interval, and an upper micritic/dolomitic interval (**figure 4.12**).

The lower interval is approximately 17m-thick. It is mainly composed of decimetric beds (ranging across 10-40 cm), interbedded with thin mudstone partings (< 10 cm) and very thin micritic beds; the thinner beds are frequently deformed (wavy base and top). Thicker beds may display a wavy top, or a lenticular geometry. They are composed of grey-blue to pink, commonly bioturbated micrites; in some beds a very fine lamination was preserved. In the upper portion of the micritic interval, some thin micritic breccia horizons were recognized.

The upper, dolomitic interval is substantially similar to the lower one in bed thickness, geometry and internal structures; weathering color is more yellowish, and grey in fresh cuts. Plant remains are often found; locally a few scattered miliolids were recognized.

Facies interpretation

Although no specific reference was found, it is commonly recognized that this unit formed in a lacustrine setting, due to the presence of charophyte remains (E. Mutti, pers. comm.). The upper, dolomitized interval, possibly represents a transition to a coastal setting (sabkha s.l.); similar relationships between lacustrine and sabkha deposits were reported within lower units of the

Paleocene of the Ager basin in its western sector (Rossi, 1993).

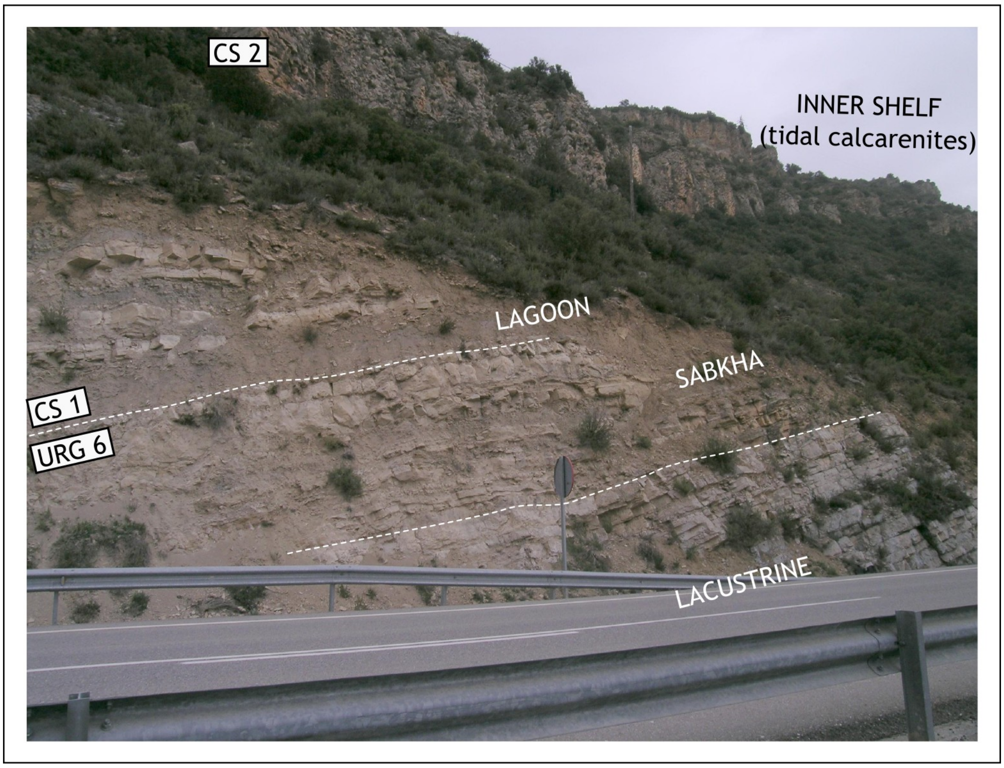

Figure 4.12 - Lower Ypresian continental/marine transition in the southern Ager basin; facies and unit names reported later in the text were added; C-13 roadcut near La Baronia de Sant Hoisme

4.2.1.3 – *Cadì Formation – southern Ager basin.*

The Cadì formation is exposed both in the northern and southern flanks of the Ager syncline; the northern and southern successions will be treated separately, because of some uncertainties in their lateral relationships.

In the southern Ager basin, it is continuously exposed from the eastern Coll d'Orenga sector to the Rio Noguera Ribagorçana to the west. It is mainly composed of shallow-marine calcarenites, and subordinate mudstones and sandstones.

It can be subdivided in 3 informal units; the following description is referred to the exposure along section [4].

UNIT CS1 – shallow-marine carbonates and mudstones

It comprises the first ~10m of the succession, and is mainly composed of fossiliferous mudstones that include two packages of fine-grained calcarenites and subordinate micrites and sandstones/siltstones.

Mudstones

Unit CS1 mudstones are characterized by a dark blue color and fossil content. The basal interval is characterized in its upper portion by an oyster coquina horizon, followed by a thin muddy layer extremely rich in plant fragments. The intermediate and upper mudstone layers host some scattered benthic foraminifers (mainly miliolids).

Calcarenites

These are represented mainly by miliolid wackestones, with rare Alveolina specimens; gastropods and oysters are occasionally found, as well as plant fragments. They are commonly very bioturbated, but thin horizontal laminations are locally observed.

Micrites

Micrites in this interval are typically white-colored, an host scattered miliolids.

Sandstones

A few, very thin sandy-silty beds were observed at the base of the lower calcarenitic body. They display thin, wavy to horizontal laminations

Facies interpretation

Unit CS 1 records a facies association very similar to the one recorded in Unit URG 4. The dark, OM-rich fossilifeous mudstones and the fine-grained, miliolid-bearing calcarenites are consistent with a low-energy lagoonal setting (cf. **figure 4.12**).

Figure 4.13 - Small- and large-scale cross-bedded sets (above) and close-up view (below) of the tidal grainstones of Unit CS2

UNIT CS 2 - Cross-bedded calcarenites

This unit represents most of the succession of the Cadì Formation, and it is almost exclusively composed of calcarenites, ranging from wackestones to coarse grainstones/packstones. The lower 30 m of this succession are represented by prevalently coarse-grained (**figure 4.13**, below), white calcarenites, particularly rich in alveolinae, gasteropods and lamellibranchs. These calcarenites are organized into 6 main coarsening-upwards cycles, with thicknesses ranging between 2 and 6 meters; these lithocycles are constituted by a relatively thin basal packstone/wackestone layer, transitionally overlain by a large scale cross-stratified grainstone/packstone unit (**figure 4.13**, above). This association displays a great vertical variability, mostly in terms of relative thickness of the more energetic sediment (grainstones) within each cycle; e.g., in the basal interval of Unit CS 2, calcarenites are represented by thin (decimetric), lenticular grainstone beds with sigmoidal cross-stratification (*sensu* Mutti et al., 1985, 1994), included within a mudstone/wackestone succession; in the intermediate portion of Unit CS 2, the cycles are almost exclusively composed of grainstones, and cycles are bounded by erosional surfaces.

Bioturbation is common throughout the whole succession, but it is more intense in the finer horizons.

The attitude of cross-bedding, characterized by concave-upwards surfaces with tangential lower terminations, changes from one cycle to the other, and in some cases within the same cycle.

In the upper portion of Unit CS 2, alveolinae are gradually replaced by nummulites. This portion of the succession is substantially similar to the one described above, although the packstone/wackestone intercalations become finer grained, more intensely bioturbated and nodular, and relatively thicker if compared with the coarser units.

This interval is represented by 5-4 cycles, for a total thickness of approximately 15 m; at their top, a rhodolitic surface was found (cf. *Solenomeris*?), overlain by an almost completely covered muddy interval.

Facies interpretations

The calcarenitic bodies that compose Unit CS 2 were formerly interpreted as tidal deposits (subtidal bioclastic tidal bars *sensu* Mutti et al., 1973, 1985), although they were not studied in detail. This interpretation was mainly based on the bimodality of the paleocurrents and on the presence of small- and large-scale sigmoidal bedding (*sensu* Mutti et al., 1985, 1994). Following the interpretation suggested in these papers, the relative abundance of well-sorted, coarser-grained bioclastic units with steeper foresets *vs* finer-grained, bioturbated units with low-angle to subhorizontal bedding, would reflect the variable intensity of tidal currents; it is assumed that these variations were mainly related with high-frequency relative sea-level variations (a similar interpretation was proposed in Mutti et al., 1994 and 1996 for the deposits of the Lower Baronia Sandstones, cf. below) although a thorough description of this depositional system, based on the study of the lateral variability of depositional geometries and facies, would be necessary to correctly assess these features.

On a broader view, the fining-upwards trend and the replacement of alveolinids with nummulitids, observed within the upper portion of this unit, suggest a progressive deepening-upward.

UNIT CS 3 – mixed unit

This unit was described in Mutti et al. (1994, see “stop descriptions”), Rubino et al. (1985), Ghielmi (1991). It encompasses a mixed carbonate/siliciclastic horizon at its base, and at least two calcarenitic bars included within a muddy succession (poorly exposed); the calcarenites as well develop a mixed composition (“hybrid”, sensu De Rossa & Zuffa, 1979; see **4.2.1.5**) in the eastern sector of the basin (Rubino et al., 1985).

Along the C-13 roadcut (section [4]), Unit CS 3 is repeated three times because of a transcurrent fault system roughly parallel to the exposure.

Mixed interval

The lower, mixed unit is ~3m-thick, and is characterized by strong bioturbation, abundant fossil and glauconite content and scattered pebbles. Despite the bioturbation, within this interval a W-dipping, low-angle oblique bedding was preserved (erosional gully at the base of “Les Alteres” cliff). Towards the east, a conglomerate bed scours the top of this unit (Rubino et al., 1985; **figure 4.14**).

Calcarenites

A 4m-thick cross-bedded calcarenite lies directly above the mixed interval. It is composed by nummulitic grainstones/packstones, organized in horizontal to oblique beds characterized by oblique laminations and forming a thinning-upward succession. In the eastern sector of the basin, this unit is instead characterized by an overall coarsening-upward trend, associated with large scale oblique bedding (Rubino et al., 1985).

A mudstone interval (badly exposed) separates this calcarenitic unit from the overlying one.

The latter is always thinner (commonly ~2-3 m) and displays a well-developed sigmoidal bedding (*sensu* Mutti et al., 1985, 1994), with E-directed cross stratifications.

It is almost entirely composed of nummulitic grainstones (a few alveolinae were encountered too), and shows a limited content in glauconite.

Above Unit CS 3, a thick (up to 30 m) mudstone wedge (almost entirely unexposed) separates the deposits of the Cadì fm. from the Baronia Sandstones above.

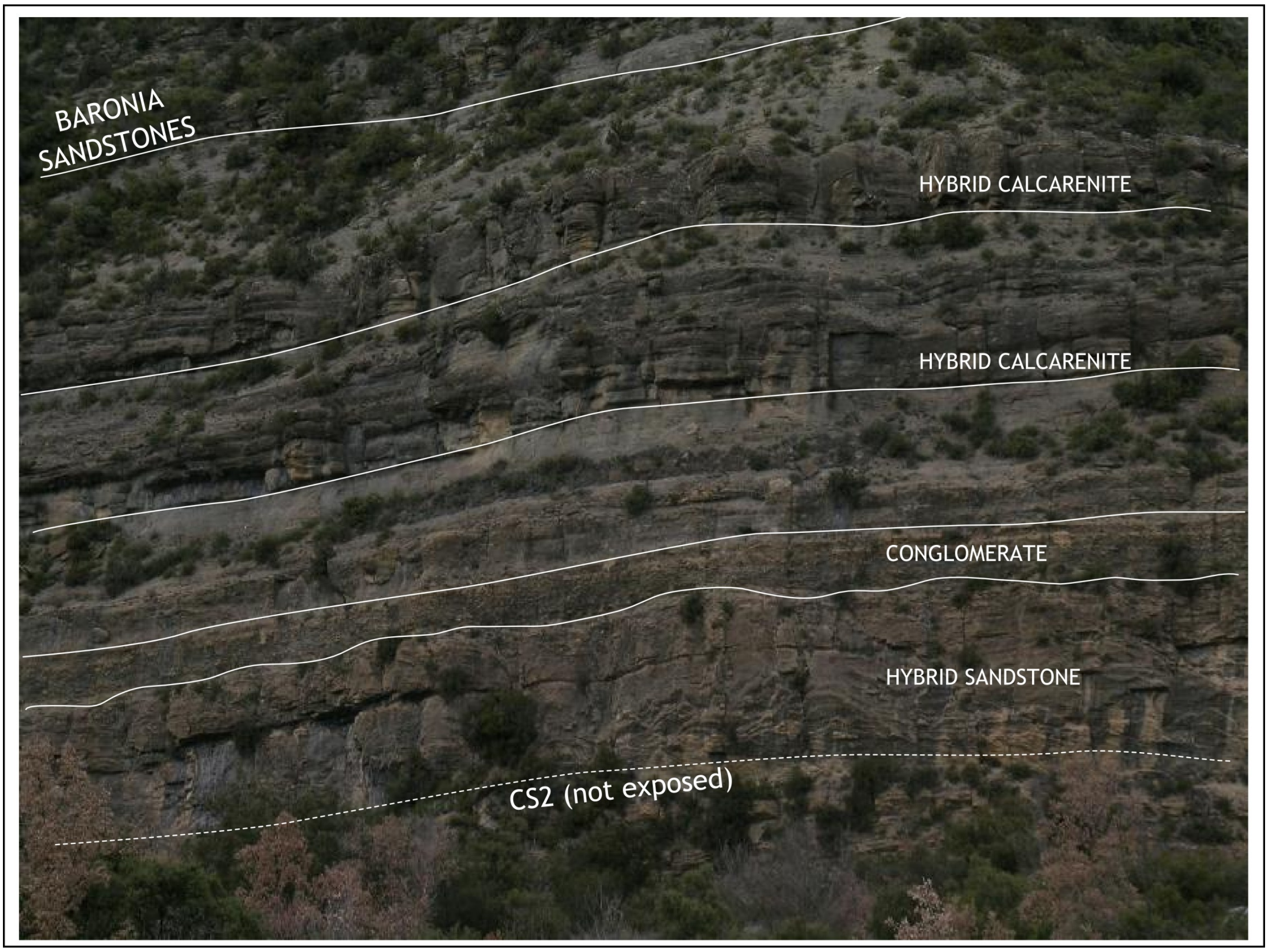

Figure 4.14 - Unit CS 3 exposure in the Barranc de S.ta Margarita (NW of section [10]). Field of view is approximately large 30 meters

Facies interpretations

Unit CS3 represents a very complex interval; in a general view, the presence of siliciclastic detritus and the reactivation of well-developed bioclastic tidal bars (Rubino et al., 1985; Ghielmi, 1991; Mutti et al., 1994) suggest a relative shallowing if compared with the upper beds of Unit CS2.

However, the abundant content in glauconite and the (apparent) condensed succession represented by this whole unit on the basis of biostratigraphic data (**2.5.3** and figure **2.21**) complicate its interpretation (Mutti et al., 1994, "stop descriptions").

The basal conglomerate/pebbly sandstone gets progressively coarser-grained towards the east; similarly, the sand content within the bioclastic bars increases in the same direction (Rubino et al., 1985), similarly to the deposits of the Lower Baronia Sandstones (see **4.2.1.5**). However, it is not clear whether the conglomerate and the sandstones share the same origin.

The less speculative interpretation for this unit is that its base constitutes a sequence boundary, i.e., it is associated with an abrupt relative sea-level fall, that contextually caused an increase in terrigenous inputs within the basin; the overlying bioclastic tidal bars are interpreted, following Ghielmi (1991) and Mutti et al. (1994), as transgressive deposits.

Still following these former interpretations, the overlying mudstone wedge is interpreted as an highstand deposits.

4.2.1.4 – *Cadì Formation – northern Ager basin.*

Similarly to the southern succession, the Cadì fm. in the northern Ager basin is mainly composed by calcarenites, commonly grainstones-packstones (section [12]). However, a greater terrigenous influx is recorded within this succession. It was subdivided into three informal units, not equivalent to the ones defined in the southern sector.

UNIT CN 1 – shallow-marine limestones and conglomerates

This unit is exposed along the eastern bank of the Rio Noguera Pallaresa. It is ~30m-thick, and it is mainly composed of conglomerates, calcarenites and subordinate dark mudstones.

They are stacked in cycles of variable thickness (<1 to 7-8 m; cf. **figure 4.3**), at least in the lower portion of this interval (in the upper portion, the conglomerate layer is commonly absent or replaced by pebbly calcarenites). Each cycle is typically composed of a lower, dark mudstones layer, an intermediate conglomerate layer and an upper calcarenitic layer (**figure 4.15**). The contact between the mudstones and the conglomerates is commonly erosional, characterized by shallow scours.

The conglomerates are clast-supported, composed of well-rounded, coarse (up to ~5 cm) limestone pebbles (Mutti et al., 1985, 1988); in their upper portion they include some concentrations of bioclasts (commonly *Alveolina* shells); from the base towards the top of Unit CN1, the conglomerate layers are richer in bioclasts, and in some cases they are replaced by pebbly grainstones (**figure 4.15**).

Calcarenites are substantially different from the ones exposed in the southern sector. Although their bioclast composition is largely similar, they are characterized by a nodular fabric disrupting their original bedding. Therefore, internal bedding surfaces display an irregular wavy profile; frequently, a thin layer of dark mudstones is present along these surfaces. In rare cases, an internal, crude oblique stratification is preserved; restored bedding dips towards the south.

Facies interpretation

This succession was interpreted by E. Mutti (pers. comm.) to have formed in a setting where Montsec-sourced fan-deltas (*sensu* Mutti et al., 2000) interacted with coastal deposits (mud flats and inner shelf carbonates).

UNIT CN 2 – lower mixed unit

This unit is better exposed close to the western bank of the Rio Noguera Pallaresa. It can be subdivided in a lower sandy interval and an upper calcarenitic interval.

The lower, roughly 10m-thick interval, is composed of mixed sandy/bioclastic layers and a gravelly coarse sandstone, characterized by a sharp base with abundant rounded to subangular lithic (siliciclastic and carbonatic) pebbles; grain-size is relatively coarse (medium to coarse sand) also in the mixed layers (**figure 4.16**). Pebbles are commonly smaller than the ones observed in Unit CN 1. *Alveolina* shells and bivalve fragments were recognized amongst the bioclastic detritus; scattered pebbles and abundant plant fragments (locally concentrated in distinct layers) are observed throughout the interval.

The upper portion of Unit CN 2 is approximately 30m-thick; it is mainly composed of calcarenites, very similar to the ones described in Unit CN 1; therefore they display a similar nodular fabric, and sometimes display an irregular, erosional base and a basal division rich in sand and/or pebbles. These calcarenites are mainly grainstones, rich in *Alveolina* and *Orbitolites*.

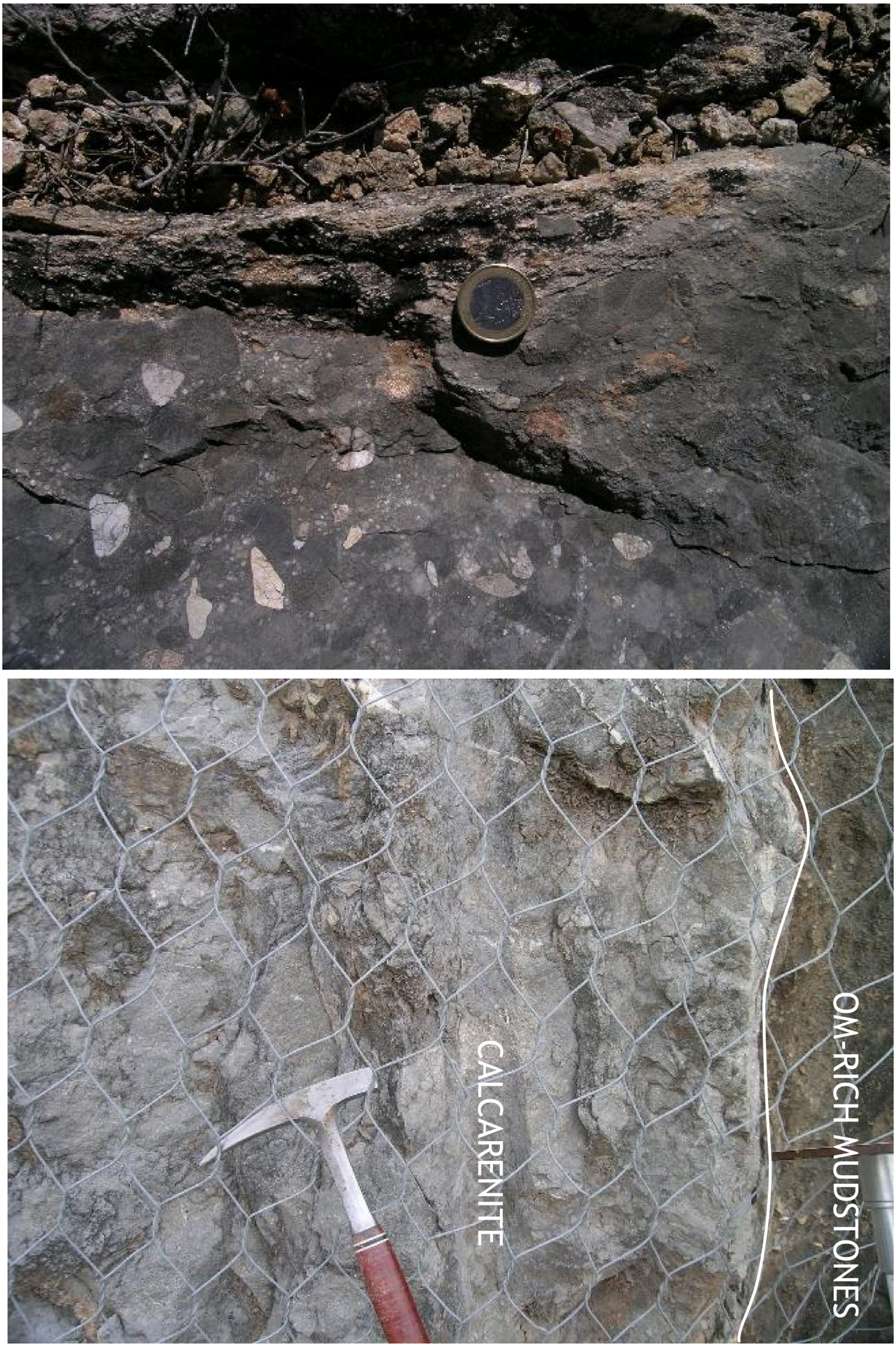

Figure 4.15 - Characteristic deposits of unit CN1 (section [12]). Above: Fossiliferous conglomerate draped by a thin calcarenitic layer; below: sharp contact between the calcarenitic deposits and the OM-rich mudstones; the succession is younger to the right.

Figure 4.16 - Hybrid calcarenites of unit CN2; above: sand-rich calcarenite; the succession is younger to the left; below: close-up view of the sandy and pebbly calcarenitic facies.

Towards the top of Unit CN 2, the succession is badly exposed; relatively thinner calcarenite beds crop out discontinuously and are largely similar to the lower ones; however,sand content is significantly lower, or absent; *Orbitolites* are apparently absent; rare *Nummulites* were observed.

Facies interpretations

The limited exposures of the Cadì fm. in the northern Ager basin do not allow a complete description of these facies. However, the sandy and pebbly inputs recorded in Unit CN 2 suggest a setting similar (though a little more distal) to the one described in Unit CN 1. The deltaic nature of these inputs is supported by the abundant presence of plant remains; the rather bad sorting suggest deposition from poorly-efficient flows. Coherently with the lower fan-delta deposits, their source should be the Paleo-Montsec, although the provenance of the siliciclastic lithic sediments is unknown (a possible candidate would be the dismantling of the Arèn sandstones and/or the continental deposits of the Tremp-Ager Group).

Based on these data, the facies association observed within Unit CN2 is interpreted as distal fan-delta deposits interbedded with inner shelf deposits, and progressively transgressed by the latter.

UNIT CN 3 – upper mixed unit

It is included within the top of Unit CN 2 and the middle/upper Ypresian unconformity (see **4.4.2.1**) FIG. It is ~25m-thick in the studied exposure and it shows some similarities with the lower portion of Unit CN 2. Lithology is represented by calcarenites, that may be either sandy/pebbly (frequently with small angular clasts) or sand-poor. Plant fragments are commonly found within the sandier horizons, although in minor abundance when compared with the lower CN3 deposits. Alveolinae are still very common; nummulites too are commonly found, and locally form thin concentrations devoid of alveolinae.

The uppermost interval of Unit CN 3 is a carbonate breccia of variable thickness (30-50 cm in the studied exposure; **figure 4.17**), with an erosional base scouring an underlying nummulitic pebbly limestone.

The breccia is composed by clasts pertaining to the Cadì fm., although it also contains scattered with fossils (oysters and corals) that are absent in the underlying beds. The breccia is sustained by a sandy matrix, apparently injected from the overlying middle-upper Ypresian sandstones, that locally display soft-sediment deformation features.

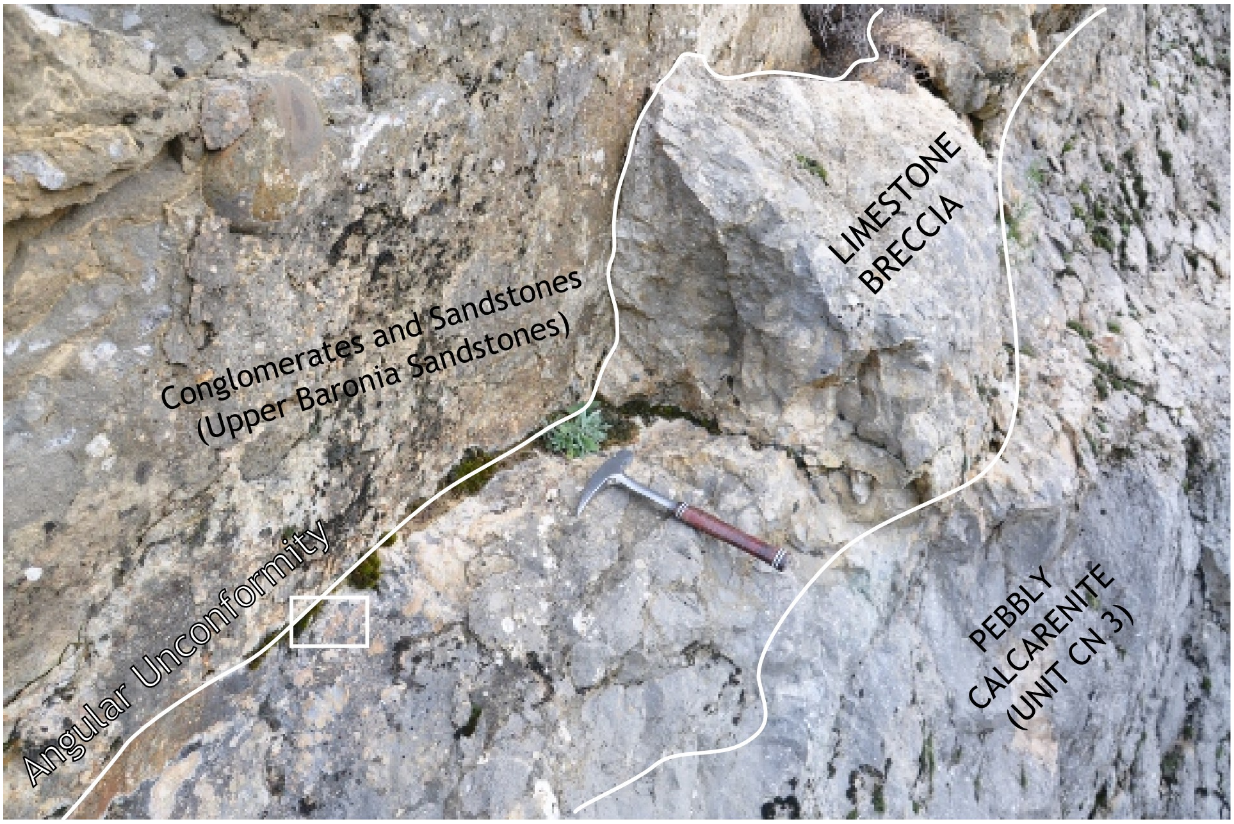

Figure 4.17 - Close-up views of the unconformable contact on top of the Cadì limestones in the northern limb of the Ager syncline. Notice the heterogeneous composition of the breccia below the unconformity.

Facies interpretations

This succession is dominated by inner shelf calcarenites, apparently affected by an outer shelf influence in their upper portion (mixed *Alveolina*/*Nummulites* populations). Compared with the upper portion of unit CN 2, it records a reprise of the terrigenous inputs, with mixed layers interleaved within the calcarenitic succession. Associated to this trend is a growing abundance of angular millimetric clasts, that possibly finds its acme in the breccia located along the interface with the overlying unconformity.

The facies association represented by this succession is largely similar to the one described in the lower portion of Unit CN 2 (distal fan-delta deposits interbedded with inner/outer shelf deposits).

The angular clasts might represent reworked sediment from detrital scree-like accumulations formed along nearby (unpreserved) reefs or sea-cliffs. The upper breccia could represent an in-place equivalent of these accumulations, and therefore might have formed much later than the underlying deposits.

4.2.1.5 – *Lower Baronia Sandstones*

The deposits that form this unit, only exposed along the southern flank of the Ager syncline, were described in detail by Mutti et al. (1972, 1985, 1994; Rubino et al., 1985; Ghielmi, 1991); their descriptive features are synthesized below.

The Lower Baronia Sandstones are mainly composed of a succession of hybrid arenites (*sensu* De Rossa & Zuffa, 1979) and subordinate sandy/silty mudstones and calcarenites. The “hybrid” concept defines mixed carbonate/siliciclastic strata in terms of provenance and redistribution of their constituent materials, operated by marine currents. In the case of the Baronia Sandstones, deltaic inputs and shelfal carbonate production provide the sediment; tidal currents produce the mixing, and distribute these sediments in function of their circulation patterns within the basin (Mutti et al., 1985).

Hybrid arenites

As a general rule, the Lower Baronia Sandstones are organized in bundles of large scale cross-bedded, coarsening upwards beds, with a lower, relatively fine-grained and thin-bedded interval with horizontal to low-angle oblique bedding (bottomsets), transitionally passing to an upper, coarser (fine to medium sand), high angle, forestepping interval (foresets; **figure 4.18**). The top of the bundles is commonly sharp and sub-horizontal, and it is overlain by intensely bioturbated muddy sandstones (less frequently mudstones), locally rich in glauconite; in turns, the bioturbated sandstones are sharply overlain by a new cycle starting with the bottomset facies.

This cyclical stacking is repeated, with minor variations, 4 times within the lower ~60m of the succession (Rubino et al., 1985; Ghielmi, 1991; Mutti et al., 1994). Towards the west (sections [2] and [3]), this interval is characterized by a reduction in the size and dip of the large-scale foresets, together with an increase in the amount of bioturbation. All the cross-bedded units within this lower interval display a dominant current direction towards the west.

Above this lower interval some significant changes occur, involving both the clast composition and the depositional structures.

The fifth "cycle", although locally displaying features similar to the lower units, is characterized by a greater lateral variability of thickness, composition, depositional structures and paleocurrents. Instead of large scale cross-bedding (bottomsets/foresets), this interval is more commonly composed of a package of lenticular beds, with variable lateral extension, characterized by thin cross-laminations, typically mono-directional within a single bed; the paleocurrents may reverse from one bed to the other. The packages of lenticular beds display a sharp base and top and are commonly included within muddy sandstones. Bioclastic detritus is more abundant with respect with the lower intervals (Rubino et al., 1985; **figure 4.19**).

In the uppermost portion of the Lower Baronia sandstones, a further sandstone unit is present. This was only encountered in section [4], and it may have a limited areal extent. Its internal stacking pattern is similar to the "lenticular" deposits described above.

Figure 4.18 (next page)- Lower Baronia Sandstones: Above: general view of the succession at Les Alteres (section [7]); below: the typical facies association of a sigmoidal tidal bar, sensu Mutti et al., 1985; hammer (circled) for scale; section [8].


N
S
Bioclastic
tidal bars
Upper bioclastic tidal bar
of Unit CS3
Lower Tsunami bed
Base of the Lower Baronia Sandstones

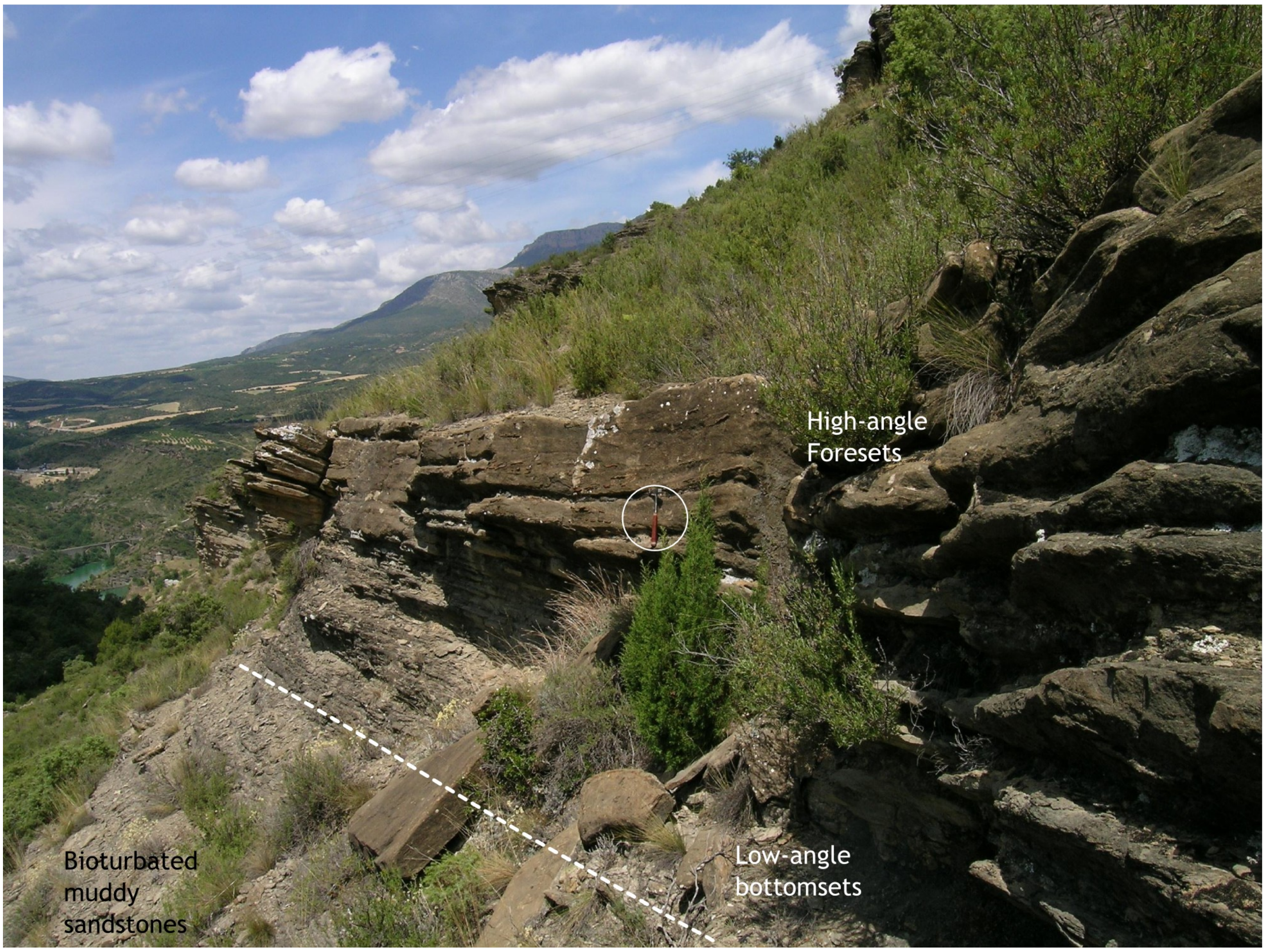
High-angle
Foresets
Bioturbated
muddy
sandstones
Low-angle
bottomsets


2 EURO CENT

Figure 4.19 (former page) - Hybrid tidal deposits in the upper portion of the Lower Baronia Sandstones; notice the alternation of dark (terrigenous) and light (bioclastic) bands, and the variability of paleocurrent directions; section [2].

Calcarenites

Two types of calcarenitic beds are present within the Lower Baronia Sandstones.

Calcarenitic horizons encountered in the upper portion of the Lower Baronia Sandstones are composed of grainstones and subordinate packstones/wackestones, containing alveolinae and nummulites, together with abundant skeletal debris (mostly lamellibranchs and echinids); their geometry and internal structures are similar to the ones described in the sandstones.

Two main layers can be distinguished, although they dramatically change in thickness and may be locally discontinuous (e.g. section [4]).

The second type of calcarenitic beds is represented by normally-graded beds, frequently laminated and rippled on their top, with sharp, erosional base, tabular to lenticular bedding, and including, or laterally replaced by carbonatic boulders to blocks originally pertaining to the Cadì fm. (Mutti et al., 1985; **figure 4.20**).

Figure 4.20 (next page) - Tsunami deposits in the middle and upper portion of the Lower Baronia Sandstones; above: limestone clasts within a graded bioclastic bed. Below: olistolith (circled; long axis ~7 m) within a muddy sandstones succession; Barranc de S.ta Margarita.


MIDDLE
BARONIA
SANDSTONES

Facies interpretations

The interpretation of the above-described unit was anticipated in the introductory part of this section (**4.2.1.5**), and it follows the original interpretations of Mutti et al. (1985). The authors described the succession of the Lower Baronia Sandstones as an accumulation of subtidal deposits (cf. Mutti et al., 1973), mainly composed by composite tidal bars (either hybrid or bioclastic) and bioturbated muddy sandstones.

Tidal bars were described as prograding sandstone bodies that formed during periods of relatively low sea-level, under the action of strong tidal currents, and reworked and mixed intrabasinal bioclatic and extrabasinal siliciclastic sediments (hybrid arenites *sensu* de Rossa & Zuffa, 1979). The finer-grained, commonly bioturbated deposits represented instead deposits formed below the depth at which the currents were able to build up large bodies; this facies periodically became ubiquitous throughout the basin, in response to oscillations of the relative sea-level.

The authors interpreted the strong tidal regime to have originated because of the narrow morphology of the basin, that caused resonance of tides, i.e. the amplification of the tidal wave, and the development of circulation patterns of the tidal currents within the basin, that changed with time, similarly to other modern and ancient analogs (e.g., the Gulf of California; Meckel, 1975). They proposed a model of the circulation of the tidal currents, based on facies distributions; dominant ebb tides typically built the hybrid bars, importing terrigenous sediments from the east, while flood flows most frequently imported bioclastic detritus from the west (i.e. from the open sea and from the structural highs located at the basin margins (e.g., the Millà Anticline). Within the upper part of the Lower Baronia Sandstones, the presence of bioclastic tidal bars was associated with a change in the current patterns related with a rapid relative sea-level rise (attributed to tectonic subsidence).

Evidence for a tectonic disturbance may be the variation in subsidence patterns occurring in the western portion of the panel of the Attached Document 3 (cf. Rubino et al., 1985; Mutti et al., 1994, their Plate III), apparently associated with the basal boundary of the fifth bundle of hybrid arenites. This unit is not yet a bioclastic tidal bar, but it displays a more abundant content of bioclastic detritus than the lower units (Rubino et al., 1985), a different facies association (as described above and in Ghielmi, 1991), and a very different geometry of the bars. The change in paleocurrents that can be observed within this unit at least indicates that a reorganization of the tidal currents took place starting from this period.

Finally, the graded bioclastic beds associated with olistoliths were also described by Mutti et al. (1985). They represent deposits related with tsunamis, that imported shelfal sediments from the west and deposited it as a turbidity current. At the same time, the occurrence of large blocks (Rubino et al., 1985) testified the dismantling of an exposed carbonate ramp. The actual provenance of these blocks is not clear, since the process itself could have the potential of displacing for great distances even large blocks.

4.2.1.6 – *Middle Baronia Sandstone*

This unit was not studied in detail, since its base sharply delimits the LFG/UFG boundary at the top of the studied interval; it is mainly composed by coarse estuarine, locally channelized deposits to tidal flat deposits (Mutti et al., 1985). Similarly to the Lower Baronia Sandstones, they rest unconformably on the basin margins, and locally erode within the underlying units (op. cit.); the occurrence of this unit was related with a major sea-level fall that followed the deposition of the fine-grained upper deposits of the Lower Baronia Sandstones.

4.3.1 – Tremp basin

The lithostratigraphic subdivision proposed by Barberà et al. (1997) was adopted, with a few modifications, in order to describe the marine Lower Ypresian of the Tremp basin. The continental Lower Ypresian and the Paleocene follow the subivision proposed by Schmitz & Pujalte (2005), which was in turn modified from Cuevas (1992).

4.3.1.1 - *Vallcebre Formation*

The Vallcebre Formation in the Tremp basin is mainly represented in its innermost sectors (east of the Rio Noguera Pallaresa), where it took the local names of Suterranya & S. Salvador fm. (Cuevas, 1992). Near S. Salvador de Tolo', it is represented by x carbonate bodies interbedded within a continental succession.

Within the studied transect, a possible equivalent of the Vallcebre fm. was described by Baceta et al. (2011) in the Esplugafreda exposure (section [23]). Above that, they recognized an erosional surface associated with local accumulations of *Microcodium* debris.

Facies interpretations

Pujalte & Schmitz (2005) interpreted the micritic horizon as a palustrine deposit. The erosional surface is associated by the authors to the Middle Paleocene Unconformity.

4.3.1.2 – *Esplugafreda Formation*

The Esplugafreda fm. (**figure 4.21**) is mainly composed of bright red mudstones and lenticular sandstones and conglomerates. According to Schmitz & Pujalte (2005), it may be subdivided in a lower unit, resting on an erosional boundary (see above), represented by a ~10-m thick horizon of purple mudstones, and an upper unit (~ 150m-thick in the Esplugafreda exposure) mainly composed of red mudstones, sandstones and conglomerates, with locally abundant gypsum nodules and veins (in more internal sectors of the basin, these concentrations are replaced by massive gypsum beds). Both units display an abundant content in carbonate nodules, commonly concentrated along distinct layers.

Sandstones and conglomerates form a great number of lenticular bodies, with maximum thickness of metric scale, and lateral extension that may reach 500m.

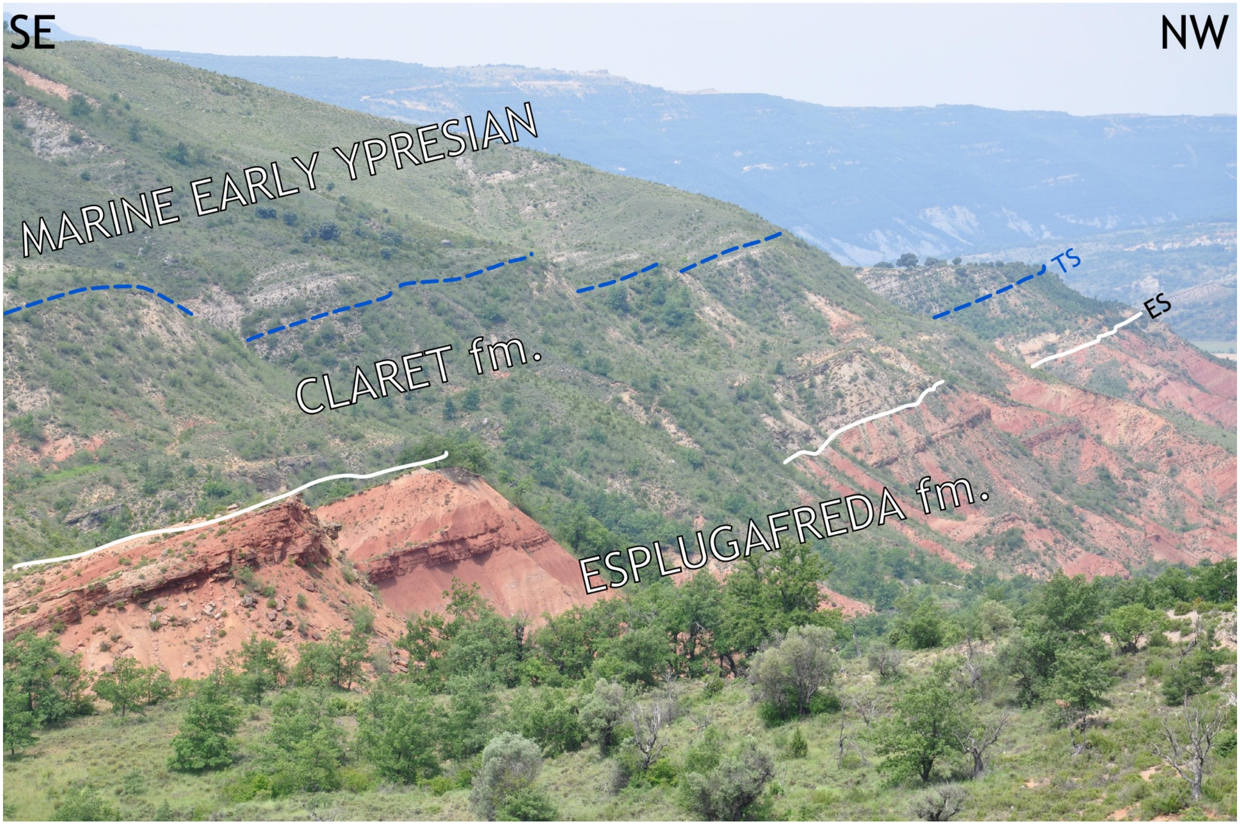

Figure 4.21 – Esplugafreda outcrops; ES: erosional surface; TS: transgressive surface.

Facies interpretations

This unit is mainly composed of paleosols. It displays some similarities with the coeval Units URG 1, 2 and 3, (such as the presence of evaporitic deposits in its upper part), but the pedogenic facies are distributed in a totally different way; the fluvial deposits as well (channelized sandstones and conglomerates) are more ubiquitous than in the Ager basin, where they are limited to the lower "Upper Red Garumnian".

4.3.1.3 – *Claret Formation*

This unit is almost continuously exposed along the northern and central-eastern sectors of the Tremp basin (although in the latter it is more difficult to define its lower boundary). It is patchily exposed along the southern sector of the basin, although a sandy horizon – supposed to be an equivalent of the Claret Conglomerate (**2.4.3.1**; and below) – is locally exposed (Eichenseer & Luterbacher, 1992; Waehry, 1999).

It is separated from the Esplugafreda fm. by an irregular erosional surface (Pujalte & Schmitz, 2005).

This formation was instituted by Cuevas (1992), and partially reviewed by Pujalte & Schmitz (2005). It is apparently thicker in the northern sector (~ 70m), but its actual thickness may have a local variability larger than what observed on a broader scale.

In Pujalte & Schmitz (2005) it was subdivided into five units ("intervals"); in the present work, a sixth unit is included, that encompasses the continental-marine transition of the Ilerdian transgression (**2.4.3.2**, and below).

UNIT CL1

It is a strongly discontinuous unit, with a maximum thickness attaining a few tens of meters and representing the local fill of the incision that separates the Claret fm. from the underlying Esplugafreda fm. (Pujalte & Schmitz, 2005). This unit encompasses a lower sandy unit (locally including a basal conglomerate, (cf. Section [20]), characterized by decimetric beds mainly composed of yellowish medium to fine-grained sandstones (and subordinate coarse sandstones in its lower portion), commonly displaying oblique laminations (roughly west-dipping). These beds are commonly separated by centimetric to decimetric silty intercalations; in the Tremp section, there is evidence of cross-cutting relationships between a lower body, composed of low-angle cross-bedded sandstones and silty layers, and an upper body where the sandstones occur as lenticular amalgamated beds with SW-dipping cross-laminations (**figure 4.22**, middle).

In section [23], Pujalte & Schmitz (2005) described the highest portion of Unit CL1 (not exposed in section [20]) as a composed by grey/yellow and red silty mudstones.

Facies interpretations

The deposits of this succession were interpreted by Pujalte & Schmitz as the fluvial infilling of an incised valley. This interpretation is followed; the Tremp exposure is here interpreted as a small complex of fluvial channels shifting over a coarse basal lag; the oblique bedding may be attributed to a small point bar.

UNIT CL 2

It is represented by the classic “Claret Conglomerate”. A general description of this unit is in chapter **2.4.3.1**.

The Claret Conglomerate (**figure 4.22**, above and below) typically encompasses two-three superposed bodies, summing up to ∼7-8 m, but gradually decreasing in thickness (and grain size) towards the north-west (Schmitz & Pujalte, 2003, and references therein); each of them is composed of lenticular beds with sharp, deep-scouring erosional base, lateral and vertical normal grading and crude oblique stratifications (flood-generated sigmoidal bars in Mutti et al., 1996, 2000; their fig.2; **figure 4.22**, above); paleocurrents are mainly oriented to the south and south-west. Mudstone intercalations are present between the different bodies; in section [20] these mudstones are typically blue-grey, while in the northern sector (section [23] and near Arèn) they are red and light red, and host soil nodules.

The Claret Conglomerate is topped by a pebbly, medium to coarse sandstone.

Figure 4.22 (next page) - xposures of the coarse deposits of the Claret fm.

Above: upper part of unit CL2; in the middle: unit CL1; notice the cross-cutting relationships between fine-grained, cross-bedded deposits; jacob staff for scale; C-1311 road-cut.Below: load-deformed unit CL1 in the Rio Palau exposure after the deposition of Unit CL2. Notice that the mudstones are not pedogenized, suggesting the presence of a relatively permanent water body south of the classic exposures of the Claret Conglomerate. Field of view is approximately 4 m wide.


SW
NE


CONGLOMERATE (CL2)
LOAD-DEFORMED SANDSTONES (CL1)

Facies interpretations

As anticipated in chapter **2.4.3.1** there are some controversies on the interpretation of the origin of the Claret Conglomerate. Both interpretations are focused on the wide areal extension and sheet-like geometry of the whole body. Angella (1999) and Mutti et al. (2000) described these deposits as mouth-bar complexes of high-gradient fluvial systems originated in the Axial zone, and discharging catastrophic floods in ephemeral basins. Schmitz & Pujalte (2003) instead interpreted this unit as braided river deposits, developed at the end of a transgressive interval; the abundant production of coarse detritus was attributed to enhanced continental runoff, related with a period of global climatic change during the initial stage of the Paleocene-Eocene Thermal Maximum (CHAP).

The braided river interpretation could be questioned by the distribution of paleocurrents within the Claret Conglomerate, that are commonly oriented to the south and south-west (i.e., towards the axis of the basin; cf. **4.3.1.4**); finally, the load deformation occurring to Unit CL 1 (or deposits lateral to of the lower part of Unit CL 2; **figure 4.22**, below) suggest rapid accumulation and, possibly, dynamic load related with intense floods; these are coherent with a prograding pattern, resulting from the superposition of "sigmoidal flood units" *sensu* Mutti et al. (1996; 2000).

UNIT CL 3

It is represented by a laterally continuous horizon of yellow silty mudstones of variable thickness (up to ~20m), locally hosting lenticular sandstone beds and scattered carbonate nodules (Pujalte & Schmitz, 2005).

Facies interpretation

This unit was interpreted as a paleosol horizon, formed under conditions of relatively low sedimentation rates ("Yellow Soils" from Schmitz & Pujalte, 2007) if compared with the paleosols of the Esplugafreda fm.; its formation was also associated to the re-establishment of arid conditions after a subhumid stage of intense runoff represented, in their interpretation, by the Claret megafan (unit CL2). This unit may locally include relatively thin, lenticular sandstone beds.

UNIT CL 4

It is mainly composed of red mudstones with gypsum nodules; locally (e.g. section [20]) the nodules are replaced by thick gypsum beds. (Pujalte & Schmitz, 2005). This interval commonly ranges in thickness around ~10 m.

Facies interpretation

Schmitz & Pujalte (2003) interpreted this horizon, in accord with former researchers (e.g. Eichenseer & Krauss, 1985) to have formed under very arid conditions.

UNIT CL 5

This unit was marginally described by Baceta et al. (2011), as a red mudstones horizon with scattered carbonate nodules. Actually, this interval grades to (or it is entirely represented by) a grey mudstone with yellow mottling.

Facies interpretation

Unit CL 5 records the transition from an arid paleosol succession to a wetter facies (grey paleosols); this transition was related by Eichenseer & Luterbacher (1992) to a rise of the groundwater level that anticipated the Ilerdian transgression in the inner sectors of the Tremp basin.

UNIT CL 6

This unit encompasses the transition from continental to marine setting; it was described by Eichenseer & Krauss (1985), Eichenseer and Betzler (1987) and Eichenseer & Luterbacher (1992). Its type section is located along the C-1311 roadcut, west of Claret; it is also well-exposed in sections [22] and [23], but some of its most significant elements may be missing in these locations.

It encompasses a succession composed of: a lower, grey to dark grey mudstones with abundant plant fragments, frequently concentrated along distinct layers, and micritic limestones with charophyte remains; an upper, grey mudstones interval, characterized by lenticular accumulations of bioclastic debris (extremely rich in *Alveolina* shells). Within the muddy sediments, oyster shells and gastropods of the genus *Potamides* are frequently found. In the Claret outcrop, this interval is some ~10 m thick, although its upper boundary is transitional with the deposits of the Tendrui fm. (see below).

Facies interpretations

This succession was classically interpreted (Eichenseer & Luterbacher, 1992, and references therein) as the transition from a palustrine setting to a low-energy coastline; this transition is recorded by marsh to mud-flat deposits with residual bioclasic beaches ("cheniers").

4.3.1.4 – *Equivalents of the upper Tremp Formation along the southern margin of the Tremp basin*

In section [14], a patchy exposure along a road-cut allows the study of the uppermost continental beds of the Paleocene and Early Ypresian.

In this location, two main sandstone bodies were encountered, included within a succession of varicolored mudstones. Not considering the large covered intervals, 4 informal units can be defined.

UNIT UTF 1 – *Varicolored mudstones*

This unit is ~15 m-thick, and hosts a succession of dark red to light red and yellow silty/sandy mudstones, with rare interbedded thin-bedded (decimetric) fine-grained sandstones. Grey mottling is ubiquitous within this unit; the top of the unit is characterized by a thin red horizon with abundant gypsum nodules.

Facies interpretation

The mudstones within this succession represent paleosols formed during a transition from arid to sub-humid conditions (red to yellow paleosols; cf. Kraus & Riggins, 2007). The upper gypsiferous layer is probably associated with the reappraisal of arid conditions.

Figure 4.23 (next page) – Exposures of the upper Tremp fm. In the southern Tremp basin and measured log. Section [14], road cut between Alsamora and Puente de Monatañana.

Above: supposed equivalent of the Claret Conglomerate.; the grey star indicates the syn-PETM horizon (see chapter 5.6.1).

Below: possible equivalent of the basal part of the Claret fm. sensu Pujalte & Schmitz, 2005. In both pictures, the brown line indicates the contact with the Quaternary; circled Jacob staff for scale.

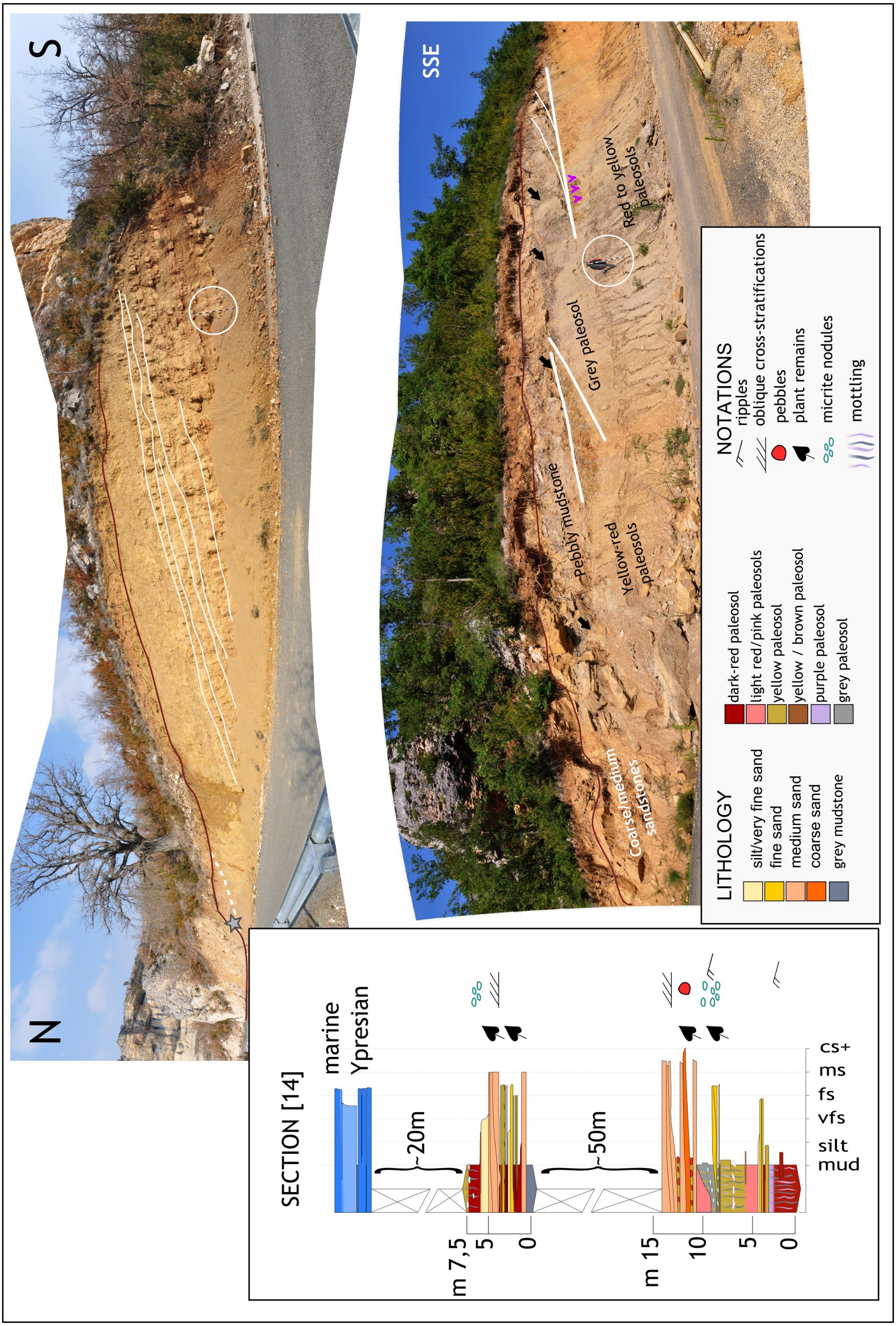
N
S
SSE
Red to yellow paleosols
Grey paleosol
Pebbly mudstone
Yellow-red paleosols
Coarse/medium sandstones
LITHOLOGY
silt/very fine sand
fine sand
medium sand
coarse sand
grey mudstone
dark-red paleosol
light red/pink paleosols
yellow paleosol
yellow / brown paleosol
purple paleosol
grey paleosol
NOTATIONS
ripples
oblique cross-stratifications
pebbles
plant remains
micrite nodules
mottling
SECTION [14]
marine Ypresian
~20m
~50m
m 7,5
5
0
m 15
10
5
0
mud
silt
vfs
fs
ms
cs+

UNIT UTF 2 – *Varicolored mudstones and sandstones*

This unit encompasses the top of the lower exposure, and displays some significant changes if compared with Unit UTF 1 (cf. **figure 4.23**, below). It is mainly represented by yellow to grey (yellow-mottled) mudstones with scattered carbonate nodules and interleaved by abundant lignitic remains in lenticular deposits and cross-bedded fine-grained sandstones. This interval is truncated by a lenticular body entirely composed by intensely mottled, yellow to light red mudstones, draped on its top by another lignitiferous layer.

The overlying unit is partially covered; however, two main lithologies can be recognized: yellow-red pebbly mudstones, with rare carbonate nodules, and lenticular sandstones, thinning out to the south, with maximum thickness ranging between 20 to 60 cm, relatively coarse grain-size (medium to coarse sand) and commonly displaying thin horizontal laminations.

20-25 m of cover are interposed between the top of this unit and the upper one.

Facies interpretation

The color, mottling and carbonate nodules present within the mudstones indicate a pedogenic origin. The cross-cutting relationships recognized in the lower part of Unit UTF 2 suggest deposition in a channelized system related with a fluvial environment; it is possible that the lower grey mudstones represent overbank or point bar deposits formed during a period of relatively high humidity, while the lenticular yellow-red mudstones were formed as a channel-abandonment deposit, lately affected by pedogenic processes.

UNIT UTF 3

This unit rests on poorly exposed grey-blue mudstones; it is represented by a ~7 m-thick package of sandstones and subordinate red mudstones (**figure 4.23**, above). Sandstones are organized in two thickening- and coarsening-upwards (very fine to medium sand) cycles, and typically display north-dipping cross-bedding with lenticular geometries.

Facies interpretations

This bed was probably the one designated as an equivalent of the Claret Conglomerate by Waehry (1999, Ribagorçana section), since it is the last coarse-grained unit exposed below the lower Ypresian limestones (Guardia Unit, **4.3.1.6**). Because of local structural complications, the thickness interposed between these two units was measured farther eastwards (section [15]).

The lower grey-blue mudstones might not be paleosols, or they are poorly-developed; the grey color suggest formation in a humid, if not watery environment. The overall geometry of the sandstone body suggests periodic progradation towards the south; pedogenesis occurred during relatively short periods of abandonment.

This body is interpreted as a deltaic mouth bar.

UNIT UTF 4

Above the sandstone interval rests a ~2 m-thick succession (interrupted by cover) of sandy to silty yellow-red mudstones, with blue mottling and abundant scattered carbonate nodules.

Facies interpretation

This horizon is interpreted as a pedogenic interval, similar to the "yellow soils" resting above the Claret Conglomerate of Unit CL 3; they are similarly interpreted as "cumulate" paleosols.

4.3.1.5 – *Tendrui Formation-axial sector of the Tremp basin*

Considering the great lateral variability occurring within the deposits of the Tremp basin, the axial and marginal (southern) sectors will be treated separately.

The Tendrui Formation roughly includes all of the shallow-marine deposits of the Lower Ypresian of the Tremp basin. In the lithostratigraphic subdivision proposed by Barberà et al. (1997), it includes as "members" the limestone bodies exposed along the southern margin of the Tremp basin. The central "Farga" and "Puigcercos" Formations should be similarly considered as members of the Tendrui Formation, given that they occur within that as bodies of very limited areal extension (at least in the studied north-south transect).

On a broader view, the axial deposits of the Tendrui fm. can be described as an alternation of mudstones and relatively thin-bedded and fine-grained sandstones and calcarenites (**figure 4.24**); most of these beds display a mixed carbonate/terrigenous composition (Waehry, 1999); similarly, the mudstones display variations in their carbonate content expressed by color bands (darker vs lighter grey/blue; Fonnesu, 1984).

The Tendrui fm. displays a faunal composition that reflects a general deepening-upwards trend

(Eichenseer & Luterbacher, 1992, and references therein). Under this perspective it may be subdivided in a basal unit, characterized by abundant miliolids and alveolinids, and the rest of the succession richer in nummulitids and dyscocyclinids. Within the latter, and below the Serra-Puit Unit (see below), three intervals were classically distinguished (Luterbacher, 1973) in terms of characteristic fossils. These are the "*Turritella* marls", characterized by local coquina layers almost exclusively composed of this gastropod, the "*Pattalophyllia* shales" (solitary corals scattered within the mudstones) and the "*Nummulites globulus* clays", that were considered the unit formed in the deepest setting recorded within the whole succession.

Figure 4.24 – Exposure of the lower part of the Tendrui fm.; barranco de St. Adrià, between sections [21] and [22].

Figure 4.25 (next page) – Deltaic sandstone lobes. Above: proximal lobe with well-developed horizontal laminae to climbing ripples; section [23], lateral equivalent of the Farga Unit; in the middle and below: bioclast-rich distal lobes; section [20].

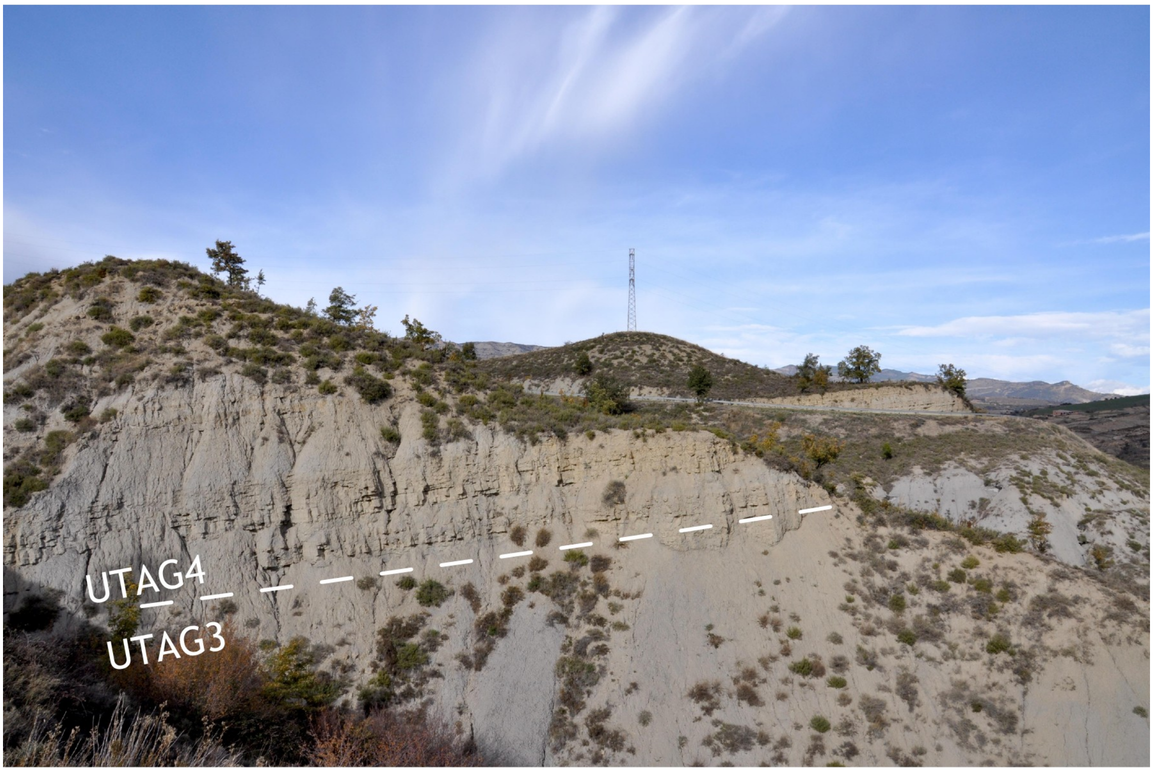
UTAG4
UTAG3

Sandstones and mixed carbonate-siliciclastic beds

Fine-grained sandstones (and mixed beds) are almost ubiquitous within the Tendrui fm, and are typically arranged in cycles (sandstone/mudstone couplets) of metric to decametric thickness (Waehry, 1999; **figure 4.25**); locally, a hierarchy of cycles may be recognized (possibly up to 4 orders within the decametric scale), but the lateral correlation of each individual unit, and so their cyclostratigraphic significance, at least at the smallest scale, may be largely speculative.

The sandstones and mixed beds frequently display current structures (typically horizontal laminations; rarely well-developed oblique laminations and HCS; hydraulic segregation of bioclasts; **figure 4.25**); more commonly, these beds are intensely bioturbated; however, as a general rule, in the upper portion of the Tendrui fm. (above the Serra-Puit Unit, see below) it is easier to find well-preserved depositional structures.

Calcarenites

Calcarenites are rarely observed within this succession. They are mainly concentrated in the basal part (Alveolina and miliolids grainstones with *Lucina corbarica*; Luterbacher, 1970), and close to the top (see S.Llucia Unit in **4.3.1.6**) of the succession, where they display a relatively abundant terrigenous content and nodular fabric.

Facies interpretation

The sandstone/mudstone couplets of the Tendrui fm. were interpreted as the product of fluvio-deltaic processes (Mutti et al., 1994; 1996; 2000; Angella, 1999; Waehry, 1999) and, specifically for the studied interval, as proximal to distal sandstone lobes and associated prodelta mudstones.

The local abundance of calcarenitic detritus raises the probem of its provenance; Waehry (1999) distinguished between deposits associated with an expansion of the marginal carbonate environments (such as the ones cited above), and reworked layers ("bioclastic debris flows"); Angella (1999) favored the role of flood-related processes in sweeping the carbonate ramps and locally redistributing intrabasinal carbonate detritus.

The cyclical stacking that characterizes most of the succession was tentatively interpreted in terms of cyclostratigraphy by Eichenseer & Luterbacher (1992) and later, with a better chronostratigraphic control by Waehry (1999); both recognized a short-term eccentricity modulation (~95 ky periodicity), and Waehry inferred also the presence of a higher-order modulations (precessional scale); however, the recent reviews of the Early Paleogene chronology (see **2.5.1.3**), that significantly expanded the duration of the Lower Ypresian, suggest that these results may have been apparent. Further complications were discussed by Luterbacher (1998), concerning the presence of condensed successions, and erosion along sequence boundaries, that in the Tremp basin might have enhanced biozonal boundaries; another implication is that, despite the exceptional continuity and thickness of this foreland succession, its temporal record might be irregularly squeezed and expanded.

FARGA UNIT

This unit is equivalent to the lower portion of the Puigmaçana-Serrat de Cal Senàs depositional system of Fonnesu (1984), the braid delta lowstand deposits of the Ager Sequence in Eichenseer & Luterbacher (1992; cf. **figure 2.9**) and the Upper Sequence of the Claret Deltaic System of Angella (1999).

It is well-exposed at the base of section [22], and it is composed of three bundles of poorly sorted medium sandstones, the last of which is truncated by a lenticular orthoconglomerate (**figure 4.26**). It possibly represents the only exposure of a larger complex developed along the northern margin in the earliest Ypresian of the Tremp basin (Eichenseer & Luterbacher, 1992). Each bundle displays a low angle cross-stratification, possibly because of the orientation of the exposure. The conglomerate is characterized by a sigmoidal geometry (*sensu* Mutti et al., 1996), and a dihedral cut allows the recognition of a SW dip of the scour surface.

A lateral equivalent of this unit was observed in a small exposure in the Puigmaçana village and it is represented by thin (centimetric to decimetric) beds of coarse to medium sand occurring a few meters above the Ilerdian transgression; one of these beds is particularly rich in pebbles and is characterized by a concentration of gastropods (cfr *Potamides*).

Figure 4.26 (next page) – Deltaic mouth bars deposits of the Farga Unit in the Tendrui exposure (Section [22]); below: detail of the sigmoidal conglomerate bed (see text)


S
N
MOUTH-BAR COMPLEX
PALUSTRINE LIMESTONES AND OM-RICH MUDSTONES

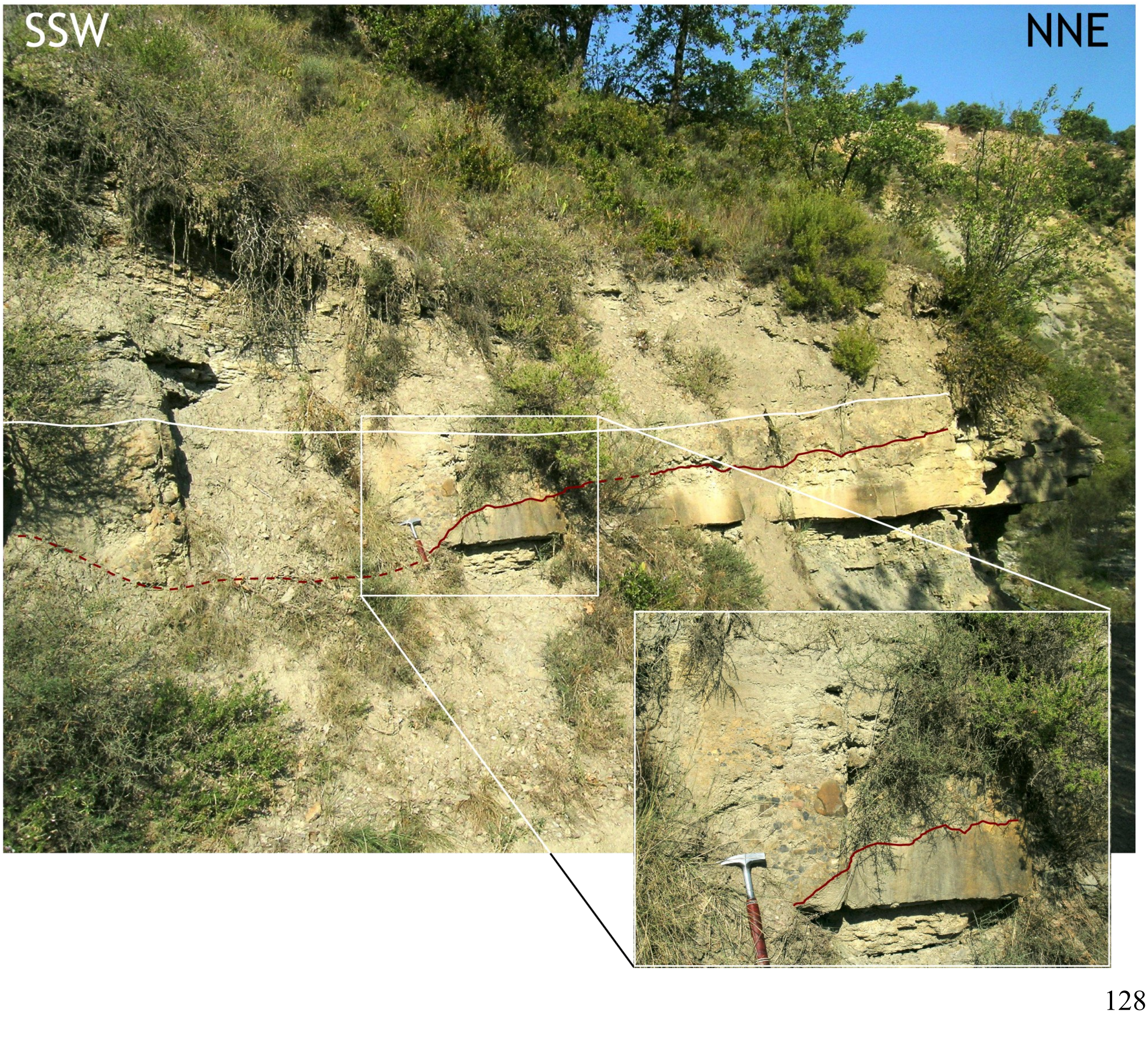
SSW
NNE

Facies interpretation

These deposits were described in detail by Angella (1999) and interpreted as fluvial mouth bar deposits, fed by northern rivers. They were earlier considered braid delta deposits (Eichenseer & Luterbacher, 1992, and references therein), that composed the lowstand wedge of the Ager Sequence .

The relevance of this unit stands in the fact that it represents a short-lived, but significant, input of deltaic deposits during the early stage of the Ilerdian transgression.

"PUIGCERCOS" UNIT

This unit is characterized by a very limited areal extent, to the point that its actual presence in the Puigcercos exposure is quite doubtful. The body that Barberà et al. (1997) were considering with their "Puigcercos Formation" is actually exposed within the Rio Palau exposure (section [20]), and was decribed in detail by Fonnesu (1984). It is located at the base, or close to the base of the Tendrui fm. (details concerning its stratigraphic position, mainly in relation with the "Farga unit" were investigated by Angella, 1999); this unit probably scours within the lower CL6 unit, because it apparently occurs on the same stratigraphic level.

This body is an Alveolina/miliolid grainstone, characterized by bimodal sigmoidal-shaped (sensu Mutti et al., 1985) cross bedding, and an overall lenticular geometry (**figure 4.27**). These depositional structures and geometries were not recognized in the Puigcercos exposure ("Espadat" hill, a few kms to the southeast of the Rio Palau exposure).

Similar deposits attributable to this unit are located in the eastern sector of the basin (near St. Miquel de la Vall) and in the Rio Isabena Valley near Serraduy (Eichanseer & Luterbacher, 1992).

Facies interpretation

This unit was interpreted by Fonnesu (1984) as a bioclastic tidal channel, formed during the earliest stages of the Ilerdian transgression; Angella (1999), although recognizing a similar stratigraphic position, opted for a positive geometry of the body, and preferred an interpretation as a bioclastic barrier island. The tidal interpretation is here preferred.

Figure 4.27 – Tidal deposits of the Puigcercos Unit; Rio Palau exposure, section [20].

SERRA-PUIT UNIT

It is equivalent to the Serra-Puit depositional system of Fonnesu (1984) and partially equivalent with the Eroles Sandstones member of Barberà et al. (1997). At basinal scale, its most recurrent expression is a tabular package of thick, locally amalgamated medium to fine-grained sandstones, associated with interposed muddy siltstones and discontinuous sandy calcarenitic layers. Locally (e.g., the Serra Puit hill, north of Guardia de Noguera), these sandy deposit are replaced by pebbly coarse sandstones with crude oblique laminations, and paleocurrents oriented to the west (**figure 4.28**).

Similarly to its marginal carbonate equivalent (Alsina-2 unit, see below CHAP), the Serra-Puit beds host shallow-water fossils (alveolinids) that sharply contrast with the deeper faunal compositions recorded within the underlying "*Nummulites globulus* Shales" (see above).

Facies interpretation

The Serra Puit depositional system was attributed a deltaic origin since the work of Fonnesu (1984); according to the criteria proposed by Mutti et al. (1996, 2000) for the deltaic systems of the foreland basins, it may be interpreted as relatively low-efficiency deltaic complex, with proximal lobes ("Eroles facies") attached to a distal mouth bar ("Serra-Puit facies").

Figure 4.28 - Coarse sandstones of the Serra-Puit Unit resting on open shelf mudstones, near Villamolat (section [19])

4.3.1.6 – *Tendrui Formation-southern sector of the Tremp basin*

Carbonate deposits dominate along the southern border of the Tremp basin, and within the studied interval are organized in five distinct bodies mainly composed of calcarenites (**2.4.5.1**). These were named Guardia, Estorm, Alsina, Alsina-2 and S. Llucia units (**figure 4.29**)

The axial muddy deposits of the Tendruy fm. are both lateral to- and interbedded with the calcarenitic bodies, in the shape of mudstone wedges that pinch out towards the south. The lateral relationships between the marginal calcarenites and the axial mudstones and sandstones are still problematic; this feature will be discussed individually for each unit.

Stratigraphic studies and environmental interpretations were provided by Luterbacher (1973), Fonnesu (1984), Eichenseer & Luterbacher (1992), Barberà et al. (1997) and finally Waehry (1999).

The carbonatic deposits were studied in the field in descriptive terms, concerning bed thickness, typology of the stratal boundaries and major compositional features (macrofossils, sand and mud content, sedimentary structures); insights on their composition was provided by the observation of microfacies from 30 samples collected in section [16], with the aid of C. Papazzoni (UNIMORE).

INTERPRETED PANORAMIC VIEW OF THE SOUTHERN CARBONATE RAMP OF TREMP BASIN

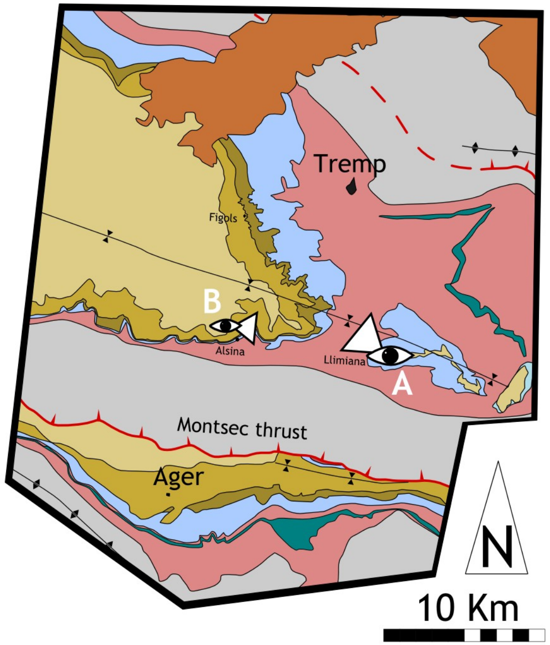

INTERPRETED PANORAMIC VIEW OF THE EASTERN SIDE OF THE "BARRANC DE LA MULLER" (SECTION [16])

LIMESTONE BANKS ① Guardia and Estorm Units ② Alsina Unit ③ Alsina2 Unit ④ S.ta Llucia Unit

Figure 4.29 (former page) - views of the southern carbonate ramp of the Tremp basin. Some features and units discussed in the text were highlighted.

GUARDIA UNIT

This unit is the most extended of the southern carbonate banks towards the north, laterally grading into a muddy succession between the villages of Guardia de Noguera and Puigmaçana.

It is almost entirely composed of nodular grainstones/packstones with abundant alveolinids and miliolids. Towards the north, the grainstones/packstones are transitionally replaced in the lateral and vertical sense by beds with a finer lithology (commonly very nodular packstones/wackestones, cf. **figure 4.31**, above, and **4.32**, below; retreating homoclinal ramp of Eichenseer & Luterbacher, 1993), and nummulitids replace the alveolinids in the upper portion of this unit. In sections [19] and [20], the Guardia Unit is almost entirely replaced by mudstones with interbedded thin sandy and calcarenitic layers; also lateral to the Guardia Unit are the Puigcercos and Farga units (see above, **4.3.1.5**; Fonnesu, 1984; Angella, 1999).

In the southern sector, the Guardia Unit is typically composed of well-cemented decimetric grainstone/packstone beds, with upper wavy bedding surfaces (probably of early diagenetic origin) and dark mudstone interbeds (not always present), organized in m-scale packages. These packages commonly display a sharp wavy top and a transitional base, represented by a nodular/lenticular facies with nodule dimensions decreasing towards the bottom of the package (it is roughly a thickening-upwards succession; cf. **figure 4.30**, above). This "finely nodular" interval rests either on mudstones or on the top of a former calcarenitic package.

Porcellanaceous foraminifera, particularly alveolinids, frequently associated with Orbitolites, constitute a characteristic paleontological feature of these beds. Lamellibranchs of the genus Lucina are commonly found in life position in the lower portion of the succession; other lamellibranchs, gastropods and echinids are also common; rotalid foraminifers were rarely observed.

The Guardia Unit is the most thickness-conservative amongst the marginal carbonate banks of the Tremp basin in the E-W direction (cf. Barberà et al., 1997, **figure 2.21** and the panel of Attached Document 2), ranging across 20-30 m along the southern flank of the basin.

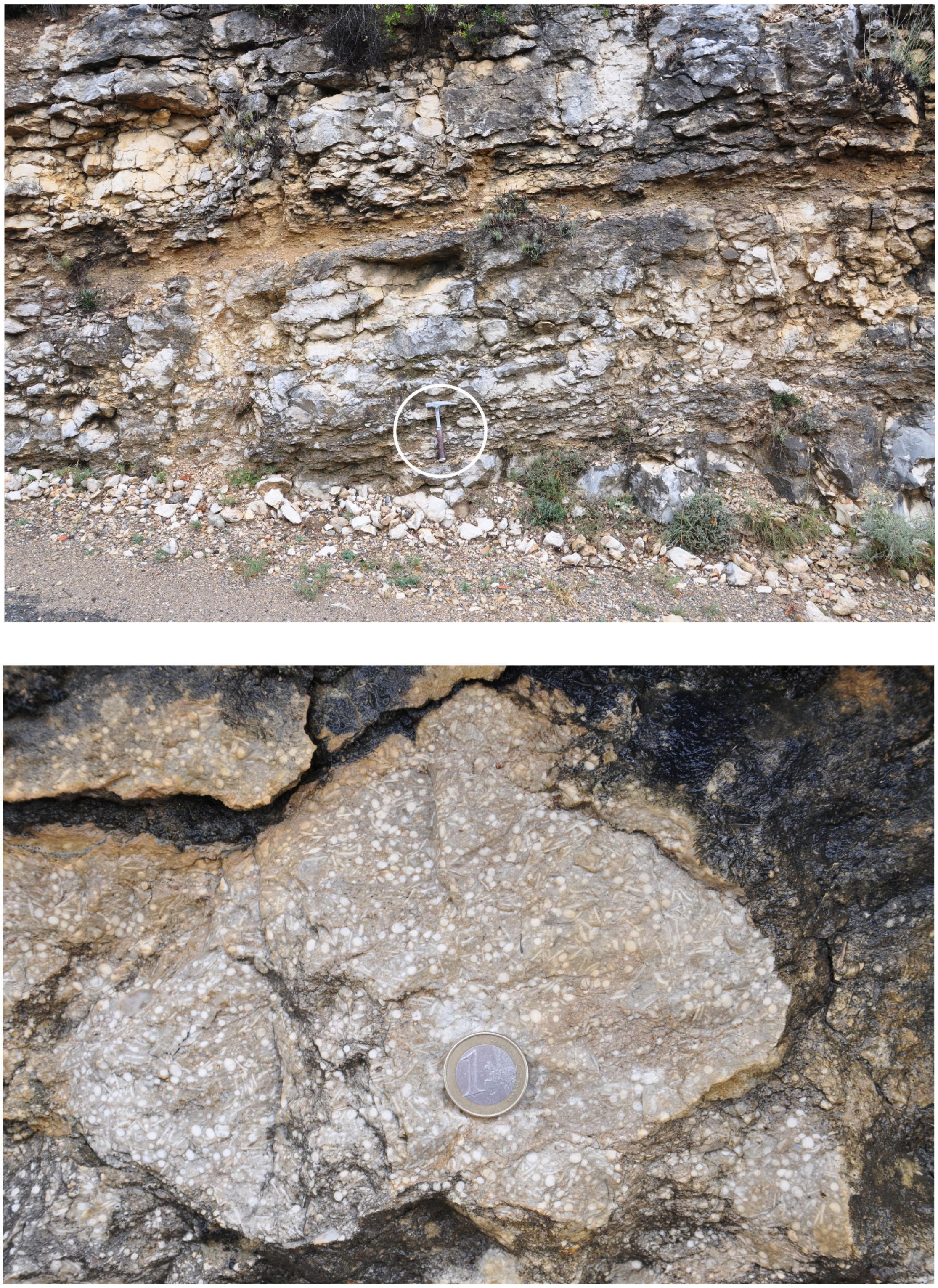

Figure 4.30 – Inner shelf deposits (Alveolina + Orbitolites bars; lower Estorm Unit; section [16]*). Notice the apparent thickening-upwards stacking of the nodular facies; below: close-up view of the coarser grainstone facies.*

Figure 4.31 – Above: Classic exposure of Guardia de Noguera; towards the south, it is not clear whether the muddy deposits between the Guardia and Estorm Units are lateral to, or onlapping above the Guardia Unit (cf. correlation panel, attached document 2).Below: mixed sandstone/bioclastic bed equivalent to the base of the Estorm Unit in the axial sector (sensu Angella, 1999).

Figure 4.32 – Inner shelf deposits; above: lower part of the Alsina-2 Unit; notice the grey and yellow bands (see text; circled hammer for scale; section [16]). Below: strongly nodular calcarenites, equivalents of the Guardia Unit on the northern Tremp basin (section [23]).

Figure 4.33 – Transitional inner/outer shelf deposits; upper part of the Estorm Unit. Section [16]

Figure 4.34 – Outer shelf sandy tabular beds with nummulitids/discocyclinids. Above: equivalent of the Estorm Unit (S. Llucia/Guardia de Noguera crossroad, south of section [17]); below: muddy equivalent of the Alsina Unit (probably onlapping above it; see text); section [19], below Villamolat.

Facies interpretations

The deposits of the Guardia Unit record the earliest stages of the Ilerdian transgression in the southern marginal sector, and are classically interpreted to have formed in a lagoonal/protected shelf environment (e.g., Luterbacher, 1970; 1973); however, the common presence of echinids, at least in the southern margin, suggests a poorly-restricted environment, anyway located within the inner sector of the carbonate ramp (C. Papazzoni, pers. comm.).

The cyclically-stacked packages rich in coarse bioclasts were interpreted as intertidal-subtidal littoral deposits, controlled either by wave or tidal activity (Luterbacher, 1970; Eichenseer & Luterbacher, 1992; Waehry, 1999); the characteristic sharp top of these bodies was interpreted to have formed as a transgressive erosional feature (ravinement surface).

ESTORM UNIT

The Estorm Unit is almost undifferentiated from the Guardia member in the southern margin of the Tremp basin, and separates from the latter in the proximity of Moror; then it rapidly pinches out (or transitionally passes to mudstones) to the north. Angella (1999) observed a layer, of mixed siliciclastic/bioclastic composition, which can be correlated with the lower part of the Estorm member (*sensu* Barberà et al., 1997) throughout the inner Tremp basin; near Guardia de Tremp, the uppermost part of the Estorm unit before shifting to the tabular facies is apparently composed of bars prograding towards the north (cf. **figures 4.29** and **4.31**).

The lower part of this unit (Estorm mb. *sensu* Barberà et al., 1997) in the southern sector is substantially similar to the Guardia unit in terms of lithology and fossil content. However, within the lower Estorm unit, a few boundstone horizons can be encountered, apparently more developed in the western sector of the ramp (cf. Barberà et al., 2011); these contain rhodolites and locally-abundant corals. In thin section, corals appear frequently bioeroded by colonies of the foraminifer *Solenomeris*, in a relation similar to the one described by Plaziat & Perrin (1992) in the northern sector of the Tremp basin (Arèn-Merli region). As pointed out by Eichenseer & Luterbacher (1992), the reefal buildups observed in the southern Tremp basin are characterized by a patchy distribution, while in the northern sector they form larger and more complex bodies.

In the upper part of the Estorm Unit, the grainstone/packstone beds are gradually replaced by packstones and wackestones; similarly, paleocommunities shift quite abruptly from alveolinid- to nummulites-dominated associations. The finer-grained beds of the upper Estorm unit are typically organized in metric to decimetric layers characterized by strong bioturbation and a finely nodular structure (**figure 4.33**); these beds in turn grade vertically to nummulitic mudstones (**figure 4.36**)

Although the base of this unit can be easily followed towards the center of the basin (Angella, 1999), its actual lateral relationships with the axial deposits are more difficult to assess.

Within sections [17] and [19], it apparently passes to tabular beds, similar in facies to the ones described in the upper/northern relatives of the Guardia Unit (nodular nummulitic wackestones/packstones); these beds are interbedded with nummulitic mudstones and are organized in decametric packages with an overall thinning-upwards stacking pattern, and grade to the north to a mixed carbonate-siliciclastic composition (Angella, 1999). At least three main cycles of this kind can be recognized throughout the basin in the stratigraphic interval equivalent o the Estorm Unit.

The basal layer adopted by Angella (1999) as a keybed shows similar characteristics, although its mud content is much lower (it is substantially a grainstone/packstone for most of its extension), and the terrigenous component is more limited to the north (sections [21] and [22]), and apparently concentrated in the lower part of the bed.

Facies interpretations

The overall succession represented by the Estorm Unit can be interpreted as the vertical and lateral transition from inner to outer shelf, mainly on the basis of faunal and lithological change (cf. Eichenseer & Luterbacher, 1992, and references therein).

The lower bioclastic deposits (grainstones) of the southern Tremp basin are interpreted similarly to the ones of the Guardia Unit.

Facies relationships between the southern calcarenitic deposits and the northern mixed/siliciclastic deposits were treated by Angella (1999) and Mutti et al. (2000), and are reported above in **4.3.1.5**. A more specific interpretation was proposed by Angella for his keybed, seen as the product of a tsunami event (cf. “Bioclastic debris flows” of Waehry, 1999), related with tectonic activity occurring in the northern sector (cf. the lower Ilerdian unconformity in the Arèn-Iscles sector documented by Fonnesu, 1984).

ALSINA UNIT

This unit is very limited in areal extension, and it is characterized by a peculiar facies, well expressed in the exposure of section [16], but apparently relatively common in different locations of the basin (Eichenseer & Luterbacher, 1992).

It rests on nummulitic wackestones/mudstones, and in section [16] its basal portion is composed of nummulitic wackestones/floatstones with scattered corals.

Above that a ~10 m thick, lenticular body develops (**figure 4.35**), with large-scale oblique stratification dipping towards the basin axis (north-dipping in section [16]). The oblique strata are part of sigmoidal units, with a sub-horizontal top marked by nodular horizons, and steeply-dipping (up to 25°) tangential foreset strata. The internal structure of the sigmoids is cross-bedded, with a distinctive foreset geometry; foresets typically prograde in the same direction of the larger-scale clinostratifications, but with a lower angle.

Each sigmoidal unit progrades and slightly aggrades over the former one (**figure 4.35C**), and each unit is separated from the successive by relatively fine-grained (wackestone) intervals. The bulk of the body is composed by packstones/wackestones and subordinate grainstones, with abundant large nummulites, fragments of lamellibranchs and echinids.

The lower part of the sigmoidal units gently downlaps towards the north, within a few hundreds of meters, and grades to a package of subhorizontal beds, represented by an alternation of glauconite-bearing packstones and wackestones (**figure 4.35E**), characterized by a fossil association of discocyclinids and ortophragminids, plus echinid fragments and, locally, large oysters.

Within sections [16] and [17], similar lenticular bodies are exposed in this same stratigraphic position (i.e., above the Estorm Unit), but it wasn't possible to observe them closely.

Facies interpretations

These bodies are classically interpreted as "*Nummulites* banks" (Eichenseer & Luterbacher, 1992, and references therein), that are peculiar calcarenitic accumulations, exclusive to the fossil record. The interpretation of *Nummulites* banks is still quite problematic (Arni, 1965; Fournie, 1975; Aigner, 1982; Racey, 2001; Guido et al., 2010). Besides a general agreement on their occurrence in a middle-outer ramp setting, the mechanisms of accumulation are still unclear, primarily because of the absence of modern analogues.

According to the cited papers, *Nummulites* banks can be interpreted either as dynamic, current-driven accumulations, or as in-situ buildups. The latter hypothesis is based on analogies with rimmed-shelf systems, and on the relatively common occurrence of these bodies over structural highs (one example was described in the northern Tremp basin by Eichenseer & Luterbacher, 1992).

Although discriminating between these hypotheses is beyond the scope of the present work, the cross-bedding that internally characterizes the sigmoidal units of these banks indicates accumulation under the action of currents; however, these sigmoidal units might also represent a marginal detrital facies developing on the front of a larger buildup (e.g. a reef).

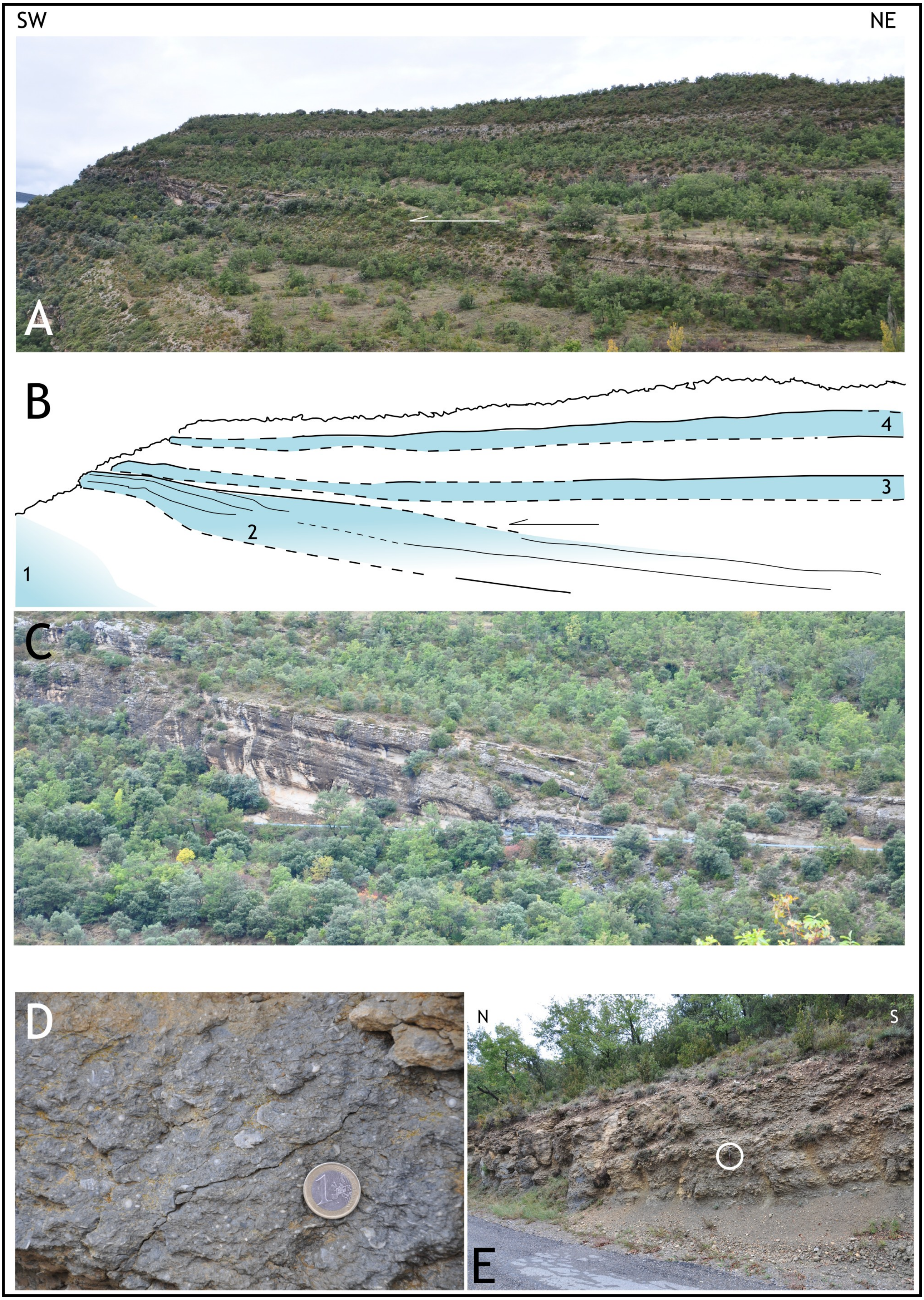
SW
NE
A
B
4
3
2
1
C
D
N
S
E

Figure 4.35 (former page) - Nummulites bank of the Alsina Unit. A, B: panoramic and interpreted view of the western side of the Barranc de la Muller (section [16]) See fig. 4.29 for unit names. C: detail of the cross-bedded sets. D: close-up view of the packstone facies of the Nummulites bank. E: bottomsets of the Nummulites bank, eastern side of the Barranc de la Muller (circled hammer for scale).

Towards the west (section [14]), this facies apparently forms a larger buildup, although direct correlations in this interval are less reliable.

Towards the north, in section [17], the Alsina Unit is replaced by a regular alternation of tabular, nodular nummulitic beds and nummulitic mudstones (see Guardia and Estorm Units), organized in two-three main cycles (**figures 2.34**, below, and **2.36** and cf. with panel in Attached Document 2).

The lateral relationships between the *Nummulites* banks of the Alsina Unit and the tabular beds are probably different than the ones observed in the lower units. In the western exposure of the Barranc de la Muller (section [16]), tabular nummulitic packstones/grainstones sharply onlap the Alsina Unit; its internal sigmoidal geometry and the transition of the clinoform beds to basal bottomsets suggests an abrupt frontal termination of the bank; the shift from nummulites-dominated communities to the deeper ortophragminids/discocyclinids-dominated communities also indicate a sharp depth gradient on its frontal part (C. Papazzoni, pers. comm.); finally, the presence of glauconite might imply, always in the frontal sector of the bank, a very low sedimentation rate.

A possible implication of these features is that the *Nummulites* banks acted as a physical barrier between the southern ramp and the axial sector, following an event of steepening of the ramp itself.

ALSINA-2 UNIT

This unit is represented by lenticular packages, not exceeding ~10 m in thickness of grainstones and packstones/wackestones, locally resting with an onlap relationship on the Alsina Unit (Waehry, 1999).

In most locations (e.g. section [14]; northern section [16]), however, a wedge of nummulitic mudstones separates these two units. In the Southern Tremp basin, at the interface between these mudstones and the Alsina-2 Unit, a few sandstone layers are commonly found, ranging in thickness from a few centimeters to 20-30 cm; these beds are commonly composed of fossil-poor, fine to very fine-grained sandstones with well-preserved depositional structures (planar to wavy laminae to HCS).

The Alsina-2 unit is typically composed of thin-bedded (decimetric) grainstones in its lower part, with abundant miliolids and alveolinids, gradually passing to a packstones/grainstones nummulitic facies. In section [13, 14] these beds are relatively coarse-grained, and the nummlitids and alveolinids commonly occur together; in section [16] the two populations are more sharply separated. In this exposure, the lower interval (**figure 4.32**, above) is characterized by a 3 m thick alternation of white, relatively finer-grained beds and grey beds containing coarser bioclasts (commonly alveolinae). In thin section, these two facies are both characterized by a significant content in geniculate red algae (*Disticoplax sp.*; C. Papazzoni, pers. comm.), with peak abundances in the white layers, where they are associated with small benthic foraminifera.

Above this interval, the upper portion of the Alsina-2 Unit (roughly 4-5 m thick in the studied exposures) is characterized by an increased mud content, abundant nummulites and, locally, by very small coralline buildups. It is composed by grainstones and packstones/wackestones, the latter progressively more common upwards. Within this interval, the upper bedding surfaces of the coarser units frequently display a red color.

Facies interpretations

The succession recorded within the Alsina-2 Unit substantially depicts an abrupt transition from an outer ramp setting (nummulitic mudstones) to a shallower environment (*Alveolina* grainstones), followed by a progressive deepening (nummulitic packstones/wackestones). The lateral changes in paleocommunities is probably due to a slight diachronicity of the transgression in the W-E direction (i.e., from sections [13, 14] to section [16]).

The lateral relationships between the Alsina-2 Unit and the axial deposits are relatively clear, at least concerning the lower boundary of this unit, since the initial shallowing is clearly reflected in the sedimentological and paleontological features of the Serra-Puit Unit (see above, **4.3.1.5**). The transition between the two units is probably recorded in a thick, strongly bioturbated horizon of mixed carbonate-siliciclastic deposits exposed along section [17]. This horizon probably represents carbonate deposits that formed in a relatively quiet setting between distributary mouth bars, such as the one exposed along the Serra-Puit hill. In this interpretation, the terrigenous content might have been originated by overspilling fluvial floods; successive mixing might have been operated by bioturbation.

S. LLUCIA UNIT

This is a thick (up to 30 m) and widespread unit that extends from the southern margin of the basin to the Guardia de Noguera/Mur sector. North of this location it terminates abruptly, or its is laterally replaced by an alternation of mudstones, sandstones and calcarenites (see below) similarly to the Guardia and Estorm units.

It rests on a wedge of nummulitic mudstones that includes some layers of relatively thin (<50 cm) fine to very fine-grained sandstones with well-developed HCS, as well as thin-bedded (centimetric to decimetric) nummulitic grainstones. Within this muddy unit a further calcarenitic bank can be followed within the same extension of the S. Llucia unit (**figure 4.36**, and general panel in Attached Document 2).

This lower layer ranges from ~3 (south) to ~7 m (north) in thickness, and it is composed of an alternation of grainstones and packstones commonly richer in nummulites than in alveolinids; it is locally cross-bedded (e.g., section [17]).

The S. Llucia unit is mainly composed of thick accumulations of grainstones/packstones with an high variability in fossil content and grain size, both vertically and longitudinally. Commonly its base is richer in nummulites, and its middle/upper portions are richer in alveolinae. Locally (e.g. along the road between S. Llucia and Mur) its lower portion is cross-bedded, with concave-upwards foresets prograding towards the north. Along the exposure on the southern slope of the Mur hill (roughly a few hundreds of meters westward of section [17], the S.Llucia Unit is clearly organized in two main banks, separated by a few m-thick wackestone layer; the lower unit is richer in mud along this exposure, and it is organized in metric packages of nodular packstones in alternation with wackestones/mudstones. Nummulites are much more common, especially within the lower bank. Further towards the south, in the exposures of section [16], alveolinids are almost ubiquitous, with the exception of the very first layers at its base. The overall organization of the S. Llucia Unit in this location is represented by metric packages in turn composed of 20-30 cm-thick beds.

In sections [13, 14], this unit is interleaved with mudstone layers, so that it crops out in four banks composed of massive to thin-bedded grainstones (thinner beds, composed of alternated grainstones/packstones and wackestones characterize the upper part). Alveolinids are absent (or very rare), and Nummulites are almost ubiquitous.

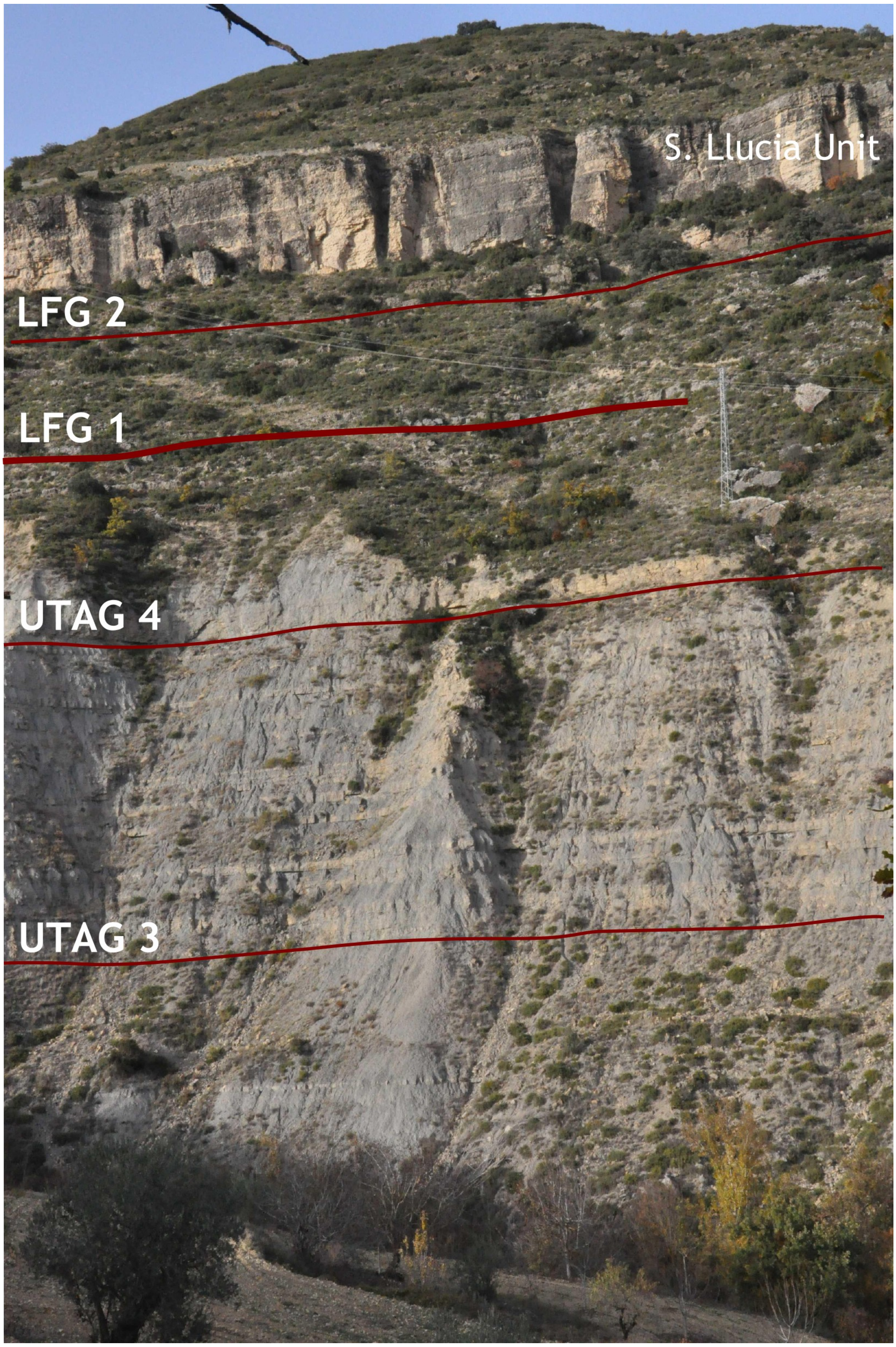

Figure 4.36 – Upper part of section [17], near Guardia de Noguera. Notice the muddy succession replacing the Estorm and Alsina Units (compare with panel in the Attached document 2).

Facies interpretations

The S. Llucia Unit is composed by deposits formed during a major expansion of the southern carbonate systems; similarly to the Estorm Unit, an inner to outer shelf transition is recorded both in the longitudinal and vertical direction (Fonnesu, 1984).

The S. Llucia Unit is affected by some problems in the correlation with the axial deposits of the Tremp basin. Similarly to the lower carbonate banks, it is lateral to a muddy succession that, in section [20], hosts thin-bedded sandstones, organized in three thinning-upwards cycles. The uppermost cycle includes a mixed to nodular calcarenitic interval, with a sharp base evidenced by a ~30 cm-thick fine sandstone bed with HCS. This unit can be observed near Figols and along the road between Puigvert and Villamolat. Sandstones and calcarenites are commonly rich in nummulites, with the exception of an individual grainstone characterized by mixed *Alveolina* and *Nummulites* specimens. This bed was interpreted as the deposit of a major storm, or tsunami (Mutti et al, 1994), and thus considered a key-horizon of regional significance.

Different correlations were proposed for these calcarenites in relation with the S. Llucia Unit (Fonnesu, 1984, Waehry, 1999, and Angella, 1999). Fonnesu and Angella correlated these units at their top; Waehry instead proposed an equivalence of the axial calcarenites with a further carbonate unit located on top of the S. Llucia Unit in his Alsina and Ribagorçana logs. This is a complex localized accumulation of nummulitic grainstones to packstones/wackestones. In sections [13, 14] they are separated by the S. Llucia Unit by a ~20-30 m-thick mudstone wedge, while in section [16] this wedge is absent or reduced to a few meters of mudstones/wackestones. However, in section [17], this “upper” calcarenitic layer is absent, and a muddy succession with interbedded thin sandstones is present.

4.3.1.7 – *Puigverd Formation*

The base of the Puigverd fm. delimits the studied interval in the Tremp basin. It is composed of relatively thick, tabular and channelized sandstones, within a predominantly muddy succession.

Its lower boundary was correlated on a purely physical-stratigraphic basis, establishing a relationship between:

1. a coarse sandstone body with crude oblique bedding and paleocurrents directed towards the north, recognized on top of the carbonate deposits of the S. Lllucia unit in section [16] (**figure 4.37**, below),

2. a 2 m-thick, tabular, graded (medium to very fine sand) sandstone layer, characterized by abundant bioclastic content (with mixed alveolinids and nummlitids), well-developed current ripples and large-scale HCS, exposed near Figols (**figure 4.37,** above) and directly followed up to the Mur sector, and,
3. the first sandstone beds exposed above the top of the S. Llucia Unit in sections [17] and [13, 14].

This correlation in part follows the one proposed by Waehry (1999, his FG2/FG3 boundary), with exception of its position within section [16] (much higher in the cited paper).

Facies interpretations

The occurrence of coarse-grained and thick-bedded siliciclastic deposits above the S.Llucia limestones suggests a similarity with the Serra-Puit Unit. The coarse deposits observed in section [16] may be interpreted as deltaic mouth-bar deposits, like other similar units discussed in the text; analogously, the tabular graded sandstones with HCS constitute relatively proximal deltaic sandstone lobes.

The significance of the boundary related with these sedimentological changes imply a relative sea-level fall (although less pronounced than the one recorded at the base of the Serra-Puit Unit), that initiates the generalized shallowing trend that characterizes the Upper Figols Group and the overlying Castigaleu and Castissent Groups (Fonnesu, 1984; Mutti et al, 1994).

A possible event of deformation related with uplift in the southern sector might have triggered this change, as is suggested by the complex subsidence patterns recognized on top of the S. Llucia Unit (that also generated the different correlations proposed by former authors).

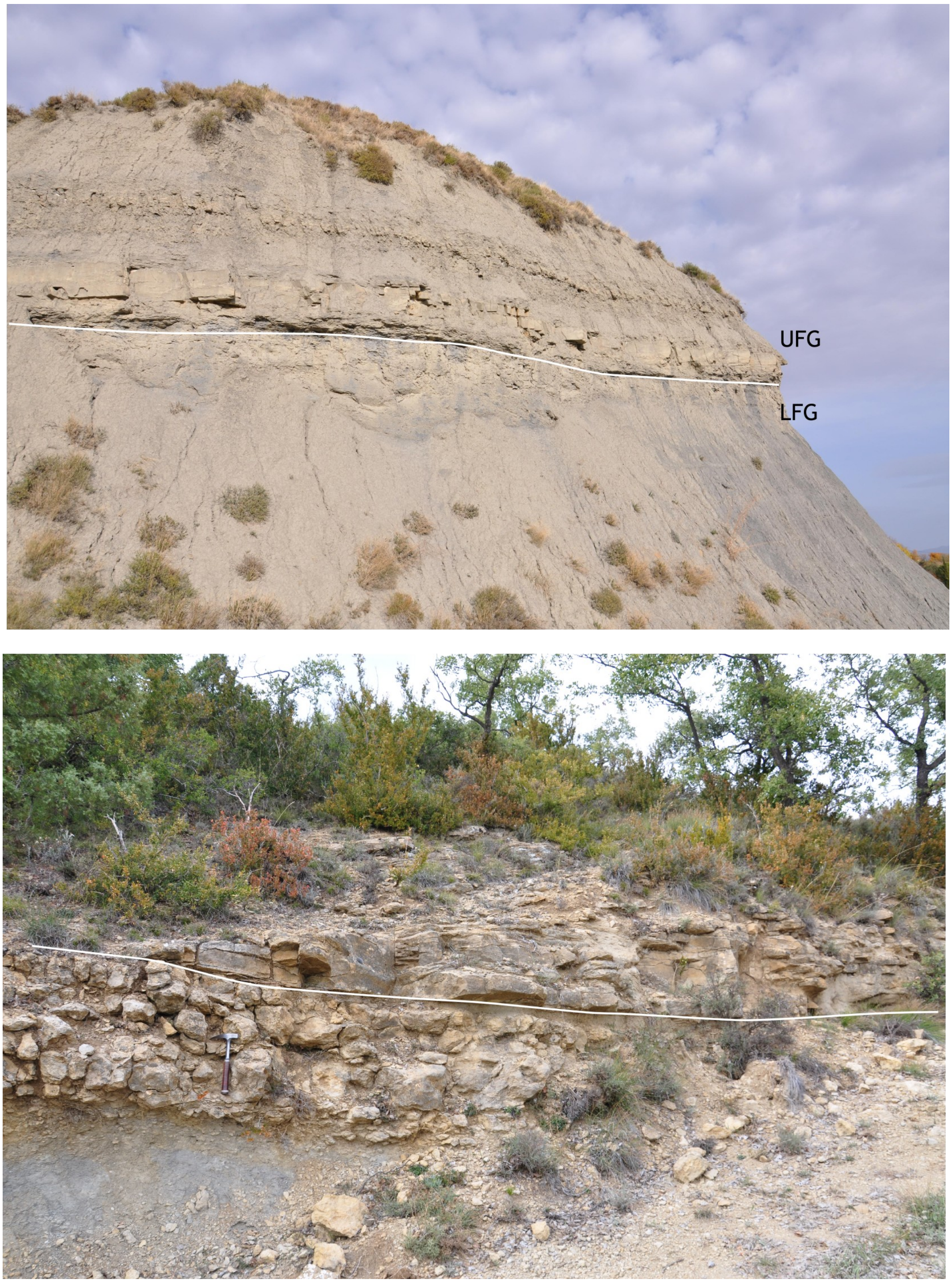

Figure 4.37 - Lower boundary of the Puigvert fm. (LFG/UFG boundary). Above: thick deltaic sandstone lobe near Figols (section [20]); below: mouth bar deposits overlie outer shelf deposits in the southern sefctor of the basin (section [16]).

4.4 – Physical stratigraphy

4.4.1 – Geometric reconstruction of the southern ramp of the Tremp basin

A tentative reconstruction of the geometric relationships between the main carbonate banks in the southern margin of the Tremp basin was performed in the “Barranc de la Muller”, between the villages of Alsina and Moror; this small valley allows a 3D evaluation of the succession (**figures 4.38** and **4.39**).

Stratigraphic logs were measured on both sides of the valley, and cross-sections were plotted on 1:5000 ortophotomaps and topographic maps produced by the Institùt Cartografic de Catalunya.

Stratal dips were directly measured in different locations with the use of a Silva compass (**figure 4.38**); these measures couldn't be uniformly applied, mainly because of the irregularity of stratal surfaces, so they were integrated with dip calculations derived from map views.

The results should be compared with the general panel (Attached Document 2) and with the flattenings discussed in **4.4.4**.

The profile obtained is highly interpretative (**figure 4.39**), but it provides some indications on the main deformational stages occurring in the Early Ypresian succession on the hangingwall of the Montsec Thrust.

The most significant of these indications are the following:

1. the package including the Guardia, Estorm and Alsina Units is affected by the major local stratigraphic expansion;
2. the Guardia and Estorm Units, here directly superposed, are tilted altogether before the deposition of the Alsina Unit;
3. the Alsina Unit is onlapped both by relatively deep-water deposits (nummulitic mudstones) and more sharply by the Alsina-2 Unit;
4. the Alsina-2 Unit is interested as well by onlap of progressively deeper muddy deposits;
5. the Alsina-2 and S.Llucia Units display an overall aggradational pattern.

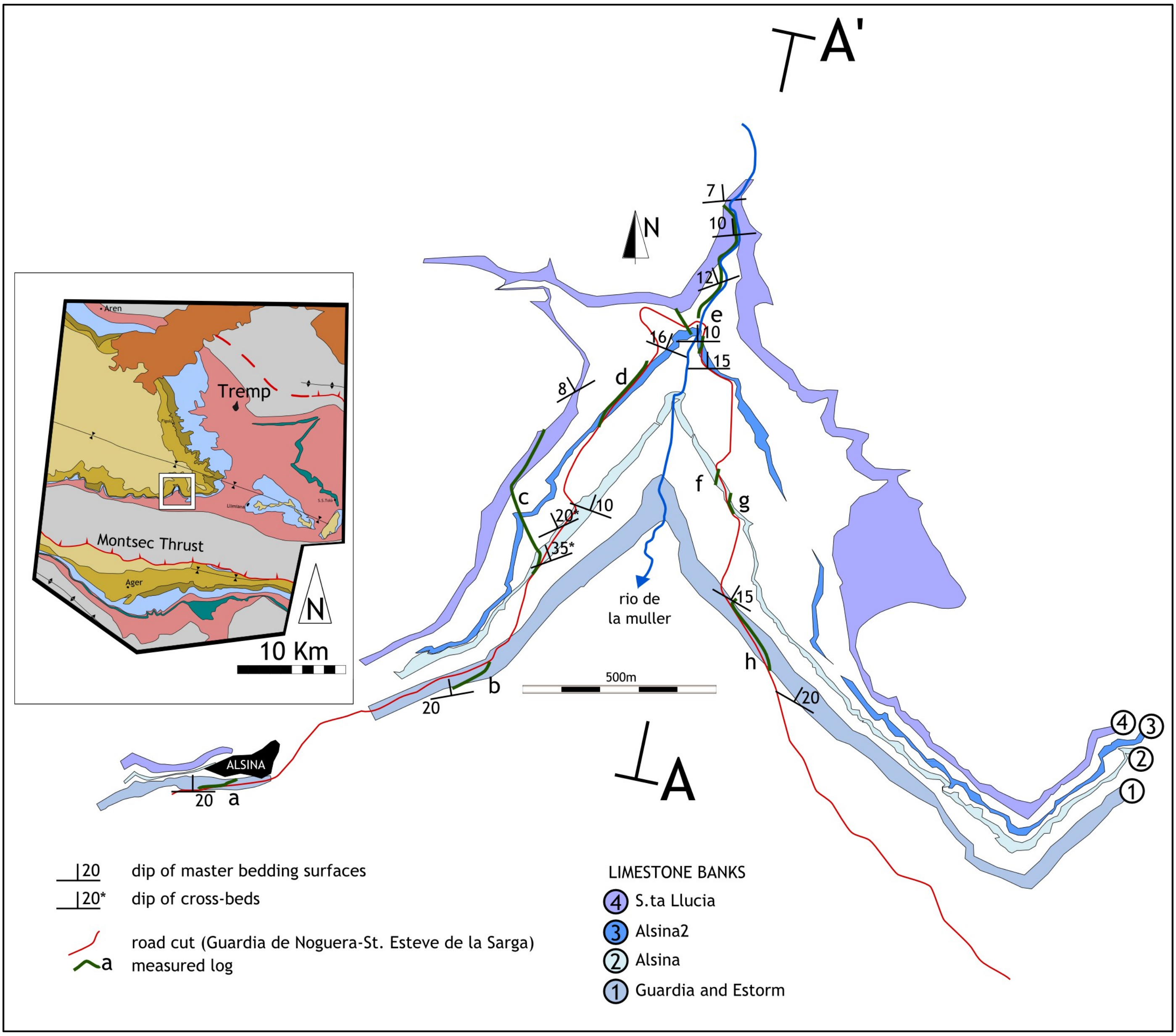

Figure 4.38 - Photogeological map of the "Barranc de la Muller" (section [16])

Figure 4.39 (next page) - Interpretive cross-section, based on field and map data, representing the geometry of the main carbonate banks developed on the southern margin of the Tremp basin (cf. figure 4.38).

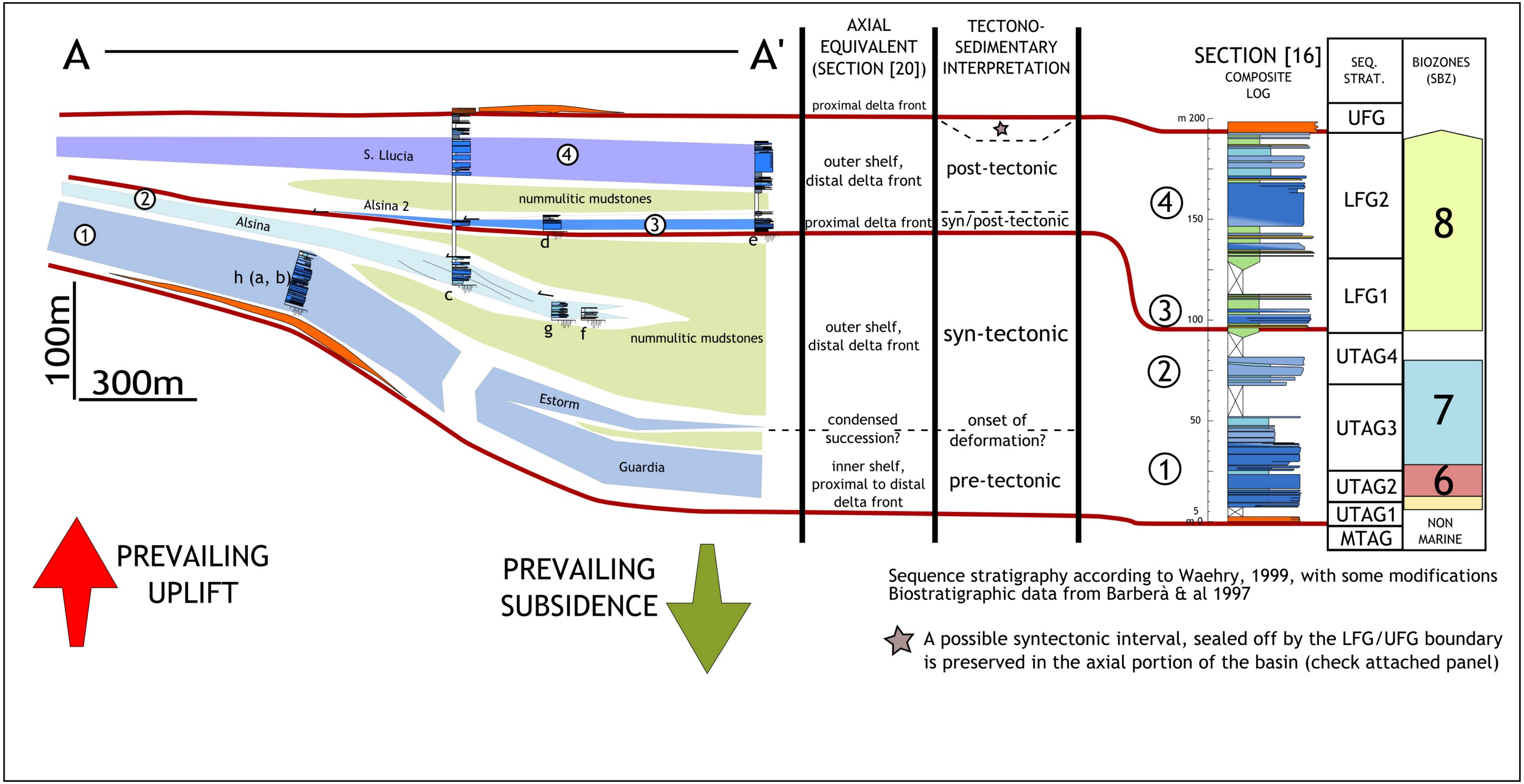

A
A'
100m
300m
S. Llucia
Alsina 2
Alsina
h (a, b)
c
d
e
f
g
nummulitic mudstones
nummulitic mudstones
Estorm
Guardia
PREVAILING UPLIFT
PREVAILING SUBSIDENCE
AXIAL EQUIVALENT (SECTION [20])
proximal delta front
outer shelf, distal delta front
proximal delta front
outer shelf, distal delta front
condensed succession?
inner shelf, proximal to distal delta front
TECTONO-SEDIMENTARY INTERPRETATION
post-tectonic
syn/post-tectonic
syn-tectonic
onset of deformation?
pre-tectonic
SECTION [16]
COMPOSITE LOG
m 200
150
100
50
5
m 0
SEQ. STRAT.
UFG
LFG2
LFG1
UTAG4
UTAG3
UTAG2
UTAG1
MTAG
BIOZONES (SBZ)
8
7
6
NON MARINE
Sequence stratigraphy according to Waehry, 1999, with some modifications
Biostratigraphic data from Barberà & al 1997
A possible syntectonic interval, sealed off by the LFG/UFG boundary is preserved in the axial portion of the basin (check attached panel)

On a broader scale, this description may be further integrated, (cf. Attached Document 2 and **4.4.4**).

The Guardia Unit is relatively thickness-conservative along the southern margin (cf. Eichenseer & Luterbacher, 1992), and towards the basin axis, it is separated by the Estorm Unit, suggesting the presence of angular relationships amongst the two (Angella, 1999), or a facies change of the upper part of the Guardia Unit towards the north. In the general panel, most of the increase of subsidence apparently occurs within Guardia de Noguera and Villamolat, within sequence UTAG 2.

Waehry (1999) came to a similar conclusion, establishing that it was during this period that the axial succession began to onlap towards the south. Angella (1999), who correlated the base of the Estorm Unit with a tectonic unconformity in the northern Tremp basin, came to a different conclusion (a truncation of the mudstone wedge).

The main difference in the two interpretations stands in a gradualistic vs dramatic occurrence of tectonic deformation (see **4.4.3**)

A long-term synsedimentary growth of the Montsec high is recorded within the interval comprised between the high portion of the Guardia Unit and the Alsina-2 Unit.

Correlated with this marginal growth, is the enhanced axial subsidence recorded in a time interval roughly equivalent with the separation of the Guardia and Estorm Units that eventually brought to maximum flooding conditions.

A striking feature is the fact that, although sea-level changed periodically, only at the end of this deformational stage a major (or, at least, more evident) relative sea-level fall occurs.

This interpretation implies that the LFG succession substantially formed during a stage of relative tectonic quiescence (see also **4.4.4**)

4.4.2 – Adopted subdivision: major surfaces

In order to assess a physical-stratigraphic framework, major unconformities and flooding surfaces must be located and correlated within the two basins.

4.4.2.1 – *Major unconformities*

Five major unconformities are included within the studied interval, that delimit major sequence-stratigraphic units. These may be considered allogroups *sensu* Mutti et al. (1988), although the basal unconformity (MPU) should only be considered as a reference layer.

1. **MPU** (Middle-Paleocene Unconformity). This unconformity is located within the top of the Vallcebre fm. and the base of the Upper Red Garumnian; its areal and temporal scale were mainly defined on chronostratigraphic criteria (Feist & Colombo, 1983; Baceta et al., 2011), and it is apparently related with a global sea-level fall. It probably follows an initial stage of tectonic reorganization of the southern Pyrenean foreland (cf. Rosell et al., 2001); in the Ager basin, it might be associated with the initial deformation related with the uplift of the St. Mamet and Millà highs (cf. Rossi, 1997). It is therefore tentatively chosen as a reference layer for the definition of a "Middle Tremp-Ager Group", mainly of Thanetian age, related with the initial development of the Paleo-Montsec high as a physical barrier that divided the two basins.

2. **UPU** (Upper Paleocene Unconformity). This unconformity is located along the incised-valley fill at the base of the "Claret Formation" in the Tremp basin; in the Ager basin, a possible equivalent may be the karst surface on top of the Upper Thanetian miliolid beds (Unit URG4), and the angular unconformity between the continental and marine deposits in the northern sector of the basin. Facies interpretations suggest that the base of the Claret Conglomerate, and its possible equivalent in the southern Ager basin (cf. Unit URG5) may be a better reference layer in order to identify the occurrence of a major tectonic event (e.g., uplift in the Axial zone and steepening of the frontal part of the Boixols-Turbon Thrust); the two events may however be related (generalized uplift and creation of a sedimentary hiatus; later response of the deltaic systems). This unconformity defines the base of the UTAG in the Tremp basin (*sensu* Waehry, 1999), and so in the Ager basin.

3. **LYU** (Lower Ypresian Unconformity). This unconformity is exposed in the northern sector of the Tremp basin (Fonnesu, 1984), and it is clearly related with tectonic activity along the Boixols

thrust front. The southern equivalents are basically unknown and different interpretations have been provided by former authors. In the present work, the stage of synsedimentary deformation described in the southern margin of the Tremp basin includes the stratigraphic horizon that was considered most likely to correlate with this unconformity (Angella “keybed”, 1999), suggesting a slight diachronicity between deformation on the Boixols and Montsec highs in this period. Therefore this unconformity, instead of delimiting an allogroup, is probably correlative to a syntectonic succession (cf. **4.4.3**).

4. **MYU** (Middle Ypresian Unconformity). This is the classic unconformity related with the base of the Figols Group in the Ager basin. Chronostratigraphic data (see **2.5.3** and Appendix 1) correlate this unconformity with the major sea-level fall recorded in the Tremp basin at the base the Alsina-2 and Serra-Puit Units. Where syntectonic growth could be observed, this unconformity seals off the growth strata.

5. **MUYU** (Middle-Upper Ypresian Unconformity). This unconformity separates the LFG and UFG, and its expression in the Tremp basin is still quite problematic. The wedge-shaped interval between the top of the S.Llucia Unit and the base of the UFG might constitute the record of syntectonic deposition.

4.4.2.2 – *Transgressive and Maximum Flooding surfaces*

The correlation of transgressive and MF surfaces in the two basins is more speculative.

In the continental deposits of the MTAG, the transgression occurred during the late Thanetian probably have an equivalent in the western Tremp basin; however, its correlation in the Tremp basin is unknown.

The flooding surface associated with the Ilerdian transgression is classically documented in both basins (e.g. Luterbacher, 1969). Other transgressive events are recorded within the Tremp basin during stages of expansion of the southern carbonate ramp (Eichenseer & Luterbacher, 1992; Angella, 1999), but their correlation within the axial sector is largely hypothetical; in most cases transgressive and maximum flooding surfaces cannot be properly distinguished when defining small-scale sequences in the muddy axial succession.

Within the LFG the main transgressive event is recorded by the thick calcarenitic accumulations of the S.Llucia Unit in the Tremp basin; in the Ager basin, a possible equivalent would be the represented by the bioclastic deposits formed in the upper part of the Lower Baronia Sandstones

(Mutti et al., 1994b, c), although these two units may be slightly diachronous.

Different criteria may be applied in the recognition of maximum flooding surfaces, but a practical one is based on the occurrence of basin-wide marine mudstones, i.e., the drowning of carbonate shelves and deltas. When compared with “conceptual” maximum-flooding surfaces, defined on the presence of condensed successions different results may occur (cf. Waehry, 1999 and Eichenseer & Luterbacher, 1992).

In the Tremp basin, the MFS of the UTAG was associated with a condensed succession (roughly located within SBZ 6) that could actually be recognized on the basis of nearby reference layers: examples are the “*Spondylus* beds”, an horizon of peak abundance in planktic foraminifers and the base of the *Turritella* Marls (Eichenseer & Luterbacher, 1992, and references therein). Only in the marginal areas there is evidence for the formation of glauconite, but it occurs on different stratigraphic levels; in the axial sector, its formation was probably hampered by the persistence of deltaic inputs also in periods of sea-level rise (discussed by Angella, 1999).

In the Ager basin, the glauconitic deposits in the upper part of the Cadì fm., and the presence of an (apparent) condensed succession (as reconstructed on the basis of biostratigraphic data, CHAP) might indicate an equivalent of the Tremp basin's MFS; Mutti et al. (1985, 1994c) adopted the dip-slope on top of the Cadì fm. as a regionally-correlatable MFS.

Within the Lower Baronia Sandstones, the common occurrence of glauconite is probably related with higher-frequency relative sea-level variations (Mutti, 1992; Mutti et al., 1994a); similarly to the UTAG, the main dip-slope on top of the Lower Baronia Sandstones was interpreted as a MFS (Mutti et al., 1994c).

In the Tremp basin, a correlative MFS is probably located on top of the S.Llucia Unit.

4.4.3 – Minor sequences

The subdivision in small-scale sequences was operated only in the Lower Ypresian interval. The criteria followed for this subdivision are treated in **3.2.5**; the main controlling factors on the development of the smaller scale units are, ultimately, sea-level variations.

The elementary sequences defined by former workers cannot be correlated properly between the two basins, signifying that local factors (e.g. different rates of subsidence related with the different structural settings) might have caused a different response of the depositional systems. Tectonics could have enhanced both sequence boundaries along the basin margins and transgressive to highstand conditions within their axial sectors (Mutti et al., 1994a).

The smallest sequences defined by Waehry (1999) in the Tremp basin couldn't be properly traced along all of the sections, and only his “Large scale” units were adopted (UTAG 1-4 and LFG 1-2). Within the LFG of the Ager basin, a possible equivalence with the LFG 1 and 2 of the Tremp basin was proposed (see **figure 2.9**).

The difficulties in measuring a transect of the UTAG in the Ager basin hamper a similar correlation. According to Mutti et al. (1994, stop descriptions; E. Mutti, pers. comm.), the unit here informally designated as CS3 (see **4.2.1.3**) represent the lower part of a sequence (lowstand to transgressive), formed in response to a major relative sea-level fall. The succession of the Cadì fm. was therefore subdivided in two main sequences, UTAGa and UTAGb.

On the basis of chronostratigraphic data (see **2.5.3**), there may be equivalence between the UTAG b in the Ager basin with the syntectonic interval represented by the middle-upper portion of the UTAG in the Tremp basin. Subsidence patterns measured in the Tremp basin (see below) locate within the SBZ5 or SBZ6 the beginning of the main stage of differential subsidence, i.e., a time interval likely to be recorded within the UTAG b “condensed” interval (see CHAP; it is also possible for this condensed succession to be originated by the presence of one or more significant hiatuses within the base of the UTAGb and the base of the FG).

4.4.4 – Subsidence patterns

The subsidence patterns, associated with the uplift of the Paleo-Montsec high, cannot be properly extimated within the Ager basin, because of difficulties in establishing N-S correlations.

Within the Upper Red Garumnian succession, Rossi (1997) recognized a differential pattern occurring in his sequences 1 and 2 (roughly equivalent to Units URG 1 and 2) between the depocentral area of the southern sector (section [4]) and the incipient highs of the St. Mamet and Millà anticlines.

Rosell et al. (2001, and references therein) interpreted the continental conglomerates exposed in the northern limb of the Ager syncline as the first evidence of the presence of an ancestral Monstec high. However, also the correlation between the northern and southern sector is only based on a litostratigraphic equivalence of the deposits here collected in Unit URG1; this hypothesis will be tested in chapter **5**.

Figure 4.40 (next page) - Correlation panel in the range of the Paleocene/Eocene boundary in the southern limb of the Ager basin. See the text below for comments

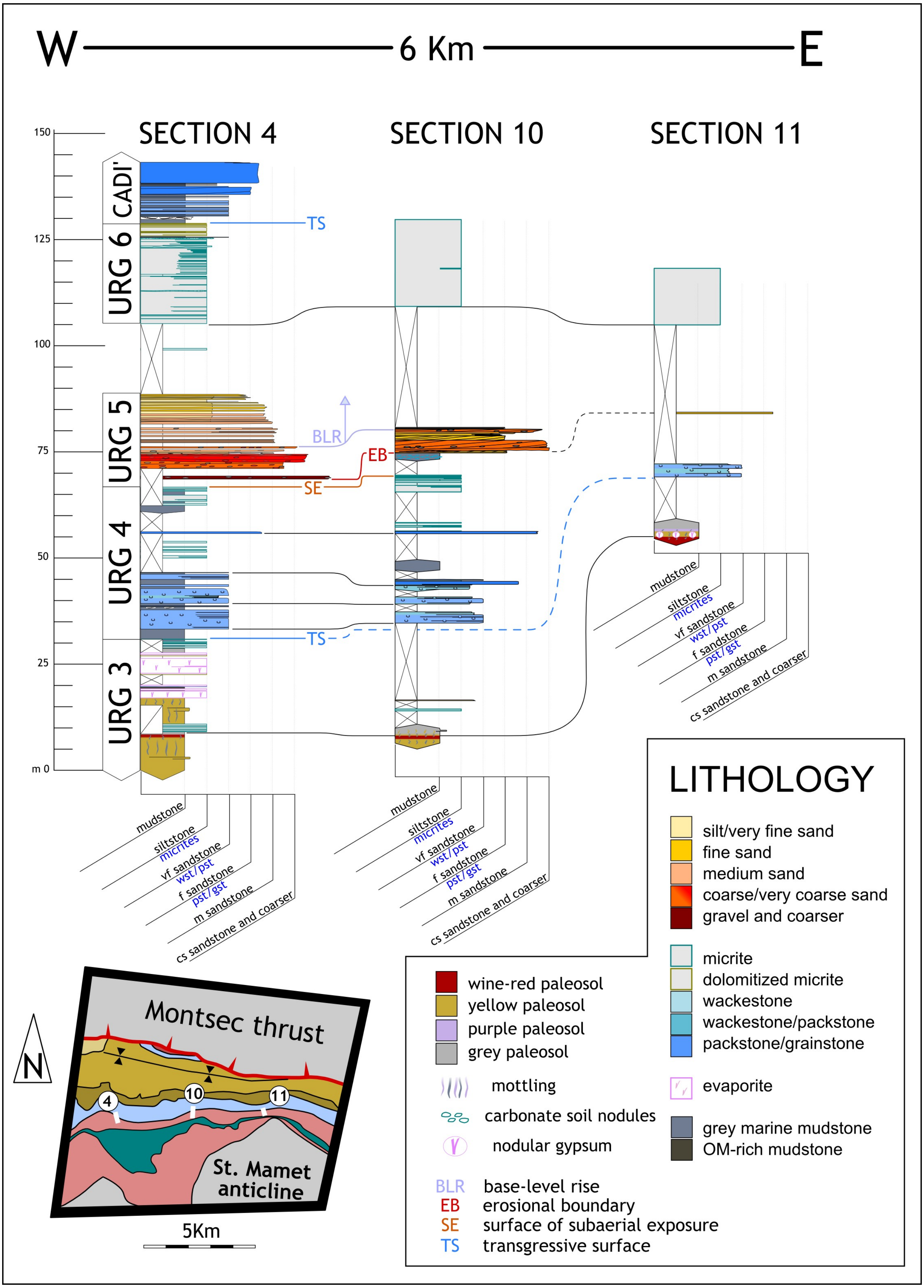

W
6 Km
E
SECTION 4
SECTION 10
SECTION 11
150
125
100
75
50
25
m 0
CADI'
URG 6
URG 5
URG 4
URG 3
TS
BLR
EB
SE
TS
mudstone
siltstone
micrites
vf sandstone
wst/pst
f sandstone
pst/gst
m sandstone
cs sandstone and coarser
LITHOLOGY
silt/very fine sand
fine sand
medium sand
coarse/very coarse sand
gravel and coarser
micrite
dolomitized micrite
wackestone
wackestone/packstone
packstone/grainstone
wine-red paleosol
yellow paleosol
purple paleosol
grey paleosol
mottling
carbonate soil nodules
nodular gypsum
evaporite
grey marine mudstone
OM-rich mudstone
BLR base-level rise
EB erosional boundary
SE surface of subaerial exposure
TS transgressive surface
N
Montsec thrust
4
10
11
St. Mamet anticline
5Km

On the other hand, differential subsidence occurred in the southern Ager basin in the upper portion of the Upper Red Garumnian succession, as it is testified by the panel in **figure 4.40**.; more specifically, a stratigraphic expansion occurred during the late Thanetian within the St. Mamet high to the east (section [11]) and the depocentral sector to the west (section [4]). However, the actual boundaries of the syntectonic interval could not be constrained, because of bad exposures and structural complications in the sector north of the St. Mamet anticline.

The Lower Baronia Sandstones were studied in more detail, and gave results similar to the ones reported by former researchers, i.e., a relatively stable and generalized subsidence in the lower part of the succession and a more irregular pattern in the upper portion (see Attached Document 3).

In the Tremp basin, subsidence patterns within the continental deposits of the Upper Red Garmnian couldn't be properly ascertained. Apparently, axial enhanced subsidence is recorded within the Esplugafreda fm.; former workers (e.g. Waehry, 1999) suggested that angular relationships were recorded at the top of this interval, stressing on the tectonic significance of the deposits of the Claret Conglomerate. The change in subsidence for each of the discussed sequences can be observed in the reconstructions of **figure 4.41**.

The diagrams of **figure 4.42** quantifies the variation of the Lower Ypresian subsidence patterns measured in sections [16] and [20], expressed as:

$$\text{Rate of Subsidence Variation} = (Ta-Tm)/Tm$$

(Ta = axial thickness; Tm = marginal thickness)

The most striking feature is the strong variation recorded within sequence UTAG 2, that is interpreted as the main phase of tectonically-enhanced subsidence; Angella hypothized the presence of an angular unconformity at the boundary between sequences UTAG2 and 3 (upper part of the Estorm Unit. Conversely, the LFG is interested by minor expansion, as also suggested by the aggradational pattern discussed in **4.4.1**.

Figure 4.41 (next 3 pages) - Progressive flattenings in the Tremp basin. Ages are given for reference purposes. See the text for comments.

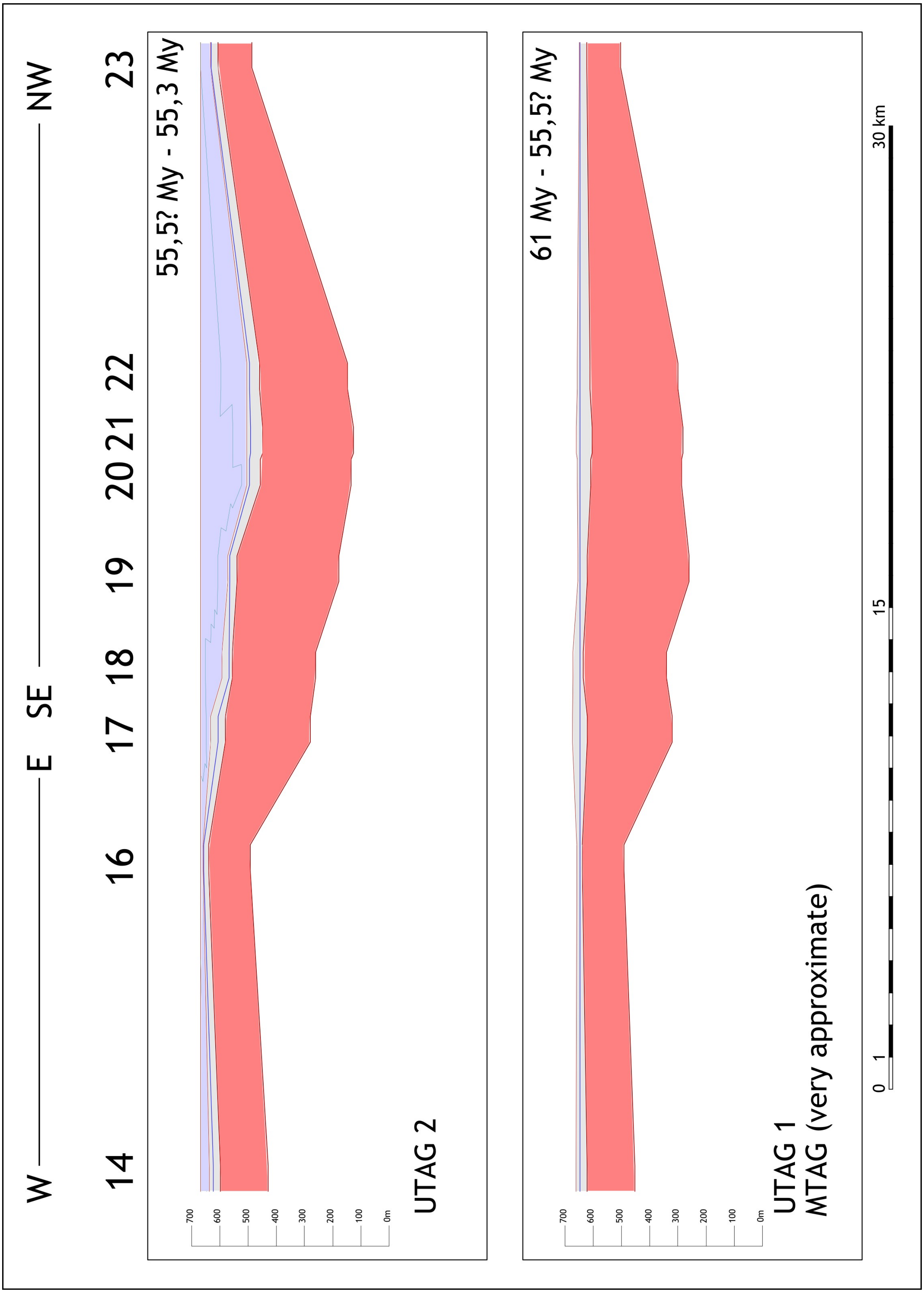
W — E SE — NW
14
16
17
18
19
20
21
22
23
55,5? My - 55,3 My
UTAG 2
61 My - 55,5? My
UTAG 1
MTAG (very approximate)
700
600
500
400
300
200
100
0m
0
1
15
30 km

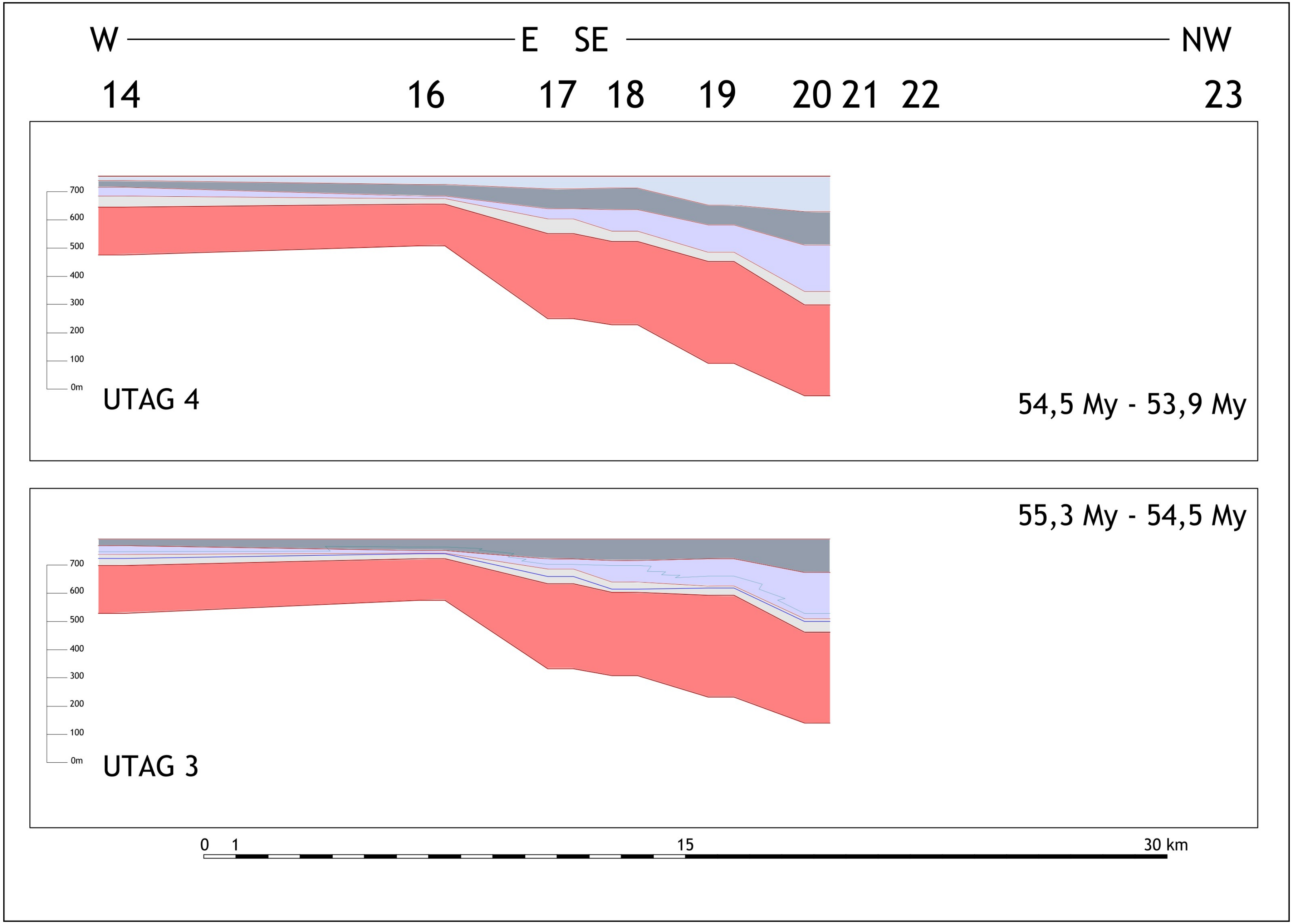
W
E
SE
NW
14
16
17
18
19
20
21
22
23
700
600
500
400
300
200
100
0m
UTAG 4
54,5 My - 53,9 My
55,3 My - 54,5 My
UTAG 3
0
1
15
30 km

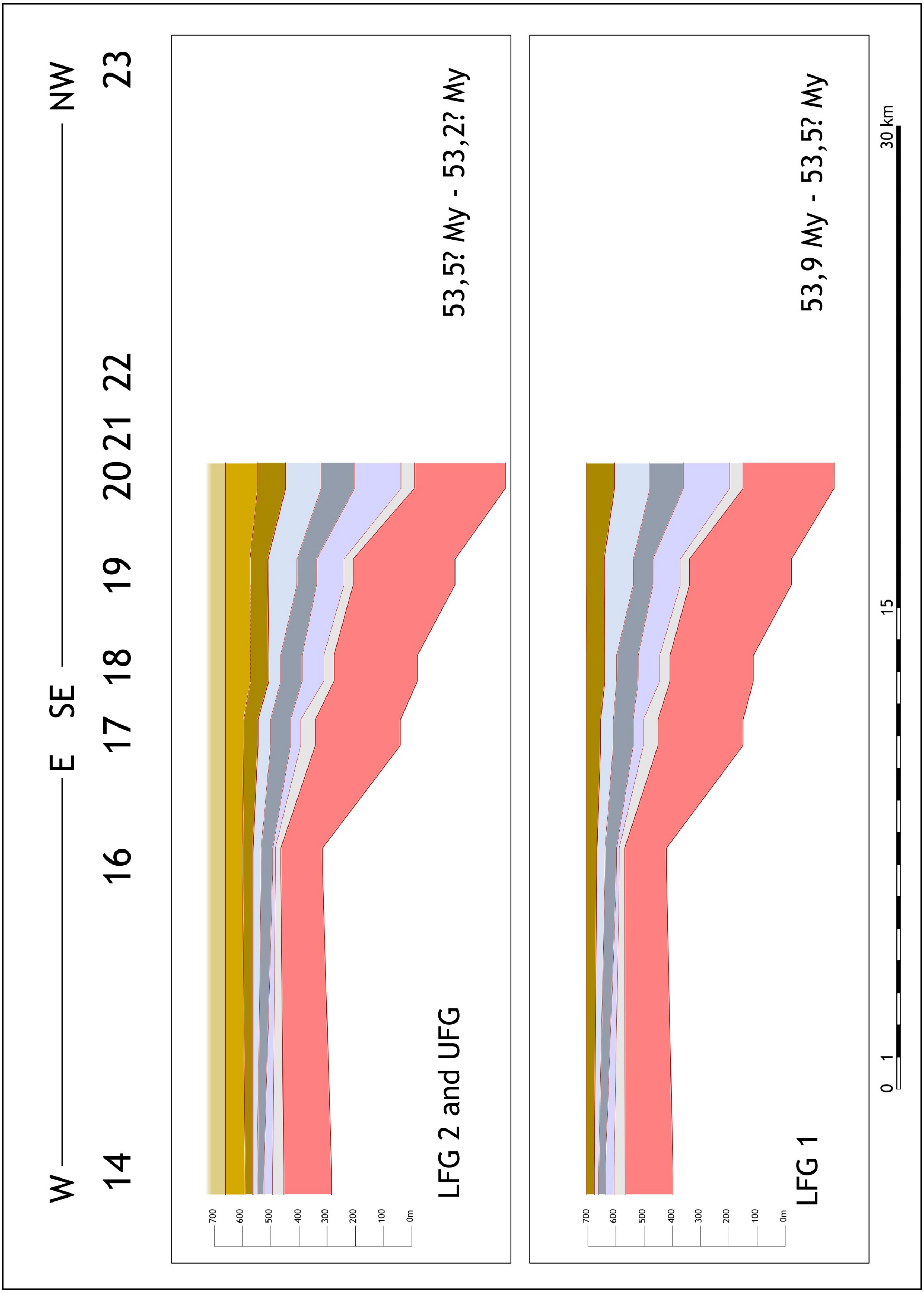
W
E SE
NW
14
16
17
18
19
20
21
22
23
LFG 2 and UFG
53,5? My - 53,2? My
LFG 1
53,9 My - 53,5? My
0m
100
200
300
400
500
600
700
0
1
15
30 km

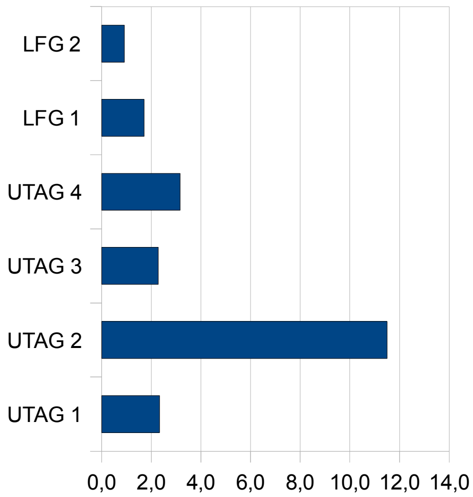

Figure 4.42 – Rates of differential subsidence recorded between section [16] and section [20]; notice the abrupt increase represented by sewuence UTAG 2.

5 – ISOTOPE STRATIGRAPHY

In this chapter, the isotopic investigations performed for this work are presented. Isotope data – primarily concerning carbon isotopes – are used as a stratigraphic tool for correlation. Environmental considerations do not come only from isotopic investigation (that would require at least a parallel study on other geochemical parameters), but through the comparison of the isotopic results with the sedimentary features, such as facies and sequence stratigraphy, that characterize the sampled units.

5.1 – Isotope stratigraphy: fundamentals

The main principle of stable isotope geochemistry is that stable isotopes of a given element are present in nature in a constant ratio, and that, during chemical reactions, the different isotopic species distribute differently in the products of the reaction, due to an external controlling factor. In other words, isotopic abundances in a given compound (e.g., the calcite from a shell or in a pedogenic precipitate) can indicate under which conditions the compound have formed.

This mechanism is termed "fractionation".

5.1.1 – Notation

Isotopic abundances are expressed by the ratio between the heavy and the light isotope. This ratio is not expressed as an absolute value, but as the offset with respect to a given standard ratio (a "delta", ∂). E.g., the $\partial^{13}C$ is expressed as:

$$[(^{13}C/^{12}C)_{sa}/(^{13}C/^{12}C)_{st} - 1] \times 1000$$

With $(^{13}C/^{12}C)_{sa}$ = sample absolute isotopic ratio; $(^{13}C/^{12}C)_{st}$ = standard absolute isotopic ratio.

5.1.2 – Oxygen isotopes

A seminal paper of Urey (1948) first demonstrated the relationships occurring between the relative abundance of stable oxygen isotopes (^{16}O and ^{18}O) in calcium carbonate, and the temperature at which the compound is precipitated. This relation can be summarized by the fact that heavier isotopes are less prone to participate to a chemical reaction, unless more energy is available to the system, i.e., in conditions of higher temperatures. Formally, this is expressed by a function, of which slightly different versions were proposed in time.

During the '50s and '70s various approaches were undertaken in order to apply this investigative approach to the geological successions, and obtain an estimate of oceanic paleotemperatures, primarily by analyzing the calcite shells of planktic (Emiliani, 1954a, 1954b, 1966) and benthic foraminifers (Shackleton, 1974). The latter approach resulted more functional to the problem, primarily because the upper layers of the oceanic waters – i.e., where planktic foraminifers live – could be interested by relevant isotopic compositional changes, if compared with bottom waters, during cycles of deglaciation.

In the '80s and '90s, isotope investigations applied in cores collected by oceanic drilling programs allowed to reconstruct the temporal variability of the $^{18}O/^{16}O$ ratio, that was summarized by Zachos et al. (2001) for the Tertiary and the Quaternary. The observed variability primarily reflected the presence/absence of permanent ice caps, and the long- and short-term changes of glacial and interglacial periods.

Together with long-term trends, a number of anomalous negative shifts was observed, that in the early Paleogene are represented primarily by transient warming/cooling trends occurring over (geologically) very shorts amounts of time. This theme is discussed later in this chapter.

5.1.3 – Carbon isotopes

The abundance of stable carbon isotopes (^{12}C and ^{13}C) is primarily related with the carbon cycle, and it is dependent of a large number of factors. Paleoclimatic research focuses on the variability of carbon isotopic composition to estimate the composition of atmospheric CO_2, (Cerling, 1991), reconstruct paleoenvironmental conditions (Cerling, 1984; Cerling et al., 1989), eventually to discriminate between different trophic strategies in continental floras of the past (Cerling et al., 1993). In recent years, the stability of the carbon isotopic signal allowed to perform stratigraphic correlations, especially in continental settings where poor biostratigraphic resolution is available (Cojan et al., 2000; Schmitz & Pujalte, 2003; Magioncalda et al., 2004).

In fact, the isotope stratigraphic chart compiled by Zachos et al. (2001) shows a good correlation in the variability of oxygen and carbon compositions.

Similarly to the oxygen record, the carbon record shows correlative anomalous negative excursions occurring over relatively short time intervals, that researchers attribute to isotopically-light greenhouse gases enrichment of the atmosphere; these shifts, often easier to be recognized if compared with the related shifts in oxygen isotopes, were the drivers for short-term climatic anomalies with dramatic effects on the environment, biota and sedimentation.

5.2 – Early Paleogene climate trends

On the basis of the variability of isotope composition with time (Zachos, 2001), a relatively simple scenario can be depicted. Starting from the K/Pg boundary, an overall warming trend reaches peak warm conditions in the early Eocene (Early Eocene Climatic Optimum, EECO). This peak is further emphasized by the fact that after its recession, never again such warm conditions were reached.

The warming trend that brings to the EECO, as expressed by oxygen isotopes, is perturbed by a long-term (~ 2My) positive excursion in the Selandian-Thanetian, and by short term climatic anomalies – represented by negative isotopic excursions, named “EPG hyperthermals”, the most prominent of which is the Paleocene-Eocene Thermal Maximum (PETM). In recent years, higher-resolution investigations showed the occurrence of many other similar events, although always of smaller magnitude. The most relevant amongst these subordinate anomalies is the Eocene Thermal Maximum 2 (ETM2), occurring at the beginning of the EECO. All of these events were chronostratigraphically constrained (Westerhold et al., 2007; 2008; 2011). The onset of the sharp carbon isotopic excursion of the PETM is the actual criterium for the location of the P/E boundary (AUBRY REF).

5.2.1 – PETM

The PETM (in some publications referred-to as LPTM, LPE, IETM) or, better, its carbon isotopic excursion, has been object, since its discovery (Kennett and Stott, 1991), of a large number of studies. The main reason stands in the magnitude of the anomaly that, together with its short duration (~ 20 ky for the reaching of peak negative values, ~100ky for its recession, Rohl et al., 2000?), is considered as a primary analog for the modern enrichment of the atmosphere with greenhouse gases and global warming.

Causes of this event are still lively discussed. Unlike the other EPG hyperthermals, whose occurrence apparently correlates with astronomical cycles, the PETM is not related to a predictable pattern (Zachos et al., 2011). Two main theories try to explain the geologically-sudden enrichment of the atmosphere in isotopically-light carbon, that rapidly would have led to greenhouse conditions and global warming.

The first hypothesis relates this enrichment as the effect of large-scale dissociation of methane hydrates (Dickens et al., 2005), possibly caused by the collapse of shelf-margins (Katz et al., 1999).

The second hypothesis associates this carbon-cycle perturbation to magmatic events, and the opening of the North-Atlantic Volcanic Province was seen as a tightly related event (Schmitz et al., 2001; Carozza, 2009).

For the purposes of this work, the effects of the PETM are more relevant.

Estimates on the oxygen isotope shift and independent climatic proxies indicate a warming of the deep oceanic waters up to 4°C (Zachos et al, 2001), with surface temperatures rising in a range of 5°-10°C (Zachos et al., 2003). This warming caused a global increase in the dissolution rate of carbonates on the ocean floor (Thomas et al., 1999) and increased weathering in the continental realm, possibly associated with increased humidity (Gibson et al., 2000). An increase in terrigenous influx (represented by an enrichment in kaolinite) was as well documented in deep marine successions (Gibson et al., 1993; Bolle et al., 1998; Knox, 1998; Zachos et al., 2011; Lourens et al., 2005) and was interpreted either as an effect of increased weathering (Gibson et al., 2000) or increased subaerial erosion (Thiry and Dupuis, 2000; Schmitz et al., 2001); an additional confirmation of increased flux of sediments to the sea was recently reported by Devleeschower et al. (2011) on the basis of an enrichment in continental organic matter and increased magnetic susceptibility in the basinal successions of the Eastern Pyrenees.

Relevant effects on the biota were recorded as well.

Larger benthic foraminifera underwent a major event of extinction and the subsequent radiation of new forms (Larger Benthic Foraminifera Turnover, LBFT; Thomas, 1998; Pujalte et al., 2009a); peaks of occurrence in the nannofossil genus *Apectodinium* were recorded globally (Crouch et al., 2001), and tropical foraminifera underwent a similar widespread diffusion (Kelly et al., 1996; Lu et al., 1998).

In the continental realm, the most relevant event is the dispersal of plants and mammal faunas in the northern hemisphere (Koch et al., 1992).

5.2.2 – ETM2

If compared with the PETM, no major biotic changes are associated with this horizon, but common features, besides the warming of oceanic waters recorded by oxygen isotopes, are represented by an increase of carbonate dissolution and terrigenous input to deep seas (Lourens et al., 2005). This event, similarly to other minor hyperthermal anomalies in the early Paleogene, is apparently related with astronomical cyclicities and, more precisely, with short-term eccentricity modulations (Lourens et al., 2005; Zachos et al., 2010).

5.3 – Rationale for isotopic investigation

The SCPFB hosts a foreland Early Paleogene succession displaying many features that suggest an interaction of both tectonic and climatic controls over the sedimentary succession (Mutti & al, 1994). According to the latter paper, in some parts of the succession it may still be difficult to clearly recognize the effective roles of the two factors, and a great number of stratigraphic studies have been performed to define the sequence stratigraphic framework of the succession (see geologic framework).

As previously stated, the study of stable isotopes allows global correlation of major climatic trends and events; the Early Paleogene is probably the oldest thoroughly investigated stratigraphic interval in terms of chronology of these events.

In this work we consider both the chronostratigraphic significance of the hyperthermals, since these events develop and recede globally on relatively short amounts of time (tens to few hundreds ka), and their long-term climatic variations that may be put in relation with the succession.

Former isotopic studies performed in the study area followed similar purposes; examples are the study of the K/Pg boundary in the Ager basin (López-Martínez et al, 1996), or the detection of the PETM along the northern sector of Tremp basin (Schmitz & Pujalte, 2003, 2007), or the isotopic characterization of the correlative “Campo Section” westward of the study area (Molina et al, 2003).

The analyses performed for this work were undertaken on a variety of lithologies, and although a temporal series of such heterogeneous data is in itself poorly significant, the characterization in age and lithology is shown in carbon/oxygen diagrams, so that vertical successions can be correctly interpreted.

Stable isotopes of carbon and oxygen were studied in marine and continental carbonates, and a tentative study of organic matter carbon stable isotopes was performed in the Paleocene of Ager basin. As it is made evident by some samples, oxygen isotopes in carbonates turned out to be the least preserved signal. In some cases facies and isotopic analyses coupled allowed the recognition of diagenetic horizons (such as the negativization trend produced by the subaerial exposure of late-Thanetian marine carbonates in Ager basin); and finally, local environmental effects on isotopic compositions were observed (such as the positive values recorded in sabkha carbonates in the upper

Thanetian of Ager Basin).

5.3.1 – Materials and Methods

Sample preparation and analysis were carriedout at the Isotopic Geochemistry Laboratory at the Università degli Studi di Parma Earth Sciences Department.

5.3.1.1 – *Carbonates*

SAMPLE COLLECTION

Carbonate samples were collected as hand samples always trying to get unaltered, non-surficial samples; carbonate soil nodule samples were collected individually by digging a few tens of centimeters in the hosting paleosol.

Carbonate samples were generally sub-sampled with a dentist drill, unless individual samples turned out to be too small (e.g., the carbonate soil nodules were generally split and drilled in the middle, with the exception of some nodules from section [14], that were individually treated as bulk because of their small size – in any case, no bulking of multiple nodules was performed).

Continental limestones (commonly micrites) were sub-sampled in order to subdivide original micrite, burrow fills, altered horizons (most of the times related with Microcodium bioerosion) and any other macroscopic feature.

Marine limestones were most of the times treated as bulk samples, in the absence of a microsampling device, with the exception of a few samples where a presumably original micritic matrix was abundant enough to be drilled separately from the rest of the sample.

Almost all of the carbonates analyzed were close to pure, low-Mg limestones; exceptions are discussed below.

PREPARATION AND ANALYSIS

The powders obtained from drilling, and subsequent powdering in an agate mortar, were commonly weighed between 6.0 and 12.0 mg, then prepared with a manual vacuum line, through which they were reacted with excess 100% phosphoric acid at ~$5*10^{-3}$ atm and 25°C for at least 12 hours.

A few samples, containing a significant dolomitic component (see **5.4.1.3**), underwent a two-steps procedure in order to separate carbon dioxide produced by calcite or dolomite reaction: samples were weighed between 20.0 and 40.0 mg, reacted with 100% phosphoric acid, and carbon dioxide produced by the fast reaction of calcite was extracted for spectrometer analysis after two hours; the reaction was then continued for two more hours and further products of the reaction from calcite were totally removed. Finally, after at least 72 hours of reaction, carbon dioxide freed from dolomite reaction was extracted and analyzed.

Carbon dioxide analysis was performed with a Thermo Finnigan Delta S mass spectrometer by 8 comparisons with an internal standard (MAB99); data were then expressed in permille with reference to the V-PDB international standard.

About 25% of the samples were double analyzed, with an analytical plus instrumental error summing up to ±0,2‰.

5.3.1.2 – *Organic matter*

One of the main purposes of the isotopic study in Ager basin Paleocene was the correlation of the thinned northern succession with the thick southern one; because of the scarcity of pedogenic nodules in the latter, a tentative survey on organic matter carbon isotopes was performed.

Similar studies were formerly performed in Early Paleogene continental settings (Domingo & al 2009) for the PETM interval in Tremp basin as well as in other locations all over the world (e.g., Magioncalda et al, 2004), showing the coupling of the inorganic (carbonate) and organic matter carbon isotopic signal.

SAMPLE COLLECTION

Carbonate paleosols were collected preferentially at some tens of centimeters from the surface, if possible avoiding internal discontinuities such as slickensides, and in the absence of modern vegetation.

Ager basin Paleocene southern section (section [4]) was sampled in detail in its lower and upper portions, while in its middle portion the presence of a stronger plant cover hampered the possibility to collect good samples for the purposes of this survey.

PREPARATION AND ANALYSIS

Paleosol samples were dried at low temperature (~30°C), then powdered with an agate mortar and successively reacted with 25% HCl for 60 minutes, while manually kept in suspension. Since samples showed a $CaCO_3$ content between 20% and 50%, about 3 ml of acid were used for each gram of sample. After the decarbonation, samples were neutralized using a centrifuge; during this process, the organic matter differentiates inside the test tube as a thin black layer on top of the clay.

Since the amount of organic matter cannot be clearly quantified in this phase, decarbonated samples are dried again at low temperature, and again powdered and homogenized using the agate mortar.

The organic carbon content and its isotopic composition were estabilished in double analysis with a coupled elemental analyzer/mass spectrometer (analyses were performed by A. di Matteo at the Isotopic Geochemistry Laboratory at the Università degli Studi di Parma Earth Sciences Department) after weighing of the samples between 20 and 40 mg, in function of their abundance in organic matter.

PREMISE FOR DATA EXPOSITION

All $\partial^{18}O$ and $\partial^{13}C$ data are expressed in ‰ vs V-PDB; if not explicit, terms in the text such as “negative” or “positive” are to be intended with respect to this standard.

5.4 - Ager basin Paleocene – isotope signatures

5.4.1 – Carbonate data

Diagrams 1, **2** and **3** display the results of the stable isotopes analyses performed in some Paleocene successions exposed in the Ager basin; sample locations are provided in **figure 5.1** and in detail in figures **5.3** and **5.4**.

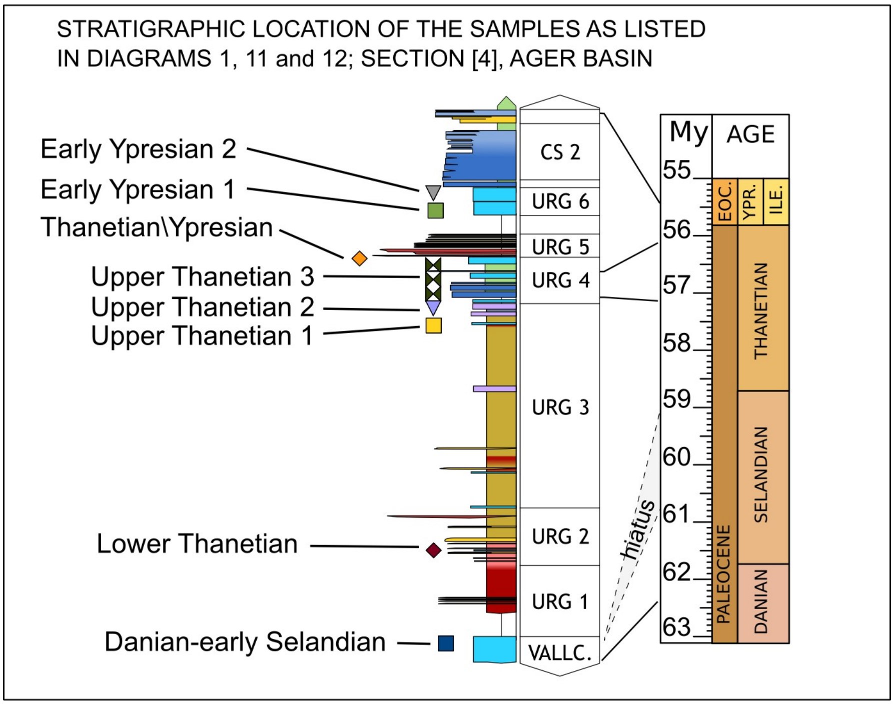

Figure 5.1 – Stratigraphic location of the different groups of samples in Section [4]; compare with the informal units listed in 4.2.1.2

Data from carbonates come from different kinds of rocks, that can be categorized in the following groups:

a. paleosol carbonate nodules;

b. freshwater limestones;

c. sabkha dolomitized limestones;

d. shallow marine limestones.

Some of these attributions were given after the isotopic analyses (see below) and are here anticipated for completeness.

Although the number of samples is below statistic significance, it is clear that samples from different environments and stratigraphic intervals are generally clustered around characteristic isotopic compositions; each case (and relative outliers) will be discussed below.

A macroscopic feature emerging from these data is the short range of oxygen isotopic compositions characterizing the continental carbonates, that are instead relatively scattered around different carbon isotopic compositions - apparently in relation with their stratigraphic position; marine and sabkha deposits are instead concentrated in a small range of $\partial^{13}C$ values, and display a slight clustering in oxygen values, although differences in lithology require them to be treated separately.

In the following paragraphs, the data are discussed per unit and lithology, plus some observations concerning outlier results.

Diagram 1
SOUTHERN AGER BASIN
section [4]

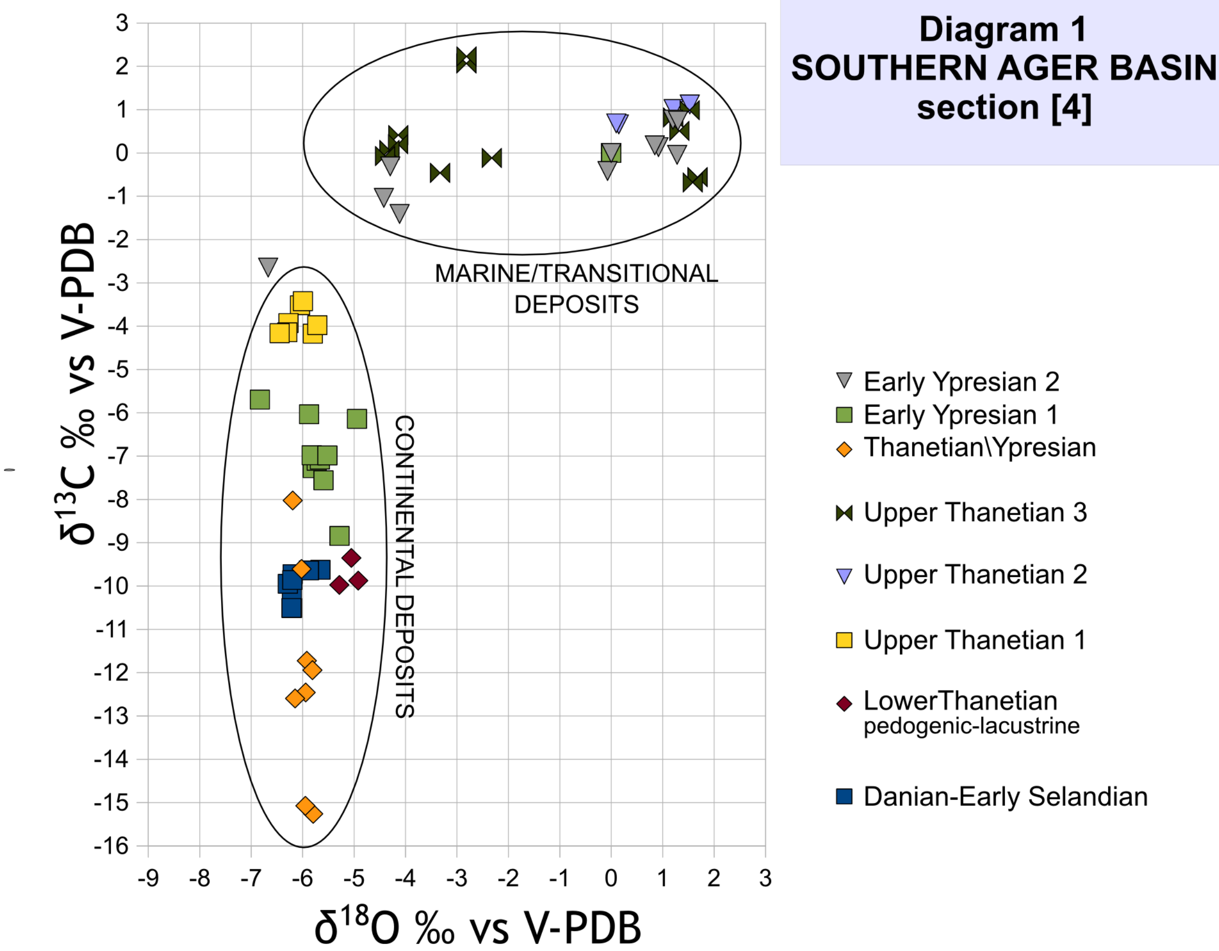

Compared isotopic values for Ager basin carbonates in the Paleocene-earliest Eocene interval. Squares: lacustrine or palustrine deposits; diamonds: supposedly pedogenic limestones; triangles: sabkha limestones (average calcite+dolomite composition); papillons: bulk marine limestones.

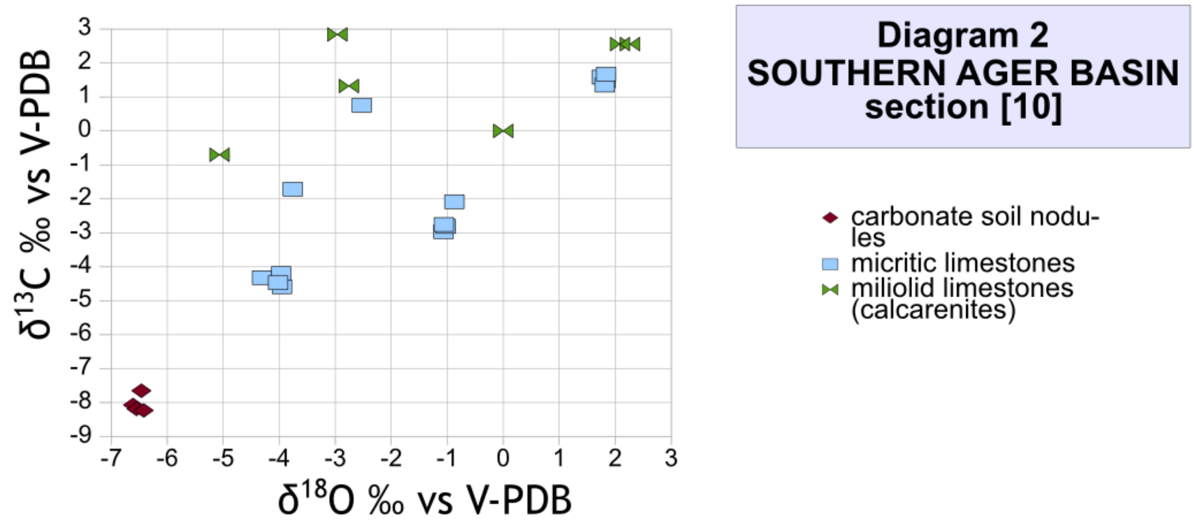

Compared isotopic values for late Thanetian carbonates.

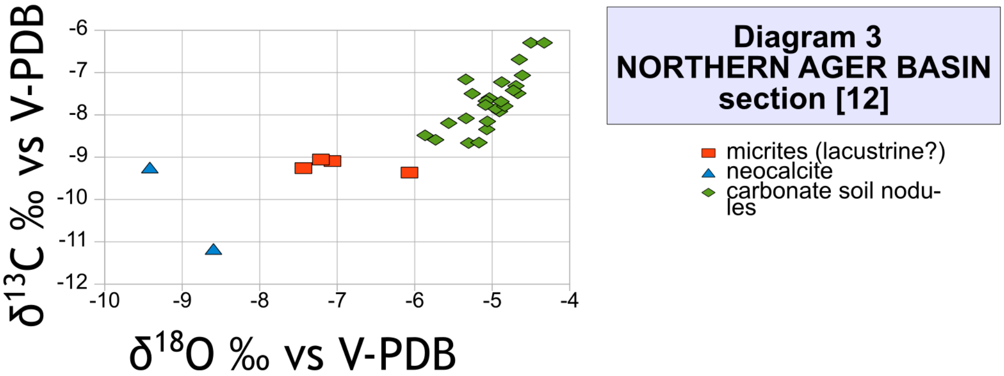

Compared isotopic values for northern Ager basin carbonates sampled from section [12]. Neocalcite data represent subsamples from the lacustrine micritic samples (see text). The whole succession is supposed to be of Danian - lower Thanetian age

5.4.1.1 – *Paleosol carbonate nodules*

Along the southern flank of Ager syncline (sections [10] and [4] in **diagram 4**), pedogenic soil nodules are very uncommon; with the exception of the early upper Thanetian "pseudo-conglomeratic limestones" - that constitute a pedogenic feature of palustrine deposits (see **4.2.1.2**, Unit URG 2) – only a few nodules were collected in-situ above the late upper Thanetian emersion surface (see **4.2.1.2**, Unit URG 5). Nodules are instead very common along the Paleocene exposure at the northern flank of the basin (supposed equivalent of Unit URG 1, see **4.2.1.2**).

These data can be compared with the ones collected by Schmitz & Pujalte (2003, 2007) at the northern side of the Tremp basin of upper Paleocene and early Ypresian age, and analogous data from this work from the southern Tremp basin (see **5.6.1**).

The range of isotopic values characterizing the studied nodules is typical of ancient paleosols; notice that $\partial^{13}C$ values never reach the negative peaks of the PETM carbon isotopic excursion. Notice also the small range of oxygen isotopic values that perfectly overlaps the ones from other continental limestones (cf. **diagram 1**).

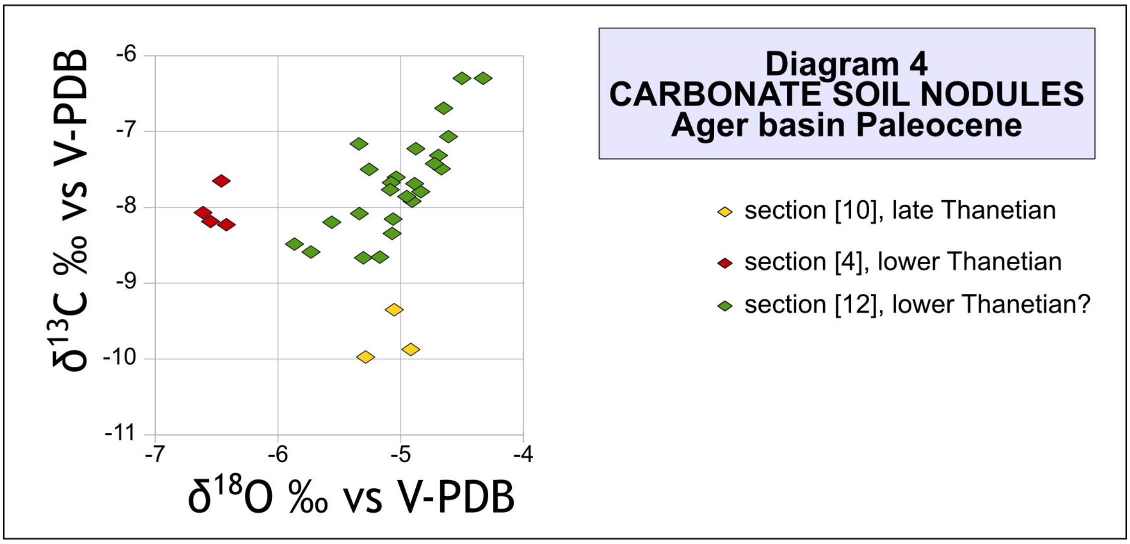

"Thanetian/Ypresian pebbles"

A peculiar type of data was collected in an horizon suspected to be closely related to the location of the Paleocene/Eocene boundary.

These data refer to micrite pebbles from the basal conglomerate of Unit URG 5 (see **4.2.1.2**) – encountered only in section [4], at the base of a deltaic succession – that were suspect to be either reworked karstified micrites from an underlying exposure surface (cf. below) or reworked soil nodules. **Diagram 5** and **figure 5.2** show the isotopic compositions of some different clasts.

Two main categories of micritic clasts were observed i.e., white and yellow (plus rare pinkish tests), with yellow clasts more common in proximity of exposed surfaces or along fractures; white micrite clasts are more common away from these features. This early observation suggests a diagenetic origin for the yellow color (see **figure 5.2**).

Sandstone clasts were observed as well (red and grey sandstones). These showed to be relatively rich in carbonate, as well as for most – if not all – continental sandstone bodies in the Ager basin Paleocene and Maastrichtian. No insight was performed to verify the origin of the carbonate, but it is known that upper Cretaceous marine limestones constitute the most common source of detrital carbon in the Paleogene of the southern Pyrenees.

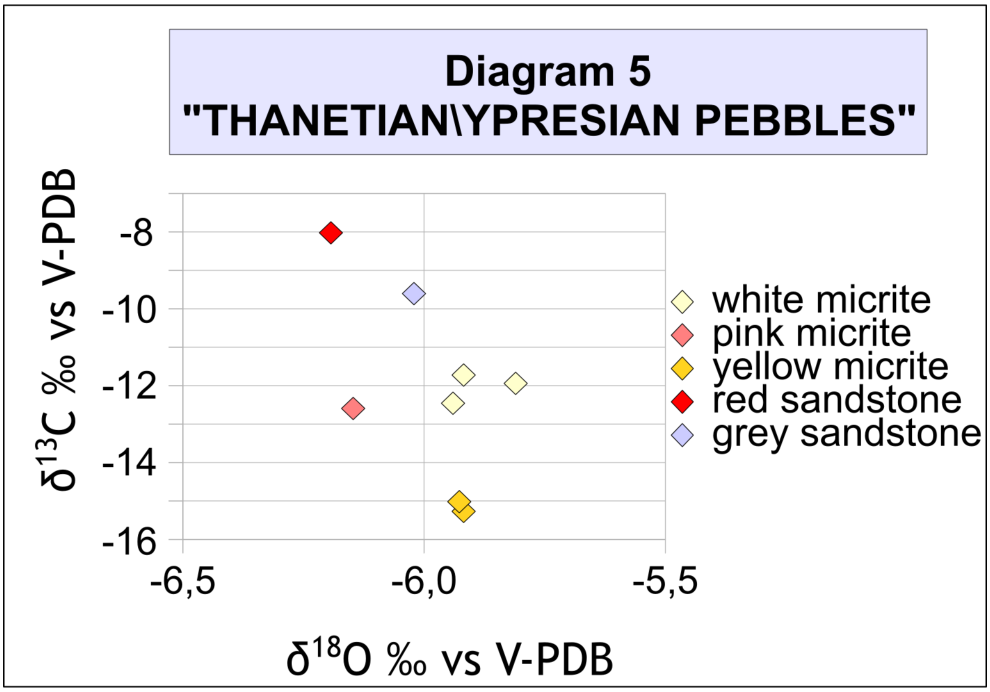

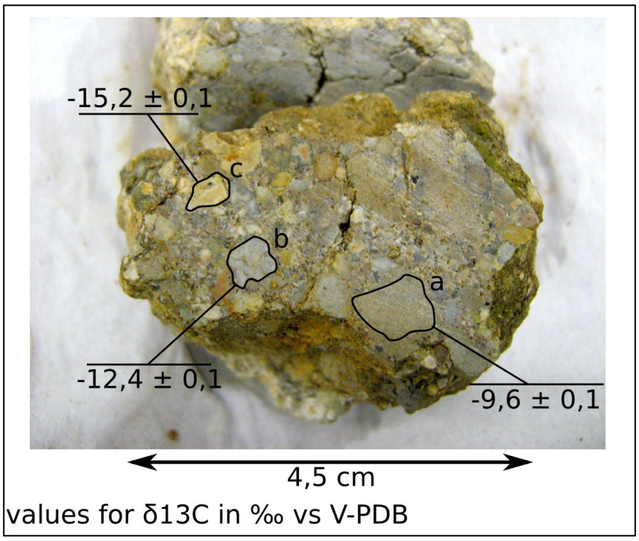

Figure 5.2 – Hand sample of the basal conglomerate of Unit URG 5; some of the analyzed clasts and relative carbon isotope values are evidenced. A: carbonate sandstone; B: white micrite; C: yellow micrite.

Isotope data from these samples display a small range of $\partial^{18}O$ compositions, and a very wide range of $\partial^{13}C$ values. Micrites show the most negative carbon values, with a clear offset from white to yellow samples.

A possible interpretation for carbon data is that micrite clasts represent reworked nodules from an eroded paleosol. Other stratigraphic data (see the stratigraphic isotopes trends section) suggest an equivalence of the deltaic succession with the "Claret conglomerate" (**4.3.1.3**) of the Tremp basin, that formed at the onset of the PETM carbon isotopic excursion, as testified by soil nodules displaying negative-peak isotopic values comparable to our data (Schmitz & Pujalte, 2003; this work **5.6.1**). Since the data set is small, and because of the poor exposure of the intervals immediately above the terrigenous succession, some arguments could contradict this hypothesis.

The first one is that Schmitz & Pujalte's paper (2003) reports less negative (pre-PETM) values below the Claret conglomerate; another paper, from Domingo et al. (2009), who performed organic carbon isotopic analyses in some of the intervals sampled by Schmitz & Pujalte, reports the first syn-PETM values just below the lower surface of the Claret conglomerate (**figure 2.14**). Considering that sampling for organic matter allows to collect data even where soil nodules are absent, it can be concluded that the PETM isotopic excursion started before the deposition of the Claret conglomerate – whose erosional base could even have removed a relevant portion of the succession. Moreover, the onset of the PETM have been demonstrated to occur in a very short time (10 to 20 ka; Röhl et al., 2000), so that peak negative values were already established during the early phases of the isotopic excursion.

A second question considers soil nodules from below the deltaic beds in section [10] (see **diagram 4**, "section [10], late Thanetian") that display carbon values more consistent with pre- or post- PETM conditions, if compared with data from former papers. Bed-by-bed correlation suggests that up to 5 m of succession were eroded in section [4] with respect to section [10] (see **figures 4.40** and **5.6**); but erosion surely occurred also in section [10], as it is testified by the sharp base of the sandstone beds and the abundance of mudstone clasts in the lower third of the unit. This allows the hypothesis of the removal of an hypothetical, relatively thin soil horizon, formed during the onset of the PETM.

The isotopic values of the "Thanetian/Ypresian pebbles" are problematic in themselves.

The low degree of variability in oxygen values might imply an obliteration of the primary isotopic signal by meteoric waters in a porous body. Despite the poor outcrop conditions, it can be said that the conglomerate is certainly encased between mudstone layers that should have protected it from massive fluid inputs; but, although it appears very limited in lateral extent, it could possibly be crossed by a nearby fault, that might have allowed communication with meteoric fluids.

A probable alteration signal is represented by carbon isotopic values from yellow micrite clasts. These are offset by a -2 to -3‰ from white micrite clasts data. Since yellow tests show the same size (few mm) and low-roundness of white tests, and their distribution in the rock sample is almost mutually-exclusive (see above), it is inferred that yellow clasts are weathered, originally-white clasts. The difference in isotopic composition between the two sample categories should then be representative of recent weathering, instead of a long-term action of fault-related or underground fluids, because in such a porous body it would be expected to uniformly alter micrite composition.

Further insight would be needed to unambiguously sustain the here presented interpretation for the isotopic data from this peculiar horizon. An alternative hypothesis might be the shallow erosion of the underlying karstified micrites followed by a strong, late-diagenetic imprint. The same should account for the erosion and resedimentation of any other stratigraphically-lower limestone body.

Billi et al. (2007) report isotopic shifts of the same magnitude and in the same range in modern karstic settings. These regard calcite concretions from fault surfaces, that showed a strong relative depletion in C and O heavy isotopes if compared with nearby unfractured rocks. Data from calcite fracture fills in the present work show some similarities (see neocalcite data in **diagrams 6** and **7** from samples close to faults), but no macroscopic evidence of recrystallization have been found in the micrite clasts here documented. Finally, the cited paper refers the presence of hydrothermal activity as the main driver of dissolution and fluid development, and no informations of such activity have ever been reported in the study area.

5.4.1.2 – *Freshwater limestones*

Different layers of micritic limestones were formed in the early Paleogene continental succession of the Ager basin. They are described in **4.2.1.1** and **4.2.1.2**.

Thanks to the clear clustering in the isotopic composition of these rocks (cf. **diagram 1**), they can be treated separately by stratigraphic position.

Danian – early Selandian

A former isotopic investigation was carried out and published by López-Martínez et al. (1996), focused on the late Maastrichtian – early Paleocene interval, trying to constrain the location of the K/Pg boundary. The paper provides a few data from the base of the Vallcebre formation along the southern flank of the Ager syncline; this unit is the base of the Ager basin succession here examined.

Galbrun et al. (1993) assigned this unit a Danian age, possibly including the base of the Selandian and the lower Thanetian at its top; it hosts a number of internal discontinuities (Colombo & Cuevas, 1993) interpreted as karst surfaces. These surfaces host a large discontinuity (Middle

Paleocene Unconformity; see chapters **2** and **4**).

Three samples (tagged "Vallcebre fm., Southern Ager basin, sec [4]", in **diagram 6**), made of nearly-pure micritic calcite, were collected in the upper 10 meters of the unit, and sampled for isotopic analysis based on different color patterns of a fresh cut (white, yellow, pink and red).

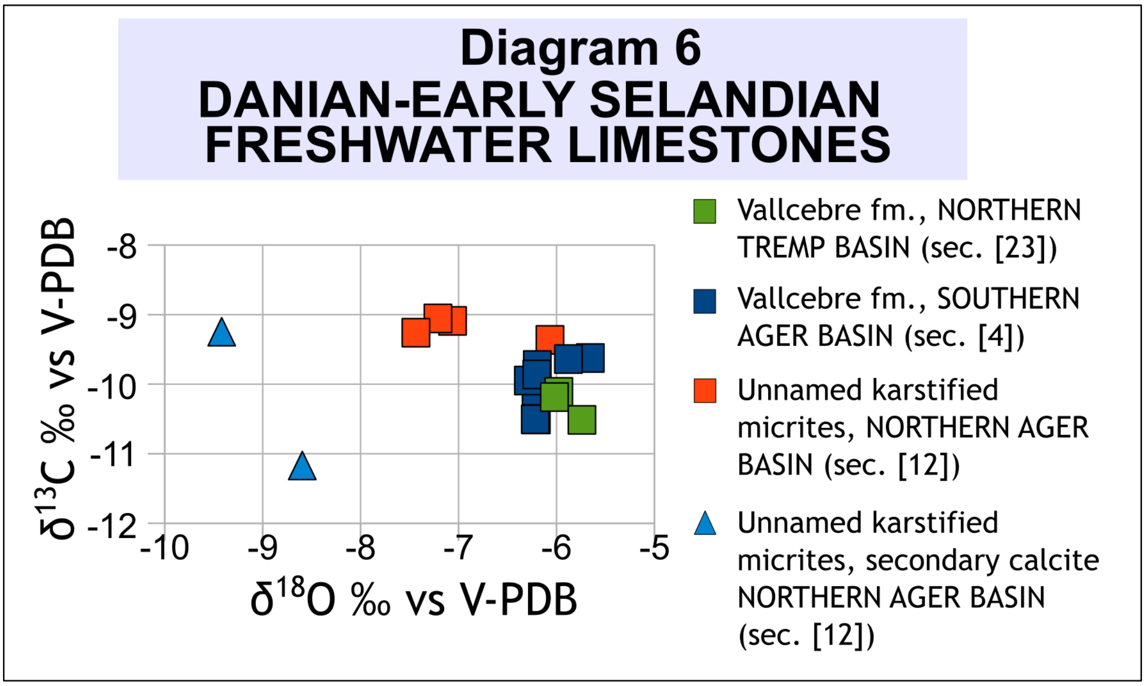

All the results (see **diagram 6**) fall in a small window of negative values for both oxygen and carbon isotopes of respectively -6±0,25‰ and -10±0,5‰. These data are consistent with the non-marine limestone data from López-Martínez et al. (1996), although oxygen values are more negative by a 2‰ if compared with the results the authors reported from the base of this same unit.

A sample collected in the proximity of Esplugafreda, in the northern sector of the Tremp basin (see **diagram 6**), from a few decimeters thick grey micritic layer, and reported to be the local expression of the Vallcebre formation (Baceta et al., 2011; **4.3.1.1**) shows comparable results.

These data are compared with a sample collected on top of a thick pinkish limestone body that crops out at the base of the inverted – presumably – Paleocenic succession at the northern flank of Ager syncline; this body is supposed to be an equivalent of the Vallcebre formation (cf. Rosell et al., 2011; **figure 2.7**), although it is unreported in maps and publications. Since no paleontological data are available, a tentative correlation was performed using isotopic data.

A sample of brecciated pink-yellow micrite was subsampled in its blocky, matrix and recrystallized components and analyzed for isotopes. Results are very slightly offset to the average of the ones pertaining to the Vallcebre formation, by a ~0,7‰ heavier in carbon and ~1‰ lighter in oxygen, with the exception of secondary calcite, showing greater scatters (up to ~1‰ lighter values for carbon and ~3‰ for oxygen), possibly imputable to a fault-related fluid fractionation. Unremarkable differences have been observed between the blocky and matrix micrite.

Other potential southern equivalents of this unnamed limestone body (in terms of lithology and thickness) are located in the late Cretaceous succession, some ~150m below the Vallcebre formation, and in the upper Paleocene. Data from oncolites belonging to the Mesozoic limestone are provided in López-Martínez et al. (1996), and display comparable values for oxygen, but heavier values for carbon (at least a ~4‰). Other Paleocene freshwater limestones as well show comparable values for oxygen, but carbon results are always abundantly heavier (this work, see **diagram 1** - “Upper Thanetian 1” and “Early Ypresian 1”, and text below). A further alternate correlation would consider the karstified micrites of the Late Thanetian (se **4.2.1.2**, Unit URG 4), but their isotopic signatures as well display totally different values (cf. **diagram 9**).

Although further insight would be necessary to uncontrovertibly correlate the northern Ager freshwater limestones with the Danian Vallcebre fm., stratigraphic and isotopic data make this correlation very likely.

Thanetian

Limestones from the continental succession in the lower-intermediate interval of the Paleocene succession (Unit URG 2, see **4.2.1.2**) show a characteristic nodular facies (sometimes named “pseudoconglomeratic”) and are included in a paleosol facies association unique to this interval.

Isotopic results from these layers can be observed in **diagrams 1** and **4** and show a composition close to the values of Danian limestones and to pedogenic carbonates.

Upper Thanetian

Limestones from the upper Thanetian show variable isotopic composition, but are quite clustered in relation with the stratigraphic position and facies.

The freshwater lower unit (tagged “Upper Thanetian 1” in **diagram 1**; high part of Unit URG 2, see **4.2.1.2**) if compared with lower freshwater limestones displays a similar isotopic composition for oxygen and a much heavier composition for carbon (by a ~6‰).

Early Ypresian

At the base of the Eocene (see **5.5.6.2** and **6..3** for the age attribution), a thick succession of massive to finely-stratified micritic limestones precedes the Ilerdian marine ingression in the Ager basin.

The lower portion of this unit (tagged “Early Ypresian 1”; see **4.2.1.2**, Unit URG 6) is made of nearly-pure calcite, while the upper part is characterized by a variable, although subordinate, dolomite content, and will be treated below.

$\partial^{18}O/\partial^{13}C$ data from early Ypresian 1 limestones are more scattered than the ones from lower freshwater limestones (see **diagram 1**). The scattering may be explained by shifting values that are made evident in the carbon isotope-stratigraphic series (see **diagram 12** and **figure 5.6**), since they represent a period of progressive enrichment of the carbonates in the heavier isotope (from about -9‰ to -6‰).

5.4.1.3 – *Sabkha dolomitized limestones*

Non-marine limestones bearing a dolomitic component are reported by Colombo & Cuevas (1993) in the upper Thanetian and early Ypresian of the Ager basin. In the upper Thanetian, these are represented by white micrites deposited in association with gypsiferous mudstones and gypsum beds (top of Unit URG 3, **4.2.1.2**); in the early Ypresian, they form the upper part of a micritic succession of non-marine limestones (“Early Ypresian 1 limestones”, see above and Unit URG 6, **4.2.1.2**) and they are topped by lagoonal mudstones and limestones (Unit CS 1, see **4.2.1.3**); macroscopic features are a yellowish color, saccharoid texture and local microbreccia layers.

Diagram 7 shows the isotopic composition of some dolomite-bearing beds in the two stratigraphic intervals; the procedure for the separation of calcite and dolomite isotopic compositions was presented above (see “preparation and analysis” paragraph).

Calcite carbonate displays values comparable to the ones of marine carbonates. Dolomitization apparently causes a concentration of heavier isotopes, both for carbon and oxygen (with the exception of a sample showing an unaltered composition in carbon isotopes).

Data from the two stratigraphic intervals are slightly distinct, but it is interesting to observe that the sample collected at the top of the evaporitic interval shows heavier compositions. For the late upper Thanetian dolomite-bearing beds, there is little doubt that these data reflect deposition by precipitation in a sabkha environment, and that dolomite was formed as an early diagenetic product typical for this setting (cf. Selmo, 1993).

Early Ypresian beds, instead, might have undergone some later diagenesis, since the section where they were observed and sampled is crossed by normal faults; some layers are rich of neoformational calcite veins and plagues. Moreover, no anhydrite or gypsum layers have been observed in this interval, nor they have ever been documented in the Ager basin.

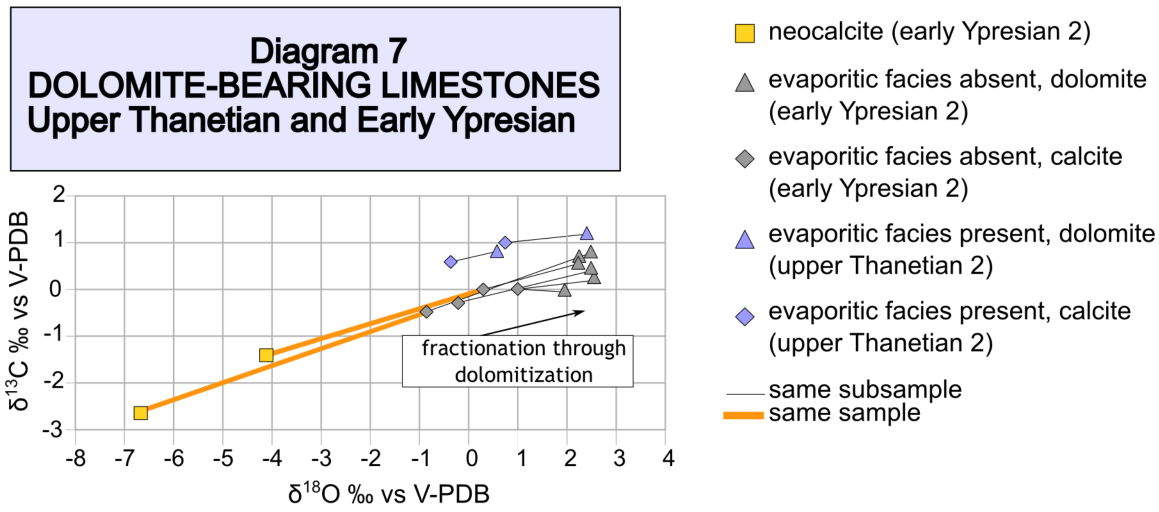

Isotopic values for dolomite-bearing limestones. Notice the difference with recristallyzed calcite

Late-formation calcite data are displayed in **diagram 7**, and it can be observed that that fractionation occurred during dissolution e/o recrystallization, but brought isotopic composition to sharply lighter values.

The isotopic and geological data suggest that dolomite in early Ypresian non-marine limestones formed as an early diagenetic product in a setting similar to the one from late Thanetian. Evaporites could have formed in a different location of the basin, and it is likely that this arid stage correlates with early Ypresian evaporites cropping out in the axial portion of Tremp basin (Eichenseer & Kraus, 1985).

Considering an alternative hypothesis for the case of Early Ypresian 2 beds would require specific conditions.

Commonly dolomitization requires extreme conditions to occur, and the sabkha environment is one of the few settings where dolomitization may take place at surficial temperatures; the process would otherwise require very high temperatures and commonly takes place in hydrothermal conditions; in the case of evaporitic settings, different mechanisms and conditions may contribute to catalyze the substitution of Mg and Ca ions (Selmo, 1993).

If dolomitization of these beds were related to buried-rock fluid alteration – as the presence of faults might allow – it would require either a meteoric Mg-enriched fluid or hydrothermal conditions (cf. Selmo, 1993). No evidence for these conditions can be reconstructed from literature or field data; moreover, vitrinite data from the Maastrichitan portion of the underlying continental succession (Garcia-Valles et al., 1993) reflect very low burial temperatures.

5.4.1.4 – *Shallow marine limestones*

The late Thanetian transgression occurring in Ager basin causes the deposition of fine-grained shallow water carbonates (Unit URG 4, see **4.2.1.2**); the upper part of the succession was then exposed to subaerial conditions following a relative sea-level fall. Because of the fine grain-size and of the small size of shells and shell debris, these carbonates were treated as bulk.

Three main lithofacies characterize this interval that are, a calcarenitic facies (miliolid wackestones rich in fine-grained skeletal debris, associated with rare packstone/grainstone layers) mostly present in the lower portion of this interval, and micritic limestones, with rare miliolids, that occupy the upper portion; finally, blue mudstones/marls, common to the full interval and interbedded between the limestone beds (see **4.2.1.2** for more details). Isotopic analyses were performed only on the limestone facies.

Diagrams 8 and **9** show the isotopic values collected from two correlative sections ([4] and [10]; see also **figure 5.6**).

Micritic and calcarenitic facies are well differentiated in their isotopic values, by the fact that carenites display a characteristic signature with positive $\partial^{13}C$ and negative $\partial^{18}O$ values; micrites show a wider range of compositions, that can be roughly summarized in "heavy" and "light" compositions: "heavy" samples display slightly positive to positive values (in the range of ~1-2‰) for both oxygen and carbon isotopic compositions, while "light" samples are characterized by negative values over a relatively larger range of values (~ 0 to -4‰).

Apparently, micrites in the "heavy" range represent facies similar or adjacent to the sabkha micrites; in any case, these samples are not dolomite-bearing such as the sabkha deposits formerly discussed.

"Light" samples characterize the part of the succession hosting a karst surface at the top of the late upper Thanetian carbonates. Microcodium bioerosion is very common in these layers; subsamples collected in clearly Microcodium-altered surfaces did not show a significant data offset from bulk subsamples, with the exception of the topmost sample, where Microcodium data showed a clearly lighter composition.

Layers displaying "light" isotopic compositions are therefore interpreted as originated as a similar facies as to the one with "heavy" composition, and successively undergone meteoric-water driven early diagenesis during subaerial exposure (Allan & Matthews, 1982; cf. Goldstein, 1991; Immenhauser at al., 2002).

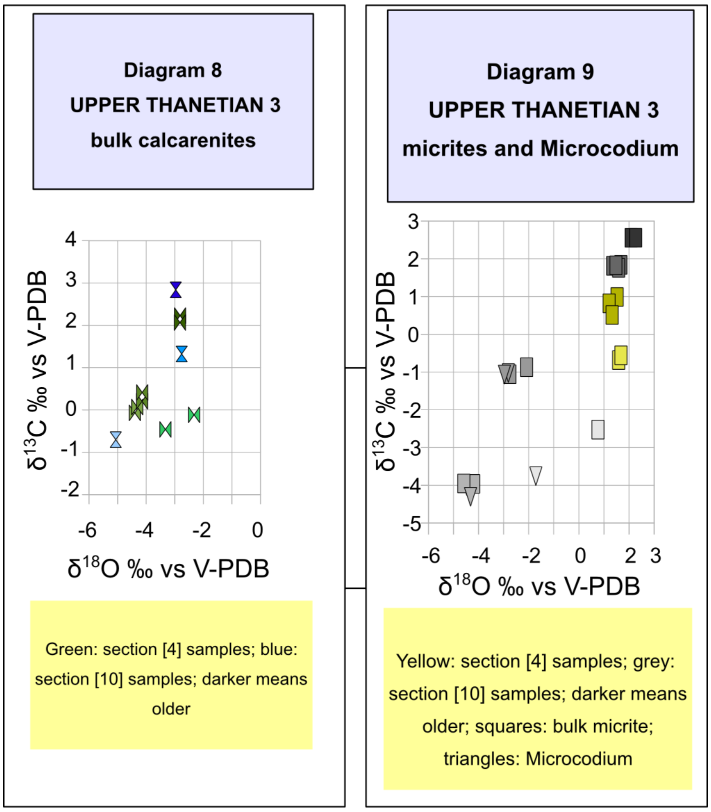

5.4.2 – Organic matter data

In the absence of a common typology of sample, the northern and southern Ager basin successions were compared on the basis of organic matter carbon isotopic composition from bulk paleosols.

First of all, a comparison was made between carbonate and OM data from section [12]; this is shown in **figure 5.3**, where organic and inorganic carbon apparently share a common vertical trend, suggesting a common relation in the two data (i.e., OM and carbonate carbon shifts may both be driven by changing climatic/environmental parameters).

Bulk paleosol samples were then collected in the nodule-poor southern succession (section [4]) and compared.

Values range between -23‰ and -25‰ in section [12] and between -20‰ and -27‰ in section [4]. Most of the samples present values in the same range of the ones reported by Domingo et al. (2009) at the top of the continental section (late Thanetian – early Ypresian) in the axial portion of Tremp basin.

Diagram [10] summarizes the results ordered by facies.

Data scatter in this diagram is related with the different stratigraphic position; yellow paleosols averagely show lighter compositions with respect to red paleosols. The latter are characterized by a relatively small range of isotopic compositions in the upper Thanetian of section [4] and fall in the same data range of the red paleosols of section [12]. The “heavy” sample from section [4]'s red paleosols represents the last widespread horizon of this kind close to the top of the Thanetian.

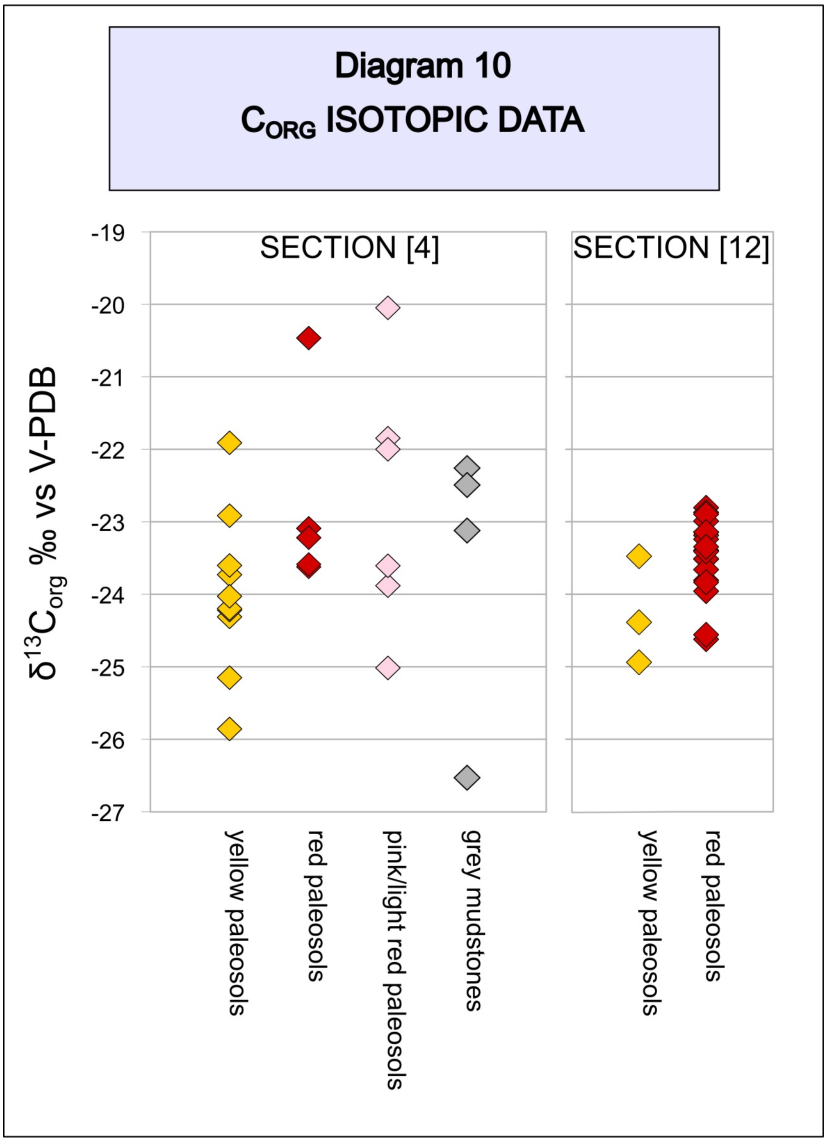

5.5 – Ager basin Paleocene – stratigraphic isotope trends

5.5.1 - Data reliability

Stratigraphic trends interpretations in the following paragraphs are based on some assumptions.

The first is that carbonate isotopic data from freshwater limestones can be interpreted the same way of data from pedogenic soil nodules (e.g., Cojan et al, 2000; Schmitz & Pujalte 2003, 2007).

The second assumption is that original oxygen isotope values in carbonates are less likely to be preserved than carbon data; moreover their shifts, especially in marine deposits, might be below the resolution of this work.

Carbonate carbon data are then considered to be the most reliable for stratigraphic interpretation; original OM carbon data might have been preserved, but no strong evidence for this can be presented, with the exception represented by section [12] (see **figure 5.3**), where OM and inorganic carbon isotope data can be compared; most of these results indicate a systematic offset between 15 and 16,5 ‰, that largely overlap the offset recorded in modern paleosols (14-16‰; cf. Cerling et al., 1989), therefore indicating a good preservation of the carbon isotopic signal.

5.5.2 - Overview – carbonate data

A significant feature of the isotopic data of section [4] (see **diagrams 11** and **12**) is the presence of a threshold, separating continental from marine/paralic limestones, in the range of -4‰ to -5‰ for oxygen and -3‰ for carbon stable isotopes. These two populations must be kept apart for interpretative purposes.

As remarked in a previous section (see section **5.4.1**), $\partial^{18}O$ data from continental carbonates show little variability, with shifts apparently antithetic with the ones observed in carbon data.

A problematic issue is represented by the Upper Thanetian 1 freshwater limestones samples (cf. isotopic signatures), displaying heavier carbon values if compared with other continental limestones (by a 3‰ and 6‰ if compared with early Ypresian and Paleocene samples respectively – also considering Paleocene data from Schmitz & Pujalte, 2003). The reason for this might be a radically different climate in the Ager basin's upper Thanetian (if compared with Tremp basin), and/or the formation of this unit in an evaporitic setting. Field data do not support directly the latter hypothesis, but evaporitic conditions surely developed below and above this unit (see stratigraphy). Better-defined vertical trends can be observed in the late Thanetian – early Ypresian interval, and in the supposedly Thanetian deposits at the northern flank of the Ager basin, and are shown and discussed in paragraphs below.

A comparison with Paleocene global trends could be speculative, primarily because of the data gap from the middle portion of the succession, and because of the lack of well-constrained chronostratigraphic data from the Paleocene of the Ager basin; a comparison can be made with carbonate isotopic data from the Esplugafreda section (northern Tremp basin) by Schmitz & Pujalte (2003). Features in common with the present work are the relatively-low variability of oxygen data, and the lighter values in the lower Thanetian with respect to the late Thanetian ones.

These results are opposite to the global trend shown in the late Paleocene data from Zachos et al. (2001), and are likely to represent a local feature limited to the southern Pyrenees foreland.

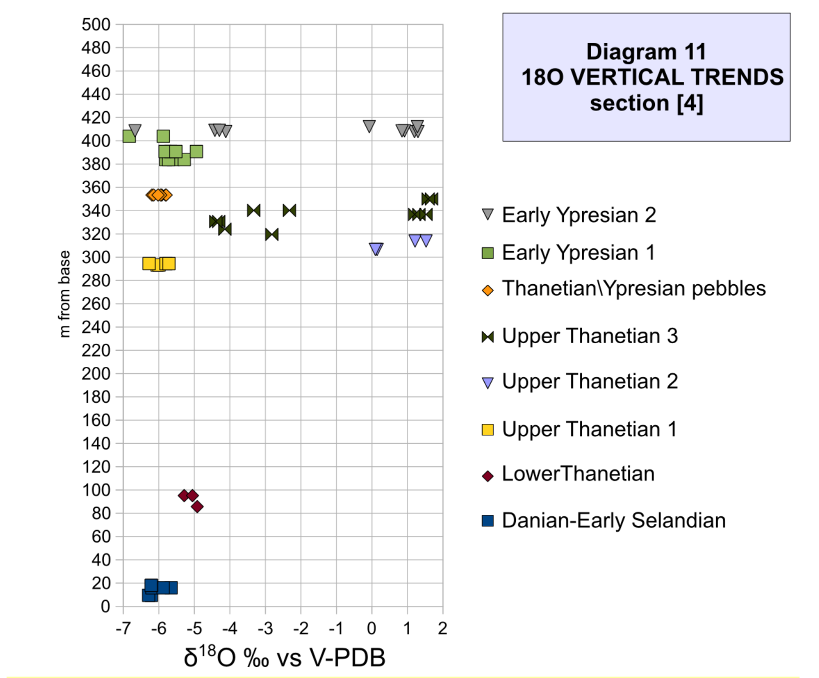

Vertical variation of carbonate oxygen isotopic composition.
Squares: lacustrine or palustrine deposits; diamonds: supposedly pedogenic limestones; triangles: sabkha limestones (average calcite+dolomite composition); papillons: bulk marine limestones.

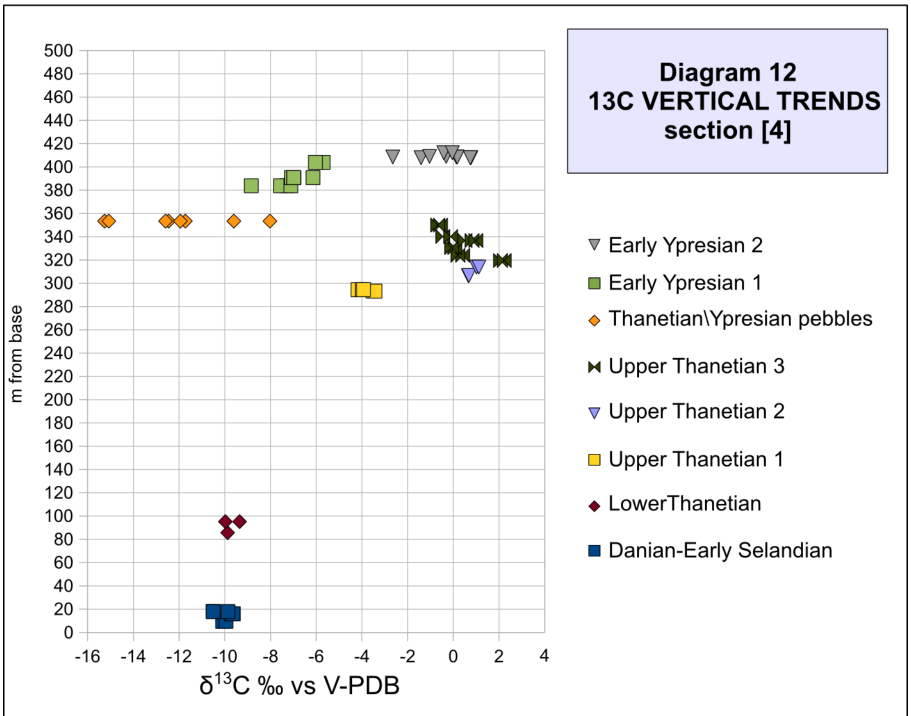

Vertical variations in carbonate carbon isotopic composition;
Squares: lacustrine or palustrine deposits; diamonds: supposedly pedogenic limestones; triangles: sabkha limestones (average calcite+dolomite composition); papillons: bulk marine limestones.

5.5.3 – Northern Ager basin, Danian – lower Thanetian (?)

Section [12] is the only section where inorganic and OM isotope data were studied altogether.

Figure 5.3 shows the vertical variations of inorganic $\partial^{18}O$ and $\partial^{13}C$, and organic $\partial^{13}C$, that are plotted against the stratigraphic log. Data from bulk micrites at the base of the succession are plotted for completeness (see **5.4.1.2**).

The succession records an overall positive shift in stable isotopes values by a ~1‰, with values ranging in a wider interval (up to ~2,5‰ in carbon data). Where the record is better resolved (i.e., in the interval rich in pedogenic carbonate nodules), data show some major shifts, two of which are very well coupled in carbonate data (in concomitance with units tagged AF1 and AP2); OM carbon data seemingly follow the same pattern.

Figure 5.3 (next page) - Stratigraphic log and isotope trends in the continental deposits of section [12]. Color shades are provided in order to highlight relevant horizons discussed in the text.

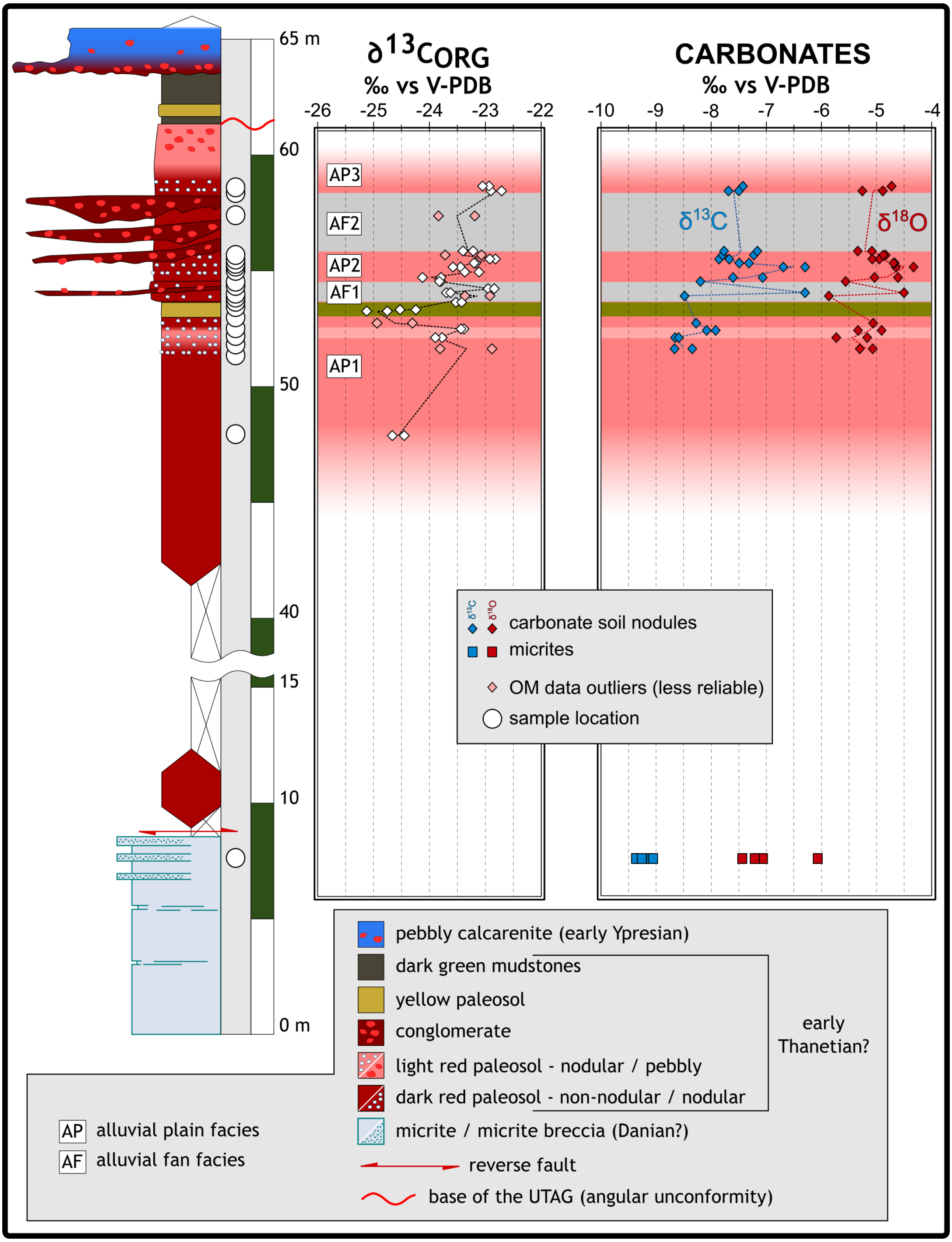

If compared with the rock record, this progressive enrichment in heavy isotopes shows up in a coarsening succession (from mud-dominated to sandy and pebbly paleosols; see **4.2.1.2**);

conversely, the deposition of a coarse unit (AF2 in **figure 5.3**) does not occur together with a significant change in isotopic values; this may reflect a sharp increase in sedimentation rate in that specific interval, up to two or three times with respect to the mud-dominated portions of the succession. This inference, anyway, assumes that no significant breaks occur during the deposition of the alluvial plain facies, but at least one break occurs in concomitance with the formation of the yellow paleosol horizon just below the AF1 unit. This is testified by field observations, since this horizon crops out as an hardened crust, probably the effect of a relatively prolonged interruption of sedimentation – and associated early diagenesis. A potential trace of this process stands in the strong negative shift in organic carbon isotopes measured in this horizon (notice that carbonate soil nodules are here absent).

5.5.4 – Southern Ager basin Paleocene

Figure 5.4 shows the vertical variations of organic and inorganic carbon along section [4].

Since sampling resolution was variable because of different outcrop conditions, the organic and inorganic record cannot be properly compared, but a better insight can be achieved by considering some sedimentological features.

Figure 5.5 displays in better detail the lower portion of the alluvial succession, including organic carbon data and a comparison with section [12].

No petrographic or compositional studies have been performed on these strata, but a detailed case-study from Kraus and Riggins (2007) on late Paleocene – early Eocene continental deposits from Bighorn basin (Wyoming) has been used as a guideline for field interpretation. The main difference from the chosen model lies in the definition of the "light red" paleosols, probably a facies different from the one found associated with the pseudoconglomeratic micrites within Unit URG 2; the latter may be more closely related with the "purple" facies.

Kraus & Riggins's model offers an interpretation of paleosol facies based on physical and geochemical data, displaying a relation between drainage/moisture conditions and paleosol color; this relation is synthesized in the legend of **figure 5.5**.

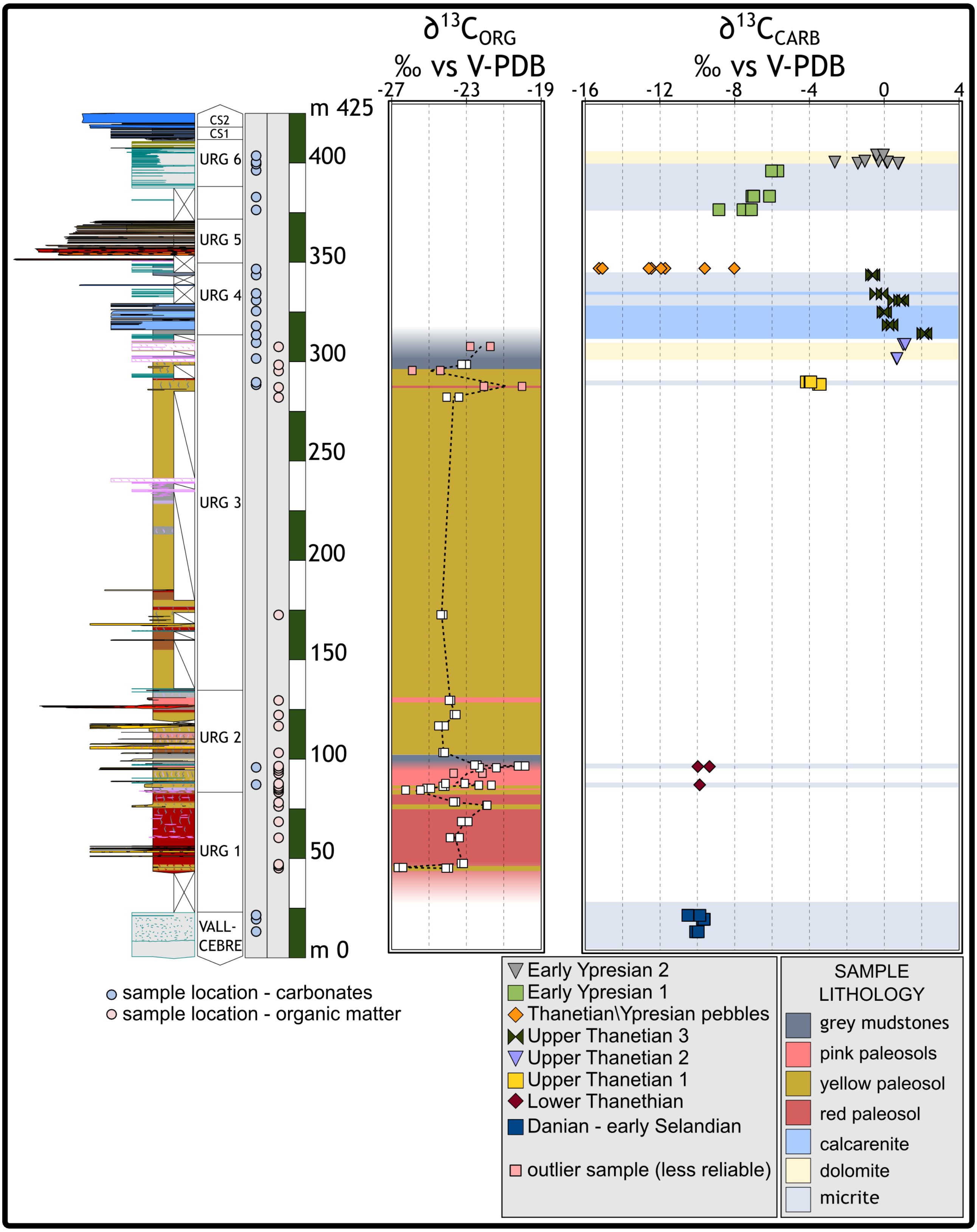

Figure 5.4 – Stratigraphic log and carbon isotope trends in the continental deposits of section [4].

5.5.4.1 – *Unit URG 1*

Despite the lower frequency of sampling in section [4], lower red paleosols are seemingly characterized by a small range of organic carbon isotopic compositions between – 23 and – 24 ‰ vs V-PDB. The same range applies for most of the samples collected in section [12].

A couple of yellow paleosol horizons develop near the base and the top of this interval, showing antithetic shifts in C_{ORG} isotopic values. The lower one shows a slightly lighter composition with respect to the red paleosols, and it hosts a thin layer of OM-rich blue-green mudstone presenting a peak light carbon isotopic composition. Conversely, the upper yellow horizon shows a composition heavier than the ones from red paleosols. This horizon, anyway, develops directly above a sandy layer of fluvial origin, and the color and isotopic composition might reflect different conditions from paleosols forming in interfluves.

The lower red paleosols are further characterized in their upper portions by color mottling and gypsum nodules, both scattered in the sediment and organized in layers. The presence of these concretions, described by Colombo and Cuevas (1993) as rhizomal features, is not apparently accompanied by relevant changes in C_{ORG} isotopic composition.

5.5.4.2 – *Unit URG 2*

The facies association is mainly represented by yellow, intensely mottled paleosols, together with pink layers commonly underlying or including pseudoconglomeratic limestones (see **4.2.1.2**); some layers of fluvial sandstones are intercalated as well.

This interval roughly corresponds to the lower portion of Sequence 2 of Rossi (1997) that correlates the palustrine deposits with coastal lakes in the western portion of Ager basin; all these observations agree with relatively wetter conditions with respect to the lower red paleosols.

Isotopic data initially display very negative values associated with a yellow-brown horizon particularly rich in gypsum concretions. Two sharp positive peaks are then recorded in concomitance with the main layers of palustrine/pedogenic limestones; values then drop significantly just above the limestone layers.

The pink mudstones commonly grade to blue-grey mudstones, following former papers (Rossi, 1997; Kraus & Riggins, 2007), are interpreted as gley paleosols, possibly representing the horizon that formed under peak moisture conditions.

5.5.4.3 – *Unit URG 3*

Unlike Tremp basin, whose late Thanetian deposits are primarily represented by red paleosols (cf. Rosell, 1967, 2001; Cuevas Schmitz & Pujalte, 2003; see **4.3.1.2**), yellow paleosols dominate during this period in the Ager basin. Unfortunately, the study of this interval is hampered by a bad exposure, and a red/yellow color banding observed at the base and at the top of this interval might actually represent its original aspect.

Pedogenic facies suggest a relatively wet or poorly drained environment, eventually shifting to drier conditions in the subordinate red paleosol horizons.

C_{ORG} isotopic data are very scarce in this interval, and are apparently limited in the range of -24‰.

5.5.5 – Ager basin Paleocene N-S correlation

Although a paleosol facies change from the north to the south cannot be excluded (cf. Oms et al., 2007), red paleosols to the north are more likely to be correlated with a similar unit to the south; actually, major changes should be expected to occur in the E-W direction, i.e., from the inner basin to the continental-marine transition: instead, pedogenic facies belts appear laterally continuous over many kms in this direction.

Organic matter carbon isotopic data suggest an equivalence between the northern red paleosols and the lower exposed interval of the red paleosols of the southern succession, because they share a similar range of isotopic compositions, including a negative excursion occurring along a yellow paleosol horizon, implying a Thanetian age for the northern paleosols; this correlation is presented in **figure 5.5**.

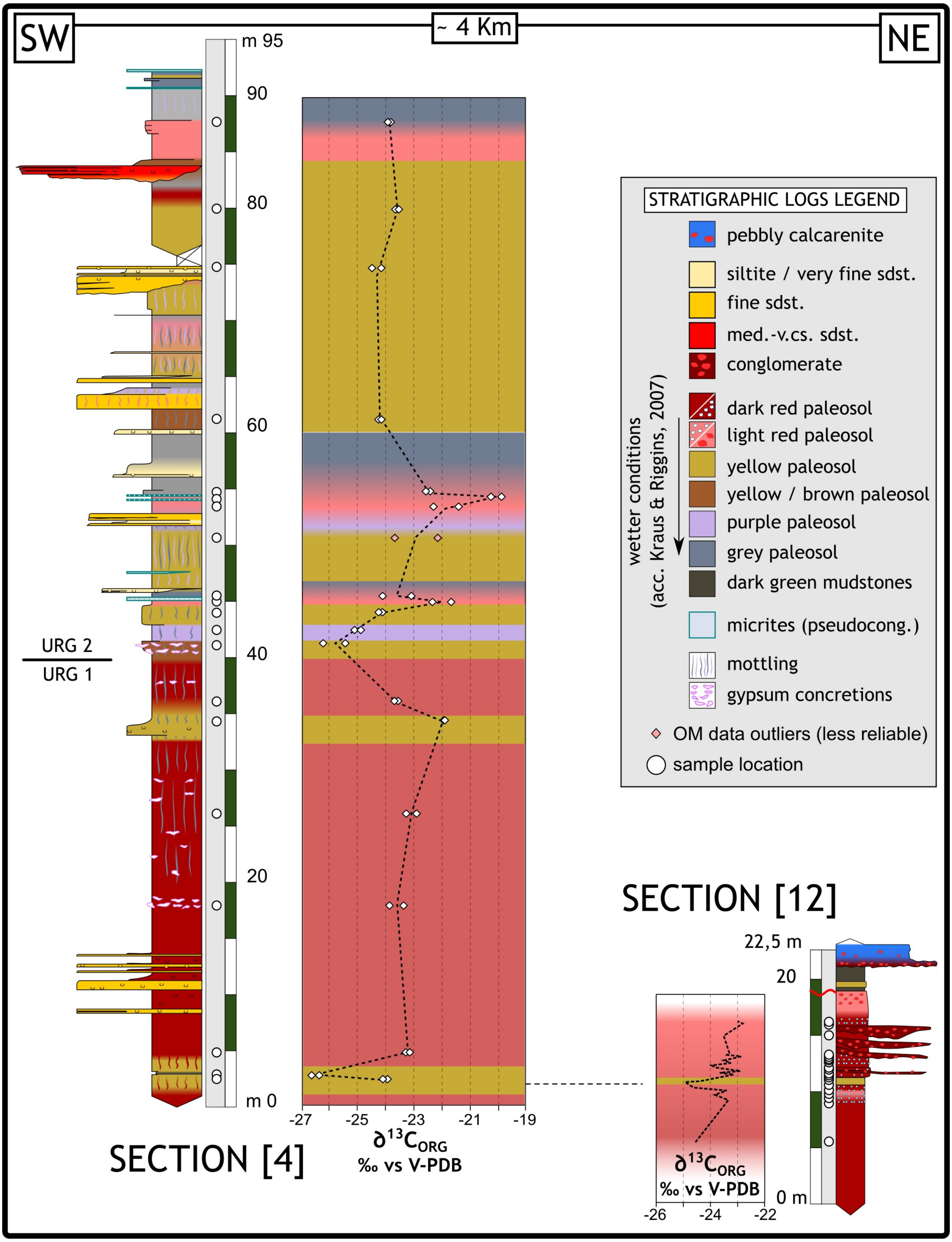

Figure 5.5 – Stratigraphic logs and organic carbon isotope trends in sections [12] and [4]. A tentative correlation is proposed (see text).

5.5.6 – Ager basin upper Thanetian – early Ypresian

Data from carbonates across the Paleocene/Eocene boundary (Units URG 4 to 6; see **4.2.1.3**) provide a better comprehension of the significance of isotopic data from different units. **Figure 5.6** shows the correlated data between the sections [4] and [10].

5.5.6.1 – *Marine upper Thanetian*

"Upper Thanetian 2" sabkha deposits are sharply overlain by marine limestones. Both display a clear distinct isotopic signal (near-zero values for O and C isotopes in sabkha dolomitized limestones; compositions heavier in carbon than oxygen clearly characterize marine calcarenites).

Marine micrites in the same range display instead values similar to the ones for sabkha deposits. Since no evidence for dolomite in these horizons has been found, they can be interpreted as almost original marine values; the ones obtained from bulk calcarenites are likely to be disturbed by secondary cement formed in pores.

Micrites dominate in the upper part of the section. In section [10], they display a clear pattern of negativization in isotopic values, that are likely to fit with former observations of a surface of subaerial exposure and Microcodium bioerosion. An interesting feature is that, at the top of the micritic succession, slightly positive values have been observed in both sections, as if a short marine influx would have occurred before fully continental conditions were met.

5.5.6.2 – *Non-marine early Ypresian*

Above the exposure horizon, pedogenic soil nodules display negative values substantially in agreement with pre- or post-PETM values measured in the Tremp basin (FIG-INTRO).

White micrite clasts from the conglomerate at the base of a deltaic succession bear very negative $\partial^{13}C$ values (see "Thanetian/Ypresian pebbles" in **5.4.1.1**). If their interpretation as reworked pedogenic nodules is correct, these are in agreement with syn-PETM values for continental carbonates (notice that sandstone clast data have been omitted in **figure 5.6**).

Moreover, lacustrine carbonates above the deltaic deposits seemingly display a progressive enrichment in ^{13}C, with ∂ values intermediate between PETM's negative peak and post-PETM values, possibly indicating that the lacustrine deposits formed during PETM's remission of the carbon isotopic excursion.

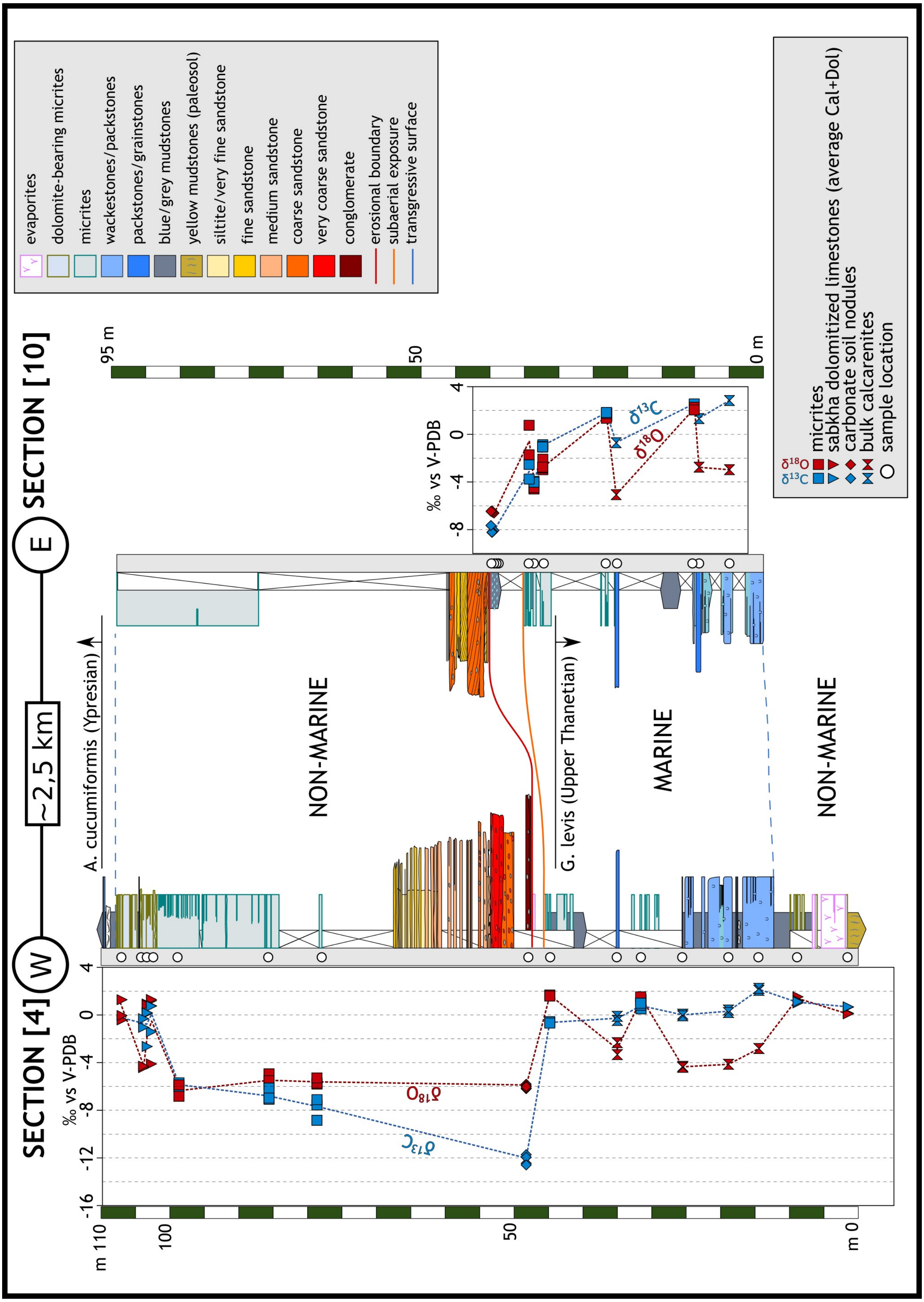

Figure 5.6 – Stratigraphic logs and carbonate isotope trends across the Paleocene/Eocene boundary, southern Ager basin. Biostratigraphic data from Ferrer (1973), Rossi (1997).

Sabkha deposits above this interval show very different values, clearly more scattered than the ones from “upper Thanetian 1” sabkhas. These shifts could be associated with slight facies changes and variable chemical composition.

The stratigraphic implications of these data are that part, or the whole stratigraphic interval including the initial stage of the Paleocene-Eocene Thermal Maximum in the Ager basin was eroded, and that the deltaic deposits of Unit URG 5 formed successively to this event, i.e. they are of basal Ypresian age. Similarly to the Claret Conglomerate in the Tremp basin, this unit (and the overlying continental micrites) probably formed during the main body of the PETM carbon isotope excursion.

5.6 – Tremp basin late Thanetian/early Ypresian – carbonate isotope data

5.6.1 – PETM along the southern margin of the Tremp basin.

The PETM carbon isotopic excursion was investigated in the southern flank of Tremp syncline, within the upper deposits of the Tremp fm. (see **4.3.1.4**).

A correlation with the northern Claret Conglomerate was presented in Eichenseer & Luterbacher (1992) and Waehry (1999), who inferred that the highest sandstone body below the Ilerdian marine limestones in the southern Tremp basin was a fine-grained facies equivalent of the Claret Conglomerate. This unit can be easily traced from west to east, at the Congost de Mont Rebei roadcut (west of La Clua), southwest of Beniure, along the roadcut from St. Esteve de la Sarga to Castellnou del Montsec, near Alsina and Moror, up to the eastern outcrops of Tremp Basin, in the Llimiana-San Salvador de Toló region.

The Mont Rebei roadcut (section [14]) is the only location where a few meters of mudstone paleosols can be studied above and below the sandstone body. Horizons of pedogenic soil nodules can be observed and sampled, although the record provided is discontinuous.

Figure 5.7 displays the results of the isotopic analyses performed carbonate soil nodules: a clear negative shift (~4‰) has been measured between paleosols from below and above the presumed equivalent of the Claret Conglomerate, substantiating the correlation proposed by former workers. The absence of observable paleosol nodular horizons between the negative shift and the base of the Ilerdian carbonate succession hampers the possibility to locate the final stage and to evaluate the timing of the Ilerdian transgression at the southern border of Tremp basin (since former workers –

e.g. Schmitz & Pujalte, 2003 – have shown that the isotopic excursion apparently terminates just below the first marine strata in the Tremp basin depocenter).

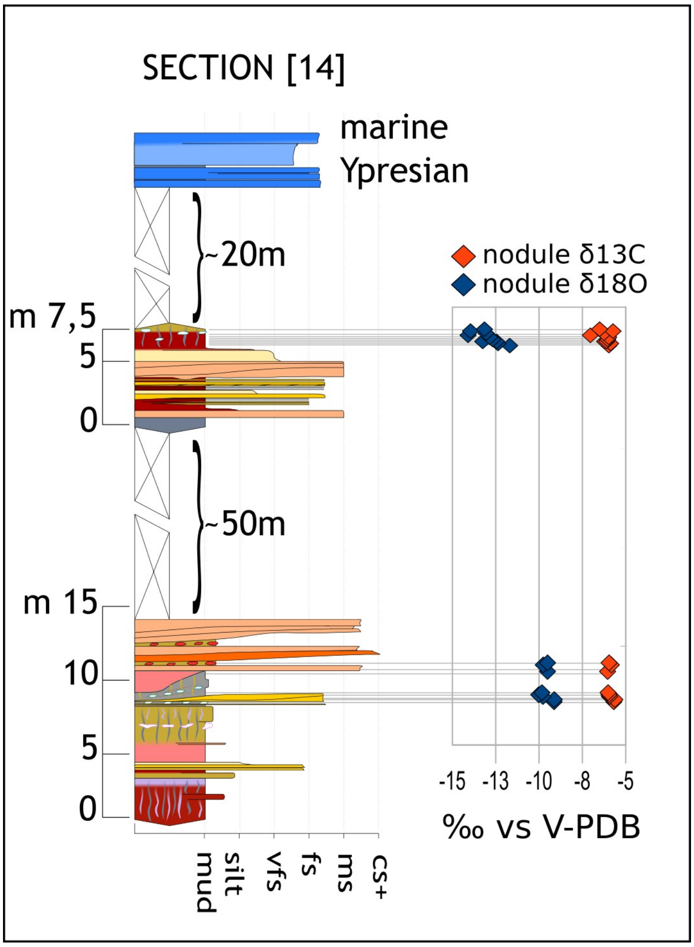

Figure 5.7 – Carbonate isotope data in the range of the Paleocene/Eocene boundary in the southern Tremp basin.

5.6.2 – Tremp basin lower Ypresian.

The Alsina roadcut (section [16]) offers one of the better exposures of the carbonate deposits of southern Tremp basin during the early Ypresian. The studied succession is represented by four limestone bodies interbedded with mudstones, the latter usually covered.

These units were described in detail in **4.3.1.6**.

A tentative isotopic investigation was performed along this section, in order to evaluate the preservation of the isotopic signal and compare it with global Ypresian isotopic trends.

The succession is mainly composed by calcarenites, with an abundant content of larger benthic foraminifers. Foram tests are commonly filled by secondary calcite; the carbonate matrix of the calcarenites is frequently composed by skeletal debris, and only in a few samples a peloidal matrix was observed. A few horizons are characterized by red bioclasts, possibly because of subaerial early alteration (e.g., upper part of the Alsina-2 Unit, see **4.3.1.6**)

Analyses (results in **figure 5.9**) were performed on alveolina and nummulites shells, and bulk rock. In the lack of a microsampling device, a dentist drill was used to collect small samples (between 2.5 and 6.0 mg) in the middle of the foram tests (i.e., attempting to collect carbonate material from the prolocus). This approach would reduce the amount of early secondary calcite in the analyzed samples; furthermore, early and late secondary calcite (i.e., from fenestral structures and joint fills respectively) were separately analyzed in a few samples in order to assess the potential disturbance in shell isotope data. 24 samples were collected and 42 subsamples were analyzed; 30% of the subsamples were double-analyzed; carbon data showed an error below the instrumental error (0,1‰); oxygen data rarely exceeded the instrumental error by less than 0,1‰.

Results

Similarly to the case of the Paleocene samples, oxygen isotopic data display a very irregular behavior; conversely, where different subsamples were analyzed from a same stratigraphic level, carbon isotopic data display minor intrasample variability between nummulites and alveolina samples (commonly below a 0,25 ‰); bulk data instead are commonly more negative (in the range of -0,5 ‰) from foraminifera samples.

Red bioclasts as well are characterized by relatively lighter isotope values when compared with (apparently) unaltered foram specimens from the same stratigraphic level.

Secondary calcite was separately analyzed in a few samples, where relatively large pore fills (supposedly fenestral structures) or a calcite-filled joint were observed, in order to compare their isotopic compositions with the ones from secondary calcite filled shells. Results fall very close to the average rock composition in carbon isotopes; oxygen data, instead, show a variable negative scatter from other subsamples collected in the same stratigraphic levels.

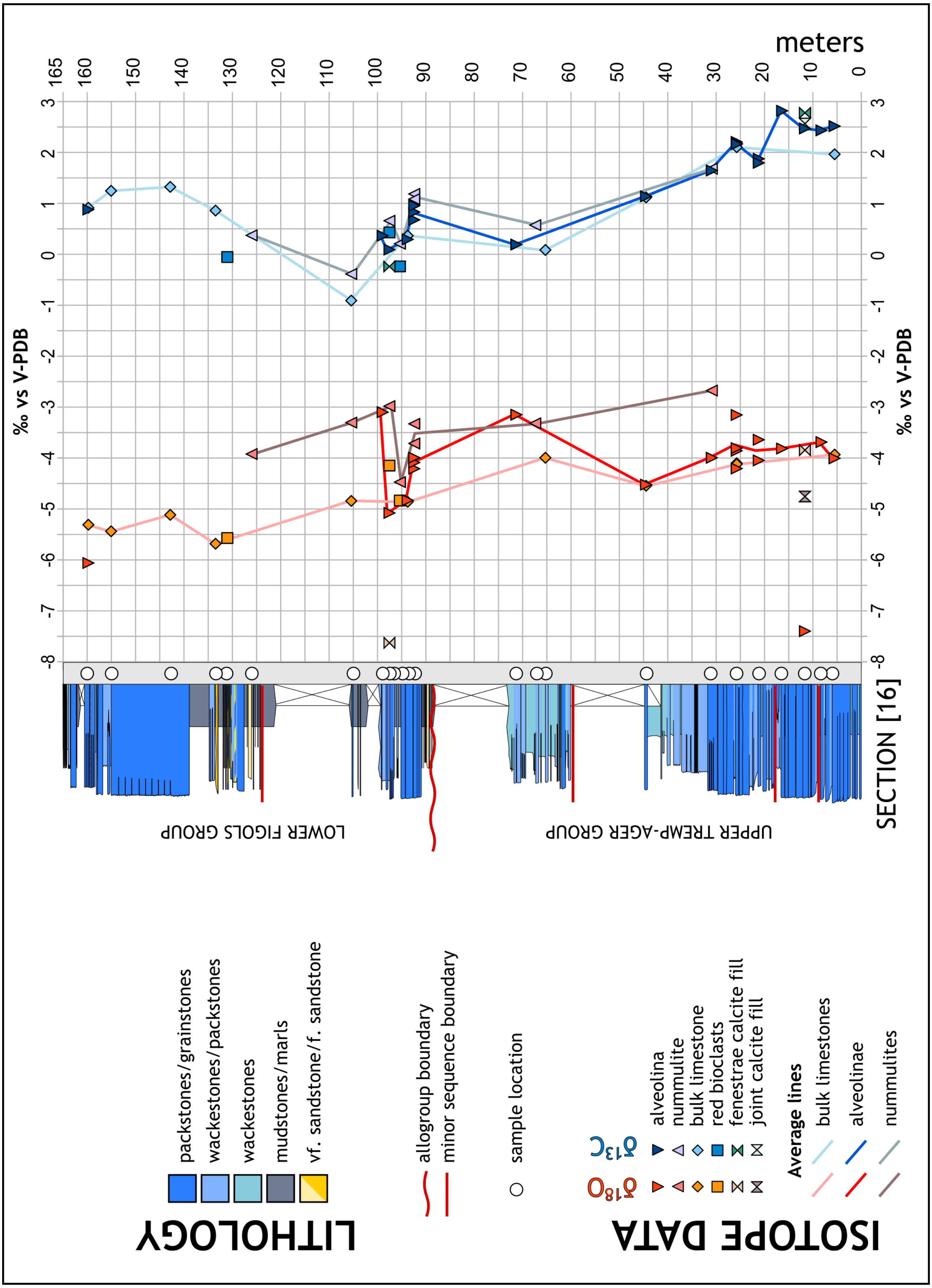

Figure 5.8 – Carbonate isotope trends from the lower Ypresian of section [16], southern Tremp basin.

INTERPRETATION

Since all of the samples measured were interested by some degree of secondary calcite fill, interpretations of isotopic data may be very speculative. Some help may be provided by comparison with independent isotope-stratigraphic research from coeval deposits.

A local comparison can be performed with Molina et al. (2003) study from the “Campo section”, the parastratotype for the regional “Ilerdian” (Lower Ypresian) stage (see **figure 5.9**). The Campo section is located in proximity with the western shelf margin of Tremp basin, some 45km north-west of section [16] in the present work. In the cited paper, oxygen and carbon stable isotopes from Alveolina shells were studied in an interval including the Upper Tremp-Ager Group that is represented in section [16] by the two main lower limestone units. Although the paper didn't detail sample selection and preparation, it is evident from the provided log that a wide spectrum of lithologies was sampled, similar to the one characterizing the present work (from marls to grainstones). It is here assumed that recrystallization affects Alveolina shells also in the Campo section, at least concerning the samples collected in the calcarenitic layers.

A global term of comparison is offered by the well-known global isotopic curves compiled by Zachos et al. (2001), and from a very detailed isotopic log provided by Zachos et al. (2010) from an individual site (ODP site 1262, Walvis Ridge, southern Atlantic). The latter may be considered as a reference data set for marine isotope values in the early Eocene, given that site 1262 is the most complete log ever recorded in this time interval.

The correlation provided between the two sections follows the one proposed by Waehry (1999).

Oxygen data.

The strongly negative values of oxygen isotopes collected in this work – and their large range of variability (approximately from -3 to -5‰ in Alveolina shells) – clearly indicates that these values are no more representative of original marine values. An influx of meteoric waters (quite realistic in a shallow water setting periodically interested by strong fluvial inputs) is a likely cause for the negative values. No significant correlation with carbon data was observed. Comparison with the Campo section data (Molina et al., 2003) shows a similar range of variability in oxygen data.

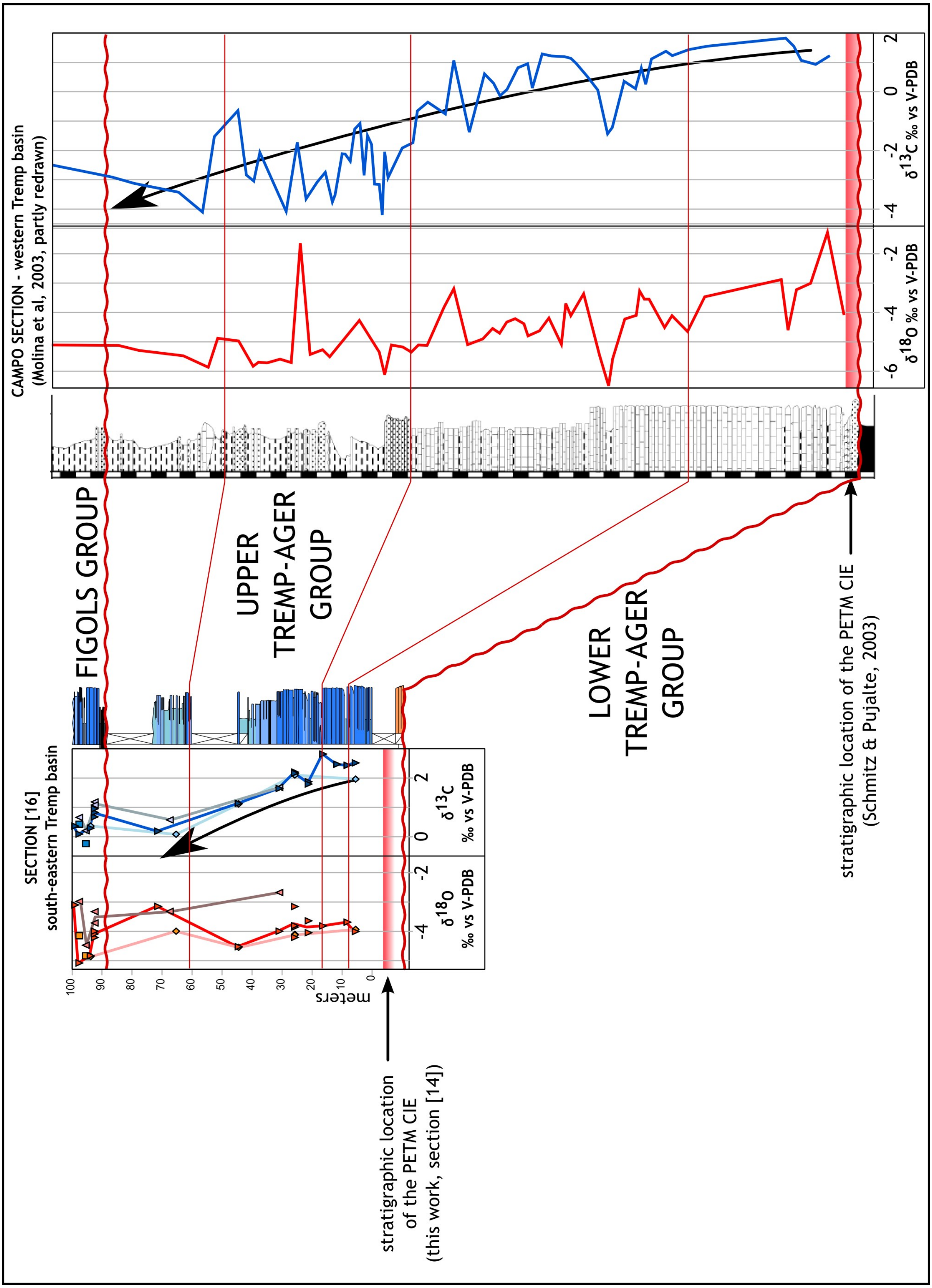

Figure 5.9 – Comparison of the lower Ypresian isotope data collected in the present work and from Molina et al. (2003).

Carbon data.

The range of variability in marine carbon data from section [16] is wide as well (from approximately -1 to 3‰). Differently from oxygen data, these results closely fall in the range of variability from carbon isotope data measured in abyssal logs (Zachos et al., 2010); this in itself doesn't imply that these values are truly representative of original values, since the time interval represented by section [16] sampled interval should be characterized by a thinner range of variability (0,5 to 2‰ in Zachos et al., 2010).

It is interesting to notice that Molina et al. (2003) carbon results are, on an average, much more negative; moreover, an overall vertical negative trend was observed by the authors, with an abrupt shift close to the top of their measured section (coincidently with the deposition of a glauconite-bearing terrigenous layer ("REE turbidites" in Payros et al., 2000; the presence of glauconite was recognized by E. Mutti, pers. comm.). This negative shift was interpreted by the authors as the effect of a diagenetic imprint. Since a similar negative trend is observed in the correlative portion of the present data, some hypotheses must be made.

A first, daring, hypothesis, would be that carbon isotope data from section [16] are actually very close to the original values, and that diagenetic imprint wouldn't have shifted bulk values; they would positively offset from abyssal data under the influence of some local factor (e.g., a characteristic heavier composition in waters from the SCPFB, if compared with oceanic waters).

An alternative possibility is that the negative trend could have been already present in the original values, and diagenetic disturbances would have offset these values in a homogeneous manner (e.g., a partial dissolution of calcite causing the ablation of lighter isotopes).

These two hypotheses would be in agreement with the general ^{13}C depletion trend in carbon isotopes occurred during the early Ypresian between the PETM and the EECO (Zachos et al., 2001; 2011).

On the other hand, in both sections, carbon isotope data become more negative when passing from coarse calcarenites (grainstones and packstones) to finer lithologies (wackestones and marls), implying a different degree of recrystallization (volumetrically more relevant in the coarser lithologies). Given the sharply negative oxygen values for recrystallized calcite – in contrast with carbon values, displaying compositions close to the average rock – it is possible that during recrystallization the carbon isotopic composition would have been homogenized between the bulk rock constituents, while major fractionation would have interested oxygen isotopes.

Since the negative trend is experienced in a deepening succession, it isn't likely of having been originated from subaerial exposure. Comparisons can be made with isotopic data from the exposed lowermost portion of the Figols Group in section [16], that displays a clear negative shift in carbon (as well as in oxygen) isotope values: considered altogether with sedimentological and paleoenvironmental informations (see **4.3.1.6**), this unit forms in clearly shallower conditions and it is likely to have experienced short periods of subaerial exposure (this also hampers the recognition of the ETM2 isotope shift, since it should be located close to the UTAG/LFG boundary). Another term for comparison is the well-assessed exposure surface of marine deposits in the late upper Thanetian of Ager basin (see above).

In conclusion, carbon isotope data from section [16], although suggestive for their similarity with original global marine values, are not clear enough to recognize clear trends and anomalies.

Integration with chronostratigraphic data (partly inferred from the correlation with the thoroughly studied axial Tremp section, section [20] in this work) might allow the hypothesis that the negative trend in carbon isotopes is related with the warming stage occurring between the PETM and the EECO.

6 – DISCUSSION

The problem of defining allogroup boundaries (*sensu* Mutti et al., 1988) is mainly related with the correct recognition, within the stratigraphic succession, of events that significantly changed the morphology of the basins, and consequently the areal distribution of sediments and depositional systems.

Within foreland basins, uplift of the source areas causes an increase in the gradient of fluvial systems, renewed erosion of basement rocks and partial dismantling of the sedimentary covers; piggy-back basins are affected by thrust-related folding, and growth patterns and angular unconformities affect the deposits in their marginal areas.

The Tremp and Ager basins allow the study of these features during the initial stages of uplift of the structural high that separate them (the Montsec thrust). This problem was investigated by reconstructing the physical stratigraphic framework of the syntectonic successions.

However, some of the main elements of the correlation remain quite elusive, either because of the difficulties in correlating unconformities between the marginal and depocentral areas (where they are likely to shift to paraconformable or conformable surfaces), or because of poor chronostratigraphic coverage. A further problem is the apparent co-occurrence, over relatively short time intervals, of allogroup boundaries and global eustatic or climatic events (see **6.4**) that might have enhanced or diminished the expression of such boundaries on the field.

6.1 – Southern Tremp basin

In the present work a new correlation is proposed for the Tremp basin between its marginal and depocentral areas. It is mainly based on the physical stratigraphic framework and correlation proposed by Waehry (1999), with some modifications. The most significant of these modifications concern the sequence UTAG 2 that in the present work displays a greater differential subsidence.

Angella (1999) correlated the base of sequence UTAG 3 with an angular unconformity, of early Ypresian age, located in the northern margin of the Tremp basin (Arèn), and tentatively explained the differential subsidence in the UTAG 2 interval in the Guardia/Tremp sector as the apparent effect of a poorly-exposed, angular unconformity at the UTAG2/UTAG3 boundary. The main inference of this correlation was the occurrence of a major compressional phase in the Tremp basin. Following a similar hypothesis from Mutti et al. (1988), this event was related with the deformational stage that led, in the Ager basin, to a transition from the carbonate ramp deposits of the Cadì fm. to the terrigenous deposits of the Baronia Sandstones.

Differently from Mutti et al. (1988), Angella established that the allogroup boundary associated with this general deformational stage (base of the Figols Group) was located in a lower position in the Ager basin, i.e., at the base of the UTAG b sequence.

The recognition of a sharp angular unconformity in the Lower Ypresian of the southern Tremp basin is mainly hampered by problems of exposure; also, the lateral relationships between the carbonate ramp and the deltaic deposits might be distorted by different rates of sedimentation and accretion patterns of the main carbonate banks.

The interpretative model proposed in the present work tries to depict a more gradualistic scheme for the evolution of the Tremp basin in the Lower Ypresian (**figure 6.1**).

The reconstruction of the geometries of the southern margin of the basin (see **4.4.1**) indicates the occurrence of synsedimentary uplift of the Montsec high during the formation of sequences UTAG 3 and 4; axial correlations suggest that strong differential subsidence initiated within sequence UTAG 2. This helps to identify an interval of synsedimentary growth of the Montsec high, that accelerated shortly after the Ilerdian transgression and was significantly diminished by the time of deposition of the Serra-Puit and Alsina-2 Units (early middle Ypresian; see **2.5.3**, **4.3.1.5**, **4.3.1.6**).

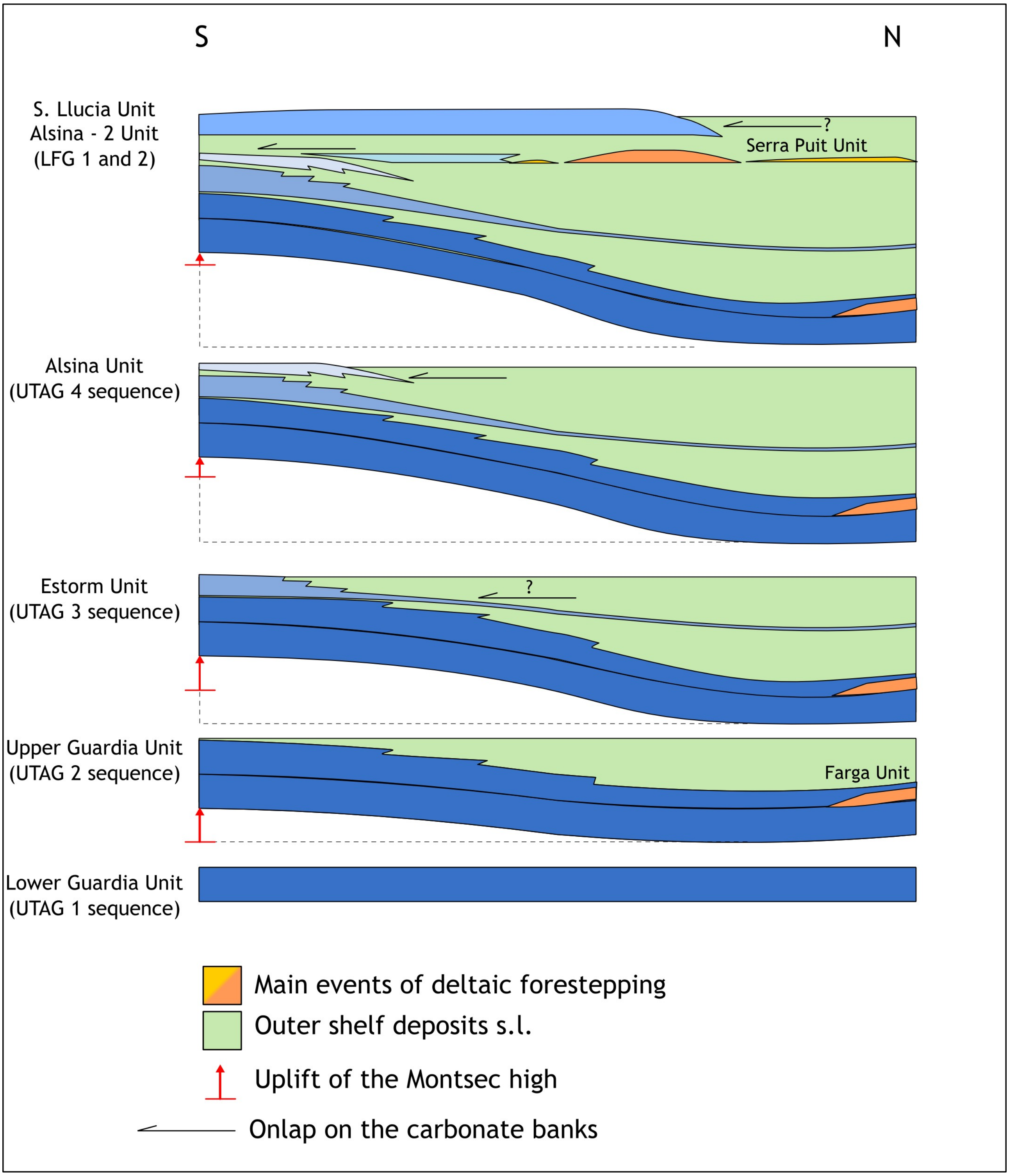

Figure 6.1 – Evolutionary model of the southern ramp of the Tremp basin (not to scale)

6.2 – Ager basin N-S correlation: Paleocene

In the Ager basin many problems are still to be settled, and mainly involve the poor chronostratigraphic coverage of its successions. In the present work, some light was shed on the age of the angular unconformity between the continental Paleocene and the marine Ypresian in the northern Ager basin; the results are synthesized in **figure 6.2**.

Isotope data (see **5.5.6**) support the hypothesis of a correlation between the siliciclastic deposits of Unit URG 5 in the southern Ager basin (see **4.2.1.2**) and the Claret Conglomerate s.s. (i.e., Unit CL 2, see **4.3.1.3**). This correlation was formerly proposed on the basis of a litho- and biostratigraphic approach (e.g., Sole-Sugrañes, 1970), substantially correlating the uppermost siliciclastic body below the first marine deposits with Lower Eocene fossils. In the present work a more direct correlation of these two units is proposed, with the implication of a common climatic driver for the deposition of these bodies (see below).

E-W correlations of this unit (see **4.4.4**) also demonstrate that it formed during a stage of strong differential subsidence between the St. Mamet anticline and the depocentral sector of La Baronia de Sant Hoisme. The actual timing of this deformation cannot be properly ascertained, because of difficulties in defining and correlating its base. The detailed correlation panel of the western Ager basin proposed by Rossi (1997) only displays major disturbances in subsidence patterns in the lower part of the "Upper Red Garumnian"; the author's E-W correlation of the lower part of this succession (roughly equivalent to units URG 1 and 2, see **4.2.1.2**) displays enhanced subsidence between the Millà and St. Mamet anticlines.

On the other hand, isotope data from the northern succession of the Ager basin indicate that the "uppermost siliciclastic body below the first Eocene marine deposits" did not form during or close to an isotope anomaly comparable to the PETM C.I.E. (see **5.5.3**); i.e., the continental conglomerates of this succession are probably much older than the Claret Conglomerate.

Still on the basis of isotope data, the underlying continental deposits are likely to correlate with the basal portion of the succession studied in the southern Ager basin (see **5.4.1.2** and **5.5.4**), similarly to the reconstruction proposed by Rosell et al. (2001).

This implies the presence of a very large hiatus associated with the basal Ypresian unconformity that, in the most conservative hypothesis, would correspond to ~300 m of succession in the southern basin, with a temporal extension of at least 1-2 My.

This reconstruction is coherent with the classic model that locates in the Paleocene the early stage of uplift along a proto-Montsec.

The presence in this sector of an early high is testified by the northern conglomerates (Rosell et al., 2001, and references therein). The possible evidence in the southern sector for a correlative unit are the widespread sheet sandstones within Unit URG 1 (see **4.2.1.2**); the isotope correlation might support this hypothesis.

The general picture suggest a syntectonic evolution for the Upper Red Garumnian in the Ager basin. In order to highlight this interpretation, a “Middle Tremp-Ager Group” (MTAG) subdivision is here proposed. Its base corresponds with the Middle-Paleocene Unconformity; despite the fact that its significance as an allogroup boundary (tectonic unconformity) may be controversial (see **2.3.1.1**), it may be used as a reference layer, because of its basin-wide traceability.

The top of the MTAG is defined by the tectonic event that is commonly related with the deposition of the Claret Conglomerate (uplift of the Boixols thrust in the Tremp basin; Waehry, 1999); a contemporary event along the Montsec high is probably represented by the basal Ypresian marine conglomerates in the northern Tremp basin (see **4.2.1.4**, Unit CN 1). The tectonic significance of these conglomerates was first inferred by Mutti et al. (1985).

In the southern Ager basin, as well as for the Tremp basin, this unconformity might not be directly related with the Claret Conglomerate. Better correlative surfaces are probably the incised valley described by Pujalte & Schmitz (2005) in the Temp basin, and the karst surface developed on top of the Thanetian marine carbonates (Unit URG 4; see **4.2.1.2**), since both of these surfaces indicate a major sea-level fall before the Paleocene-Eocene boundary. Therefore, the basal unconformity of the UTAG was designated as the Upper Paleocene Unconformity.

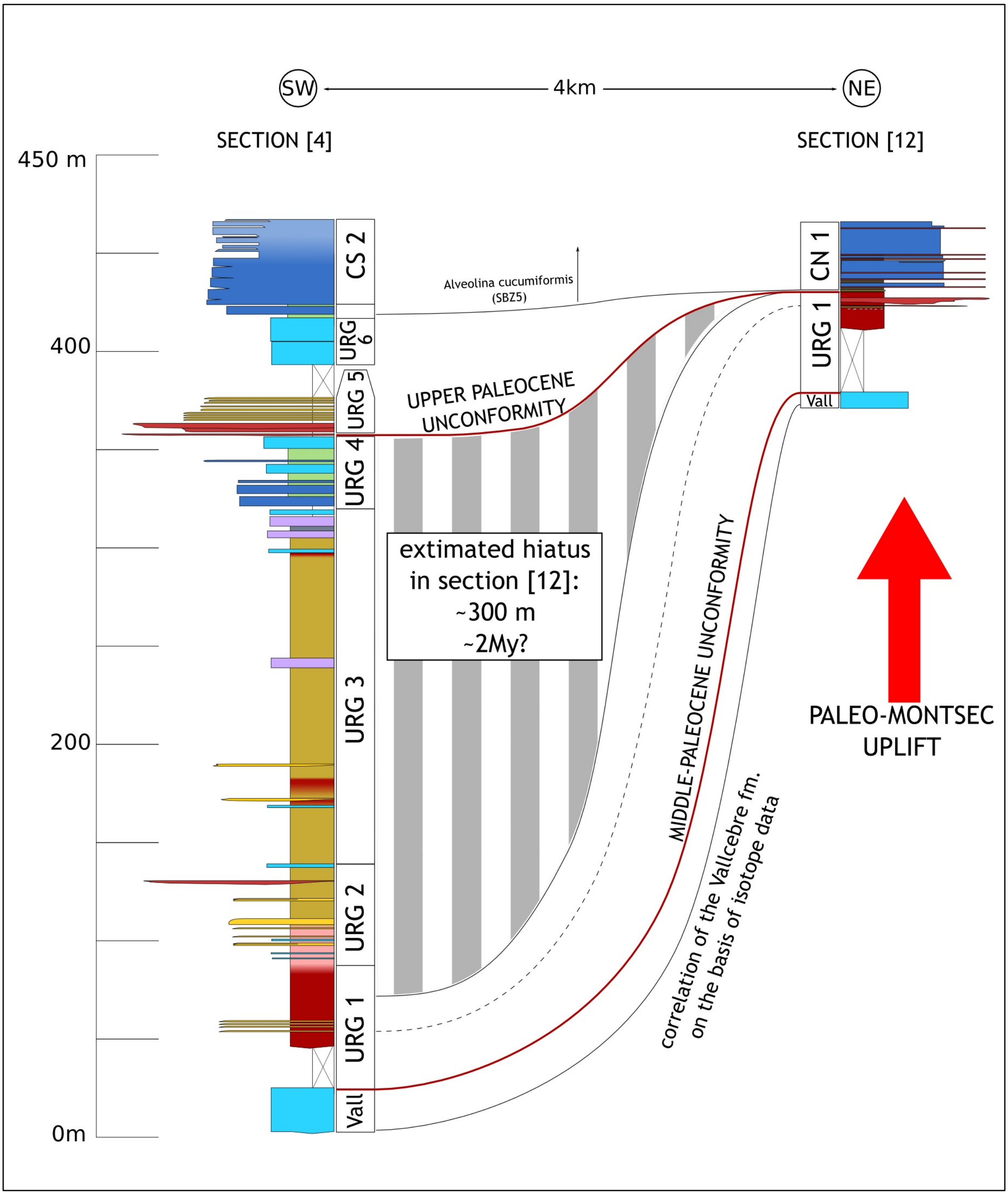

Figure 6.2 – Correlation proposed for the Paleocene of the Ager basin; see text for an explanation.

6.3 – Ager basin N-S correlation: Lower Ypresian

N-S correlations in this interval are limited to sedimentological arguments and based on a comparison with the southern margin of the Tremp basin. These considerations are mainly centered on the significance of the CS 3 Unit / UTAG b sequence in the southern Ager basin and its correlation with the northern succession.

Biostratigraphic data from Ferrer et al. (1973) place the basal part of the northern marine succession (Unit CN 1, see **4.2.1.4**) in the earliest Ypresian (see Attached Document 1), i.e., these beds are probably coeval with the southern units CS 1 and/or CS 2 (see **4.2.1.3**).

Therefore, Unit CS 3 might be equivalent to the upper part of the northern succession, or younger. Mutti et al. (1994, stop descriptions) suggested various possible interpretations of the basal glauconite-bearing conglomerate of Unit CS 3. It could either be associated with a ravinement surface, a sequence boundary or a tectonic unconformity. The latter hypothesis was followed by Angella (1999), whose interpretation of the base of the Figols Group implied that the angular unconformity, observed on top of the Cadì fm in the northern Ager basin (see **2.4.4**), was related to the mixed deposits of unit CS 3. This reconstruction is depicted in **figure 6.3**.

An alternative hypothesis should consider the correlation of unit CS 3 with the upper part of the northern succession (Units CN 2 and 3, see **4.2.4**). The main reason for this is the abundant occurrence of mixed carbonate-siliciclastic deposits in both units and their organization in two main cycles – possibly two small-scale sequences, that could be equivalent to the two main packages of bioclastic to mixed tidal bars that form the upper part of the CS 3 unit.

In the Tremp basin, the syntectonic succession outlined in **4.4.1**, **4.4.3** and **6.1** formed during a relatively well-constrained time-interval, that is expressed in the southern Ager basin by a condensed or lacunous succession (see **2.5.3**); with the available data, the two possibilities cannot be properly worked out.

An hypothetical reconstruction is proposed in **figure 6.4** and **6.5**, that involves in both basins a gradual uplift of the Montsec high.

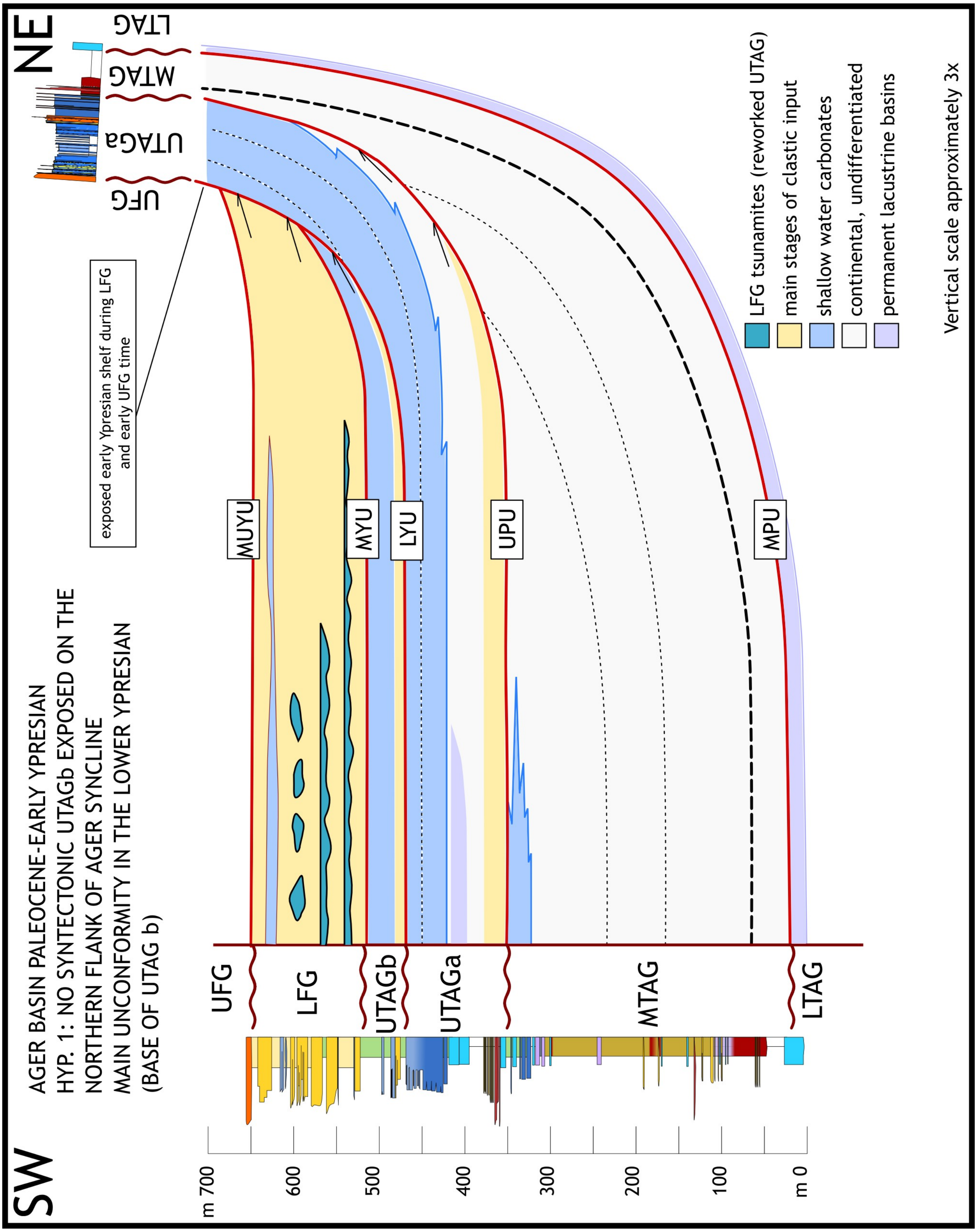

Figure 6.3 - refer to ***4.4.2*** *for the names of the unconformities*

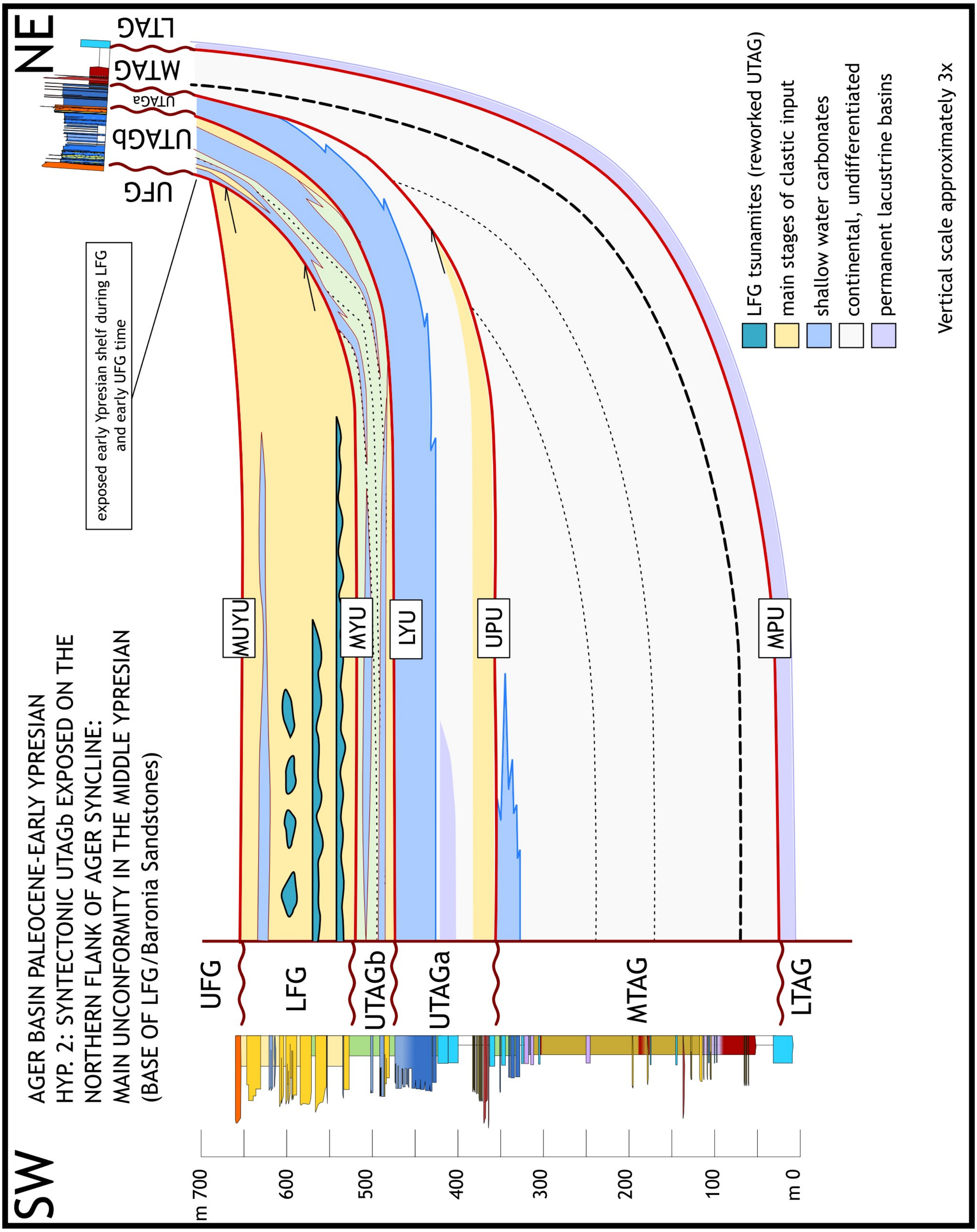

Figure 6.4 - refer to 4.4.2 for the names of the unconformities

Figure 6.5 (next page) - Figure 6.5 – Correlation of the UTAG between the Tremp and Ager basins, and reconstruction of the N-S stratigraphic relationships in Ager basin based on the hypothesis of syntectonic sedimentation occurring on both sides of the Montsec High during the Lower Ypresian.

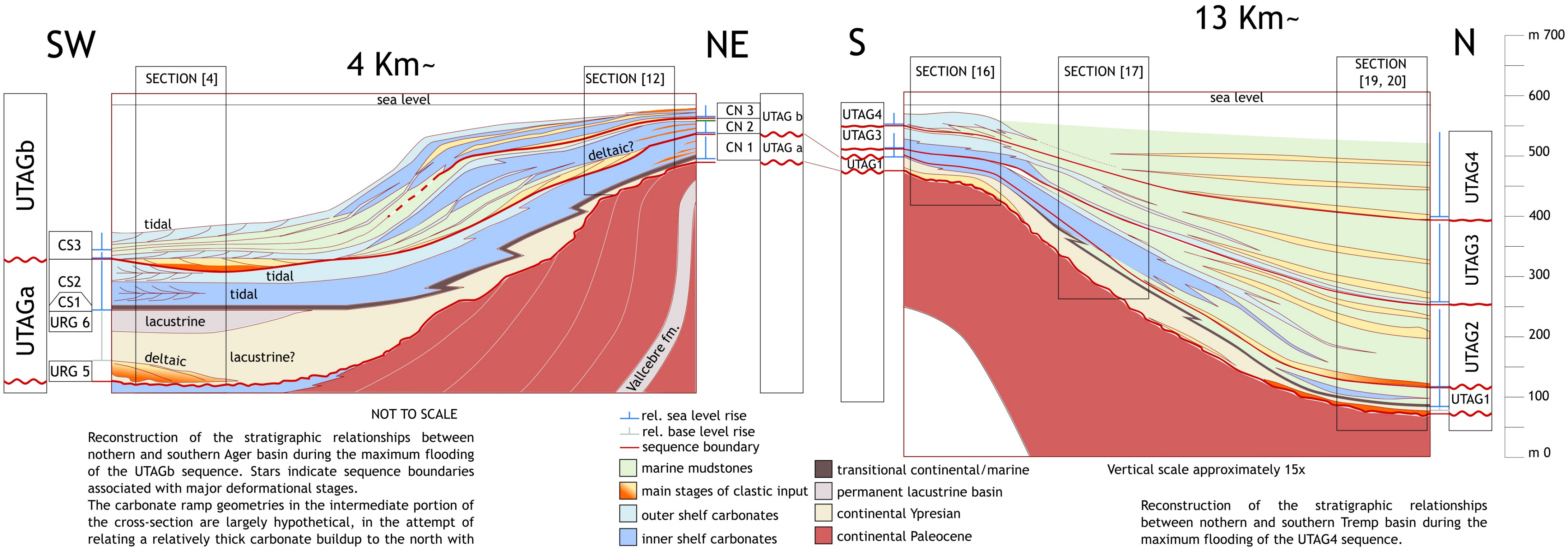

Reconstruction of the stratigraphic relationships between nothern and southern Ager basin during the maximum flooding of the UTAGb sequence. Stars indicate sequence boundaries associated with major deformational stages.
The carbonate ramp geometries in the intermediate portion of the cross-section are largely hypothetical, in the attempt of relating a relatively thick carbonate buildup to the north with a condensed succession to the south.

Reconstruction of the stratigraphic relationships between nothern and southern Tremp basin during the maximum flooding of the UTAG4 sequence.
The location of the boundary between LTAG and MTAG in the southern Tremp basin is unknown

The beginning of the deformation is placed at the base of sequence UTAG 2 in the Tremp basin, that is correlated on a (relatively weak) biostratigraphic basis with the base of sequence UTAG b. Coarse clastics occur in both basins (basal part of Unit CS 3 and Farga Unit in the Tremp basin; base of the Ager sequence *sensu* Eichenseer & Luterbacher, 1992).

Deformation continues during much of the Lower Ypresian along the Montsec high; concurrent subsidence in the depocenters and eustatic rise (which peaked slightly above the base of sequence UTAG 3, according to the global correlations proposed by Waehry, 1999) cause the formation of condensed successions in both basins. The lower structural position of the Ager basin, already testified by the late Thanetian transgression causes a more prolonged starvation of the depocentral area. At the same time, along its northern margin, small, poorly-efficient fandeltas (*sensu* Mutti et al., 1996, 2000) interact with localized carbonate buildups. In the deeper area of the basin, only tidal action succeeds in accumulating reworked bioclastic materials.

Deformation was diminished in the middle Ypresian but, at this time, the morpho-structural assset and the generalized uplift could have reached critical conditions (e.g. in the gradient of fluvial systems) that caused the widespread occurrence of deltaic deposits of the Figols Group.

In this interpretation, the UTAG b sequence, and its coeval units in the Tremp basin (UTAG 2, 3, 4; Ager sequence in Eichenseer & Luterbacher, 1992) represents a "boundary sequence" (*sensu* Mutti et al., 1994a), i.e., a sequence formed when depositional systems, originated as the product of a specific morpho-structural or climatic setting, blend with others that would become dominant in a successive stage. The case of the UTAG b might explain the different positions proposed for the base of the Figols Group (cf. Mutti et al., 1988; 1994c; Angella, 1999).

6.4 – Climate issues

The problems discussed in the former sections are ultimately related with the definition of allogroups and allogroup boundaries. This might be a general problem of foreland basins when thick syntectonic successions are preserved; in some cases, defining a reference horizon is easier and more useful than defining complex units where the timing of deformation is actually diachronous.

The case of the Tremp and Ager basins is complicated by the fact that sequence boundaries and systems tracts can be either enhanced or diminished due to interaction of tectonic uplift, tectonic subsidence, eustatic rise vs fall (Mutti et al., 1985; 1988; 1994). Moreover, in the Early Paleogene, long-term climatic variations and short-term anomalies could have interacted with the sedimentary processes.

The example of the Claret Conglomerate (Unit CL 2, see **2.4.3**; **4.3.1.3**) is emblematic, since its correlation with the onset of the PETM was ascertained in both basins (Schmitz & Pujalte, 2003; this work, **5.5.1** and **5.5.6**). Its interpretation as a continental deltaic deposit (Angella, 1999) is followed, also acknowledging the data recently presented by Pujalte et al. (2011), who found a marine deltaic deposit of PETM age in the M.te Perdido area (west of the South-Central Pyrenean Unit), and interpreted these deposits as the deltaic equivalents of the Claret Conglomerate (a braid-plain deposit in their interpretation). Paleocurrents and facies of the Claret Conglomerate suggest instead its occurrence as a north-sourced fan delta system, discharging high energy flows in ephemeral continental basins located in the axial sector of the Tremp basin (see **4.3.1.3**); these continental fan deltas probably switched to the marine setting together with the depositional profile towards the north-west.

The ascertained global effects of the PETM are relatively poor, and mainly involve biological effects, and an increase in the export of continental sediments to the sea; sea-level effects are more doubtful, and different reconstructions place on this level both flooding surfaces and eustatic falls.

The short-term increase of rainfalls over a relatively arid landscape suggested by Schmitz & Pujalte (2003) might explain the occurrence of catastrophic floods, at least in the South-Central Pyrenean foreland: e.g., opposite effects of the PETM (increased aridity) were described by Kraus and Riggins, 2007, in the Willwood fm. of the Bighorn Basin, Wyoming.

Similarly to the case of the Claret Conglomerate, the basal deposits of the Figols Group (Serra Puit Unit, Lower Baronia Sandstones) might have been affected by an increase of clastic production related with the ETM2 thermal anomaly. The base of chron C24n may be used as a reference layer for this event; similarly, the base of the Figols Group runs closer to this magnetic inversion.

The ETM2 anomaly was tentatively investigated in the southern Tremp basin; a negative shift was actually found, but it is clearly younger than the base of the Figols Group (see **2.5.3**), and it is likely to have formed because of an influx of meteoric waters during the lowstand phase represented by the Alsina-2 and Serra Puit Units; short-term subaerial exposure of the calcarenites of the Alsina-2 Unit is also likely to have occurred, as the presence of “red horizons” within it might suggest.

6.5 – Evolutionary model

The cartoons of **figure 6.6** in the next two pages resume the inferred evolution of the Tremp and Ager basins during the Paleocene and Lower Ypresian, on the basis of the arguments discussed in this chapter. Rectangles indicate the relative position of the studied sectors within the model.

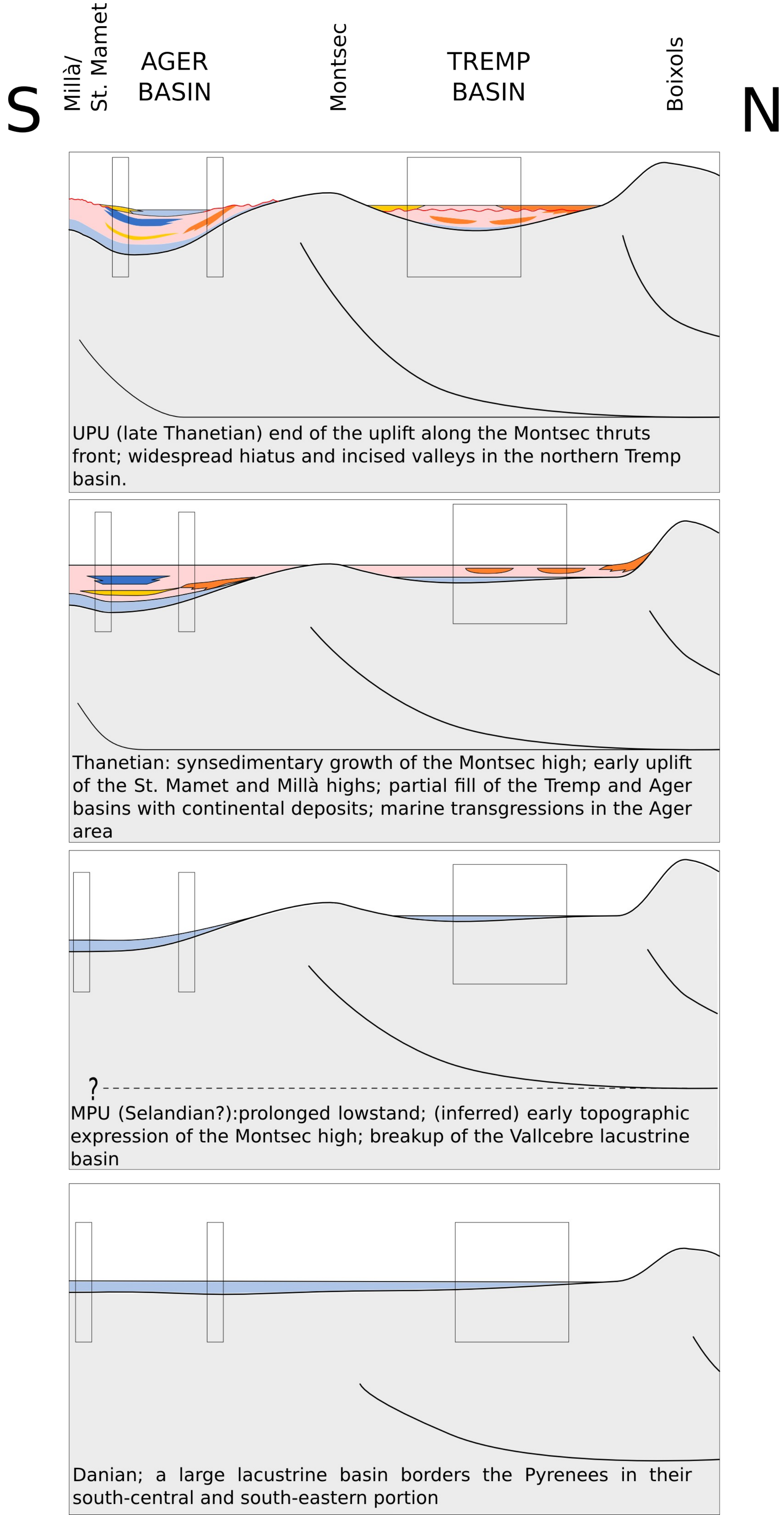

UPU (late Thanetian) end of the uplift along the Montsec thruts front; widespread hiatus and incised valleys in the northern Tremp basin.

Thanetian: synsedimentary growth of the Montsec high; early uplift of the St. Mamet and Millà highs; partial fill of the Tremp and Ager basins with continental deposits; marine transgressions in the Ager area

MPU (Selandian?):prolonged lowstand; (inferred) early topographic expression of the Montsec high; breakup of the Vallcebre lacustrine basin

Danian; a large lacustrine basin borders the Pyrenees in their south-central and south-eastern portion

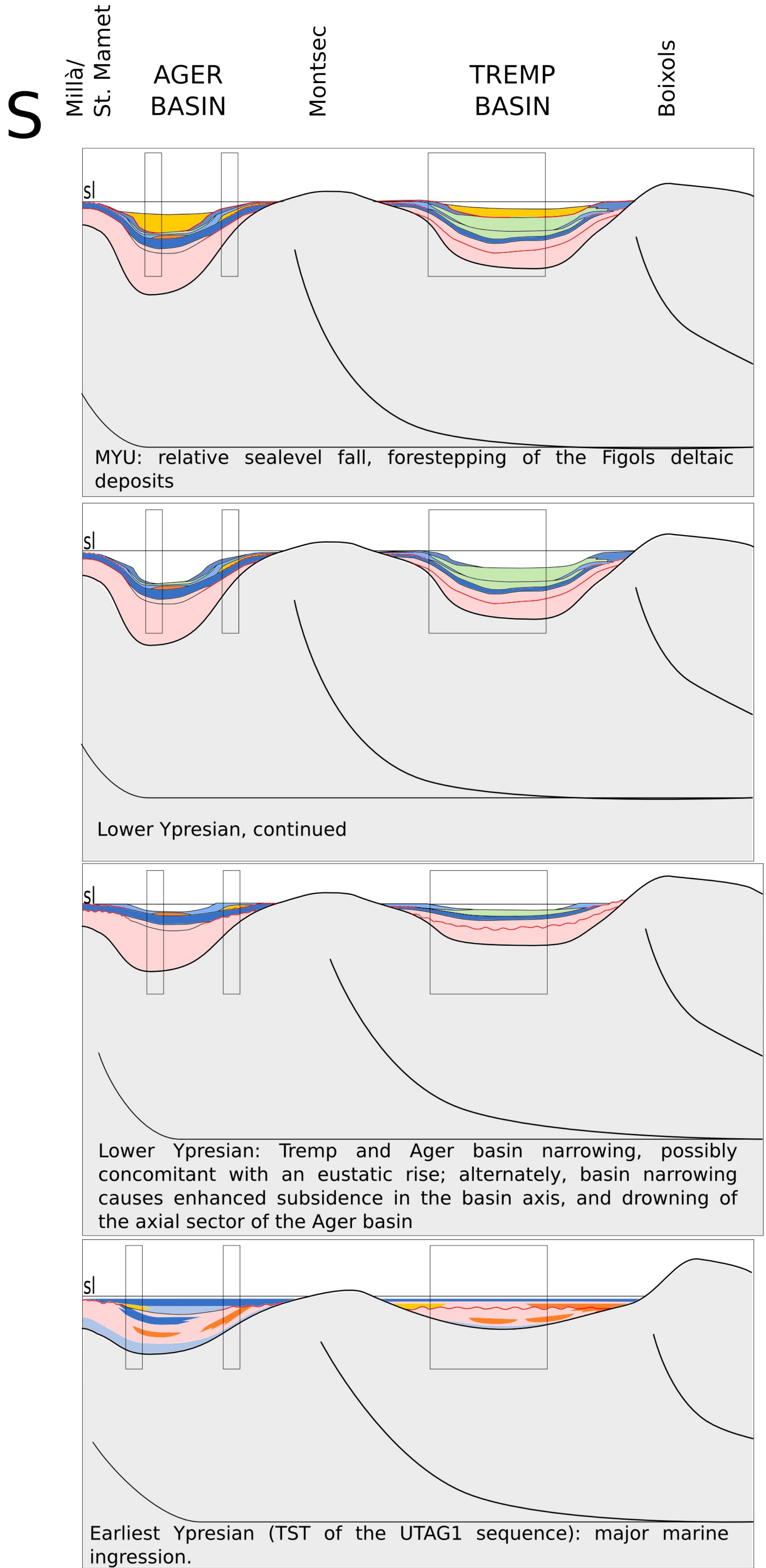

MYU: relative sealevel fall, forestepping of the Figols deltaic deposits

Lower Ypresian, continued

Lower Ypresian: Tremp and Ager basin narrowing, possibly concomitant with an eustatic rise; alternately, basin narrowing causes enhanced subsidence in the basin axis, and drowning of the axial sector of the Ager basin

Earliest Ypresian (TST of the UTAG1 sequence): major marine ingression.

7 - CONCLUSIONS

In the present work, the correlation between the Ager and Tremp basins was investigated during the early stages of development of the Paleo-Montsec, i.e., the strucutral high that divided these basins. The work involved both fieldwork and laboratory analyses.

Fieldwork consisted in the measurement and facies analysis of about 4000 m of stratigraphic logs, both reviewing formerly-measured sections and integrating new detailed data where needed. New detailed stratigraphic logs encompass the Paleocene and early Ypresian of the Ager basin (see Attached Document 1).

The objective of this field activity was the construction of a N-S transect across the Tremp ad Ager basins. A detailed reconstruction of the internal geometries of the marginal sector of the Tremp basin was also performed, in order to identify synsedimentary activity of the Montsec high and relate it with general subsidence patterns recorded in the whole basin.

In order to overcome some correlation problems, mainly related with the structural setting of the Ager basin, carbon and oxygen stable isotope analyses were performed, with the main purpose of using them as local and global correlation tools.

The main outcome of this activity was a preliminary isotopic characterization of the continental deposits of the Paleocene of the Ager basin, that allowed the location of the Paleocene/Eocene boundary as defined by current GSSPs, i.e., the onset of the Paleocene-Eocene Thermal Maximum. More specifically, this boundary turned out to be probably eroded by a clastic succession of Ypresian age. The occurrence of the PETM was also documented in the southern Tremp basin, although it was not possible to properly locate the P/E boundary.

These data helped in the realization of a correlation panel, where physical stratigraphic correlations are supported by both available and new chronostratigraphic data, that were reviewed and updated in the light of recent Early Paleogene age models.

The final result of this investigation was the proposal of a new descriptive model for the deformational stages occurred during the Paleocene and lower Ypresian along the Montsec thrust front.

ACKNOWLEDGEMENTS

I am deeply grateful to Emiliano Mutti, for having introduced me to the geology of the Southern Pyrenees , for having provided the financial support in the early period of my Ph.D, and, most of all, for his teachings in the field of sedimentary geology. Furthermore, I had the great opportunity to co-work for the Centro Universitario Studi sull'Appennino Settentrionale in Bobbio (PC, Italy), founded by E. Mutti, where I had access a great amount of scientific papers. The investigations performed by the former students of Professor Mutti were fundamental for understanding, and tentatively working out the problems of the Tremp-Ager correlation. The unpublished theses of Fonnesu (1984), Ghielmi (1991), Waehry (1999) and Angella (1999) are the most significant of these.

Many thanks to Stefano Angella, for having provided me his Ph.D. thesis and raw data.

I am also indebted to Marco Roveri and Roberto Tinterri, who encouraged, supported and helped me out in every possible way, both on the field and in the interpretation of data.

Many thanks to Giuliana Villa and Maria Sgavetti, for their help, support encouragement and suggestions.

Thanks to Davide Caré and Marco Fonnesu for their friendship, and help on the field in the study of the Baronia Sandstones.

Thanks to Antonio Longinelli, Paola Iacumin, Antonietta di Matteo, Enrico M. Selmo and at the Isotopic Geochemistry Laboratory (Università degli Studi di Parma, Earth Sciences Department), for having introduced me to the study of stable isotopes and for their precious suggestions in the interpretation of data. Also thanks to E.M. Selmo, A. di Matteo and E. Galli for their help in the preparation of samples; to A. di Matteo for having performed the analyses on organic matter.

Thanks to Rocco Gennari, for having introduced and helped me in the study of paleomagnetism; to Vinicio Manzi, for his suggestions concerning cyclostratigraphy and data exposition.

Many thanks to Ferran Colombo, for constructive comments on my research and precious suggestions. Also, thanks for having provided me some old publications on the Early Paleogene of the Southern Pyrenees.

Thanks to Luis Ardevol, Juan I. Baceta, Miguel L. Blanco, Poppe de Boer, and Victoriano Pujalte for their comments and suggestions.

Thanks to Simone Cau and Kei Ogata, for their friendship, help and encouragements, for all the time we shared together both on the field and in the office.

Thanks to the people of the Hostal del Doll at La Baronia de Sant Hoisme, for their hospitality, kindness and great kitchen during my stay in the Pyrenees.

Finally, no thank you is big enough for my family, my lover and my friends.
I owe everything to you.

This work was partially supported by research funds of PETROBRAS, S.A.

The Ph.D. Thesis was built using OpenOffice 3.3 for typewriting and diagrams; Inkscape 0.48 was used for graphics; Remasoft 3.0 for paleomagnetic analyses.

AGNINI, C., FORNACIARI, E., RAFFI, I., RIO, D., RÖHL, U., WESTERHOLD, T. (2007) - ***High-resolution nannofossil biochronology of middle Paleocene to early Eocene at ODP Site 1262: Implications for calcareous nannoplankton evolution***, Marine Micropaleontology, v. 64, pp. 215-248.

AIGNER, T. (1982) – ***Event-stratification in nummulite accumulations and in shell beds from the Eocene of Egypt***, in EINSELE, G., SEILACHER, A. (eds.), *Cyclic and event stratification*, Springer, 1982.

ALLAN, J.R. & MATTEWS, R.K. (1982) – ***Isotope signatures associated with early meteoric diagenesis***, Sedimentology, v. 29 (6), pp. 797-817.

ANGELLA, S. (1999) – ***Analisi stratigrafico-sedimentologica del Gruppo di Figols all'interno dei bacini di Ager e Tremp***, Ph.D. Thesis, Università degli Studi di Parma.

ARNI, P. (1965) – ***L'evolution des Nummulites en tant que facteur de modification des depots littoraux***, Mémoires du Bureau de Recherches Géologiques et Minières, 1965, SP. PUB. pp. 7-20.

AUBRY, M.P. (1996) – ***Towards an upper Paleocene-lower Eocene high resolution stratigraphy based on calcareous nannofossil stratigraphy***, Israel Journal of Earth Sciences, v. 44, pp. 239-253.

AUBRY, M.P., OUDA, K., DUPUIS, C., VAN COUVERING, J.A., ALI, J.R., BERGGREN, W.A., BRINKHUIS, H., GINGERICH, P.D., HEILMANN-CLAUSEN, C., HOOKER, J., KENT, D.V., KING, C., KNOX, R.W.o'B., LAGA, P., MOLINA, E., SCHMITZ, B., STEURBAUT, E., WARD, D.R. (2007) – ***The Global Standard Stratotype-section and Point (GSSP) for the base of the Eocene Series in the Dababiya section (Egypt)***, Episodes, v. 30 (4), pp. 271-286.

BACETA, J.I., PUJALTE, V., SERRA-KIEL, J., ROBADOR, A., ORUE-ETXEBARRIA, X. (2004) – ***El Maastrichtiense final, Paleoceno e Ilerdiense inferior de la Cordillera Pirenaica***, in VERA, J.A. (ed.), *Geologia de España*, Madrid, pp. 308-313.

BACETA, J.I., PUJALTE, V., WRIGHT, V.P., SCHMITZ, B. (2011) – ***Carbonate platform models, sea-level changes and extreme climatic events during the Paleocene/early Eocene greenhouse interval***, 28th IAS Meeting of Sedimentology, Zaragoza, pre-meeting field trip guidebook.

BARBERÀ, X., MARZO, M., REGUANT, S., SAMSÓ, J.M., SERRA-KIEL, J., TOSQUELLA, J. (1997) – ***Estratigrafia del Grupo Fígols (Paleógeno, cuenca de Graus-Tremp, NE de España)***, Revista de la Sociedad Geológica de España, v. 10 (1-2), pp., 67-81.

BETZLER, Ch., VAN DER HURK, A., EICHENSEER, H., LUTERBACHER, H.P. (1989) – ***Secuencias deposicionales del Paleógeno en la cuenca de antepaís surpirenaica (ríos Llobregat a Cinca)***, XXII Congreso Español de Sedimentología, Bilbao.

BERGGREN, W.A., KENT, D.V., SWISHER III, C.C., AUBRY, M.P. (1995) – ***A revised Cenozoic geochronology and chronostratigraphy***, in BERGGREN, W.A., et al. (eds.), *Geochronology, Time scales and Global Stratigraphic Correlation*, Tulsa, Society for Sedimentary Geology Sp. Publ., v. 54, pp. 129-212.

BERGGREN, W.A., MILLER, K.G. (1988) – ***Paleogene tropical planktonic foraminiferal***

biostratigraphy and magnetochronology, Micropaleonology, v. 34 (4), pp. 362-380.

BERGGREN, W.A., PEARSON, P.N. (2005) – ***A revised tropical and subtropical Paleogene planktonic foraminiferal zonation***, Journal of Foraminiferal Research, v. 35, pp. 279-298.

BILLI, A., VALLE, A., BRILLI, M., FACCENNA, C., FUNICIELLO, R. (2007) – ***Fracture-controlled fluid circulation and dissolutional weathering in sinkhole-prone carbonate rocks from central Italy***, Journal of Structural Geology, v. 29, pp. 385-395.

BOLLE, M.P., ADATTE, T., KELLER, G., VON SALIS, K., HUNZIKER, J. (1998) – ***Biostratigraphy, mineralogy and geochemistry of the Trabakua Pass and Ermua sections in Spain: Paleocene-Eocene transition***, Eclogae Geologicae Helvetiae, v. 91, pp. 1-25.

CALABRESE, L. (1999) – ***Stratigrafia fisica ed analisi di facies del Gruppo di Figols (Eocene, Pirenei centro-meridionali). Studio sulle relazioni tra sistemi carbonatici e silico-clastici***, Ph.D. Thesis, Università degli Studi di Parma.

CARMINATTI, M. (1991) – ***Stratigrafia fisica e modellizzazione sismica inversa del Gruppo di Figols affiorante tra la Val Isabena e la val Esera (Eocene inferiore, Pirenei centro-meridionali, Spagna)***, Ph.D. Thesis, Università degli Studi di Parma.

CAROZZA, D. (2009) – ***Carbon cycle box modeling studies of the Paleocene-Eocene thermal maximum***, M.Sc. Thesis, McGill University, Montreal.

CERLING, T.E. (1991) – ***Carbon dioxide in the atmosphere: evidence from Cenozoic and Mesozoic paleosols***, American Journal of Science, v. 291, pp. 377-400

CERLING, T.E. (1984) – ***The stable isotopic composition of modern soil carbonate and its relationship to climate***, Earth and Planetary Science Letters, v. 71, pp. 229-240.

CERLING, T.E., QUADE, J., WANG, Y., BOWMAN, J.R. (1989) – ***Carbon isotopes in soils and paleosols as ecology and paleoecology indicators***, Nature, v. 341, pp. 138-139.

COJAN, I., MOREAU, M.G., STOTT, L.E. (2000) – ***Stable isotope stratigraphy of the Paleogene pedogenic series of southern France as a basis for continental-marine correlation***, Geology, v. 28, pp. 259-262.

COLOMBO, F., & CUEVAS, J.L. (1993) - ***Características estratigráficas y sedimentológicas del "Garumniense" en el sector de Ager (Pre-Pirineo, Lleida)***, Acta Geologica Hispanica, v. 28 (4), pp. 15-32.

CRAMER, B.S., WRIGHT, J.D., KENT, D.V., AUBRY, M.P. (2003) – ***Orbital climate forcing of $\delta^{13}C$ excursions in the late-Paleocene-early Eocene (chrons C24n-C25n)***, Paleoceanography, v. 18 (4).

CROUCH, E.M., HEILMANN-CLAUSEN, C., BRINKHUIS, H., MORGANS, H.E.G., ROGERS, K.M., EGGER, H., SCHMITZ, B. (2001) – ***Global dinoflagellate event associated with the late Paleocene thermal maximum***, Geology, v. 29, pp. 315-318.

CUEVAS, J.L. (1992) – ***Estratigrafia del "Garumniense" de la Conca de Tremp. Prepirineo de***

Lleida, Acta Geologica Hispanica, v. 27, pp. 95-108.

DEEVLEESCHOWER, X., STORME, J.Y., CAMBIER, G., IACUMIN, P., BACETA, J.I., PUJALTE, V., YANS, J. (2011) – ***New insights on sea-level changes across the Paleocene-Eocene boundary from magnetic susceptibility and organic carbon isotope at Zumaia (Basque basin, Spain)***, 28th IAS Meeting of Sedimentology, Zaragoza.

DOMINGO, L., LÓPEZ-MARTÍNEZ, N., LENG, J., GRIMES, S.T. (2009) – ***The Paleocene-Eocene Thermal Maximum record in the organic matter of the Claret and Tendruy continental sections (South-Central Pyrenees, Lleida, Spain)***, Earth and Planetary Science Letters, v. 281, pp. 226-237.

EICHENSEER, H. (1988) – ***Facies geology of late Maastrichtian to early Eocene coastal and shallow marine sediments, Tremp-Graus basin, northeastern Spain***, Ph.D. Thesis, Tübingen University, 237 pp.

EICHENSEER, H., & KRAUSS, S. (1985) – ***The Tremp Formation (Maastrichtian/Paleogene) of the northern flank of the Tremp-Graus embayment (NE Spain)***, 6th European Regional Meeting of Sedimentology, IAS, Lleida.

EICHENSEER, H., & BETZLER, C. (1987) – ***Semiaride Gezeiten-und Strandseeablagerungen (Paläogen, Südpyrenäen)***, Heidelberger Geowissenschaften Abhandlungen, v. 8, pp. 58-59.

EICHENSEER, H., & LUTERBACHER, H.P. (1992) – ***The marine Paleogene of the Tremp region (NE Spain). Depositional sequences, facies history, biostratigraphy and controlling factors***, Facies, v. 27, pp. 119-152.

EMILIANI, C. (1954a) – ***Depth habitats of some species of pelagic foraminifera as indicated by oxygen isotope ratios***, American Journal of Science, v. 252, pp. 149-158.

EMILIANI, C. (1954b) – ***Temperature of Pacific bottom waters and polar superficial waters during the Tertiary***, Science, v. 119, pp. 853-855.

EMILIANI, C. (1966) – ***Isotopic paleotemperatures***, Science, v. 154, pp. 851-857.

FEIST, M., & COLOMBO, F. (1983) – ***La limite Crétace-Tertiaire dans le nord-est de l'Espagne du point de vue des charophytes***, Géologie Méditerraneenne, v. 10, pp. 303-325.

FERRER, J., LE CALVEZ, Y., LUTERBACHER, H., PREMOLI-SILVA, I. (1973) – ***Contribution à l'étude des foraminifères ilerdiens de la région de Tremp (Catalogne)***, Mémoires du Muséum National de Histoire Naturelle, Sciences de la Terre, v. 29.

FITZGERALD, P.G., MUÑOZ, J.A., CONEY, P.J., BALDWIN, S.L. (1999) – ***Asymmetric exhumation across the Pyrenean orogen: implications for the tectonic evolution of a collisional orogen***, Earth and Planetary Science Letters, v. 173, pp. 157-170.

FONNESU, F. (1984) – ***Estratigrafia fisica y analisis de facies de la Secuencia de Figols entre el Rio Noguera Pallaresa e Iscles (provs. De Lerida y Huesca)***, Ph.D. Thesis, Universidad Autonoma de Barcelona.

FONNESU, M. (2011) - ***Stratigrafia fisica e analisi di facies del Gruppo di Figols nella regione di Tremp (Eocene inf., Pirenei centro-meridionali)***, M.Sc. Thesis, Università degli Studi di Milano.

FOURNIE, D. (1975) – ***L'analyse sequentielle et la sedimentologie de l'Ypresien de Tunisie***, Bulletin du Centre de Récherche de Pau, SNPA, v. 1, pp. 27-75.

FREYTET, P., & PLAZIAT, J.C. (1982) – ***Continental carbonate sedimentation and pedogenesis. Late Cretaceous and Early Tertiary of Southern France***, Contributions to Sedimentology, v. 12, 217 pp.

GALBRUN, B., FEIST, M., COLOMBO, F., ROCCHIA, R., TAMBAREAU, Y. (1993) – ***Magnetostratigraphy and biostratigraphy of Cretaceous-Tertiary continental deposits, Ager basin, Province of Lerida, Spain***, Paleogeography, Paleoclimatology, Paleoecology, v. 102, pp. 41-52.

GARCÍA-VALLÉS, M., GONZÁLEZ-PRADO, J., VENDRELL SAZ M. (1993) – ***Caracterización de los lignitos garumnienses del Pirineo Central catalán***, Cuadernos de Geología Ibérica, v. 17, pp. 85-107.

GHIELMI, M. (1991) – ***La stratigrafia fisica del gruppo di Figols nella sinclinale di Ager (Spagna, Pirenei centro-meridionali)***, M.Sc. Thesis, Università degli Studi di Parma.

GIBSON, T.G., BYBELL, L.M., MASON, D.B. (2000) – ***Stratigraphic and climatic implications of clay mineral changes around the Paleocene/Eocene boundary of the northeastern US margin***, Sedimentary Geology, v. 134 (1-2), pp. 65-92.

GOLDSTEIN, R.H. (1991) – ***Stable isotope signatures associated with paleosols, Pennsylvanian Holder Formation, New Mexico***, Sedimentology, v. 38, pp. 67-77.

GRADSTEIN, F.M., COOPER, R.A., SADLER, P.M, HINNOV, L.A., SMITH, A.G., OGG, J.G., VILLENEUVE, M., MCARTHUR, J.M., HOWARTH, R.J., AGTERBERG, F.P., ROBB, L.J., KNOLL, A.H., PLUMB, K.A, SHIELDS, G.A., STRAUSS, H., VEIZER, J., BLEEKER, W., SHERGOLD, J.H., MELCHIN, M.J., HOUSE, M.R., DAVYDOV, V., WARDLAW, B.R., LUTERBACHER, H.P, ALI, J.R., BRINKHUIS, H., HOOKER, J.J., MONECHI, S., POWELL, J., RÖHL, U., SANFILIPPO, A., SCHMITZ, B., LOURENS, L., HILGEN, F., SHACKLETON, N.J., LASKAR, J., WILSON, D., GIBBARD, P. AND VAN KOLFSCHOTEN, T. (2004) - ***A Geological Time Scale 2004***, Cambridge University Press, Cambridge, 589 pp.

GUIDO, A., PAPAZZONI, C., MASTANDREA, A., MORSILLI, M., LA RUSSA, M.F., TOSTI, F., RUSSO, F. (2011) – ***Automicrite in a 'nummulite bank' from the Monte Saraceno (Southern Italy): evidence for synsedimentary cmentation***, Sedimentology, v. 58 (4), pp. 878-889.

HAQ, B.U., HARDENBOL, J., VAIL, P.R. (1987) – ***Chronology of fluctuating sea level since the Triassic***, Science, v. 235, pp. 1156-1167.

HILGEN F.J., KUIPER, K.F., LOURENS, L.J. (2010) – ***Evaluation of the astronomical time scale for the Paleocene and the earliest Eocene***, Earth and Planetary Science Letters, v. 300, pp. 139-151.

VON HILLEBRANDT, A. (1965) – ***Foraminiferen-Stratigraphie im Alttertiar von Zumaya (prov. Guipuzcoa, NW Spanien) und ein Vergleich mit anderen Tethys-Gebieten***, Bayerische Akademie der Wissenschaften, Matematisch-Naturwissenschaftliche Klasse Abhandlungen, v. 123, pp. 1-62.

VON HILLEBRANDT, A. (1975) – ***Corrélation entre les biozones de grands foraminifères et de foraminifères planctoniques de l'Ilerdien***, Bulletin de la Societé Géologique de France, Série 7, v. 17, pp. 162-167.

HONTZSCH, S., SCHEIBNER, C., GUASTI, E., KUSS, J., MARZOUK, A.M., RASSER, M.W. (2011) – ***Increasing restriction of the Egyptian shelf during the Early Eocene? - New insights from a southern Tethyan carbonate platform***, Paleogeography, Paleoclimatology, Paleoecology, v. 302, pp. 349-366.

HOTTINGER, L. (1960) – ***Recherches sur les Alvéolines du Paléocène et de l'Eocène***, Schveizerische Paläontologische Abhandlungen, v. 75-76, p. 243

HOTTINGER, L. & SCHAUB, H. (1960) – ***Zur Stufeneinteinlung des Paleocaens und Eocaens***, Eclogae Geologicae Helvetiae, v. 53, pp. 454-479.

IMMENHAUSER, A., KENTER, J.A.M., GANSSEN, G., BAHAMONDE, J.R., VAN VLIET, A., SAHER, M.H. (2002) – ***Origin and significance of isotope shifts in Pennsylvanian carbonates (Asturias, NW Spain)***, Journal of Sedimentary Research, v. 72 (1), pp. 82-94.

KAPELLOS, C. & SCHAUB, H. (1973) – ***Zur Korrelation von Biozonierungen mit Grossforaminiferen und Nannoplankton im Paläogen der Pyrenäen***, Eclogae Geologicae Helvetiae, v. 66, pp. 687-737.

KATZ, M.E., PAK, D.K., DICKENS., G.R., MILLER, K.G. (1999) – ***The Source and Fate of Massive Carbon Input During the Latest Paleocene Thermal Maximum***, Science, v. 286, pp. 1531-1533.

KELLY, D.C., BRALOWER, T.J., ZACHOS, J.C., PREMOLI SILVA, I., THOMAS, E. (1996) – ***Rapid diversification of planktonic foraminifera to the late Paleocene thermal maximum***, Geology, v. 24, pp. 423-426.

KENNETT, J.P. & STOTT, L.D. (1991) – ***Abrupt deep-sea warming, palaeoceanographic changes and benthic extinctions at the end of the Palaeocene***, Nature, v. 353, pp. 225-229.

KNOX, R.W.O (1998) – ***Kaolinite influx within Paleocene-Eocene boundary strata of western Europe***, Newsletters on Stratigraphy, v. 36, pp. 49-53.

KOCH, P.L., ZACHOS, J.C., DETTMAN, D.L. (1995) – ***Coupled isotopic change in marine and continental carbon reservoirs at the Palaeocene-Eocene boundary***, Nature, v. 358, pp. 319-322.

KRAUS, M.J., RIGGINS, S. (2007) – ***Transient drying during the Paleocene-Eocene Thermal Maximum (PETM): Analysis of paleosols in the Bighorn basin, Wyoming***, Paleogeography, Paleoclimatology, Paleoecology, v. 245, pp. 444-461.

LASKAR, J. (1989) – ***A numerical experiment on the chaotic behavior of the solar system***, Nature, v. 338, pp. 237-238.

LASKAR, J., ROBUTEL, P., JOUTEL, F., GASTINEAU, M., CORREIA, A.C.M., LEVRARD, B. (2004) – ***A long-term numerical solution for the insolation quantities of the Earth***, Astronomy & Astrophysics, v. 428, pp. 261-285.

LASKAR, J., FIENGA, A., GASTINEAU, M., MANCHE, H. (2011) – ***La2010: A new orbital solution for the long term motion of the Earth***, Astronomy & Astrophysics, v. 532 (A89), pp. 1-15.

LIEBAU, A., 1973 – ***El Maastrichtiense lagunar (Garumniense) de Isona***, XXIII Coloquio Europeo de Micropaleontologia, Madrid, pp. 87-112.

LÓPEZ-MARTÍNEZ, N., ARDÉVOL, L., ARRIBAS-MOCOROA, M.E., CIVIS, J., GONZÁLEZ-DELGADO, J.A. (1996) – ***Transición Cretácico/Terciario en depósitos continentales de la cuence de Tremp-Graus: datos preliminares de isótopos estables de C y O***, Geogaceta, v. 20 (1), pp. 62-65.

LOURENS, L.J., SLUIJS, A., KROON, D., ZACHOS, J.C., THOMAS, E., RÖHL, U., BOWLES, J., RAFFI, I. (2005) – ***Astronomical pacing of late Palaeocene to early Eocene global warming events***, Nature, v. 435, pp. 1083-1087.

LOVELL, B. (2010) – ***A pulse in the planet: regional control of high-frequency changes in relative sea level by mantle convection*** – Journal of the Geological Society, v. 167, pp. 637-648.

LU, G., KELLER, G., PARDO, A. (1998) – ***Stability and change in Tethyan plakntic foraminifera across the Paleocene-Eocene transition***, Marine Micropaleontology, v. 35 (3-4), pp. 203-233.

LUTERBACHER, H.P. (1970) – ***Environmental distribution of early Tertiary microfossils, Tremp basin, Northeastern Spain***, Exxon P&R, EPR-E-1ER-70, 48 pp.

LUTERBACHER, H.P. (1969) – ***Remarques sur la position stratigraphique de la formation d'Ager (Pyrenées Méridionales)***, Bulletin du Bureau de Recherches Géologiques et Minières, v. 69, pp. 225-232.

LUTERBACHER, H.P. (1973) – ***La sección tipo del piso Ilerdiense***, XXIII Coloquio Europeo de Micropaleontologia, Madrid, pp. 113-140.

Luterbacher, H.P., EICHENSEER, H., BETZLER, C., VAN DEN HURK, A.M. (1991) – ***Carbonate-siliciclastic depositional systems in the Paleogene of the South-Pyrenean foreland basin: a sequence-stratigraphic approach***, IAS Special Publication v. 12, pp. 391-407.

LUTERBACHER, H.P. (1998) – ***Sequence stratigRaphy and the limitations of biostratigraphy in the marine Paleogene strata of the Tremp basin (central part of the southern Pyrenean foreland basin, Spain)***, in DE GRACIANSKY, P.C., HARDENBOL, J., JACQUIN, T., VAIL, P., *Mesozoic and Cenozoic Sequence Stratigraphy of European Basins*, Society for Sedimentary Geology Special Publication, v. 60, pp. 303-309.

MACHLUS, M., HEMMING, S.R., OLSEN, P.E., CHRISTIE-BLICK, N.,(2004) ***- Eocene calibration of geomagnetic polarity time scale reevaluated: Evidence from the Green River Formation of Wyoming,*** *Geology*, v. 32, pp.137-140.

MAGIONCALDA, R., DUPUIS, C., SMITH, T., STEURBAUT, E., GINGERICH, P.D.,(2004) - ***Paleocene-Eocene carbon isotope excursion in organic carbon and pedogenic carbonate: Direct comparison in a continental stratigraphic section,*** *Geology*, v. 32, pp.553-556.

MARTINI, E.,(1971) - ***Standard Tertiary and Quaternary calcareous nannoplankton zonation***, in: FARINACCI, A., (Eds.), Proceedings of the II Planktonic Conference 2, Roma, pp. 739–785.

MECKEL, L.D. (1975) – ***Holocene sand bodies in the Colorado delta area, northern Gulf of California***, in BROUSSARD, M.L. (ed.), *Deltas, models for exploration*, Houston Geological Society, pp. 239-265.

MEIGS, A.J. & BURBANK, D.W., (1997) ***– Growth of the South Pyrenean orogenic wedge***, Tectonics, v. 16 (2), pp. 239-258.

MILANKOVITCH, M. (1941) – ***Kanon der Erdbestahlung und seine Anvendung auf das Eiszeitenproblem***, Akademie Royale Serbe, v. 133, 633p.

MILLIMAN, J.D. & SYVITSKI, J.P.M., (1992) – ***Geomorphic and tectonic control of sediment discharges to the ocean: the importance of small mountainous rivers,*** Journal of Geology v. 100, pp. 525-544.

MINELLI, N., MANZI, V., ROVERI, M., TINTERRI, R. - ***Tectonic and climate signatures on lower Eocene deposits of the Tremp-Ager basin (Pyrenees, Northeastern Spain)***, 28th IAS Meeting of Sedimentology, Zaragoza.

MOLINA, E., ANGORI, E., ARENILLAS, I., BRINKHUIS, H., M. CROUCH, E., LUTER-BACHER, H., MONECHI, S., SCHMITZ, B., (2003) - ***Correlation between the Paleocene/Eocene boundary and the Ilerdian at Campo, Spain,*** Revue de micropaléontologie, v. 46 , pp. 95–109.

MORLEY, C. (1994) – ***Tectonic overview of the South-Central Pyrenees***, in MUTTI, E., DAVOLI, G.,MORA, S., SGAVETTI, M., Eds – *The Estern Sector of The South-Central Folded Pyrenean Foreland:Criteria for Stratigraphic Analysis and Excursion Notes***,** Second High Resolution Sequence Stratigraphy Conference, 20-26 June, Tremp, Catalunya, Spain, Special Publication of the University of Parma, pp. 55-65.

MULDER, T. & SYVITSKI, J.P. (1995) – ***Turbidity currents generated at river mouths during exceptional dicharges to the world oceans***, Journal of Geology, v. 103 – pp. 285-299.

MUÑOZ, J. A., (2002) **- *The Pyrenees***, *In*: GIBBONS, W. & MORENO, M.T. (eds.) The Geology of Spain. Geological Society, London, pp. 370-385.

MUÑOZ, J. A., MARTINEZ, A., VERGÉS, J. (1986) – ***Thrust sequences in the Spanish eastern Pyrenees***, Journal of Structural Geology, v. 8, pp. 399-405.

MUTTI, E., (1992) – ***Relazioni tra stratigrafia sequenziale e tettonica,*** Mem. Soc. Geol. It. v. 45, pp. 627-655.

MUTTI, E. (1989) – ***Alcuni problemi relativi all'applicazione dei concetti della stratigrafia sequenziale all'Eocene ed al Cretacico superiore Sud-Pirenaici***, Notiziario del Gruppo Informale di Sedimentologia C.N.R.; Giornale di Geologia, v. 51 (4), pp. 55-59.

MUTTI, E., SGAVETTI, M. (1987) – ***Sequence stratigraphy of the Upper Cretaceous Aren strata in the Orcau-Aren region, South-central Pyrenees, Spain: distintion between eustatically and tectonically controlled depositional sequences***, Annali dell'Università Statale di Ferrara, Sezione di Scienze della Terra, v. 1, (1) pp. 1-22.

MUTTI, E., LUTERBACHER, H.P., FERRER, J., ROSELL, J. (1972) – ***Schema stratigrafico e lineamenti di facies del Paleogene marino della Zona Centrale Sud-Pirenaica tra Tremp (Catalogna) e Pamplona (Navarra),*** Memorie della Società Geologica Italiana, v. 11, pp. 391-416.

MUTTI, E., OBRADOR, A., ROSELL, J., (1973) – ***Sedimenti deltizi di piana di marea nel Paleogene della valle di Ager (provincia di Lerida, Spagna),*** Bollettino della Società Geologica Italiana, v. 92, pp. 517-528.

MUTTI, E., ROSELL, J., ALLEN, G.P., FONNESU, F., SGAVETTI, M., (1985) – ***The Eocene Baronia tide-dominated delta-shelf system in the Ager Basin,*** in MILA, M.D. & ROSELL, J., eds., Excursion Guidebook: VI Eur. Reg. Mtg. I.A.S. , Lerida, Spain, Excursion 13, pp. 579-600.

MUTTI, E., SEGURET, M., SGAVETTI, M. (1988) – ***Sedimentation and Deformation in the Tertiary Sequence of the Pyrenees,*** A.A.P.G. Mediterranean Basin Conference, Spec. Publ. University of Parma, Field Trip, 7, pp. 153.

MUTTI, E., DAVOLI, G.,MORA, S., SGAVETTI, M., (1994) – ***The Eastern Sector of The South-Central Folded Pyrenean Foreland: Criteria for Stratigraphic Analysis and Excursion Notes,*** Second High Resolution Sequence Stratigraphy Conference, 20-26 June, Tremp, Catalunia, Spain, Spec. Publ. University of Parma.

MUTTI, E., DAVOLI, G., FIGONI, M., SGAVETTI, M., (1994a) – **Conceptual Stratigraphic Framework,** in MUTTI, E., DAVOLI, G.,MORA, S., SGAVETTI, M., Eds., *The Eastern Sector of The South-Central Folded Pyrenean Foreland: Criteria for Stratigraphic Analysis and Excursion Notes,* Second High Resolution Sequence Stratigraphy Conference, 20-26 June, Tremp, Catalunia, Spain, Spec. Publ. University of Parma, pp. 8-15.

MUTTI, E. & SGAVETTI, M. (1994b) – ***Main stratigraphic units of the upper Cretaceous and Paleogene strata of the eastern sector of the South-Central Pyrenees***, in MUTTI, E., DAVOLI, G.,MORA, S., SGAVETTI, M., Eds., *The Eastern Sector of The South-Central Folded Pyrenean Foreland: Criteria for Stratigraphic Analysis and Excursion Notes,* Second High Resolution Sequence Stratigraphy Conference, 20-26 June, Tremp, Catalunia, Spain, Spec. Publ. University of Parma, pp. 16-24.

MUTTI, E., SGAVETTI, M., WAEHRY, W., CARMINATTI, M., DAVOLI, G., GHIELMI, M., FIGONI, M., MORA, S. (1994c) – ***Regional stratigraphy and sequence-stratigraphic aspects of the Figols Group***, in MUTTI, E., DAVOLI, G.,MORA, S., SGAVETTI, M., Eds., *The Eastern Sector of The South-Central Folded Pyrenean Foreland: Criteria for Stratigraphic Analysis and Excursion Notes,* Second High Resolution Sequence Stratigraphy Conference, 20-

26 June, Tremp, Catalunia, Spain, Spec. Publ. University of Parma, pp. 37-41.

MUTTI, E., DAVOLI, G., TINTERRI, R., ZAVALA, C., (1996) – ***The importance of ancient fluvio-deltaic systems dominated by catastrophic flooding in tectonically active basins***, Memorie di Scienze Geologiche, v. 48, pp. 232-291.

MUTTI, E., TINTERRI, R., DI BIASE, D., FAVA, L., MAVILLA, N., ANGELLA, S.,CALABRESE, L., (2000) – ***Delta front-facies associations of ancient flood dominated fluvio-deltaic systems,*** Rev. Soc. Geol. España, 13 (2), pp. 165-190.

MUTTI, E., TINTERRI, R., BENEVELLI, G., DI BIASE, D., CAVANNA, G. (2003) – ***Deltaic, mixed and turbidite sedimentation of ancient foreland basins***, Marine and Petroleum Geology, v. 20, pp. 733-755

MUTTI, E., BERNOULLI, D., RICCI LUCCHI, F., TINTERRI, R. (2009) – ***Turbidites and turbidity currents from Alpine "flysch" to the exploration of continental margins***, Sedimentology, v. 56, pp. 267-318.

NUMMEDAL, D. (2001) – ***Falling-stage systems tract in Siliciclastic Systems and its control on Reservoir Architecture and exploration strategies***, AAPG 2001-2002 Distinguished Lecture.

OKADA, H., BUKRY, D. (1980) – ***Supplementary modification and introduction of code numbers to the low-latitude coccolith biostratigraphic zonation (Bukry, 1973; 1975)***, Marine Micropaleontology, v. 5, pp. 321-325.

OMS, O., DINARÈS-TURELL, J., VICENS, E., ESTRADA, R., VILA, B., GALOBART, À., BRAVO, A.M.,(2007) - ***Integrated stratigraphy from the Vallcebre Basin (southeastern Pyrenees, Spain): New insights on the continental Cretaceous-Tertiary transition in southwest Europe,*** Palaeogeography, Palaeoclimatology, Palaeoecology, v. 255, pp. 35–47.

ORUE-ETXEBARRIA, X., PUJALTE, V., BERNAOLA, G., APELLANIZ, E., BACETA, J.I., PAYROS, A., NŒNEZ-BETELU, K., SERRA-KIEL, J.,TOSQUELLA, J. (2001) – D***id the Late Paleocene thermal maximum affect the evolution of larger foraminifers? Evidence from calcareous plakton of the Campo Section (Pyrenees, Spain),*** Marine Micropaleontology, v. 41, pp. 45-71.

PÄLIKE, H., NORRIS, R.D., HERRLE, J.O., WILSON, P.A., COXALL, H.K., LEAR, C.H., SHACKLETON, N.J., TRIPATI, A.K., WADE, B.S., (2006) – ***The heartbeat of the Oligocene climate system***, Science, v. 314, pp. 1894–1898.

PASCUAL, J.O., PARÈS. J.M., LANGEREIS, C.G., ZIJDERVELD, J.D.A., (1992) – ***Magneto-stratigraphy and rock magnetism of the Ilerdian stratotype at Tremp, Spain,*** Earth and Planetary Interiors, v. 74, pp.139-157.

PAYROS, A., PUJALTE, V., BACETA, J.I., BERNAOLA, G., ORUE-ETXEBARRIA, X., APELLANIZ, E., CABALLERO, F., FERRANDEZ, C. (2000) – ***Lithostratigraphy and sequence stratigraphy of the upper Thanetian to middle Ilerdian strata of the Campo section (Southern Pyrenees, Spain): revision and new data***, Revista de la Sociedad Geológica de España, v. 13 (2), pp. 213-226.

PLAZIAT, J.C., PERRIN, C. (1992) – ***Multikilometer-sized reefs built by foraminifera***

(Solenomeris) from the early Eocene of the Pyrenean domain (S. France, N. Spain): Paleoecologic relations with coral reefs, Palaeogeography, Palaeoclimatology, Palaeoecology, v. 96, pp. 195-231.

PUIGDEFABREGAS, C. & SOUQUET, P. (1986) – ***Tectono-sedimentary cycles and depositional sequences of the Mesozoic and Tertiary from the Pyrenees***, Tectonophysics, v. 129, pp. 173-203.

PUIGDEFABREGAS, C., MUÑOZ, J.A., MARZO, M. (1986) – ***Thrust belt develoment in the eastern Pyrenees and related depositional sequences in the southern foreland***, in ALLEN, P.A., HOMEWOOD, P., Eds, *Foreland basins*, I.A.S. Special Publication v. 8, pp. 229-246.

PUJALTE, V. & SCHMITZ, B. (2005) – ***Revisión de la estratigrafía del Grupo Tremp (Garumniense, Cuenca de Tremp-Graus, Pirineos meridionales)***, Geogaceta, v. 38, pp. 79-82.

PUJALTE, V., DINARÈS-TURELL, J., BERNAOLA, G., BACETA, J.I., PAYROS, A. (2003) – ***A reappraisal of Chron C25n in the Campo section (Huesca province, south-central Pyrenees)***, Geogaceta, v. 34, pp. 155-158.

PUJALTE, V., SCHMITZ, B., BACETA, J.I., ORUE-ETXEBARRIA, X., BERNAOLA, G., DINARÈS-TURELL, J., PAYROS, A., APELLANIZ, E., CABALLERO, F (2009a) – ***Correlation of the Thanetian-Ilerdian turnover of larger foraminifera and the Paleocene-Eocene thermal maximum: confirming evidence from the Campo area (Pyrenees, Spain)***, Geologica Acta, v. 7 (1-2), pp. 161-175.

PUJALTE, V., BACETA, J.I., SCHMITZ, B., ORUE-ETXEBARRIA, X., PAYROS, A., BERNAOLA, G., APELLANIZ, E., CABALLERO, F., ROBADOR, A., SERRA-KIEL, J., TOSQUELLA, J. (2009b) – ***Redefinition of the Ilerdian stage (early Eocene)***, Geologica Acta, v. 7 (1-2), pp. 177-194.

PUJALTE, V., ROBADOR, A., PAYROS, A., SAMSÓ, J.M. (2011) – ***Sedimentological impact of the Paleocene-Eocene thermal maximum, as recorded by the development of a supply-dominated delta system in the Ordesa-Monte Perdido National Park (Pyrenees, Spain)***, 28th IAS Meeting of Sedimentology, Zaragoza.

RACEY, A. (2001) – ***A review of Eocene Nummulite accumulations: structure, formation and reservoir potential***, Journal of Petroleum Geology, v. 24 (1) pp. 79-100.

RIBA, O. (1976) – ***Syntectonic unconformities of the Alto Caderner, Spanish Pyrenees: a genetic interpretation***, Sedimentary Geology, v. 15, pp. 213-233.

RÖHL, U., BRALOWER, T.J., NORRIS, R.D., WEFER, G. (2000) – ***New chronology for the late Paleocene thermal maximum and its environmental implications***, Geology, v. 28, pp. 927-930.

ROSELL, J., 1965 – ***Estudio geológico del sector del Prepirineo cmprendido entre los ríos Segre y Noguera Ribagorzana (pr. Lérida)***, Pirineos, v. 21 (75-78), pp. 9-214.

ROSELL, J., LINARES, R., LLOMPART, C. (2001) – ***El "Garumniense" Prepirenaico***, Revista de la Sociedad Geológica de España, v. 14 (1-2), pp. 47-56.

DE ROSSA, R. & ZUFFA, G.G. (1977) – ***Le areniti ibride della valle di Ager (Eocene, Pirenei centro-meridionali)***, Mineralogica et Petrographica Acta, v. 23, pp. 1-12.

ROSSI, C. (1997) – ***Microcodium y trazas fósiles de invertebrados en facies continentales (Paleoceno de la cuenca de Ager, Lérida)***, Revista de la Sociedad Geológica de España, v. 10 (3-4), pp. 371-391.

RUBINO, J.L., LEO, M., FONNESU, F. (1985) – ***Detailed stratigraphy of a tidal bar complex in the Eocene Baronia Sandstone, Ager Basin, South-Central Pyrenees***, Abstracts Int. Assoc. Sedimentol., 6th European Regional Meeting, pp. 657-660, Lerida.

SCHLAGER, W. (2005) – ***Carbonate sedimentology and sequence stratigraphy***, SEPM Concepts in Sedimentology and Paleontology, v. 8, 200 pp.

SCHMITZ, B., PUJALTE, V., NÚÑEZ-BETELU, K. (2001) – ***Climate and sea-level perturbationsduring the Initial Eocene Thermal Maximum: evidence from siliciclastic units in the Basque basin (Ermua, Zumaia and Trabakua Pass), northern Spain***, Palaeogeography, Palaeoclimatology, Palaeoecology, v. 165, pp. 299-320.

SCHMITZ, B. & PUJALTE, V. (2003) – ***Sea-level, humidity and land-erosion records across the initial Eocene thermal maximum from a continental-marine transect in northern Spain***, Geology, v. 31, pp. 689-692.

SCHMITZ, B. & PUJALTE, V. (2003) – ***Abrupt increase in seasonal extreme precipitation at the Paleocene-Eocene boundary***, Geology, v. 35, pp. 215-218.

SELMO, E.M. (1993) – ***Processi di dolomitizzazione nelle serie mesozoiche del veneto e trentino occidentali alla luce di uno studio geochimico-isotopico***, M.Sc. Thesis, Università degli Studi di Trieste.

SERRA-KIEL, J., CANUDO, J.I., DINARES, J., MOLINA, E., ORTIZ, N., PASCUAL., J.O., SAMSO, J.M., TOSQUELLA, J. (1994) – ***Cronoestratigrafía de los sedimentos marinos del Terciario inferior de la Cuenca de Graus-Tremp (Zona Central Surpirenaica)***, Revista de la Sociedad Geológica de España, v 7 (3-4), pp. 273-297.

SERRA-KIEL, J., HOTTINGER, L., CAUS, E., DROBNE, KATICA., FERRANDEZ, C., KUMAR JAUHRI, A., LESS, G., PAVLOVEC, R., PIGNATTI, J., SAMSÓ, J.M., J.M.,SCHAUB, H., SIREL, E., STROUGO, A., TAMBAREAU, Y., TOSQUELLA., J., ZAKREVSKAYA., E. (1998) – ***Larger foraminiferal biostratigraphy of the Tethyan Paleocene and Eocene***, Bulletin de la Societé Géologique de France, v. 169 (2) pp. 281-299.

SHACKLETON, N.J. (1974) – ***Attainment of isotopic equilibrium between ocean water and the benthonic foraminifera genus Uvigerina: isotopic changes in the ocean during the last glacial***, Colloques Internationaux du Centre National du Recherche Scientifique, v. 219, pp. 203-210.

SIBUET, J.C., SRIVASTAVA, S.P., SPAKMAN, W. (2004) – ***Pyrenean orogeny and plate kinematics***, Journal of Geophysical Reseache, v. 109, pp. 1-18.

SIMÓ, A. (1986) – ***Carbonate platform depositional sequences, upper Cretaceous, South-central***

pyrenees, Tectonophysics, v. 129, pp. 205-231-

SMITH, M.E., CARROLL, A.R., MUELLER, E.R. (2008) – ***Synoptic reconstruction of a major ancient lake system: Eocene Green River Formation, western United States***, Bulletin on the Geological Society of America, v. 120, pp. 370-374.

SOLE-SUGRAÑES, L (1970) – ***Estudio geológicodel Pirineo entre los ríos Segre y Llobregat***, Ph.D. Thesis, University of Barcelona.

THIRY, M. & DUPUIS, M. (2000) – ***Use of clay minerals for paleoclimatic reconstrctions: Limits of the method with special reference to the Paleocene-lower Eocene interval***, GFF, v. 122, p. 166-167.

THOMAS, E (1998) – ***Biogeography of the late Paleocene benthic foraminferal extinction***, in AUBRY, M.P., LUCAS, S., BERGGREN, W.A., EDS, *Late Paleocene-early Eocene Climatic and Biotic events in the Marine and Terrestrial Records*, pp. 214-243.

TINTERRI, R. (2011) – ***Combined flow sedimentary structures and the genetic link between sigmoidal- and hummocky-cross stratification***, GeoActa, v. 10, pp. 43-85.

UREY, H.C. - ***Oxygen isotopes in Nature and in the Laboratory***, Science, v. 108, pp. 489-496.

VAIL, P.R., MITCHUM, R.M., TODD, R.G., WIDMER, J.M., THOMPSON, S.III, SANGREE, J.B., BUDD, J.N., HATLEID, W.G. (1977) – ***Seismic stratigraphy and global changes of sea-level***, in PAYTON, C.E., eds, *Seismic stratigraphy – Application to Hydrocarbon Exploration*, A.A.P.G. Memoir n.26, pp. 49-205.

VAIL, P.R., AUDEMARD, F., BOWMAN, S.A., EISNER, P.N., PEREZ-CRUZ, G. (1991) – ***The stratigraphic signatures of tectonics, eustasy and sedimentation***, in EINSELE, G., RICKEN, W., SEILACHER, A., *Cycles and events in stratigraphy*, Springer-Verlag, 617-659.

VERGÉS, J., FERNÀNDEZ, M., MARTÍNEZ, A. (2002) – ***The Pyrenean orogen: pre-, syn-, and post-collisional evolution***, in ROSENBAUM, G. & LISTER, G.,S., *Reconstruction of the evolution of the Alpine-Himalayan Orogen*, Journal of the Virtual Explorer, v. 8, pp. 55-74.

WADE, B.S., PEARSON, P.N., BERGGREN, W.A., PÄLIKE, H. (2011) – ***Review and revision of Cenozoic tropical planktonic foraminiferal biostratigraphy and calibration to the geomagnetic polarity and astronomical time scale***, Earth-Science Reviews, v. 104, pp. 111-142.

WAEHRY, A. (1999) - ***Facies analysis and physical stratigraphy of the Ilerdian in the eastern Tremp-Graus Basin (south-central Pyrenees, Spain)***. Terre et Environment, Inst. Forel, Département De Minéralogie, Département de Géologie et Paléontologie, Section des Sciences de la Terre, Université de Genève, 15, 191

VAN WAGONER, J.C., POSAMENTIER, R.M., MITCHUM, R.M., VAIL, P.R., SARG, J.F., LOUTIT, T.S., HARDENBOL, J. (1988) – ***An overview of the fundamentals of sequence stratigraphy and key definitions***, in WILGUS, C.K., POSAMENTIER, H., VAN WAGONER, J., ROSS, C.A., KENDALL, G.S.C., eds., *Sea Level Changes: an Integrated Approach*, SEPM Special Publication n.42.

VAN WAGONER, J.C., MITCHUM, R.D., CAMPION, K.M., RAHMANIAN, V.D. (1990) – ***Siliciclastics sequences stratigraphy in well logs, cores and outcrops: concepts for high-resolution correlation of time and facies***, A.A.P.G., Methods in Exploration Series, n. 7, 55 pp.

WESTERHOLD, T. & RÖHL, U. - ***High resolution cyclostratigraphy of the early Eocene – new insights into the origin of the Cenozoic cooling trend***, Climate of the Past, v. 5, pp. 309-327.

WESTERHOLD, T., RÖHL, U., LASKAR, J., BOWLES, J., RAFFI, I., LOURENS, L. J., AND ZACHOS, J. C. (2007) – ***On the duration of magnetochrons C24r and C25n and the timing of early Eocene global warming events: Implications from the Ocean Drilling Program Leg 208 Walvis Ridge depth transect***, Paleoceanography, v. 22, PA2201.

WESTERHOLD, T., RÖHL, U., RAFFI, I., FORNACIARI, E., MONECHI, S., REALE, V., BOWLES, J., AND EVANS, H.F. (2008) – ***Astronomical calibration of the Paleocene time***, Palaeogeography, Palaeoclimatology, Palaeoecology, v. 257, pp. 377–403

WESTERHOLD, T., RÖHL, U., McCARREN, H., ZACHOS, J. (2009) – ***Latest on the absolute age of the Paleocene-Eocene thermal maximum (PETM): New insights from exact stratigraphic position of key ash layers +19 and-17***, Earth and Planetary Science Letters, v. 287, pp. 412-419.

WILGUS, C.K., POSAMENTIER, H., VAN WAGONER, J., ROSS, C.A., KENDALL, G.S.C (1988) – ***Sea Level Changes: an Integrated Approach***, SEPM Special Publication n.42.

ZACHOS, J.C., PAGANI, M., SLOAN, L., THOMAS, E., BILLUPS, K. (2001) – ***Trends, rhythms and aberrations in global climate 65Ma to present***, Science, v. 292, pp. 686-693.

ZACHOS, J.C., WARA, M.W., BOHATY, S., DELANEY, M.L., PETRIZZO, M.R., BRILL, A., BRALOWER, T., PREMOLI-SILVA, I. (2003) – ***A transient rise in tropical sea-surface temperature during the Paleocene-Eocene thermal maximum***, Science, v. 302, pp. 1551-1554.

ZACHOS, J.C., Mc CARREN, H., MURPHY, B., RÖHL, U., WESTERHOLD, T. (2010) – ***Tempo and scale of late Paleocene and early Eocene carbon isotope cycles: implications for the origin of hyperthermals***, Earth and Planetary Science Letters, v. 299, pp. 242-249.

APPENDIX 1

MAGNETOSTRATIGRAPHY OF THE LOWER BARONIA SANDSTONE

Figure A1 shows the sampling locations from a few samples of mudstones and sandy mudstones in the range of the Lower Baronia Sandstones of the Ager basin. The sampling was limited because of the relatively coarse-grained nature of this succession. Moreover, the mudstones below this interval are almost everywhere covered by vegetation, and samples can be taken exclusively in the last few decimeters below the base of the sandstone unit. Another sampled location lies approximately in the middle of the Lower Baronia Sandstone. For these reasons this has to only be considered a preliminary, magnetostratigraphic investigation of the Ilerdian of the Ager basin.

Samples were collected with a portable drill, and sample orientation was measured with an inclinometer; then they were analyzed after thermal demagnetization at the Alpine Laboratory of Paleomagnetism (Peveragno, CN, Italy).

A 755-2G-Enterprises cryogenic magnetometer was used to measure the magnetic intensities and directions at each step of demagnetization.

Samples were heated in progressive steps of 20°-40°, reaching unblocking T between 300° and 350°C.

All of the measured samples displayed a normal polarity, with a declination falling in the range of 10°-20°. This orientation is consistent with the ones reported by Pascual et al. (1992) for the normal samples, attributed to chron C24n, in the Ilerdian of the Tremp basin.

These data confirm the correlation of the base of the Lower Baronia Sandstones with the base of the Serra Puit depositional system in Tremp basin, supporting the Ager-Tremp correlation of the base of the Figols Group as proposed by Mutti et al. (1994; compare with Mutti et al., 1988); moreover, it is also better constrained the condensed or hiatal interval represented by the UTAG b sequence in the Ager basin (see **2.5.3**)

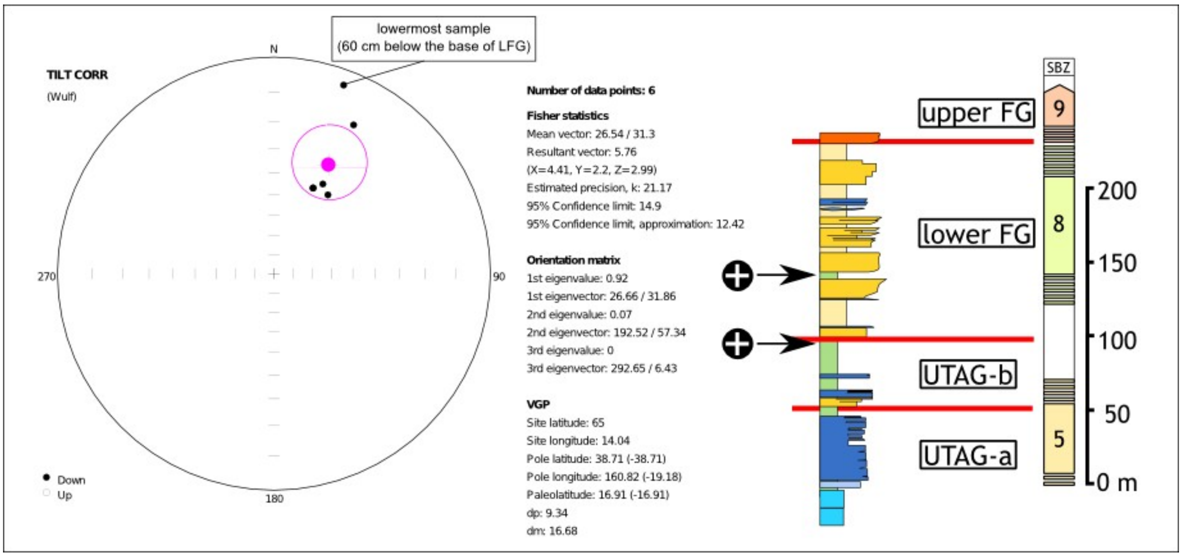
lowermost sample
(60 cm below the base of LFG)
TILT CORR
(Wulf)
N
270
90
180
Down
Up
Number of data points: 6
Fisher statistics
Mean vector: 26.54 / 31.3
Resultant vector: 5.76
(X=4.41, Y=2.2, Z=2.99)
Estimated precision, k: 21.17
95% Confidence limit: 14.9
95% Confidence limit, approximation: 12.42
Orientation matrix
1st eigenvalue: 0.92
1st eigenvector: 26.66 / 31.86
2nd eigenvalue: 0.07
2nd eigenvector: 192.52 / 57.34
3rd eigenvalue: 0
3rd eigenvector: 292.65 / 6.43
VGP
Site latitude: 65
Site longitude: 14.04
Pole latitude: 38.71 (-38.71)
Pole longitude: 160.82 (-19.18)
Paleolatitude: 16.91 (-16.91)
dp: 9.34
dm: 16.68
upper FG
lower FG
UTAG-b
UTAG-a
SBZ
9
8
5
200
150
100
50
0 m

APPENDIX 2: ISOTOPE FULL DATA SET

Section [4], CARBONATES

SAMPLE	SUB-SAMPLE	Locate	δ^{13}Ccarb	δ^{18}Ocarb	Notes
Asμ 1a	a	9,50	-10,095	-6,209	micrite
	b	9,50	-9,948	-6,287	micrite
Asμ 2a	a	16,00	-9,625	-5,654	micrite
	b	16,00	-9,724	-6,195	micrite
	c	16,00	-9,640	-5,878	micrite
Asμ 3a	a	18,00	-10,508	-6,205	micrite
	b	18,00	-9,860	-6,201	micrite
	c	18,00	-10,507	-6,216	micrite
ASG 12		85,73	-9,874	-4,918	pseudocong micrite
ASG 16	a	95,17	-9,974	-5,286	pseudocong micrite
	b	95,17	-9,350	-5,053	pseudocong micrite
ASG R03	a	293,27	-3,516	-6,049	micrire
	b	293,27	-3,423	-5,996	micrite
ASG R04	b	294,49	-4,171	-5,800	micrite
	a	294,50	-3,976	-5,714	micrite
	c	294,53	-3,928	-6,275	micrite
ASGT	a	294,55	-4,141	-6,297	micrite
	b	294,55	-4,162	-6,446	micrite
ASG R12	a	319,62	2,066	-2,817	calcarenite
	b	319,62	2,230	-2,813	calcarenite
ASG R14	a	324,04	0,413	-4,141	calcarenite
	b	324,04	0,204	-4,144	calcarenite
ASG R15	a	330,69	0,069	-4,313	calcarenite
	b	330,69	-0,070	-4,396	calcarenite
ASG R16	a	336,74	0,510	1,324	micrite
	c	336,78	0,820	1,205	micrite
	e	336,80	0,987	1,523	micrite
ASG R17	a	340,19	-0,459	-3,328	micrite
	b	340,20	-0,115	-2,323	micrite
ASG R19	a	350,01	-0,558	1,678	micrite
	b	350,01	-0,682	1,585	micrite
ASK	a	353,43	-11,725	-5,918	white micrite clast
	b	353,43	-11,942	-5,810	white micrite clast
	c	353,43	-12,594	-6,147	red\pink micrite clast
	d	353,43	-8,024	-6,193	red sandstone clast
ASX	a	353,43	-9,605	-6,021	carbonate sandstone clast
	b	353,43	-12,041	-5,889	white micrite clast
	c	353,43	-15,259	-5,794	yellow micrite clast
	d	353,43	-15,074	-5,947	yellow micrite clast
ASX 04	a	383,83	-7,276	-5,804	micrite
	b	383,83	-7,558	-5,595	micrite
	d	383,83	-7,108	-5,725	micrite
	c	383,84	-8,842	-5,284	micrite
ASX 05	a	390,80	-6,140	-4,943	micrite
	b	390,80	-7,081	-5,663	micrite
	c	390,80	-6,979	-5,823	micrite
	d	390,81	-6,983	-5,519	micrite
ASA 03	a	403,89	-5,694	-6,832	micrite
	b	403,89	-6,033	-5,873	micrite

Section [4], CARBONATES

SAMPLE	TAG (fig. 5.1)
Asμ 1a	Danian-Early Selandian; Vallcebre Formation, Southern Ager basin in Diagram 6
Asμ 2a	Danian-Early Selandian; Vallcebre Formation, Southern Ager basin in Diagram 6
Asμ 3a	Danian-Early Selandian; Vallcebre Formation, Southern Ager basin in Diagram 6
ASG 12	lower Thanetian
ASG 16	lower Thanetian
ASG R03	Upper Thanetian 1
ASG R04	Upper Thanetian 1
ASGT	Upper Thanetian 1
ASG R12	Upper Thanetian 3
ASG R14	Upper Thanetian 3
ASG R15	Upper Thanetian 3
ASG R16	Upper Thanetian 3
ASG R17	Upper Thanetian 3
ASG R19	Upper Thanetian 3
ASK	Th/Yp pebbles
ASX	Th/Yp pebbles
ASX 04	Early Ypresian 1
ASX 05	Early Ypresian 1
ASA 03	Early Ypresian 1

Section [4], SABKHA CARBONATES

SAMPLE	SUB-SAMPLE	Locate	δ^{13}Cmic	δ^{13}Cdol	δ^{18}Omic	δ^{13}Odol
ASG R08	a	306,63	0,556		-0,292	
	b	306,63	0,589	0,822	-0,365	0,576
ASG R10	b	313,94	1,001	1,206	0,744	2,404
ASAH 01	c	407,89	-1,409		-4,115	
	d	407,89	-0,493	0,691	-0,893	2,246
ASAH 02	b	408,50	0,000	0,570	0,296	2,228
	c	408,50	-2,646		-6,670	
	d	408,50	-0,301	0,427	-0,226	2,487
ASAH 03	b	409,03	-0,253	-1,063	-4,405	-2,858
	c	409,03	-0,253	-2,125	-4,405	-4,448
ASAH 04	a	412,15	-0,818		-1,169	
	b	412,15	0,008	-0,009	0,857	1,953
	c	412,15	-0,003	0,227	0,985	2,548

SAMPLE	SUB-SAMPLE	NOTES	TAG (fig. 5.1)
ASG R08	a	assoc with evaporites	Upper Thanetian 2
	b	assoc with evaporites	Upper Thanetian 2
ASG R10	b	assoc with evaporites	Upper Thanetian 2
ASAH 01	c	secondary calcite	Early Ypresian 2
	d	no evaporites	Early Ypresian 2
ASAH 02	b	no evaporites	Early Ypresian 2
	c	secondary calcite	Early Ypresian 2
	d	no evaporites	Early Ypresian 2
ASAH 03	b	no evaporites	Early Ypresian 2
	c	no evaporites	Early Ypresian 2
ASAH 04	a	no evaporites	Early Ypresian 2
	b	no evaporites	Early Ypresian 2
	c	no evaporites	Early Ypresian 2

Section [4], ORGANIC MATTER

DRP	dark red paleosol
LRP	light red paleosol
PiP	pink paleosol
PuP	purple paleosol
YP	yellow paleosol
BP	brown (-yellow) apleosol
GP	grey paleosol
GY	gypsum nodules
CSN	carbonate soil nodule

Samples	LOCATE	C% (1)	C% (2)	δ^{13}Ccarb (1)	δ^{13}Ccarb (2)	NOTES
ASG 01	42,19	0,1383	0,1363	-24,1117	-23,9433	YP
ASG 02	42,57	0,4102	0,4097	-26,3948	-26,6662	GP
ASG 03	44,62	0,0656	0,0662	-23,1489	-23,2896	DRP
ASG 04	57,99	0,0598	0,0602	-23,3698	-23,8750	DRP, GY
ASG 05	66,35	0,0723	0,0734	-23,2757	-22,9043	DRP, GY
ASG 06	74,84	0,1939	0,1953	-21,8910	-21,9296	YP
ASG 07	76,61	0,0618	0,0618	-23,6987	-23,5669	DRP
ASG 08	82,67	0,0444	0,0451	-25,4608	-26,2541	BP, GY
ASG 09	83,59	0,1199	0,1202	-24,9031	-25,1279	PuP
ASG 10	84,65	0,2471	0,2471	-24,2623	-24,1305	YP
ASG 11	85,25	0,3525	0,3495	-22,3367	-21,6642	PiP
ASG 13	86,12	0,1310	0,1290	-24,1226	-23,0905	PiP
ASG 14	91,41	0,1396	0,2152	-22,1456	-23,6858	YP
ASG 15	94,26	0,3346	0,3103	-22,2961	-21,3977	PiP
ASG 16	95,17	0,4705	0,4753	-19,8595	-20,2369	PiP
ASG 17	95,65	0,2003	0,2036	-22,5695	-22,4170	GP
ASG 18	102,19	0,1967	0,1932	-24,1642	-24,2692	BP
ASG 19	115,95	0,2980	0,2992	-24,5000	-24,1691	sandstone
ASG 20	121,87	0,1751	0,1761	-23,5402	-23,6640	YP
ASG 22	129,24	0,1068	0,1051	-23,9334	-23,8294	PiP
ASG 23	173,59	0,2515	0,2561	-24,3772	-24,2444	YP
ASG R01	286,48	0,1839	0,1853	-24,0582	-23,4015	YP
ASG R02	292,05	0,0734	0,0730	-18,8700	-22,0624	DRP
ASG R06	300,26	0,1697	0,1522	-24,4009	-25,8976	YP
ASG R07	303,4	0,1127	0,1053	-23,2559	-22,9845	DRP
ASG R09	312,73	0,1028	0,1010	-22,7963	-21,7216	GP

SECTION [12], "UNNAMED KARSTIFIED MICRITES, NORTHERN AGER BASIN" (in diagram 6)

SAMPLE	SUBS.	LOCATION	δ13Ccarb	δ18Ocarb	NOTES
Anµ	a	7,00	-9,364	-6,067	micrire matrix
	b	7,00	-9,091	-7,061	micrite clast
	c	7,00	-11,169	-8,596	secondary calcite
	d	7,00	-9,281	-9,281	micrire matrix
	e	7,00	-9,033	-9,033	micrite clast
	f	7,00	-9,245	-9,418	secondary calcite

SECTION [12], PALEOSOLS OM DATA AND CARBONATE SOIL NODULES DATA

SAMPLE	LOCATION	NOTES	δ13Ccarb	δ18Ocarb	OM – C% (1)	OM – C% (2)	δ13Corg (1)	δ13Corg (2)
ANG 01	47,28	DRP			0,0595	0,0617	-24,6643	-24,4512
ASG X01a	51,02	CSN, DRP	-8,344	-5,070	0,1100	0,0827	-23,8093	-22,8821
ASG X01b	51,02	CSN, DRP	-8,665	-5,304				
ASG X02a	51,50	CSN, LRP	-8,656	-5,170	0,1244	0,1337	-23,8949	-23,7741
ASG X02b	51,50	CSN, LRP	-8,589	-5,731	0,0883	0,0885	-23,4356	-23,3823
ANG 02	51,88	LRP						
ASG X03a	51,82	CSN, DRP	-7,919	-4,907				
ASG X03b	51,82	CSN, DRP	-8,082	-5,337				
ASG X04	52,13	DRP	-8,273	-5,062	0,0575	0,0602	-24,3057	-24,9372
ASG X05	52,65	YP			0,0626	0,0694	-24,7546	-25,1227
ANG 03	52,71	LRP			0,1132	0,1131	-24,2439	-24,5273
ASGX 06	53,03	YP			0,1566	0,1508	-23,4232	-23,5278
ASG X07	53,30	CSN, DRP	-8,484	-5,866	0,2012	0,2117	-22,9192	-23,3662
ASG X08	53,44	CSN, DRP	-6,297	-4,501	0,0715	0,0731	-23,6239	-23,6971
ASGX 09	53,61	DRP			0,0775	0,0795	-22,8412	-22,9515
ASG X10	53,93	CSN, DRP	-8,196	-5,562	0,0737	0,0724	-23,8217	-23,7951
ASG X11a	54,10	CSN, DRP	-7,067	-4,611	0,0871	0,0865	-24,1241	-23,7932
ASG X11b	54,10	CSN, DRP	-7,603	-5,037				
ANG 04	54,33	DRP			0,0739	0,0737	-23,3681	-23,1141
ASG X12a	54,55	CSN, DRP	-6,297	-4,329	0,0822	0,0782	-23,5792	-23,4451
ASG X12b	54,55	CSN, DRP	-6,692	-4,650				
ASG X13a	54,72	CSN, DRP	-7,491	-4,669	0,0779	0,0791	-23,2026	-23,1703
ASG X13b	54,72	CSN, DRP	-7,315	-4,693	0,0725	0,0709	-22,9201	-22,8212
ASG X14a	54,89	CSN, DRP	-7,857	-4,951				
ASG X14b	54,89	CSN, DRP	-7,673	-5,077	0,0864	0,0892	-23,0694	-23,7199
ASG X15a	55,07	CSN, DRP	-7,793	-4,837				
ASG X15b	55,07	CSN, DRP	-7,226	-4,877				
ASG X16a	55,24	CSN, DRP	-7,162	-5,340	0,0715	0,0687	-23,4004	-23,2188
ASG X16b	55,24	CSN, DRP	-7,767	-5,085				
ANG 05	56,75	DRP			0,0594	0,0605	-23,1902	-23,8388
ASG X17a	57,83	CSN, DRP	-7,499	-5,257	0,0694	0,0682	-22,7100	-22,9021
ASG X17b	57,83	CSN, DRP	-7,687	-4,887				
ASG X18a	58,04	CSN, DRP	-7,423	-4,726	0,0706	0,0704	-23,0495	-22,9344
ANG 06	59,04	LRP			0,0759	0,1061	-22,5293	-24,1079

SECTION [10], CARBONATES

SAMPLE	SUB-SAMPLE	Locate	δ^{13}Ccarb	δ^{18}Ocarb	Notes
MIL 01		62,70	2,839	-2,964	calcarenite
MIL 02		67,12	1,323	-2,757	micrite
MIL 03a	a	67,78	2,556	2,262	micrite
	b	67,78	2,555	2,084	micrite
MIL 04		79,16	-0,702	-5,065	calcarenite
MDB 02	c	80,54	1,828	1,476	micrite
	d	80,54	1,758	1,583	micrite
	a	80,59	1,879	1,264	micrite
	b	80,59	1,836	1,673	micrite
MDB 03	a	89,82	-0,872	-2,085	micrite
	b	89,82	-1,209	-2,941	Microcodium
	c	89,82	-1,026	-2,812	Microcodium
	d	89,82	-1,059	-2,755	micrite
MDB 04	a	91,10	-4,306	-4,321	micrite
	b	91,10	-3,951	-4,589	micrite
	c	91,10	-3,964	-4,198	micrite
	d	91,10	-4,020	-4,471	Microcodium
MDB 05	a	91,81	-2,537	0,721	micrite
	b	91,81	-3,759	-2,058	Microcodium
MDB 07		96,91	-8,069	-6,610	CSN
MDB 08		97,11	-8,186	-6,549	CSN
MDB 09		97,21	-8,229	-6,420	CSN
MDB 10		97,36	-7,651	-6,461	CSN

SECTION [23], "VALLCEBRE FORMATION, NORTHERN TREMP BASIN" (in diagram 6)

SAMPLE	SUB-SAM.	δ^{13}Ccarb	δ^{18}Ocarb
ESPμ	a	-10,111	-5,976
	b	-10,515	-5,740
	c	-10,185	-6,021

SECTION [14], CARBONATE SOIL NODULES

SAMPLE	Locate	$\delta^{13}C_{carb}$	$\delta^{18}O_{carb}$
CLL 01	9,086	-9,134	-5,685
CLL 02	9,249	-9,124	-5,625
CLL 03	9,491	-9,773	-5,940
CLL 04	9,630	-10,020	-5,970
CLL 05	9,803	-9,832	-6,018
CLL 06	11,464	-9,510	-6,045
CLL 07	11,978	-9,757	-5,829
CLL 08	12,140	-9,508	-5,961
CLL 09	72,804	-11,692	-5,972
CLL 10	72,977	-12,368	-5,869
CLUA 04	73,139	-12,447	-6,218
CLL 11	73,150	-13,251	-6,102
CLL 12	73,323	-12,680	-6,037
CLL 13	73,496	-12,848	-5,981
CLL 14	73,669	-14,097	-7,039
CLL 15	73,842	-13,057	-6,261
CLL 16	74,015	-13,953	-5,731
CLL 17	74,188	-13,151	-6,507

SECTION [16], MARINE CARBONATES

SAMPLE	SUB-SAMPLE	Locate	δ^{13}Ccarb	δ^{18}Ocarb	Notes
ALS EA 01	a	5,517	2,484	-3,997	alveolinae (CEMENTED)
	b	5,517	1,964	-3,932	matrix (sk)
ALS EA 02		8,224	2,454	-3,664	alveolinae (CEMENTED)
ALS EA 03	a	11,642	2,565	-4,755	joint secondary calcite
	b	11,642	2,471	-7,399	alveolinae (CEMENTED)
	c	11,642	2,778	-3,844	fenestral? Calcite
ALS EA 04		16,366	2,818	-3,813	alveolinae (CEMENTED)
ALS EA 06	a	21,199	1,875	-3,641	alveolina (CEMENTED)
	b	21,199	1,785	-4,113	alveolina (CEMENTED)
ALS EA 07	a	25,757	2,155	-3,808	alveolina (CEMENTED)
	b	25,757	2,206	-3,154	alveolina (CEMENTED)
	c	25,757	2,178	-4,205	alveolina (CEMENTED)
	d	25,757	2,160	-4,101	skeletal matrix
	e	25,757	2,106	-4,102	skeletal matrix
	f	25,757	2,166	-3,805	alveolina (CEMENTED)
ALS EA 08	a	30,895	1,681	-2,675	nummulite (CEMENTED)
	b	30,895	1,646	-3,994	alveolinae (CEMENTED)
ALS EA 10	a	44,477	1,129	-4,567	alveolinae (CEMENTED)
	b	44,477	1,117	-4,544	bulk calcarenite
ALS EB 02		65,297	0,085	-3,994	bulk calcarenite
ALS EB 03		67,389	0,573	-3,318	nummulites (CEMENTED)
ALS EB 04		71,291	0,186	-3,132	alveolinae (CEMENTED)
ALS EC 02	a	92,400	0,677	-4,209	alveolina (CEMENTED)
	b	92,400	0,872	-4,056	alveolina (CEMENTED)
	c	92,400	0,953	-3,992	alveolina (CEMENTED)
	d	92,400	1,187	-3,342	big nummulite-prolocular (CEMENTED)
	e	92,400	1,084	-3,751	big nummulite-marginal (CEMENTED)
ALS EC 03	a	93,754	0,294	-4,830	alveolinae (CEMENTED)
	b	93,754	0,365	-4,859	bulk algal carbonate
ALS EC 04	a	95,370	0,208	-4,472	nummulites (CEMENTED)
	b	95,370	-0,236	-4,833	skeletal red matter
ALS EC 05	a	97,531	0,079	-5,063	alveolina (CEMENTED)
	c	97,531	0,659	-2,980	nummulite (CEMENTED)
	d	97,531	-0,240	-7,628	large pore-fill secondary. Calcite
	e	97,531	0,428	-4,147	bulk red bioclasts
ALS EC 06	a	98,919	-0,503	-3,862	muddy matrix
	b	98,919	0,351	-3,044	alveolina (CEMENTED)
ALS SDS-1	a	105,424	-0,387	-3,304	nummulites (CEMENTED)
	b	105,424	-0,908	-4,842	matrix micrite
ALS ED 01		126,029	0,372	-3,921	nummulites (CEMENTED)
ALS ED 02		131,043	-0,053	-5,571	bulk red bioclasts
ALS ED 03		133,473	0,859	-5,682	bulk skeletal matter
ALS ED 04		142,837	1,324	-5,115	bulk skeletal matter
ALS ED 05		155,059	1,246	-5,438	bulk skeletal matter
ALS ED 06	a	159,762	0,878	-6,060	alveolinae (CEMENTED)
	b	159,762	0,913	-5,309	bulk skeletal matter

INTEGRATED STRATIGRAPHY OF THE UPPER PALEOCENE-LOWER EOCENE SUCCESSIONS OF THE TREMP AND AGER BASINS (SOUTH-CENTRAL PYRENEES, SPAIN)

Ph.D. Thesis, UNIVERSITA' DEGLI STUDI DI PARMA
Corso di Dottorato in Scienze della Terra, XXIII Ciclo

Ph.D. STUDENT: NICOLA MINELLI
Ph.D. COORDINATOR: Ch.mo Prof. Renzo Valloni
TUTOR: Ch.mo Prof. Marco Roveri
CO-TUTOR: Dott. Roberto Tinterri

ATTACHED DOCUMENT 1: REFERENCE SECTIONS

SECTION [4]

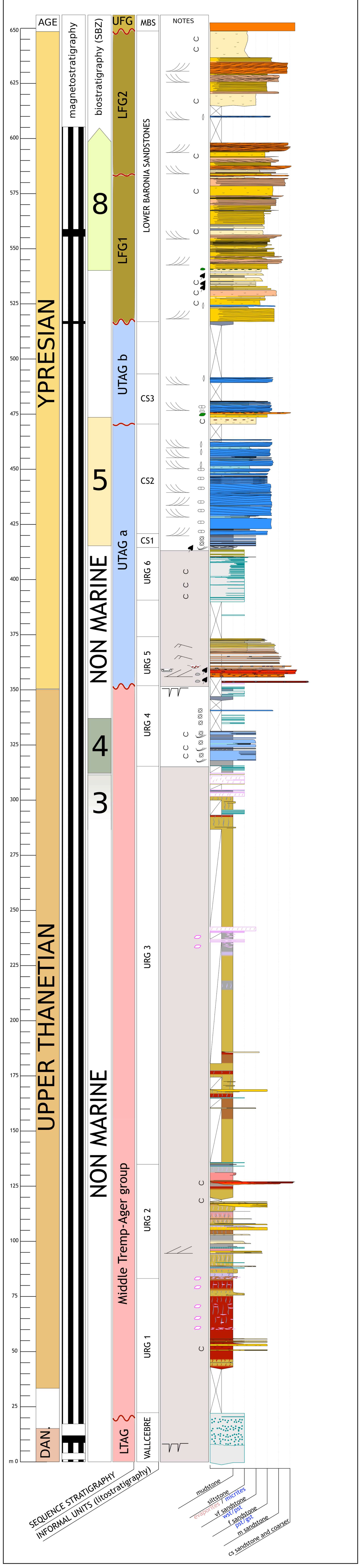

SECTION [12]

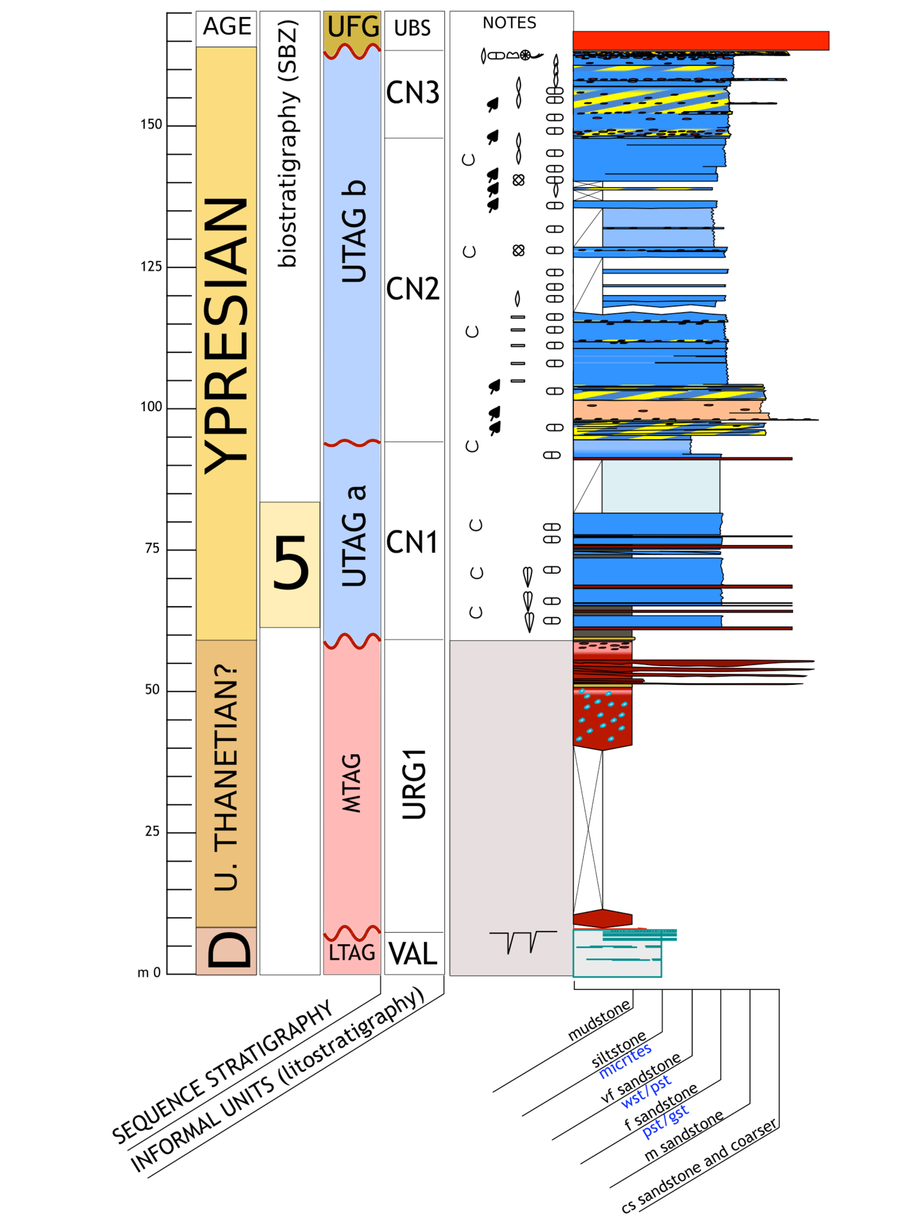

SECTION [16]

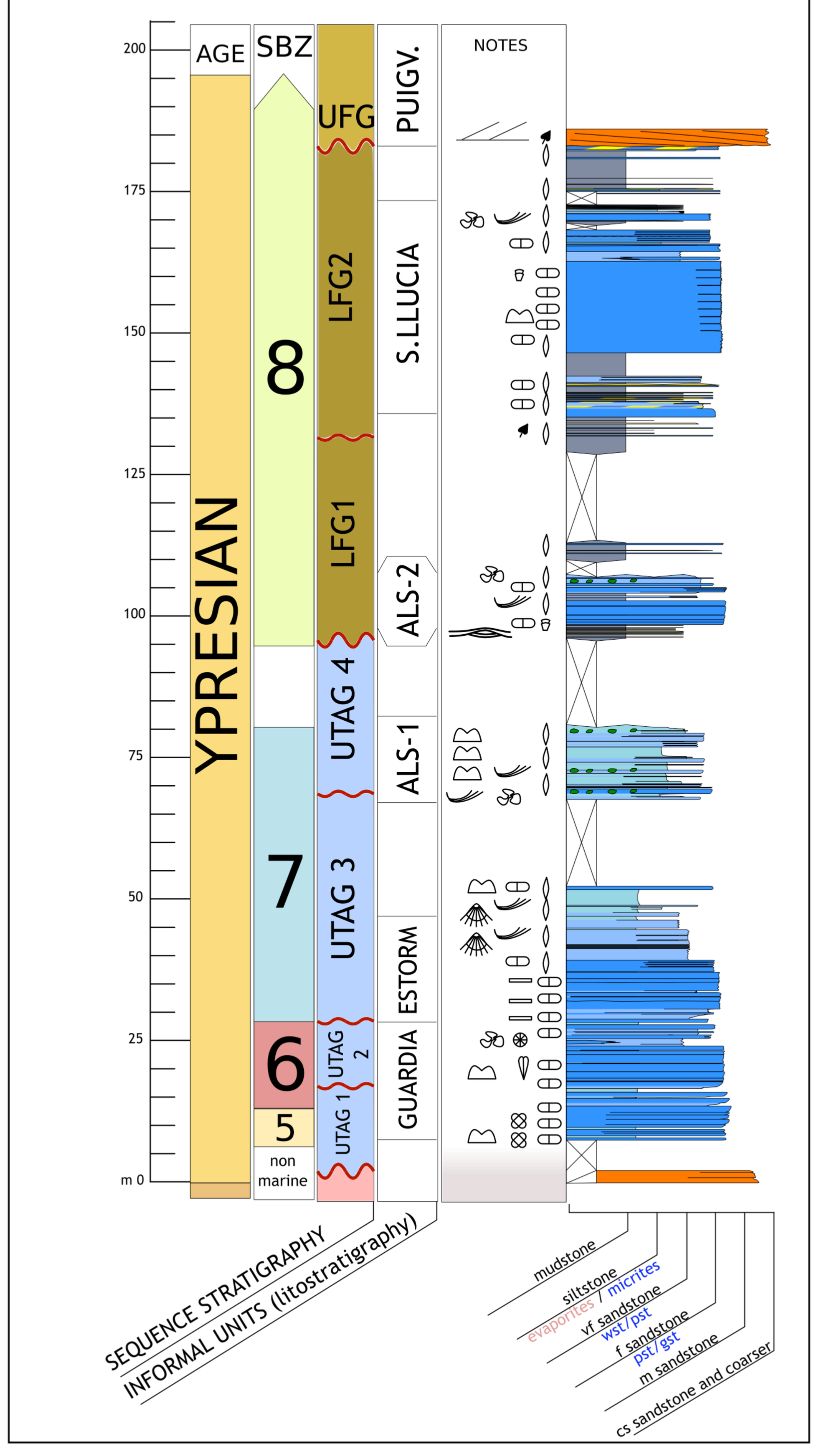

SECTION [20]

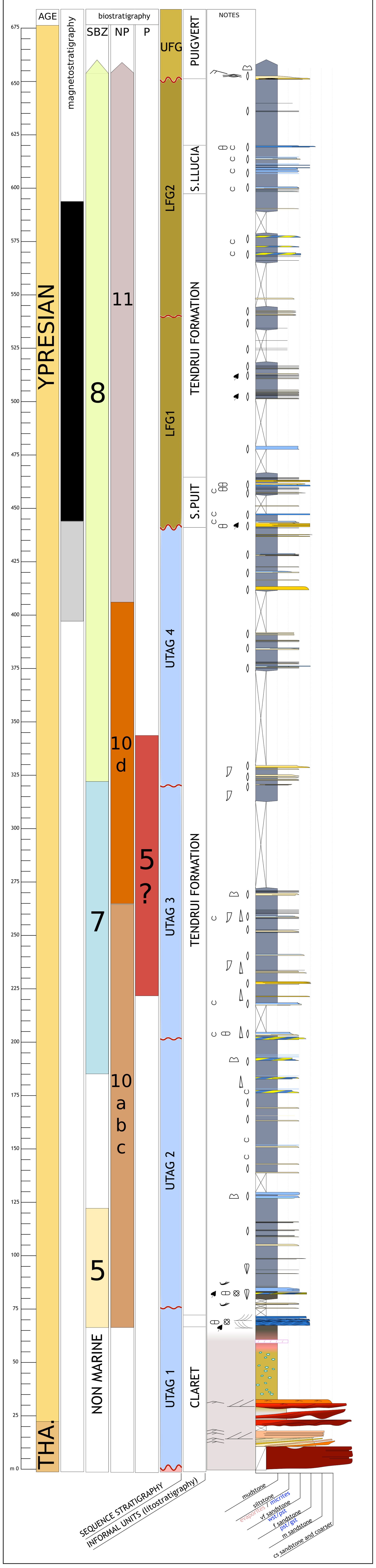

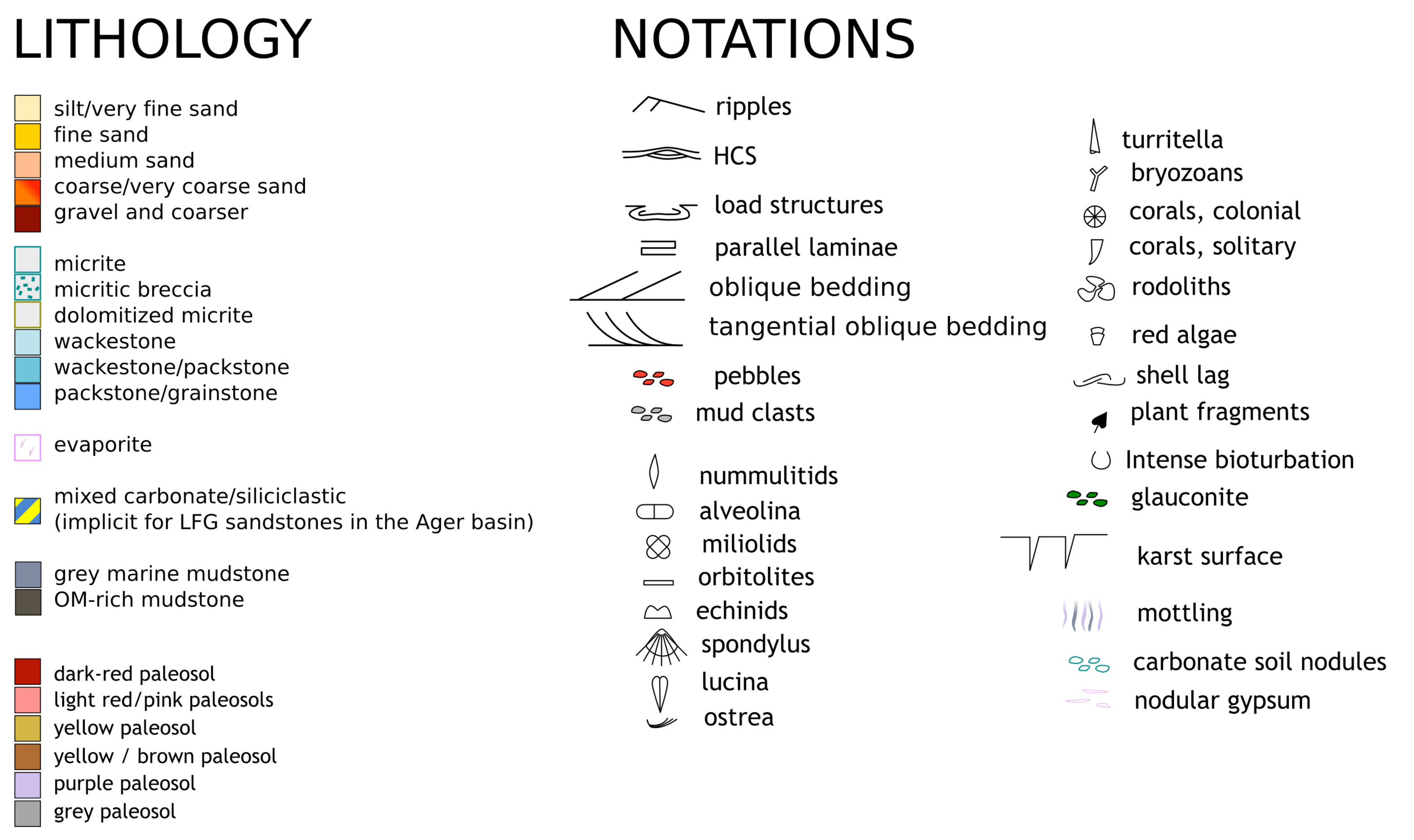

Simplified geological map of the Southern Pyrenean Foreland in the Tremp-Ager region and section locations

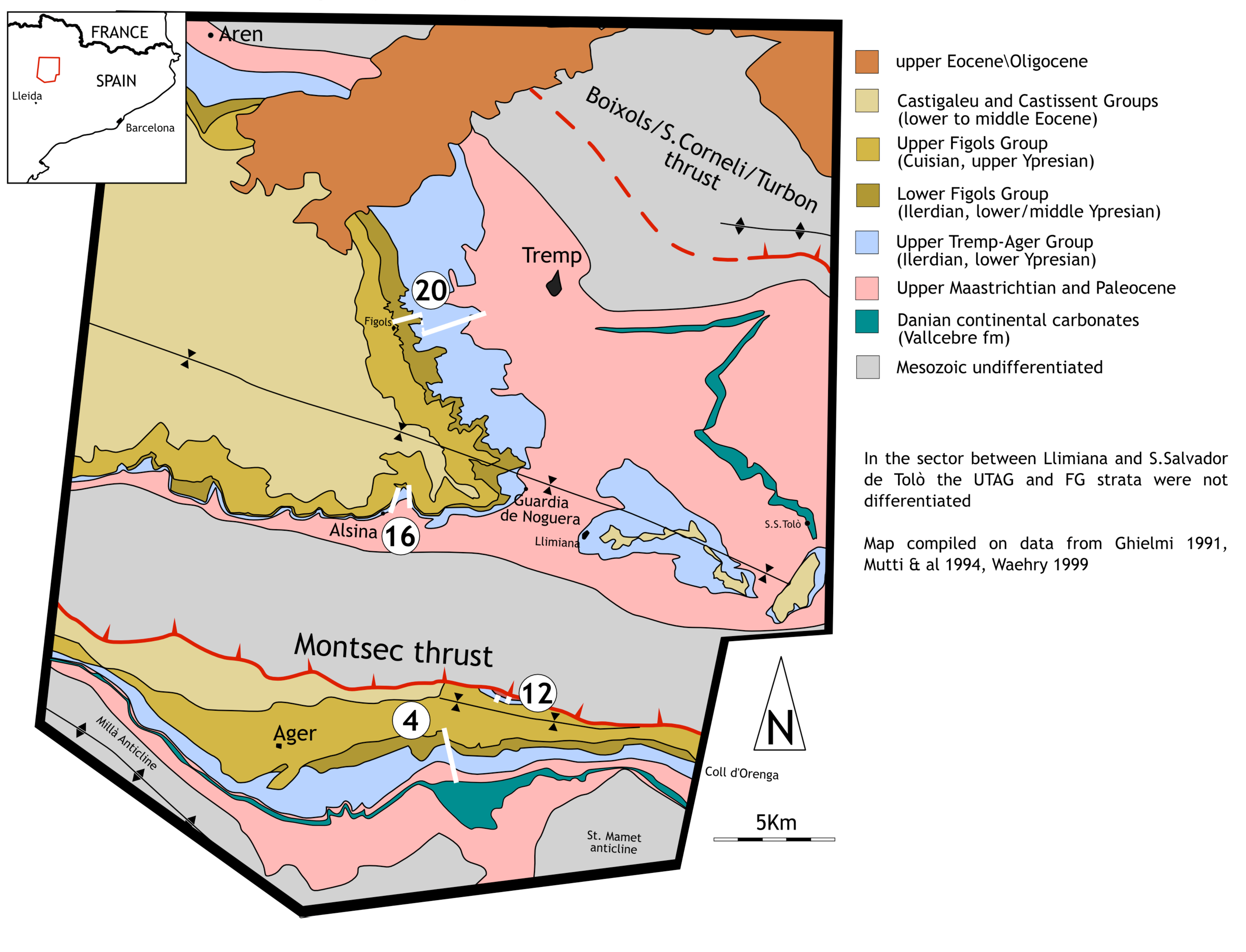

INTEGRATED STRATIGRAPHY OF THE UPPER PALEOCENE-LOWER EOCENE SUCCESSIONS OF THE TREMP AND AGER BASINS (SOUTH-CENTRAL PYRENEES, SPAIN)

Ph.D. Thesis, UNIVERSITA' DEGLI STUDI DI PARMA

Corso di Dottorato in Scienze della Terra, XXIII Ciclo

Pd. D. STUDENT: NICOLA MINELLI
Ph.D. COORDINATOR: Ch.mo Prof. Renzo Valloni
TUTOR: Ch.mo Prof. Marco Roveri
CO-TUTOR: Dott. Roberto Tinterri

ATTACHED DOCUMENT 2: GENERAL CORRELATION PANEL

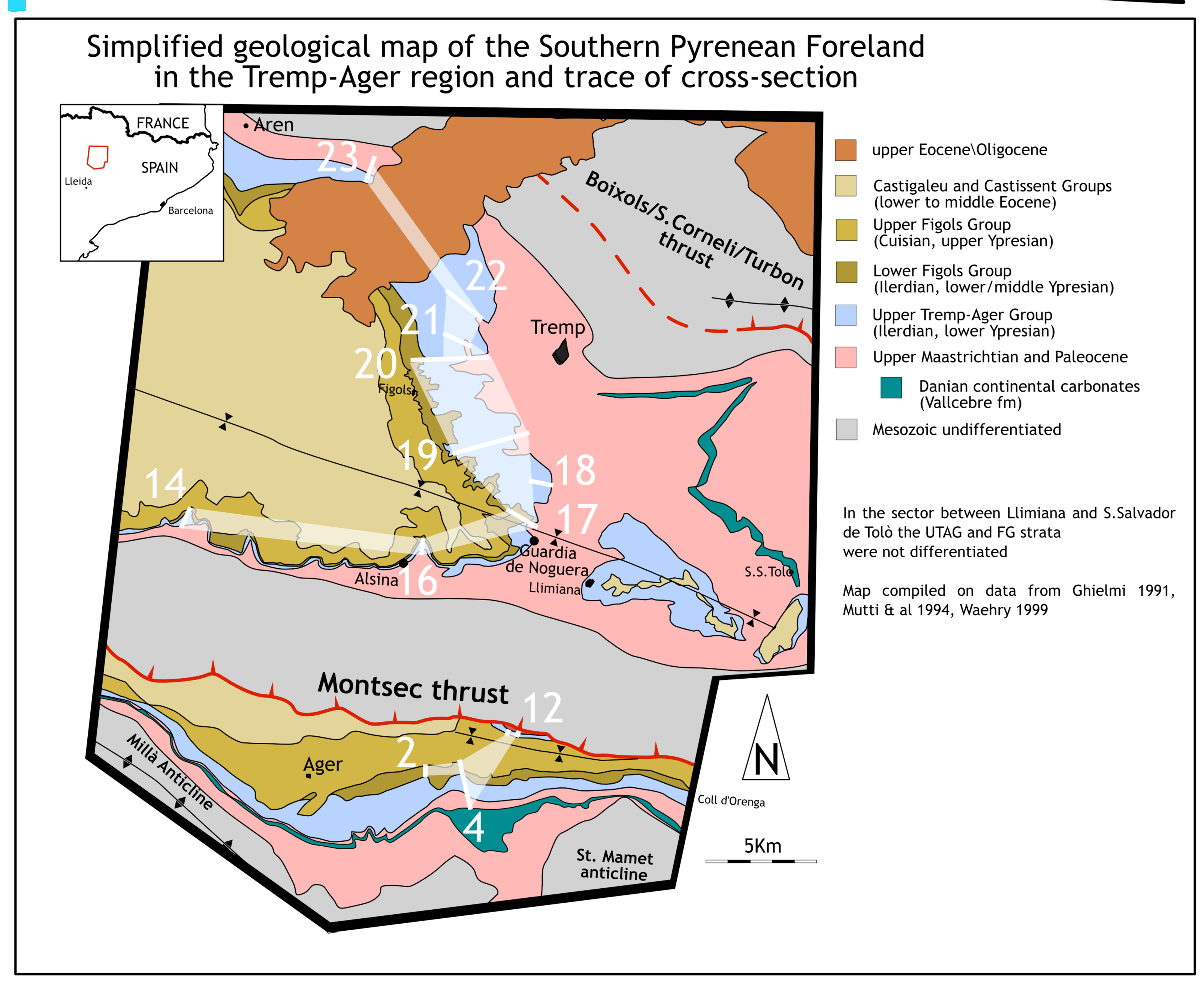

LITHOLOGY

- marine mudstones s.l.
- muddy/silty sandstones
- very fine, fine and medium sandstones
- coarse to very coarse/gravelly sandstones
- conglomerates
- micrites s.l.
- inner shelf limestones s.l.
- outer shelf limestones s.l.
- patch reef or peri-reefal deposits
- Ager basin tsunamites
- evaporites
- OM-rich mudstones
- dark-red paleosols
- light red/pink paleosols
- yellow paleosols
- purple paleosols
- grey paleosols
- covered interval

NOTATIONS

- [22] Log number
- MPU Major sequence boundary or unconformity (see text)
- Small-scale sequence boundary
- A ; 1 Small-scale sequence
- Stratal correlations
- Inner/outer shelf boundary (Alveolina/Nummulites)
- Ilerdian Transgression
- kb Tremp basin keybeds

INTEGRATED STRATIGRAPHY OF THE UPPER PALEOCENE - LOWER EOCENE SUCCESSIONS OF THE TREMP AND AGER BASINS (SOUTH-CENTRAL PYRENEES, SPAIN)

Ph.D. Thesis, UNIVERSITA' DEGLI STUDI DI PARMA

Corso di Dottorato in Scienze della Terra, XXIII Ciclo

Ph.D. STUDENT: NICOLA MINELLI

Ph.D. COORDINATOR: Ch.mo Prof. Renzo Valloni

TUTOR: Ch.mo Prof. Marco Roveri

CO-TUTOR: Dott. Roberto Tinterri

ATTACHED DOCUMENT 3: STRATIGRAPHIC CROSS-SECTION OF THE LOWER FIGOLS GROUP EXPOSED ALONG THE SOUTHERN FLANK OF THE AGER SYNCLINE

bioclastic tidal bars foresets

tidal bars foresets

tidal bars bottomsets/wavy bedding

intensely bioturbated sandstones

marine mudstones

tsunamites

dominant directions of tidal currents (red= ebb tide; blue= flood tide)

allogroup boundary or 3rd order sequence boundary

small-scale sequence boundary

EDS boundary (5th order sequence boundary)

stratal correlation

[1] log number

EDS BOUNDARIES FOLLOWING MUTTI ET AL., 1994 (PLATE III)

Simplified geological map of the Ager basin and trace of cross-sections

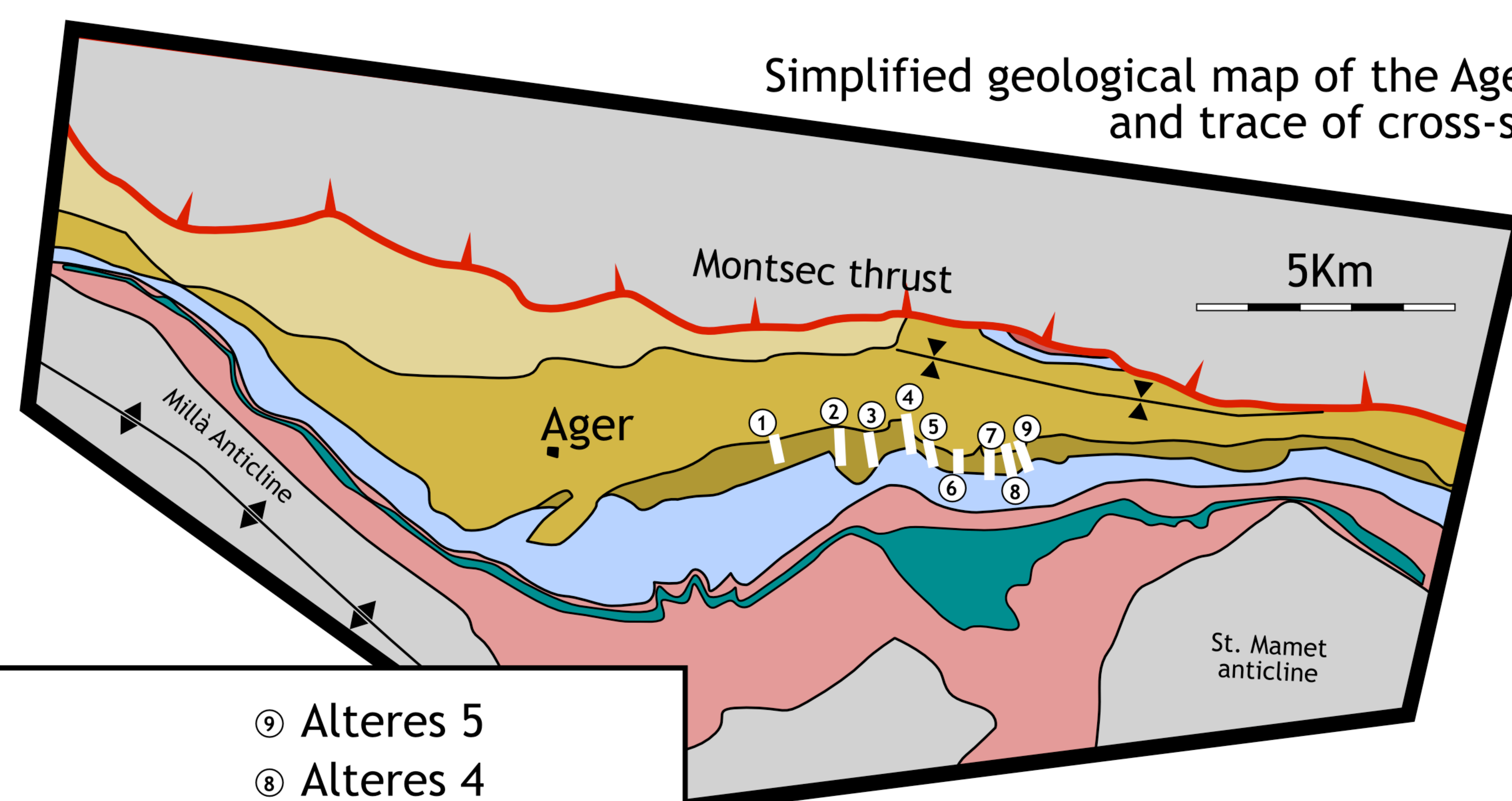

Castigaleu and Castissent Groups (lower to middle Eocene)

Upper Figols Group (Cuisian, upper Ypresian)

Lower Figols Group (Ilerdian, lower Ypresian)

Upper Tremp-Ager Group (Ilerdian, lower Ypresian)

Upper Maastrichtian and Paleocene

Danian continental carbonates (Vallcebre fm)

Mesozoic undifferentiated

Map compiled on data from Ghielmi 1991, Mutti & al 1994

Measured Sections

⑨ Alteres 5
⑧ Alteres 4
⑦ Alteres 3
⑥ Alteres 2
⑤ Alteres 1
④ Les Teuleres-C-13
③ Centralina est
② Centralina ovest
① Riu Fred ovest